FE/BE coupling for time-dependent interface problems in electromagnetics

Von der Fakultät für Mathematik und Physik
der Gottfried Wilhelm Leibniz Universität Hannover
zur Erlangung des Grades
Doktor der Naturwissenschaften
Dr. rer. nat.

genehmigte Dissertation

von

M. Sc. Ricardo Antonio Prato Torres

geboren am 12. Januar 1973 in Barranquilla/Kolumbien

2009

A Natalia

Abstract

This thesis deals with the coupling of finite elements and boundary elements for time-dependent electromagnetic interface problems in $\mathbb{R}^3$.

We consider a linear and a nonlinear eddy current problem which are induced by a current in a conductor Ω and can be described by Maxwell's equations. For the determination of the electric field in Ω and the magnetic field on the boundary we derive variational formulations for which we show existence and uniqueness. Using the Stratton-Chu representation formula we can compute the solution in the exterior domain $\mathbb{R}^3 \setminus \overline{\Omega}$.

For the approximation of the solution of the electric field in Ω we use $\mathbf{H}(\mathbf{curl}, \Omega)$-conforming vector-valued piecewise linear polynomials, and for the magnetic field on the boundary we use surface curls of hat functions. The approximation in time is done with the aid of the discontinuous Galerkin method with linear functions. For the solution of the resulting linear systems we use the fast solvers HMCR and GMRES combined with different preconditioners like multigrid and block inverses.

For the linear eddy current problem we derive a priori and a posteriori error estimates, with the resulting error indicators we perform an adaptive algorithm in space.

In the case of the nonlinear eddy current problem the magnetic permeability μ additionally depends on the magnetic field and on time. For solving the related nonlinear variational formulation we use Newton's method.

Our numerical experiments underline our theoretical results. We examine reliability and efficiency of our a posteriori error estimates and compare different preconditioners. Furthermore, we perform an adaptive algorithm using hanging edges.

Key words. Eddy current problem, FEM/BEM-coupling, discontinuous time stepping Galerkin method, a posteriori error estimates, adaptive algorithm.

Zusammenfassung

Diese Arbeit behandelt die Koplung von finiten Elementen und Randelmenten für zeitabhängige elektromagnetische Interface-Probleme in $\mathbb{R}^3$.

Wir untersuchen ein lineares und ein nichtlineares Wirbelstromproblem, die durch einen Strom in einem Leiter Ω verursacht und die durch die Maxwell-Gleichungen beschrieben werden. Zur Bestimmung des elektrischen Feldes in Ω und des magnetischen Feldes auf dem Rand leiten wir variationelle Formulierungen her, für die wir Existenz und Eindeutigkeit der Lösung zeigen. Mit Hilfe der Stratton-Chu-Darstellungsformel läßt sich die Lösung für den Außenraum $\mathbb{R}^3 \setminus \overline{\Omega}$ bestimmen.

Zur Approximation der Lösung des elektrischen Feldes in Ω benutzen wir $\mathbf{H}(\mathbf{curl}, \Omega)$-konforme vektorwertige stückweise lineare Polynome und für das magnetische Feld auf dem Rand Flächenrotationen von Hutfunktionen. Die Approximation in der Zeit wird mit Hilfe der Diskontinuierlichen Zeitschritt Galerkin Methode mit stückweise linearen Funkionen durchgeführt. Zur Lösung der resultierenden linearen Gleichungssysteme benutzen wir als schnelle Löser HMCR und GMRES in Kombination mit verschiedenen Vorkonditionierern wie Multigrid und Block-Inverse.

Für das lineare Wirbelstromproblem leiten wir a priori und a posteriori Fehlerabschätzungen her. Mit den zugehörigen Fehlerindikatoren führen wir einen adaptiven Algorithmus im Raum durch.

Im Falle des nichtlinearen Wirbesltromproblems hängt die mangetische Permeabilität μ zusätzlich vom Magnetfeld und der Zeit ab. Zur Lösung der zugehörigen variationellen nichtlinearen Formulierung nutzen wir das Newton-Verfahren.

Unsere numerische Experimente unterstreichen unsere theoretischen Resultate. Wir untersuchen die Fehlerabschätzungen auf Effizienz und Zuverlässigkeit und vergleichen verschiedene Vorkonditionierer. Weiterhin führen wir einen adaptiven Algorithmus mit Hilfe von hängenden Kanten durch.

Schlagwörter. Wirbelstromproblem, FEM/BEM-Kopplung, Diskontinuierliche Zeitschritt Galerkin Methode, a posteriori Fehlerabschätzungen, adaptive Algorithmen.

Contents

Contents

List of Figures

List of Tables

List of Tables

Introduction

Many problems in science and engineering have to deal with the analysis of electromagnetic phenomena. For solving these problems the focus lies on the study of Maxwell's equations, a system of partial differential equations which relates to the magnetic field $\mathbf{H}$, the magnetic induction $\mathbf{B}$, the electric field $\mathbf{E}$, the electric displacement $\boldsymbol{D}$, and the electric current density $\mathbf{J}$, and is given by

$$\frac{\partial \mathbf{B}}{\partial t} + \mathbf{curl}\,\mathbf{E} = 0\,, \qquad \textit{Faraday's law}$$

$$\mathrm{div}\,\boldsymbol{D} = \rho\,, \qquad \textit{Gauss' law}$$

$$\frac{\partial \boldsymbol{D}}{\partial t} - \mathbf{curl}\,\mathbf{H} = -\mathbf{J}\,, \qquad \textit{Ampère's law}$$

$$\mathrm{div}\,\mathbf{B} = 0\,,$$

where ρ denotes the distribution of charges (cf. Bastos [5], Monk [59]).

Eddy currents can be found in any conducting medium, which is subjected to a time-varying magnetic field or a relative motion between the conductive medium and the magnetic field. In applications where the displacement current existing in a metallic bounded conductor Ω is negligible compared to the conduction current, it is possible to use a magneto-quasistatic sub-model of Maxwell's equations, which is known as the *eddy current problem*.

The eddy current problem is defined in the whole space $\mathbb{R}^3$ with decay conditions for the magnetic and electric fields at infinity. One efficient method for dealing with this problem is the coupling of finite elements and boundary elements (FE/BE), such that the initial problem becomes a problem of transmission between the bounded domain Ω and the unbounded exterior domain $\mathbb{R}^3 \setminus \overline{\Omega}$. Using the Stratton-Chu formula the solution in the unbounded domain can be represented by functions on the transmission boundary. Significant theoretical and numerical results of boundary elements for exterior problems in electromagnetism can be found in MacCamy & Stephan [43, 44, 45, 46] and Nédélec [62, 64], and more recent results for instance in Bossavit [7] and Buffa et. al. [12, 14, 15].

In recent years, symmetric methods for the coupling of finite elements and boundary elements for electromagnetic problems have been developed (see e.g. Hiptmair [37, 38]), following the approach of Costabel [21]. The key concept is to use the Calderón projector

acting on the Cauchy data of the problem.

The main objective of this work is the implementation and analysis of the *h*-version of the symmetric FE/BE coupling method to solve the eddy current problem for the time dependent Maxwell's equations. For a fixed time t, the electric field is chosen as primary unknown. Furthermore, the non-local boundary condition on the FE/BE coupling interface is deduced directly from the Stratton-Chu integral representation of the electric field. Using these formulas we obtain a symmetric variational coupling formulation. For the space discretization, we use $\mathbf{H}(\mathbf{curl}, \Omega)$-conforming vector-valued polynomials to approximate the electric field in the conductor Ω and $\mathbf{H}(\mathrm{div}, \Omega)$-conforming polynomials on the transmission boundary Γ to approximate the twisted tangential trace of the magnetic field on Γ. As the resulting variational formulation is not coercive in the energy norm, we modify it by adding a penalty term.

Time-stepping methods for systems of ordinary (or partial) differential equations are frequently used to obtain a fully-discrete scheme in time and space, e.g. Costabel, Ervin & Stephan [23] introduce a full discretization for a symmetric FE/BE coupling of a parabolic-elliptic problem using the Crank-Nicolson method for the time discretization and Mund [60] applies the *discontinuous Galerkin time stepping method* to solve the time-dependent FE/BE coupling covering scalar problems (e.g. Laplace/heat equations). An extension of this time stepping method to time dependent electromagnetic problems is treated in this thesis. Using this method, the approximate solution is sought as a piecewise polynomial function of degree l in t and is not necessarily continuous in the nodes of the time mesh. Here, we consider piecewise linear test and trial functions in time. A complete analysis of the *discontinuous Galerkin method* can be found e.g. in Eriksson *et al.* [28, 27], Lippold [41], and Thomée [74].

While there is a considerable amount of work covering implementations to time-dependent Maxwell's equations and on the convergence of numerical schemes for stationary Maxwell's equations and related models (see e.g. Assous *et. al.* [3], Ciarlet & Zou [17], Meddahi & Selgas [54]), few works exist on the convergence analysis for semidiscrete or fully discrete numerical methods for the time dependent Maxwell's equations (see e.g. Ciarlet & Zou [18], Monk [58], Meddahi & Selgas [55, 56]). We provide a convergence analysis of our fully discrete system for uniform meshes in time, in that e.g. error estimates are derived at the nodal points. Moreover, an a posteriori error estimate is derived, which guarantees a quasi-optimal bound of the error in the energy norm. The residual based local error indicators allow us to present an adaptive feedback algorithm for the mesh refinement of the coupling procedure, which is presented in Algorithm 1, Page 66.

To solve the large linear equation system (3.26), Page 44, we use in our work fast solvers as e.g. the Generalized Minimal Residual Method (GMRES) (see e.g. [70]), an extension of MINRES to nonsymmetric systems, and the Hybrid Modified Conjugate Residual method (HMCR) (see e.g. [71]), a stable variant of MINRES. For the unpreconditio-

ned system the condition number $\kappa(\mathcal{A})$ of the Galerkin matrix $\mathcal{A}$, behaves like $\mathcal{O}(N)$ with respect to the number of degree of freedom N, i.e. $\mathcal{A}$ is ill-conditioned (see Table 4.1). Hence, we consider a preconditioned system, which in turn is more appropiate for iterative methods and has the same solution as our unpreconditioned linear system.

The strategy is to use a diagonal preconditioner for the matrix $\mathcal{A}$ as

$$\mathcal{P} = \begin{pmatrix} P_{\mathcal{MR}} & \\ & P_{\mathcal{V}} \end{pmatrix}$$

with

$$P_{\mathcal{MR}} = \begin{pmatrix} -2P_A & 6P_A \\ 6P_A & -12P_A \end{pmatrix}, \qquad P_{\mathcal{V}} = \begin{pmatrix} 2P_B & -6P_B \\ -6P_B & 12P_B \end{pmatrix},$$

$$P_A := (\frac{1}{k_n}\mathcal{M} + \widetilde{\mathcal{R}})^{-1} \qquad \text{and} \qquad P_B := (\mathcal{V} + \mathcal{P}_h)^{-1}.$$

The preconditioner $\mathcal{P}$ is obtained by using the **Inverses block preconditioner** (see Maischak & Tran [52]), i.e. P_A (the inverse of the FEM matrix) and P_B (the inverse of the BEM matrix) are calculated by solving an auxiliary problem with CG and using LR decomposition, respectively. Also **Multigrid** can be applied and for this case we use a $V(\nu_1, \nu_2)$-multigrid algorithm like in Hiptmair [35] for the FEM part and the multigrid method like in Stephan & von Petersdorff [75, 76] for the BEM part. In the preconditioned system with the inverses block as preconditioner the condition number $\kappa(\mathcal{PA})$ is bounded and independent of the time step (see Table 4.5, Page 91), while in the preconditioned system with multigrid as preconditioner the condition number $\kappa(\mathcal{PA})$ depends on the time step (see Table 4.7 and Figure 4.16).

In the following Ω represents a Lipschitz domain with boundary $\Gamma := \partial\Omega$.

The thesis is organized as follows. In **Chapter 1** we recall main concepts and definitions, which are necessary in the forthcoming analysis. Here, we focus on the Sobolev spaces $\mathbf{H}(\mathbf{curl}, \Omega)$, $\mathbf{H}(\text{div}, \Omega)$, and related spaces used for the analysis of Maxwell's equations. For the boundary element analysis we need the tangential trace operator $\gamma_D \boldsymbol{u} := \boldsymbol{n} \times (\boldsymbol{u} \times \boldsymbol{n})$ and the twisted tangential trace $\gamma_D^\times \boldsymbol{u} := \boldsymbol{u} \times \boldsymbol{n}$, which define the following trace spaces

$$\mathbf{H}_{\parallel}^{-1/2}(\text{div}_\Gamma, \Gamma) = \gamma_D^\times(\mathbf{H}(\mathbf{curl}, \Omega)), \qquad \mathbf{H}_{\perp}^{-1/2}(\text{curl}_\Gamma, \Gamma) = \gamma_D(\mathbf{H}(\mathbf{curl}, \Omega)).$$

Section 1.3 gives the definition of the boundary integral operators for Maxwell's equations and summarizes their mapping properties on the trace spaces $\mathbf{H}_{\parallel}^{-1/2}(\text{div}_\Gamma, \Gamma)$ and $\mathbf{H}_{\perp}^{-1/2}(\text{curl}_\Gamma, \Gamma)$. In Section 1.4 we quote the Stratton-Chu representation formula as an

essential tool to obtain the desired FE/BE coupling, and finally in Section 1.5 we recall some basic spaces and properties needed for the study of a time dependent problem.

In **Chapter 2** the spaces needed for the discretization of the spaces $\mathbf{H}(\mathbf{curl}, \Omega)$, $\mathbf{H}(\mathrm{div}, \Omega)$, $\mathbf{H}_{\parallel}^{-1/2}(\mathrm{div}_\Gamma, \Gamma)$ and $\mathbf{H}_{\perp}^{-1/2}(\mathrm{curl}_\Gamma, \Gamma)$ are presented. For this, we consider a shape-regular mesh $\mathcal{T}_h$ (with tetrahedral or hexahedral elements) on the domain Ω with mesh size $h > 0$, which induces a mesh $\mathcal{K}_h$ of triangles or of quadrilaterals on the boundary Γ. Section 2.1 defines the $k-$order Nédélec elements $\mathcal{ND}_k(\mathcal{T}_h)$, a $\mathbf{H}(\mathbf{curl}, \Omega)-$conforming space used to discretize the electric field (see Nédélec [63, 65]). These elements fulfill the $\mathbf{H}(\mathbf{curl}, \Omega)-$conformity condition, i.e. the continuity of the tangential trace between adjacent elements. In order to achieve this condition Nédélec ([63]) introduces degrees of freedom which are based on integral moments that are used for the definition of the basis functions and also for the definition of an interpolation operator. Section 2.1.4 gives an error estimate for this operator. In Section 2.2 we concisely describe the main properties of the Raviart-Thomas space $\mathcal{RT}_k(\mathcal{T}_h)$, a $\mathbf{H}(\mathrm{div}, \Omega)-$conforming space used to discretize our unknown on the boundary which satisfies $\mathcal{RT}_k(\mathcal{K}_h) = \gamma_D^\times(\mathcal{ND}_k(\mathcal{T}_h))$. With this result we obtain a discretization of the trace space $\mathbf{H}_{\parallel}^{-1/2}(\mathrm{div}_\Gamma, \Gamma)$ (see Sections 2.2.2 and 1.2.3). For the discretization in $\mathbf{H}_{\perp}^{-1/2}(\mathrm{curl}_\Gamma, \Gamma)$ we introduce in Section 2.2.3 the space $\mathcal{TND}_k(\mathcal{T}_h) := \gamma_D(\mathcal{ND}_k(\mathcal{T}_h))$ as the tangential trace space of the Nédélec space. In Section 2.3 we consider the de Rham diagram which gives us the connection between the different finite element spaces. In Section 2.4 we define discrete spaces and interpolation operators for the time dependent spaces. Moreover, we prove an inequality using a duality argument, known also as *Aubin Nitsche Trick*. This result is necessary for the proof of the a priori estimate in Theorem 3.3.1.

Chapter 3 is devoted to the time dependent eddy current problem. Initially in Section 3.1 the time dependent eddy current problem is formulated. Employing the Stratton-Chu representation formula and boundary integral operators, a symmetric FE/BE coupling formulation for the unknowns $\boldsymbol{u} \in W^1(0, T; \mathbf{H}(\mathbf{curl}, \Omega))$, which represents the electric field in the domain Ω, and $\boldsymbol{\lambda} := \mathbf{curl}\, \boldsymbol{u} \times \boldsymbol{n} \in L^2(0, T; \mathbf{H}_{\parallel}^{-\frac{1}{2}}(\mathrm{div}_\Gamma 0, \Gamma))$ is derived. A difficulty of this initial variational formulation is, that for an arbitrary and fixed t it is not coercive in the energy norm. To cope with that problem we add a penalty term to ensure coercivity. This *augmented* weak formulation is used in the following. To achieve the semi-discrete scheme we use Nédélec functions of the first order to approximate the electric field $\boldsymbol{u}$ in the interior of the domain and divergence free Raviart-Thomas functions to approximate the twisted tangential trace of the magnetic field.

In Section 3.2 we deduce a full discretization using the discontinuous time stepping Galerkin method with piecewise linear test and trial functions. An a priori error analysis for constant time step k is carried out, a convergence rate of the order $\mathcal{O}(h^r + k^2)$ is obtained in the $\mathbf{L}^2-$error estimates at the nodal points, and in the energy norm a convergence rate of the order $\mathcal{O}(h^{r_0} + k^2)$ is expected, where $r := \alpha + \min\{s, 1\}$

and $r_0 := \min\{s, 1\}$ with $\alpha > \frac{1}{2}$ and $s \in]\frac{1}{2}, 1[\cup \mathbb{N}$. Finally, we derive an a posteriori error estimate for the solution of the fully discrete discontinuous Galerkin method (see Theorem 3.3.2), using residual error estimator for the h-version. Here, singular, weakly singular, and hypersingular boundary integral operators appearing in the variational coupling formulation show up in the terms of the error estimators as well. Moreover, the residual based local error indicators allow us to present an adaptive feedback algorithm for the mesh refinement of the coupling procedure. So far an error analysis for the FE/BE coupling of electromagnetic problems was restricted to time-independent problems (see Teltscher [73] who uses results by Beck *et al.* [6] for the FE-part). As a key for extending these results to the time dependent case we have extended here the results of Mund [60] who first derived a priori and a posteriori error estimates for the time-dependent FE-BE coupling using the discontinuous Galerkin method.

In **Chapter 4** we present numerical experiments underlining the theoretical results derived in Theorems 3.3.1 and 3.3.2. For it we implement in the scientific program package MAIPROGS [50] among other the full discrete system (3.26), obtained by using the discontinuous Galerkin method, the error estimators presented in Theorem 3.3.2, and the inverse block and multigrid preconditioners presented in Section 4.2.1. To accomplish the implementation the divergence free Raviart-Thomas functions $\mathcal{RT}_1^0(\mathcal{K}_h)$ can be represented by $\mathbf{curl}_\Gamma \mathcal{S}_1(\mathcal{K}_h)$, where $\mathcal{S}_1(\mathcal{K}_h)$ denotes the space of piecewise polynomials on the triangulation $\mathcal{K}_h$ [34]. Our different numerical experiments show the realibility and efficiency of our error estimators. We also compare the different preconditioners.

Chapter 5 examines a nonlinear variant of the time dependent eddy current problem. Here the magnetic permeability μ depends on the magnetic field and on the time. For this problem we derive a variational formulation and show the existence and the uniqueness of the solution (Theorem 5.1.1). To solve the full discrete problem using the discontinuous Galerkin method we present a Newton's algorithm. A numerical experiment shows the convergence of the procedure.

Throughout this work, vector-valued functions or spaces are written in bold letters, scalar functions in normal typed letters. C denotes a generic positive constant, usually independent of the characteristic mesh size h. The symbol $\lesssim$ signifies "$\leq$ up to a multiplicative constant $C > 0$". The symbol $\simeq$ means "$\lesssim$ and $\gtrsim$".

Acknowledgements

Several people have been instrumental in allowing this project to be completed. I would like to thank my advisor Prof. Dr. E. P. Stephan, for his encouragement and patience throughout the duration of this project and for his professional advice and experience sharing. I would also like to thank to PD Dr. Matthias Maischak, for his constant encouragements, support, and help concerning the numerical analysis and numerical implementation of my investigations; his software package MAIPROGS is the basis for the numerical experiments presented in this work.

Many thanks to my colleagues of my working group at the Institute for Applied Mathematics of the Gottfried Wilhelm Leibniz Universität Hannover, specially to Elke Ostermann and Dr. Florian Leydecker, for reading my essays and offering valuable advice during these years, particularly for answering a lot of my questions; to Dr. Stephan Oestmann, Michael Andres, Leo Nesemann and Catalina Dominguez for advice, help and the numerous discussions, more or less related to this thesis. Many thanks to all of them for their friendship and camaraderie.

I wish to extend my thanks to the whole staff at the Institut for Applied Mathemathics of the Leibniz Universität Hannover. Particularly to Mrs. Carmen Gatzen and Mrs. Ulla Fleischhauer for their kindness and dedication, and their essential support on technical issues and prototyping.

I also warmly thank my family and friends in Barranquilla for standing by me in good and bad times.

This project would not have been possible without the general support of the *DAAD "Deutscher Akademischer Austausch Dienst"* and also of the *Colciencias-Laspau program* that provided me the Ph.D. scholarships, and *the Universidad del Norte (Barranquilla-Colombia)*.

Ricardo A. Prato T.

1 Foundations

1.1 Spaces for the Maxwell's equations

We start this chapter with a brief introduction into the main concepts and definitions connected with the Sobolev spaces used and some standard notation for distributions (see e.g. Girault & Raviart [29], McLean [53] and Lions & Magenes [40]).

Let $\mathcal{U} \subset \mathbb{R}^n$ be a non-empty open subset. For a sufficiently smooth $\phi : \mathcal{U} \to \mathbb{R}$ the partial derivatives of ϕ are denoted by

$$\partial^{\boldsymbol{\alpha}} \phi := \frac{\partial^{|\boldsymbol{\alpha}|} \phi}{\partial x_1^{\alpha_1} \cdots \partial x_n^{\alpha_n}}$$

where $\boldsymbol{\alpha} = \left(\alpha_1, \cdots, \alpha_n \right) \in \mathbb{Z}_+^n$ is a multi-index, i.e., an n-tuple of non-negative integers with $|\boldsymbol{\alpha}| := \sum_{i=1}^n \alpha_i$.

$\mathcal{C}^k(\mathcal{U})$ denotes the space of k times continuously differentiable functions on $\mathcal{U}$, and $\operatorname{supp} \phi$ denotes the support of ϕ, which is given by the closure in $\mathcal{U}$ of the set $\{ \boldsymbol{x} \in \mathcal{U} : \phi(\boldsymbol{x}) \neq 0 \}$.

Then,

$$\mathcal{C}_0^k(\mathcal{U}) := \left\{ \phi \in \mathcal{C}^k(\mathcal{U}) : \operatorname{supp} \phi \subset K \subseteq \mathcal{U}, \ K \text{ compact} \right\}$$

and

$$\mathcal{C}_0^\infty(\mathcal{U}) := \bigcap_{k \geq 0} \mathcal{C}_0^k(\mathcal{U}) \ .$$

The space of distributions $\mathcal{C}_0^\infty(\mathcal{U})' \equiv \mathcal{D}'(\mathcal{U})$ is the dual space of $\mathcal{C}_0^\infty(\mathcal{U})$ in the sense that a linear functional $\psi : \mathcal{C}_0^\infty(\mathcal{U}) \to \mathbb{C}$ is contained in $\mathcal{D}'(\mathcal{U})$, provided that for every compact set $K \subset \mathcal{U}$ there exist constants $C > 0$ and $k \in \mathbb{N}$ such that

$$|\psi(\phi)| \leq C \sum_{|\boldsymbol{\alpha}| \leq k} \sup_K |\partial^{\boldsymbol{\alpha}} \phi|$$

for all $\phi \in \mathcal{C}_0^\infty(\mathcal{U})$. Moreover for every $1 \leq p < \infty$ we define

$$L^p(\mathcal{U}) := \left\{ \phi : \mathcal{U} \to \mathbb{C}, \int_{\mathcal{U}} |\phi|^p \, d\boldsymbol{x} < \infty \right\} \ .$$

1 Foundations

Let $\Omega \subset \mathbb{R}^n$, $n = 1, 2, 3$ be an open and connected set. For each integer $s \geq 0$ and real number $1 \leq p < \infty$, we define the Sobolev space

$$W^{s,p}(\Omega) := \{\phi \in L^p(\Omega) : \partial^{\boldsymbol{\alpha}} \phi \in L^p(\Omega) \text{ for all } |\boldsymbol{\alpha}| \leq s\}.$$

$W^{s,p}(\Omega)$ is a Banach space with norm

$$\|\phi\|_{W^{s,p}(\Omega)} = \left(\sum_{|\boldsymbol{\alpha}| \leq s} \int_\Omega |\partial^{\boldsymbol{\alpha}} \phi(\boldsymbol{x})|^p \, dx \right)^{1/p}$$

and corresponding semi-norm

$$|\phi|_{W^{s,p}(\Omega)} = \left(\sum_{|\boldsymbol{\alpha}| = s} \int_\Omega |\partial^{\boldsymbol{\alpha}} \phi(\boldsymbol{x})|^p \, dx \right)^{1/p}.$$

Notice that the space $W^{s,p}(\Omega)$ is separable for $1 \leq p < \infty$ and reflexive for $1 < p < \infty$.

For $n = 2, 3$ and $p = 2$ define

$$H^s(\Omega) := \left\{ \phi \in \mathcal{D}'(\Omega) : \phi = u|_\Omega \text{ for some } u \in W^{s,2}(\mathbb{R}^n) \right\}.$$

Let Ω be an open subset of $\mathbb{R}^n$, m a non-negative integer and $s, p \in \mathbb{R}$ with $s \geq 0$ and $1 \leq p < \infty$ and $s = m + \gamma$ where $\gamma \in \mathbb{R}$ with $0 < \gamma < 1$. The space $W^{s,p}(\Omega)$ denotes the spaces of all distributions $\phi \in \mathcal{D}'(\Omega)$ such that $\phi \in W^{m,p}(\Omega)$ and

$$\int_\Omega \int_\Omega \frac{|\partial^{\boldsymbol{\alpha}} \phi(\boldsymbol{x}) - \partial^{\boldsymbol{\alpha}} \phi(\boldsymbol{y})|^p}{|\boldsymbol{x} - \boldsymbol{y}|^{n+\gamma p}} \, d\boldsymbol{x} \, d\boldsymbol{y} < \infty \qquad \text{for all } |\boldsymbol{\alpha}| = m,$$

equipped with the norm

$$\|\phi\|_{W^{s,p}(\Omega)} := \left\{ \|\phi\|^p_{W^{m,p}(\Omega)} + \sum_{|\boldsymbol{\alpha}| = m} \int_\Omega \int_\Omega \frac{|\partial^{\boldsymbol{\alpha}} \phi(\boldsymbol{x}) - \partial^{\boldsymbol{\alpha}} \phi(\boldsymbol{y})|^p}{|\boldsymbol{x} - \boldsymbol{y}|^{n+\gamma p}} \, d\boldsymbol{x} \, d\boldsymbol{y} \right\}^{1/p}.$$

The space $W^{s,p}(\Omega)$ is a separable, reflexive Banach space for $1 < p < \infty$ and $s \in \mathbb{R}$ with $s \geq 0$. This space with fractional order is used in the analysis of boundary values of functions and boundary integral operators.

In the following, let $\Omega \subset \mathbb{R}^3$ denote a bounded domain with a Lipschitz continuous boundary $\Gamma := \partial\Omega$ in the sense of Grisvard [30, Def. 1.2.1.2], i.e., for every $\boldsymbol{x} \in \Gamma$ there exists a neighborhood $\mathcal{U}$ of $\boldsymbol{x}$ in $\mathbb{R}^3$ and a new orthogonal coordinate system $\boldsymbol{y} = (y_1, y_2, y_3) \equiv (\boldsymbol{y}', y_3)$ and there exist

- a vector $\boldsymbol{a} \in \mathbb{R}^3$ with $\boldsymbol{x} \in \mathcal{U} := \{\boldsymbol{y} \in \mathbb{R}^3 : |y_i| < a_i, \, \forall i = 1, 2, 3\}$,

- a Lipschitz continuous function $\varphi : \mathcal{U}' \to \mathbb{R}$ with $|\varphi(\boldsymbol{y}')| \leq \frac{a_3}{2}$ for all $\boldsymbol{y}' \in \mathcal{U}'$, where

$$\mathcal{U}' := \left\{ \boldsymbol{y}' \in \mathbb{R}^2 : |y_i| < a_i, \ \forall i = 1, 2 \right\} \,,$$

such that

$$\Omega \cap \mathcal{U} = \left\{ \boldsymbol{y} \in \mathcal{U} : y_3 < \varphi(\boldsymbol{y}'), \ \boldsymbol{y}' \in \mathcal{U}' \right\},$$
$$\Gamma \cap \mathcal{U} = \left\{ \boldsymbol{y} \in \mathcal{U} : y_3 = \varphi(\boldsymbol{y}'), \ \boldsymbol{y}' \in \mathcal{U}' \right\}.$$

Essentially, this definition means that locally $\mathcal{U}$ is below the graph of some function φ and Γ is represented by the graph of φ. We shall say that Ω is a Lipschitz domain when it has a Lipschitz continuous boundary. Note that every bounded polyhedral is a Lipschitz domain.

Define $\Omega_e := \mathbb{R}^3 \setminus \overline{\Omega}$ with the outer unit normal vector $\boldsymbol{n}$ on Γ pointing from Ω into Ω_e, which exists almost everywhere for Lipschitz domains.

In the following, we introduce proper spaces which are necessary for the investigation of the Maxwell's equations. In three dimensions these are the spaces $\mathbf{H}(\mathbf{curl}, \Omega)$, $\mathbf{H}(\mathrm{div}, \Omega)$ and the trace spaces on Γ of $\mathbf{H}(\mathbf{curl}, \Omega)$ (using the tangential trace γ_{D} and the twisted tangential trace $\gamma_{D}^{\times}$) $\mathbf{H}_{\perp}^{-1/2}(\mathrm{curl}_{\Gamma}, \Gamma)$ and $\mathbf{H}_{\|}^{-1/2}(\mathrm{div}_{\Gamma}, \Gamma)$, respectively. On smooth boundaries the theory is well established, see Paquet [68], Alonso & Valli [1], Girault & Raviart [29] and Nédélec [66, Section 5.4.1]. Their results have been extended to polyhedra by Buffa [9] and Buffa & Ciarlet [10, 11, 12]. For the case of Lipschitz domains, see Buffa *et al.* [13].

Let $u \in \mathcal{D}'(\Omega)$ be a scalar function and $\boldsymbol{u} := (u_1, u_2, u_3) \in \boldsymbol{\mathcal{D}}'(\Omega) := \left(\mathcal{D}'(\Omega) \right)^3$ be a three dimensional vector function.

On Ω we consider the spaces $\mathbf{L}^2(\Omega) := (L^2(\Omega))^3$ and the space of tangential vector fields

$$\mathbf{L}_t^2(\Gamma) := \left\{ \boldsymbol{u} \in \mathbf{L}^2(\Gamma) : \boldsymbol{u} \cdot \boldsymbol{n} = 0 \text{ a.e. on } \Gamma \right\} \tag{1.1}$$

with the complex dualities

$$(\boldsymbol{u}, \boldsymbol{v})_\Omega := \int_\Omega \boldsymbol{u}(\boldsymbol{x}) \cdot \overline{\boldsymbol{v}(\boldsymbol{x})} \, d\boldsymbol{x}, \qquad \boldsymbol{u}, \, \boldsymbol{v} \in \mathbf{L}^2(\Omega),$$
$$\langle \boldsymbol{\lambda}, \boldsymbol{\zeta} \rangle_\Gamma := \int_\Gamma \boldsymbol{\lambda}(\boldsymbol{x}) \cdot \overline{\boldsymbol{\zeta}(\boldsymbol{x})} \, d\boldsymbol{x}, \qquad \boldsymbol{\lambda}, \, \boldsymbol{\zeta} \in \mathbf{L}_t^2(\Gamma).$$

Besides the usual Sobolev spaces $H^s(\Omega)$ for scalar functions and $\mathbf{H}^s(\Omega) := (H^s(\Omega))^3$ for vector fields of order $s \in \mathbb{R}$ (cf. Grisvard [30]), we use the spaces

$$\mathbf{H}(\mathbf{curl}, \Omega) := \left\{ \boldsymbol{u} \in \mathbf{L}^2(\Omega) : \mathbf{curl}\, \boldsymbol{u} \in \mathbf{L}^2(\Omega) \right\},$$
$$\mathbf{H}_0(\mathbf{curl}, \Omega) := \left\{ \boldsymbol{u} \in \mathbf{H}(\mathbf{curl}, \Omega) : \boldsymbol{u} \times \boldsymbol{n} = 0 \text{ on } \Gamma \right\},$$

$$\mathbf{H}_0(\mathbf{curl}\,0, \Omega) := \{\boldsymbol{u} \in \mathbf{L}^2(\Omega) : \mathbf{curl}\,\boldsymbol{u} = 0, \ \boldsymbol{u} \times \boldsymbol{n} = 0 \text{ on } \Gamma\},$$
$$\mathbf{H}(\mathbf{curl}\,\mathbf{curl}, \Omega) := \{\boldsymbol{u} \in \mathbf{H}(\mathbf{curl}, \Omega) : \mathbf{curl}\,\mathbf{curl}\,\boldsymbol{u} \in \mathbf{L}^2(\Omega)\},$$
$$\mathbf{H}(\mathrm{div}, \Omega) := \{\boldsymbol{u} \in \mathbf{L}^2(\Omega) : \mathrm{div}\,\boldsymbol{u} \in L^2(\Omega)\},$$
$$\mathbf{H}_0(\mathrm{div}, \Omega) := \{\boldsymbol{u} \in \mathbf{H}(\mathrm{div}, \Omega) : \boldsymbol{u} \cdot \boldsymbol{n} = 0 \text{ on } \Gamma\},$$
$$\mathbf{H}_0(\mathrm{div}\,0, \Omega) := \{\boldsymbol{u} \in \mathbf{H}_0(\mathrm{div}, \Omega) : \mathrm{div}\,\boldsymbol{u} = 0\}.$$

Furthermore, we define for $s \geq 0$

$$\mathbf{H}^s(\mathbf{curl}, \Omega) := \{\boldsymbol{u} \in \mathbf{H}^s(\Omega) : \mathbf{curl}\,\boldsymbol{u} \in \mathbf{H}^s(\Omega)\}.$$

The associated graph norms in $\mathbf{H}(\mathbf{curl}, \Omega)$, $\mathbf{H}(\mathrm{div}, \Omega)$ and $\mathbf{H}^s(\mathbf{curl}, \Omega)$ are given by

$$\|\boldsymbol{u}\|^2_{\mathbf{H}(\mathbf{curl},\Omega)} := \|\boldsymbol{u}\|^2_{\mathbf{L}^2(\Omega)} + \|\,\mathbf{curl}\,\boldsymbol{u}\|^2_{\mathbf{L}^2(\Omega)},$$
$$\|\boldsymbol{u}\|^2_{\mathbf{H}(\mathrm{div},\Omega)} := \|\boldsymbol{u}\|^2_{\mathbf{L}^2(\Omega)} + \|\,\mathrm{div}\,\boldsymbol{u}\|^2_{\mathbf{L}^2(\Omega)},$$
$$\|\boldsymbol{u}\|^2_{\mathbf{H}^s(\mathbf{curl},\Omega)} := \|\boldsymbol{u}\|^2_{\mathbf{H}^s(\Omega)} + \|\,\mathbf{curl}\,\boldsymbol{u}\|^2_{\mathbf{H}^s(\Omega)},$$

respectively.

1.2 Trace operators and trace spaces

Let $\gamma : \mathbf{H}^1(\Omega) \to \mathbf{H}^{1/2}(\Gamma)$, $\gamma(\boldsymbol{u}) = \boldsymbol{u}|_\Gamma$ denote the standard trace operator acting on vectors. We assume Ω as a polyhedral domain and that the boundary Γ is split into N faces Γ_i with $\Gamma = \bigcup_{i=1}^N \Gamma_i$. Also, we define the space

$$\mathbf{H}_-^{1/2}(\Gamma) := \left\{\boldsymbol{\varphi} \in \mathbf{L}_t^2(\Gamma) : \boldsymbol{\varphi}|_{\Gamma_j} \in \mathbf{H}^{1/2}(\Gamma_j), \ 1 \leq j \leq N\right\},$$

the **Dirichlet trace (tangential surface trace)** as

$$\begin{aligned} \gamma_{\scriptscriptstyle D} : \left(\mathcal{C}_0^\infty(\overline{\Omega})\right)^3 &\to \mathbf{H}_-^{1/2}(\Gamma) \\ \boldsymbol{u} &\mapsto \boldsymbol{n}(\boldsymbol{x}) \times (\boldsymbol{u}(\boldsymbol{x}) \times \boldsymbol{n}(\boldsymbol{x}))|_\Gamma \end{aligned} \tag{1.2}$$

and the **twisted tangential trace** as

$$\begin{aligned} \gamma_{\scriptscriptstyle D}^\times : \left(\mathcal{C}_0^\infty(\overline{\Omega})\right)^3 &\to \mathbf{H}_-^{1/2}(\Gamma) \\ \boldsymbol{u} &\mapsto \boldsymbol{u}(\boldsymbol{x}) \times \boldsymbol{n}(\boldsymbol{x})|_\Gamma \ . \end{aligned} \tag{1.3}$$

Thus, for a vectorial function $\boldsymbol{u} \in \mathbf{H}^1(\Omega)$ we obtain for almost all $\boldsymbol{x} \in \Gamma$ that

$$\gamma_{\scriptscriptstyle D}\boldsymbol{u}(\boldsymbol{x}) := \boldsymbol{n}(\boldsymbol{x}) \times (\boldsymbol{u}(\boldsymbol{x}) \times \boldsymbol{n}(\boldsymbol{x})) = \boldsymbol{u}(\boldsymbol{x}) - \big(\boldsymbol{n}(\boldsymbol{x}) \cdot \boldsymbol{u}(\boldsymbol{x})\big)\boldsymbol{n}(\boldsymbol{x}),$$

Let $\phi \in H^2(\Omega)$ be a scalar function. We then define the **surface gradient** of ϕ on Γ by

$$\mathbf{grad}_\Gamma \phi := \gamma_{\scriptscriptstyle D}(\mathbf{grad}\,\phi) \tag{1.4}$$

and the **vectorial surface rotation** on Γ by

$$\mathbf{curl}_\Gamma\, \phi := \gamma_D^\times(\mathbf{grad}\,\phi) = \mathbf{grad}_\Gamma\, \phi \times \boldsymbol{n}.$$

The **scalar surface rotation** on Γ of a vectorial function $\boldsymbol{u} \in \mathbf{H}^2(\Omega)$ with $\boldsymbol{u}\cdot\boldsymbol{n} = 0$ on Γ is given by

$$\mathrm{curl}_\Gamma\, \boldsymbol{u} := \mathbf{curl}\,\boldsymbol{u} \cdot \boldsymbol{n}$$

and the **surface divergence** by

$$\mathrm{div}_\Gamma\, \boldsymbol{u} := \mathrm{div}(\gamma_D \boldsymbol{u}) = -\,\mathrm{curl}_\Gamma(\boldsymbol{u}\times\boldsymbol{n}) = -\,\mathbf{curl}(\boldsymbol{u}\times\boldsymbol{n})\cdot\boldsymbol{n}.$$

The above definitions are valid on all regular points of Γ but can be extended to Lipschitz domains, see e.g. Buffa & Ciarlet [10, 11].

On smooth domains the following dualities hold

$$\langle \mathbf{grad}_\Gamma\, \phi, \boldsymbol{u}\rangle_\Gamma = -\,\langle \phi, \mathrm{div}_\Gamma\, \boldsymbol{u}\rangle_\Gamma\,,$$
$$\langle \mathbf{curl}_\Gamma\, \phi, \boldsymbol{u}\rangle_\Gamma = \langle \phi, \mathrm{curl}_\Gamma\, \boldsymbol{u}\rangle_\Gamma\,.$$

Next, we define spaces of tangential traces on non-smooth domains due to Buffa & Ciarlet [10, 11].

For two faces Γ_i and Γ_j with a common edge e_{ij} we define $\boldsymbol{t}_{ij}$ as the unit tangential vector and $\boldsymbol{t}_{i(j)} := \boldsymbol{t}_{ij} \times \boldsymbol{n}_i$ where $\boldsymbol{n}_i$ denotes the unit normal vector on e_{ij} w.r.t. Γ_i. Furthermore, let $\mathcal{I}_j$ denote the set of those indices i such that Γ_i shares an edge with Γ_j. Then, we define

$$\mathbf{H}_*^{1/2}(\Gamma) := \left\{ \boldsymbol{u} \in \mathbf{L}_t^2(\Gamma) :\ \boldsymbol{u}_{|\Gamma_j} \cdot \boldsymbol{t}_{j(i)},\ \boldsymbol{u}_{|\Gamma_j} \cdot \boldsymbol{t}_{ij} \in H^{1/2}(\Gamma_j) \quad \forall\, i \in \mathcal{I}_j,\ \forall\, j = 1,\dots,n \right\}$$

and

$$\mathbf{H}_\parallel^{1/2}(\Gamma) := \left\{ \boldsymbol{u} \in \mathbf{H}_*^{1/2}(\Gamma) :\ \mathcal{N}_{i,j}^{\parallel}(\boldsymbol{u}) < \infty \quad \forall i \in \mathcal{I}_j,\ \forall j = 1,\dots,n \right\}, \qquad (1.5)$$
$$\mathbf{H}_\perp^{1/2}(\Gamma) := \left\{ \boldsymbol{u} \in \mathbf{H}_*^{1/2}(\Gamma) :\ \mathcal{N}_{i,j}^{\perp}(\boldsymbol{u}) < \infty \quad \forall i \in \mathcal{I}_j,\ \forall j = 1,\dots,n \right\}, \qquad (1.6)$$

with the functionals

$$\mathcal{N}_{i,j}^{\parallel}(\boldsymbol{u}) := \int_{\Gamma_i}\int_{\Gamma_j} \frac{|(\boldsymbol{u}\cdot\boldsymbol{t}_{ij})(\boldsymbol{x}) - (\boldsymbol{u}\cdot\boldsymbol{t}_{ij})(\boldsymbol{y})|^2}{|\boldsymbol{x}-\boldsymbol{y}|^3}\,ds(\boldsymbol{x})ds(\boldsymbol{y}),$$
$$\mathcal{N}_{i,j}^{\perp}(\boldsymbol{u}) := \int_{\Gamma_i}\int_{\Gamma_j} \frac{|(\boldsymbol{u}\cdot\boldsymbol{t}_{i(j)})(\boldsymbol{x}) - (\boldsymbol{u}\cdot\boldsymbol{t}_{j(i)})(\boldsymbol{y})|^2}{|\boldsymbol{x}-\boldsymbol{y}|^3}\,ds(\boldsymbol{x})ds(\boldsymbol{y}).$$

Loosely spoken, $\mathbf{H}_\parallel^{1/2}(\Gamma)$ contains the tangential surface vector fields that are in $\mathbf{H}^{1/2}(\Gamma_i)$ for each smooth surface piece Γ_i of Γ and fulfill a suitable "weak tangential continuity" across the edges of the Γ_i. For $\mathbf{H}_\perp^{1/2}(\Gamma)$ a corresponding "weak normal continuity" is fulfilled.

The spaces $\mathbf{H}_\perp^{-1/2}(\Gamma)$ and $\mathbf{H}_\parallel^{-1/2}(\Gamma)$ are then defined as the dual spaces of $\mathbf{H}_\perp^{1/2}(\Gamma)$ and $\mathbf{H}_\parallel^{1/2}$, resp., with $\mathbf{L}_t^2(\Gamma)$ as pivot space, see [10].

The above defined surface differential operators can now be extended to other Sobolev spaces.

Lemma 1.2.1 ([10, Proposition 3.2], [11, Theorem 4.6; Proposition 4.7])
Assuming that Γ is Lipschitz regular we can extend the surface differential operators $\mathbf{grad}_\Gamma$ and $\mathbf{curl}_\Gamma$ to linear and continuous mappings

$$\mathbf{grad}_\Gamma : H^{1/2}(\Gamma) \to \mathbf{H}_\perp^{-1/2}(\Gamma),$$
$$\mathbf{curl}_\Gamma : H^{1/2}(\Gamma) \to \mathbf{H}_\parallel^{-1/2}(\Gamma)$$

and their adjoints

$$\mathrm{div}_\Gamma : \mathbf{H}_\perp^{1/2}(\Gamma) \to H^{-1/2}(\Gamma),$$
$$\mathrm{curl}_\Gamma : \mathbf{H}_\parallel^{1/2}(\Gamma) \to H^{-1/2}(\Gamma)$$

are linear, continuous and surjective. There holds

$$\mathrm{Ker}\big(\mathrm{curl}_\Gamma(\mathbf{H}_\perp^{-1/2}(\Gamma))\big) = \mathrm{Im}\big(\mathbf{grad}_\Gamma(H^{1/2})\big),$$
$$\mathrm{Ker}\big(\mathrm{div}_\Gamma(\mathbf{H}_\parallel^{-1/2}(\Gamma))\big) = \mathrm{Im}\big(\mathbf{curl}_\Gamma(H^{1/2})\big).$$

Furthermore, we have the duality pairings

$$\langle \mathbf{grad}_\Gamma \phi, \boldsymbol{u} \rangle_\Gamma = - \langle \phi, \mathrm{div}_\Gamma \boldsymbol{u} \rangle_\Gamma \qquad \forall \phi \in H^{1/2}(\Gamma),\, \boldsymbol{u} \in \mathbf{H}_\perp^{1/2}(\Gamma),$$
$$\langle \mathbf{curl}_\Gamma \phi, \boldsymbol{u} \rangle_\Gamma = \langle \phi, \mathrm{curl}_\Gamma \boldsymbol{u} \rangle_\Gamma \qquad \forall \phi \in H^{1/2}(\Gamma),\, \boldsymbol{u} \in \mathbf{H}_\parallel^{1/2}(\Gamma).$$

We are now in the position to define the following trace spaces.

$$\mathbf{H}_\perp^{-1/2}(\mathrm{curl}_\Gamma, \Gamma) := \left\{ \boldsymbol{u} \in \mathbf{H}_\perp^{-1/2}(\Gamma) : \mathrm{curl}_\Gamma \boldsymbol{u} \in H^{-1/2}(\Gamma) \right\},$$
$$\mathbf{H}_\parallel^{-1/2}(\mathrm{div}_\Gamma, \Gamma) := \left\{ \boldsymbol{u} \in \mathbf{H}_\parallel^{-1/2}(\Gamma) : \mathrm{div}_\Gamma \boldsymbol{u} \in H^{-1/2}(\Gamma) \right\},$$
$$\mathbf{H}_\parallel^{-1/2}(\mathrm{div}_\Gamma\, 0, \Gamma) := \left\{ \boldsymbol{u} \in \mathbf{H}_\parallel^{-1/2}(\mathrm{div}_\Gamma, \Gamma) : \mathrm{div}_\Gamma \boldsymbol{u} = 0 \right\}.$$

A very important result for these spaces is given by

Lemma 1.2.2 ([11, Theorem 5.4]) *The spaces $\mathbf{H}_\parallel^{-1/2}(\mathrm{div}_\Gamma, \Gamma)$ and $\mathbf{H}_\perp^{-1/2}(\mathrm{curl}_\Gamma, \Gamma)$ are dual with respect to $\mathbf{L}_t^2(\Gamma)$ as pivot space.*

We can now summarize the following mapping properties of the trace operators.

Lemma 1.2.3 *The trace operators γ_D and $\gamma_D^\times$ can be extended to linear, continuous and surjective mappings*

$$\gamma_D : \mathbf{H}^1(\Omega) \to \mathbf{H}_\|^{1/2}(\Gamma),$$
$$\gamma_D : \mathbf{H}(\mathbf{curl}, \Omega) \to \mathbf{H}_\perp^{-1/2}(\mathrm{curl}_\Gamma, \Gamma),$$
$$\gamma_D^\times : \mathbf{H}^1(\Omega) \to \mathbf{H}_\perp^{1/2}(\Gamma),$$
$$\gamma_D^\times : \mathbf{H}(\mathbf{curl}, \Omega) \to \mathbf{H}_\|^{-1/2}(\mathrm{div}_\Gamma, \Gamma).$$

Furthermore, $\gamma_D : \mathbf{H}(\mathbf{curl}, \Omega) \to \mathbf{H}_\perp^{-1/2}(\mathrm{curl}_\Gamma, \Gamma)$ and $\gamma_D^\times : \mathbf{H}(\mathbf{curl}, \Omega) \to \mathbf{H}_\|^{-1/2}(\mathrm{div}_\Gamma, \Gamma)$ possess both a continuous right inverse.

Proof. The proof for smooth domains can be found in Nédélec [66] and for Lipschitz domains in the articles of Buffa & Ciarlet [10, Proposition 2.7, Theorem 3.9, 3.10] and [11, Theorem 5.4]. ∎

The following result may be found in [10, Section 3.2] and is helpful in the computations.

Lemma 1.2.4 *For $\boldsymbol{u} \in \mathbf{H}(\mathbf{curl}, \Omega)$ there holds*

$$\mathrm{div}_\Gamma(\boldsymbol{u} \times \boldsymbol{n}) = \boldsymbol{n} \cdot \mathbf{curl}\, \boldsymbol{u}. \tag{1.7}$$

There holds the following **Green formula**:

Lemma 1.2.5 ([10, Theorem 3.9]) *For $\boldsymbol{u} \in \mathbf{H}(\mathbf{curl}, \Omega)$ and $\boldsymbol{v} \in \mathbf{H}^1(\Omega)$ there holds*

$$\int_\Omega (\mathbf{curl}\, \boldsymbol{v} \cdot \boldsymbol{u} - \boldsymbol{v} \cdot \mathbf{curl}\, \boldsymbol{u})\, d\boldsymbol{x} = \left\langle \gamma_D^\times \boldsymbol{u},\, \gamma_D \boldsymbol{v} \right\rangle_{\|,1/2,\Gamma}.$$

Here, $\langle \cdot, \cdot \rangle_{\|,1/2,\Gamma}$ denotes the $\mathbf{H}_\|^{-1/2}(\Gamma)$-$\mathbf{H}_\|^{1/2}(\Gamma)$-duality with $\mathbf{L}_t^2(\Gamma)$ as pivot space.

For $\boldsymbol{u} \in \mathbf{H}(\mathbf{curl\, curl}, \Omega)$ the **Neumann trace** $\gamma_N \boldsymbol{u} \in \mathbf{H}_\|^{-1/2}(\mathrm{div}_\Gamma, \Gamma)$ is defined by (see Hiptmair [37])

$$\langle \gamma_N \boldsymbol{u}, \gamma_D \boldsymbol{v} \rangle_\Gamma = \pm(\mathbf{curl}\, \boldsymbol{u}, \mathbf{curl}\, \boldsymbol{v})_\Omega \mp (\mathbf{curl\, curl}\, \boldsymbol{u}, \boldsymbol{v})_\Omega \quad \forall\, \boldsymbol{v} \in \mathbf{H}(\mathbf{curl}, \Omega). \tag{1.8}$$

Here, the upper signs are applied to the interior domain Ω and the lower signs are used for the exterior domain Ω_e. As for smooth fields there also holds $\gamma_N \boldsymbol{u} = \gamma_D^\times(\mathbf{curl}\, \boldsymbol{u})$.

Lemma 1.2.6 ([37, Lemma 3.3]) *The trace operator*

$$\gamma_N : \mathbf{H}(\mathbf{curl\, curl}, \Omega) \to \mathbf{H}_\|^{-1/2}(\mathrm{div}_\Gamma, \Gamma)$$

is linear and continuous and there holds for $\boldsymbol{u} \in \mathbf{H}(\mathbf{curl}, \Omega)$ with $\mathbf{curl\, curl}\, \boldsymbol{u} = 0$

$$\|\gamma_N \boldsymbol{u}\|_{\mathbf{H}_\|^{-1/2}(\mathrm{div}_\Gamma, \Gamma)} \leq C \|\mathbf{curl}\, \boldsymbol{u}\|_{\mathbf{L}^2(\Omega)}.$$

Furthermore, we define for $\boldsymbol{u} \in \mathbf{H}(\mathrm{div}, \Omega)$ the **weak normal trace** $\gamma_n \boldsymbol{u}$ by

$$\langle \gamma_n \boldsymbol{u}, \phi \rangle_{1/2,\Gamma} = (\mathrm{div}\, \boldsymbol{u}, \phi)_\Omega + (\boldsymbol{u}, \mathbf{grad}\, \phi)_\Omega \qquad \forall\, \phi \in H^1(\Omega). \tag{1.9}$$

Here, $\langle \cdot, \cdot \rangle_{1/2,\Gamma}$ denotes the duality pairing between $H^{-1/2}(\Gamma)$ and $H^{1/2}(\Gamma)$.

Lemma 1.2.7 $\gamma_n : \mathbf{H}(\mathrm{div}, \Omega) \to H^{-1/2}(\Gamma)$ *is continuous and surjective.*

Proof. The continuity can be found in Girault & Raviart [29, Theorem 2.5] and the surjectivity is proven in Nédélec [66, Theorem 5.4.1]. ∎

Remark 1.2.1 *For* $\boldsymbol{u} \in \mathcal{C}^1(\overline{\Omega})$ *there holds* $\gamma_n \boldsymbol{u} = \boldsymbol{u} \cdot \boldsymbol{n}$.

1.3 Boundary integral operators

Here, we define the boundary integral operators which are used for the coupling formulations. The fundamental solution of the Laplace equation is given by

$$\Phi(\boldsymbol{x}, \boldsymbol{y}) := \frac{1}{4\pi} |\boldsymbol{x} - \boldsymbol{y}|^{-1}, \qquad \boldsymbol{x} \neq \boldsymbol{y}.$$

There holds $\Delta\Phi(\boldsymbol{x}, \boldsymbol{y}) = 0$ and $\mathbf{grad}_{\boldsymbol{x}} \Phi(\boldsymbol{x}, \boldsymbol{y}) = -\mathbf{grad}_{\boldsymbol{y}} \Phi(\boldsymbol{x}, \boldsymbol{y})$. We then define the **scalar single layer potential** for $u \in L^2(\Gamma)$ by

$$S(u)(\boldsymbol{x}) := \int_\Gamma \Phi(\boldsymbol{x}, \boldsymbol{y}) u(\boldsymbol{x})\, ds(\boldsymbol{y}), \quad \boldsymbol{x} \notin \Gamma.$$

It can be extended to a continuous mapping $S : H^{-1/2}(\Gamma) \to H^1_{\mathrm{loc}}(\mathbb{R}^3)$ and satisfies the jump relations

$$[\gamma S(u)]_\Gamma = 0, \quad [\gamma\, \mathbf{grad}\, S(u)]_\Gamma = -u\boldsymbol{n}$$

with the normal $\boldsymbol{n}$ on Γ pointing into the exterior domain, where $[\gamma u]_\Gamma := \gamma^+ u - \gamma^- u$ denotes the jump of the trace γ of a function u over the boundary Γ and γ^+ and γ^- denote the exterior and interior traces. The second relation can be written as

$$[\gamma_n\, \mathbf{grad}\, S(u)]_\Gamma = -u, \quad [\mathbf{grad}_\Gamma S(u)]_\Gamma = 0. \tag{1.10}$$

This leads to the definition of the boundary integral operator

$$V(u)(\boldsymbol{x}) := \gamma S(u)(\boldsymbol{x}), \quad \boldsymbol{x} \in \Gamma, \tag{1.11}$$

which is continuous from $H^{-1/2}(\Gamma)$ to $H^{1/2}(\Gamma)$ and defines a positive definite bilinear form on $H^{-1/2}(\Gamma)$ (cf. Costabel [22]), and

$$\mathcal{S}u(\boldsymbol{x}) := \mathbf{grad}_\Gamma Vu(\boldsymbol{x}), \quad \boldsymbol{x} \in \Gamma, \tag{1.12}$$

which is continuous from $H^{-1/2}(\Gamma)$ to $\mathbf{H}_\perp^{-1/2}(\mathrm{curl}_\Gamma,\Gamma)$ due to the properties of $\mathbf{grad}_\Gamma$ and V. Analogously, we define the **vectorial single layer potential** for $\boldsymbol{\lambda}\in\mathbf{L}^2(\Gamma)$ by

$$\mathbf{V}(\boldsymbol{\lambda})(\boldsymbol{x}) := \int_\Gamma \Phi(\boldsymbol{x},\boldsymbol{y})\boldsymbol{\lambda}(\boldsymbol{y})\,ds(\boldsymbol{y}), \quad \boldsymbol{x}\notin\Gamma,$$

which can be extended to a continuous mapping from $\mathbf{H}_\|^{-1/2}(\Gamma)$ to $\mathbf{H}_{\mathrm{loc}}^1(\mathbb{R}^3)$ (see Buffa *et al.* [15, Theorem 3.8] or Hiptmair [37, Section 5]). We will make use of the following result by MacCamy & Stephan [45].

Lemma 1.3.1 *For* $\boldsymbol{\lambda}\in\mathbf{H}_\|^{-1/2}(\mathrm{div}_\Gamma,\Gamma)$ *there holds*

$$\mathrm{div}\,\mathbf{V}(\boldsymbol{\lambda}) = V(\mathrm{div}_\Gamma\,\boldsymbol{\lambda})\ \text{in}\ \mathbf{L}^2(\mathbb{R}^3).$$

We define the **vectorial double layer potential** for $\boldsymbol{\lambda}\in\mathbf{H}_\perp^{-1/2}(\Gamma)$ by

$$\mathbf{K}(\boldsymbol{\lambda}) := \mathbf{curl}\,\mathbf{V}(\boldsymbol{n}\times\boldsymbol{\lambda})$$

and further

$$\mathbf{W}(\boldsymbol{\lambda}) := \mathbf{curl}\,\mathbf{K}(\boldsymbol{\lambda}) = \mathbf{grad}\,V(\mathrm{div}_\Gamma(\boldsymbol{n}\times\boldsymbol{\lambda})). \tag{1.13}$$

The last equation follows from the identity $\mathbf{curl}\,\mathbf{curl}\equiv\mathbf{grad}\,\mathrm{div}-\boldsymbol{\Delta}$, the fact that $\Delta\Phi=0$ and Lemma 1.3.1. Using the continuity of $\boldsymbol{v}$ and the fact that the mapping $\boldsymbol{\lambda}\mapsto\boldsymbol{n}\times\boldsymbol{\lambda}$ is an isometry between $\mathbf{H}_\perp^{-1/2}(\mathrm{curl}_\Gamma,\Gamma)$ and $\mathbf{H}_\|^{-1/2}(\mathrm{div}_\Gamma,\Gamma)$ (this is a consequence of Lemma 1.2.3), one sees that $\mathbf{K}$ is a continuous mapping from $\mathbf{H}_\perp^{-1/2}(\mathrm{curl}_\Gamma,\Gamma)$ to $\mathbf{H}_{\mathrm{loc}}(\mathbf{curl\,curl},\mathbb{R}^3\setminus\Gamma)\cap\mathbf{H}(\mathrm{div}\,0,\mathbb{R}^3\setminus\Gamma)$ (see [15, Section 3.3] and [37, Section 5]).

The vectorial single and double layer potentials satisfy the following jump relations, (see [15, 37]): For $\boldsymbol{\lambda}\in\mathbf{H}_\|^{-1/2}(\mathrm{div}_\Gamma,\Gamma)$ there holds

$$[\gamma_D\mathbf{V}(\boldsymbol{\lambda})]_\Gamma = 0, \qquad [\gamma_N\mathbf{V}(\boldsymbol{\lambda})]_\Gamma = -\boldsymbol{\lambda}, \tag{1.14}$$

and for $\boldsymbol{\lambda}\in\mathbf{H}_\perp^{-1/2}(\mathrm{curl}_\Gamma,\Gamma)$ there holds

$$[\gamma_D\mathbf{K}(\boldsymbol{\lambda})]_\Gamma = \boldsymbol{\lambda}, \qquad [\gamma_N\mathbf{K}(\boldsymbol{\lambda})]_\Gamma = 0. \tag{1.15}$$

We now define the following vectorial boundary integral operators as exterior traces of the layer potentials for $\boldsymbol{x}\in\Gamma$

$$\mathcal{V}(\boldsymbol{\lambda}) := \gamma_D^+\mathbf{V}(\boldsymbol{\lambda}) = \gamma_D^+\int_\Gamma \Phi(\boldsymbol{x},\boldsymbol{y})\boldsymbol{\lambda}(\boldsymbol{y})\,ds(\boldsymbol{y}), \tag{1.16}$$

$$\mathcal{K}(\boldsymbol{\lambda}) := \gamma_D^+\mathbf{K}(\boldsymbol{\lambda}) = \gamma_D^+\,\mathbf{curl}_x\int_\Gamma \Phi(\boldsymbol{x},\boldsymbol{y})(\boldsymbol{n}\times\boldsymbol{\lambda})(\boldsymbol{y})\,ds(\boldsymbol{y}), \tag{1.17}$$

$$\tilde{\mathcal{K}}(\boldsymbol{\lambda}) := \gamma_N^+\mathbf{V}(\boldsymbol{\lambda}) = (\gamma_D^\times)^+\mathbf{K}(\boldsymbol{\lambda}\times\boldsymbol{n}) = \gamma_N^+\int_\Gamma \Phi(\boldsymbol{x},\boldsymbol{y})\boldsymbol{\lambda}(\boldsymbol{y})\,ds(\boldsymbol{y}), \tag{1.18}$$

$$\mathcal{W}(\boldsymbol{\lambda}) := \gamma_N^+ \mathbf{K}(\boldsymbol{\lambda}) = (\gamma_D^\times)^+ \mathbf{W}(\boldsymbol{\lambda}) = \gamma_N^+ \operatorname{\mathbf{curl}}_{\boldsymbol{x}} \int_\Gamma \Phi(\boldsymbol{x}, \boldsymbol{y})(\boldsymbol{n} \times \boldsymbol{\lambda})(\boldsymbol{y}) \, ds(\boldsymbol{y}). \qquad (1.19)$$

From the regularity properties of the potentials and the trace operators we get the following lemma (see Hiptmair [37]).

Lemma 1.3.2 *The operators*

$$\mathcal{V} : \mathbf{H}_\parallel^{-1/2}(\Gamma) \to \mathbf{H}_\parallel^{1/2}(\Gamma),$$
$$\mathcal{K} : \mathbf{H}_\perp^{-1/2}(\operatorname{curl}_\Gamma, \Gamma) \to \mathbf{H}_\perp^{-1/2}(\operatorname{curl}_\Gamma, \Gamma),$$
$$\widetilde{\mathcal{K}} : \mathbf{H}_\parallel^{-1/2}(\operatorname{div}_\Gamma, \Gamma) \to \mathbf{H}_\parallel^{-1/2}(\operatorname{div}_\Gamma, \Gamma),$$
$$\mathcal{W} : \mathbf{H}_\perp^{-1/2}(\operatorname{curl}_\Gamma, \Gamma) \to \mathbf{H}_\parallel^{-1/2}(\operatorname{div}_\Gamma, \Gamma)$$

are continuous.

Furthermore there holds

Lemma 1.3.3 ([37, Section 6]) *The boundary integral operators satisfy the following properties:*

1. *The bilinear form induced on* $\mathbf{H}_\parallel^{-1/2}(\operatorname{div}_\Gamma 0, \Gamma)$ *by* $\mathcal{V}$ *is symmetric and elliptic, i.e., there exists a constant* $c > 0$, *such that*

$$\langle \mathcal{V}\boldsymbol{u}, \boldsymbol{u} \rangle_\Gamma \geq c \|\boldsymbol{u}\|_{\mathbf{H}_\parallel^{-1/2}(\operatorname{div}_\Gamma, \Gamma)}^2 \quad \forall \boldsymbol{u} \in \mathbf{H}_\parallel^{-1/2}(\operatorname{div}_\Gamma 0, \Gamma).$$

2. *The boundary integral operator* $\widetilde{\mathcal{K}}$ *is adjoint to* $\mathcal{K} - \mathcal{I}$, *i.e.,*

$$\langle \widetilde{\mathcal{K}}\boldsymbol{u}, \boldsymbol{v} \rangle_\Gamma = \langle \boldsymbol{u}, (\mathcal{K} - \mathcal{I})\boldsymbol{v} \rangle_\Gamma \quad \forall \boldsymbol{u} \in \mathbf{H}_\parallel^{-1/2}(\operatorname{div}_\Gamma 0, \Gamma), \boldsymbol{v} \in \mathbf{H}_\perp^{-1/2}(\operatorname{curl}_\Gamma, \Gamma).$$

3. *There holds with the pairing* $\langle \cdot, \cdot \rangle_{-1/2, \Gamma}$ *between* $\mathbf{H}_\parallel^{-1/2}(\operatorname{div}_\Gamma, \Gamma)$ *and* $\mathbf{H}_\perp^{-1/2}(\operatorname{curl}_\Gamma, \Gamma)$

$$\langle \mathcal{W}\boldsymbol{u}, \boldsymbol{v} \rangle_\Gamma = -\langle V(\operatorname{curl}_\Gamma \boldsymbol{u}), \operatorname{curl}_\Gamma \boldsymbol{v} \rangle_{-1/2, \Gamma} \quad \forall \boldsymbol{u}, \boldsymbol{v} \in \mathbf{H}_\perp^{-1/2}(\operatorname{curl}_\Gamma, \Gamma).$$

4. *The bilinear form induced on* $\mathbf{H}_\perp^{-1/2}(\operatorname{curl}_\Gamma, \Gamma)$ *by* $\mathcal{W}$ *is symmetric and negative semidefinite, in particular there exists a constant* $C > 0$ *such that*

$$-\langle \mathcal{W}\boldsymbol{u}, \boldsymbol{u} \rangle_\Gamma \geq C \|\operatorname{curl}_\Gamma \boldsymbol{u}\|_{H^{-1/2}(\Gamma)}^2 \quad \forall \boldsymbol{u} \in \mathbf{H}_\perp^{-1/2}(\operatorname{curl}_\Gamma, \Gamma).$$

We now define integral operators for $\boldsymbol{\lambda} \in \mathbf{L}_t^2(\Gamma)$ and $\boldsymbol{x} \in \Gamma$ by

$$\boldsymbol{\mathcal{L}}\boldsymbol{\lambda}(\boldsymbol{x}) := \int_\Gamma \Phi(\boldsymbol{x}, \boldsymbol{y})\boldsymbol{\lambda}(\boldsymbol{y}) \, ds(\boldsymbol{y}),$$

$$\mathcal{M}\boldsymbol{\lambda}(\boldsymbol{x}) := \int_\Gamma \mathbf{curl}_x(\Phi(\boldsymbol{x},\boldsymbol{y})\boldsymbol{\lambda}(\boldsymbol{y}))\,ds(\boldsymbol{y}) = \int_\Gamma \mathbf{grad}_x\,\Phi(\boldsymbol{x},\boldsymbol{y}) \times \boldsymbol{\lambda}(\boldsymbol{y})\,ds(\boldsymbol{y}).$$

The above integral can be defined as Cauchy-principal value. Using the jump conditions one can prove the following representation of the boundary integral operators, see e.g. Mitrea *et al.* [57, Section 3] and Colton & Kress [20, Section 6.3].

$$
\begin{aligned}
\mathcal{V}\boldsymbol{\lambda} &= -\boldsymbol{n} \times (\boldsymbol{n} \times \boldsymbol{\mathcal{L}}\boldsymbol{\lambda}), \\
\mathcal{K}\boldsymbol{\lambda} &= \mathcal{M}(\boldsymbol{n} \times \boldsymbol{\lambda}) + \frac{1}{2}\boldsymbol{\lambda}, \\
\tilde{\mathcal{K}}\boldsymbol{\lambda} &= -\boldsymbol{n} \times \mathcal{M}\boldsymbol{\lambda} - \frac{1}{2}\boldsymbol{\lambda}, \\
\mathcal{W}\boldsymbol{\lambda} &= -\boldsymbol{n} \times \mathbf{grad}\,V(\mathrm{div}_\Gamma(\boldsymbol{n} \times \boldsymbol{\lambda})) = -\,\mathbf{curl}_\Gamma\,V(\mathrm{curl}_\Gamma\boldsymbol{\lambda}).
\end{aligned}
\tag{1.20}
$$

The last equation holds due to $\boldsymbol{n} \times \mathbf{grad}\,\phi = -\,\mathbf{curl}_\Gamma\,\phi$ and $\mathrm{div}_\Gamma(\boldsymbol{n} \times \boldsymbol{\lambda}) = -\,\mathbf{curl}_\Gamma\,\boldsymbol{\lambda}$.

Using these relations we can prove the useful equation

Lemma 1.3.4 *For* $\boldsymbol{u},\,\boldsymbol{v} \in \mathbf{H}_\perp^{-1/2}(\mathrm{curl}_\Gamma,\Gamma)$ *there holds*

$$\langle \mathcal{W}\boldsymbol{u},\boldsymbol{v}\rangle = -\langle V\,\mathrm{curl}_\Gamma\,\boldsymbol{u},\mathrm{curl}_\Gamma\,\boldsymbol{v}\rangle. \tag{1.21}$$

The following Lemma is necessary for the proof of the residual error estimator in Chapter 3.

Lemma 1.3.5 ([73, Lemma 4.3.2]) *For* $\boldsymbol{u} \in \mathbf{H}(\mathbf{curl},\Omega_e)$, $\boldsymbol{\lambda} \in \mathbf{H}_\parallel^{-1/2}(\mathrm{div}_\Gamma\,0,\Gamma)$ *there holds*

1. $\mathrm{div}_\Gamma\tilde{\mathcal{K}}\boldsymbol{\lambda} = 0$ *in* $H^{-1/2}(\Gamma)$,

2. $\mathrm{div}_\Gamma\mathcal{W}\gamma_D\boldsymbol{u} = 0$ *in* $H^{-1/2}(\Gamma)$.

1.4 The Stratton-Chu representation formula

In this Section we introduce an integral representation formula for the solutions of the Maxwell's equations. This is the main ingredient to derive the coupling formulations in the next chapters. The formula is based on the results of Stratton & Chu [72]. We cite here Colton & Kress [20] for smooth boundaries but the results also hold for Lipschitz boundaries, see e.g. Buffa *et al.* [12, Theorem 3].

We consider the Maxwell's equations

$$\mathbf{curl}\,\mathbf{E} - i\kappa\mathbf{H} = 0, \tag{1.22}$$

$$\mathbf{curl}\,\mathbf{H} + i\kappa\mathbf{E} = 0, \tag{1.23}$$

where $\mathbf{E}$ and $\mathbf{H}$ denote the electric and the magnetic field, resp. Thus, there holds for $\mathbf{E}$

$$\mathbf{curl}\,\mathbf{curl}\,\mathbf{E} = \kappa^2\mathbf{E}.$$

Here $\Phi(\boldsymbol{x}, \boldsymbol{y}) := \frac{1}{4\pi}\frac{e^{i\kappa|\boldsymbol{x}-\boldsymbol{y}|}}{|\boldsymbol{x}-\boldsymbol{y}|}$, $\boldsymbol{x}, \boldsymbol{y} \in \mathbb{R}^3$, $\boldsymbol{x} \neq \boldsymbol{y}$ define the fundamental solution of the Helmholtz equation. We obtain the following representation Theorem, see Colton & Kress [20, Section 6.2].

Theorem 1.4.1 (Stratton-Chu formula) *Let Ω be a bounded domain with smooth boundary and let $\boldsymbol{n}$ denote the unit normal vector to the boundary $\Gamma = \partial\Omega$ directed into the exterior of Ω. Let $\mathbf{E}, \mathbf{H} \in \mathcal{C}^1(\Omega) \cap \mathcal{C}(\overline{\Omega})$ be a solution to the Maxwell's equations (1.22) and (1.23) in Ω. Thus, there hold the Stratton-Chu formulas*

$$\begin{aligned}
\mathbf{E}(\boldsymbol{x}) = {}& -\,\mathbf{curl}\int_\Gamma \big(\boldsymbol{n}(\boldsymbol{y}) \times \mathbf{E}(\boldsymbol{y})\big)\Phi(\boldsymbol{x}, \boldsymbol{y})\,ds(\boldsymbol{y}) \\
& + \frac{1}{i\kappa}\,\mathbf{curl}\,\mathbf{curl}\int_\Gamma \big(\boldsymbol{n}(\boldsymbol{y}) \times \mathbf{H}(\boldsymbol{y})\big)\Phi(\boldsymbol{x}, \boldsymbol{y})\,ds(\boldsymbol{y}), \qquad \boldsymbol{x} \in \Omega,
\end{aligned}$$

and

$$\begin{aligned}
\mathbf{H}(\boldsymbol{x}) = {}& -\,\mathbf{curl}\int_\Gamma \big(\boldsymbol{n}(\boldsymbol{y}) \times \mathbf{H}(\boldsymbol{y})\big)\Phi(\boldsymbol{x}, \boldsymbol{y})\,ds(\boldsymbol{y}) \\
& - \frac{1}{i\kappa}\,\mathbf{curl}\,\mathbf{curl}\int_\Gamma \big(\boldsymbol{n}(\boldsymbol{y}) \times \mathbf{E}(\boldsymbol{y})\big)\Phi(\boldsymbol{x}, \boldsymbol{y})\,ds(\boldsymbol{y}), \qquad \boldsymbol{x} \in \Omega.
\end{aligned}$$

For the unbounded domain there holds

Theorem 1.4.2 (Stratton-Chu formula) *Let $\Omega_e := \mathbb{R}^3 \setminus \overline{\Omega}$, where Ω is a smooth domain and let $\boldsymbol{n}$ denote the unit normal vector to the boundary $\partial\Omega$ directed into the exterior of Ω_e. Let $\mathbf{E}, \mathbf{H} \in \mathcal{C}^1(\Omega_e) \cap \mathcal{C}(\Omega_e)$ be a solution to the Maxwell's equations (1.22) and (1.23) in Ω_e. Furthermore, we assume that $\mathbf{E}$ and $\mathbf{H}$ satisfy the Silver-Müller radiation conditions*

$$\lim_{|\boldsymbol{x}|\to\infty}(\mathbf{H} \times \boldsymbol{x} - |\boldsymbol{x}|\mathbf{E}) = 0 \tag{1.24}$$

or

$$\lim_{|\boldsymbol{x}|\to\infty}(\mathbf{E} \times \boldsymbol{x} + |\boldsymbol{x}|\mathbf{H}) = 0 \tag{1.25}$$

uniformly in all directions $\frac{\boldsymbol{x}}{|\boldsymbol{x}|}$. Then, there holds

$$\begin{aligned}
\mathbf{E}(\boldsymbol{x}) = {}& \mathbf{curl}\int_\Gamma \big(\boldsymbol{n}(\boldsymbol{y}) \times \mathbf{E}(\boldsymbol{y})\big)\Phi(\boldsymbol{x}, \boldsymbol{y})\,ds(\boldsymbol{y}) \\
& - \frac{1}{i\kappa}\,\mathbf{curl}\,\mathbf{curl}\int_\Gamma \big(\boldsymbol{n}(\boldsymbol{y}) \times \mathbf{H}(\boldsymbol{y})\big)\Phi(\boldsymbol{x}, \boldsymbol{y})\,ds(\boldsymbol{y}), \qquad \boldsymbol{x} \in \Omega_e,
\end{aligned} \tag{1.26}$$

and

$$\mathbf{H}(\boldsymbol{x}) = \mathbf{curl} \int_{\Gamma} \big(\boldsymbol{n}(\boldsymbol{y}) \times \mathbf{H}(\boldsymbol{y})\big) \Phi(\boldsymbol{x}, \boldsymbol{y}) \, ds(\boldsymbol{y})$$
$$+ \frac{1}{i\kappa} \mathbf{curl\,curl} \int_{\Gamma} \big(\boldsymbol{n}(\boldsymbol{y}) \times \mathbf{E}(\boldsymbol{y})\big) \Phi(\boldsymbol{x}, \boldsymbol{y}) \, ds(\boldsymbol{y}), \qquad \boldsymbol{x} \in \Omega_e. \tag{1.27}$$

Furthermore, there holds, see [20, (6.10)],

$$\frac{1}{i\kappa} \mathbf{curl\,curl} \int_{\Gamma} \big(\boldsymbol{n}(\boldsymbol{y}) \times \mathbf{H}(\boldsymbol{y})\big) \Phi(\boldsymbol{x}, \boldsymbol{y}) \, ds(\boldsymbol{y})$$
$$= -i\kappa \int_{\Gamma} \big(\boldsymbol{n}(\boldsymbol{y}) \times \mathbf{H}(\boldsymbol{y})\big) \Phi(\boldsymbol{x}, \boldsymbol{y}) \, ds(\boldsymbol{y}) + \mathbf{grad} \int_{\Gamma} \big(\boldsymbol{n}(\boldsymbol{y}) \cdot \mathbf{E}(\boldsymbol{y})\big) \Phi(\boldsymbol{x}, \boldsymbol{y}) \, ds(\boldsymbol{y}). \tag{1.28}$$

Thus, using $\mathbf{H} = \frac{1}{i\kappa} \mathbf{curl\,E}$, the relation (1.26) can be rewritten as

$$\mathbf{E}(\boldsymbol{x}) = \mathbf{curl} \int_{\Gamma} \big(\boldsymbol{n}(\boldsymbol{y}) \times \mathbf{E}(\boldsymbol{y})\big) \Phi(\boldsymbol{x}, \boldsymbol{y}) \, ds(\boldsymbol{y})$$
$$+ \int_{\Gamma} \big(\boldsymbol{n}(\boldsymbol{y}) \times \mathbf{curl\,E}(\boldsymbol{y})\big) \Phi(\boldsymbol{x}, \boldsymbol{y}) \, ds(\boldsymbol{y}) \tag{1.29}$$
$$- \mathbf{grad} \int_{\Gamma} \big(\boldsymbol{n}(\boldsymbol{y}) \cdot \mathbf{E}(\boldsymbol{y})\big) \Phi(\boldsymbol{x}, \boldsymbol{y}) \, ds(\boldsymbol{y}), \quad \boldsymbol{x} \in \Omega_e.$$

In Chapter 3 we use this formula for the derivation of the coupling formulations.

1.5 The Lebesgue Space $L^p(0,T;X)$

This section introduces some basic ideas and spaces needed to study time dependent problems. A complete analysis can be found in Zeidler [78, Chapter 23].

Definition 1.5.1 *Let X be a Banach space and $0 < T < \infty$.*

1. $C^m([0,T], X)$, $m \in \mathbb{N}$, denotes the space of all continuous functions $\boldsymbol{u} : [0,T] \to X$ which have continuous derivates up to order m on $[0,T]$ with the norm

$$\|\boldsymbol{u}\|_{C^m([0,T],X)} := \sum_{i=0}^{m} \max_{0 \leq t \leq T} |\boldsymbol{u}^{(i)}(t)| \tag{1.30}$$

where $\boldsymbol{u}^{(0)}$ means $\boldsymbol{u}$. We write $C([0,T], X)$ instead of $C^0([0,T], X)$.

2. The space $L^p(0,T;X)$ with $1 \leq p < \infty$ consists of all measurable functions $\boldsymbol{u} : (0,T) \to X$ for which

$$\|\boldsymbol{u}\|_{L^p(0,T;X)} := \left(\int_0^T \|\boldsymbol{u}\|_X^p \, dt \right)^{1/p} < \infty \tag{1.31}$$

holds.

Lemma 1.5.1 ([78, Proposition 23.2])

1. $\mathcal{C}^m([0,T],\mathcal{X})$ *with the norm (1.30) is a Banach space.*

2. $L^p(0,T;\mathcal{X})$ *with the norm (1.31) is a Banach space in the case where one identifies functions that are equal almost everywhere on* $]0,T[$.

3. $\mathcal{C}([0,T],\mathcal{X})$ *is dense in* $L^p(0,T;\mathcal{X})$ *and the embedding* $\mathcal{C}([0,T],\mathcal{X}) \subseteq L^p(0,T;\mathcal{X})$ *is continuous.*

4. *The set of all polynomials* $\boldsymbol{w} : [0,T] \to \mathcal{X}$, *i.e.,* $\boldsymbol{w}(t) = a_0 + a_1\,t + \cdots + a_n\,t^n$ *with* $a_i \in \mathcal{X}$ *for all* i *and* $n = 0,1,\ldots$ *is dense in* $\mathcal{C}([0,T],\mathcal{X})$ *and* $L^p(0,T;\mathcal{X})$.

Definition 1.5.2 (Evolution Triples) *We understand an evolution triple*

$$\mathcal{V} \subseteq \mathcal{H} \subset \mathcal{V}^*$$

to be the following:

1. $\mathcal{V}$ *is a real, separable, and reflexive Banach space.*

2. $\mathcal{H}$ *is a real, separable Hilbert space.*

3. *The embedding* $\mathcal{V} \subseteq \mathcal{H}$ *is continuous, i.e.,* $\|v\|_{\mathcal{H}} \leq C\|v\|_{\mathcal{V}}$ *for all* $v \in \mathcal{V}$, *for some* $C > 0$, *and* $\mathcal{V}$ *is dense in* $\mathcal{H}$.

With evolution triples we describe the fact that two spaces $\mathcal{V}$ *and* $\mathcal{H}$ *appear in evolution equations.*

Lemma 1.5.2 ([78, Proposition 23.23]) *Let* $\mathcal{V} \subseteq \mathcal{H} \subset \mathcal{V}^*$ *be an evolution triple, and* $1 < p < \infty$, $p^{-1} + q^{-1} = 1$, $0 < T < \infty$. *Then the following hold:*

1. *For* $\mathcal{X} = L^p(0,T;\mathcal{V})$ *and* $\mathcal{X}^* = L^q(0,T;\mathcal{V}^*)$

$$W_p^1(0,T;\mathcal{V},\mathcal{H}) := \{\boldsymbol{u} \in \mathcal{X} \,:\, \boldsymbol{u}' \in \mathcal{X}^*\}$$

   forms a real Banach space with the norm

$$\|\boldsymbol{u}\|_{W_p^1} = \|\boldsymbol{u}\|_{L^p(0,T;\mathcal{V})} + \|\boldsymbol{u}'\|_{L^q(0,T;\mathcal{V}^*)}.$$

2. *The embedding* $W_p^1(0,T;\mathcal{V},\mathcal{H}) \subseteq \mathcal{C}([0,T],\mathcal{H})$ *is continuous.*

3. *The set of all polynomials* $\boldsymbol{w} : [0,T] \to \mathcal{V}$, *that is* $\boldsymbol{w}(t) = \sum_i a_i t^i$ *with* $a_i \in \mathcal{V}$ *for all* i, *is dense in the space* $W_p^1(0,T;\mathcal{V},\mathcal{H})$, $L^p(0,T;\mathcal{V})$ *and* $L^p(0,T;\mathcal{H})$.

2 Interpolation

Let $\mathcal{T}_h$ be a triangulation (with tetrahedral or hexahedral elements) of the domain $\Omega \subset \mathbb{R}^3$. We assume that $\mathcal{T}_h$ is quasi-uniform with mesh size $h > 0$ and shape-regular, i.e., there exists a positive constant c_1 such that

$$\frac{h_{\mathfrak{T}}}{\rho_{\mathfrak{T}}} \leq c_1 \qquad \forall \mathfrak{T} \in \mathcal{T}_h$$

where $h_{\mathfrak{T}}$ is the diameter of an element $\mathfrak{T} \in \mathcal{T}_h$ and

$$\rho_{\mathfrak{T}} := \max \left\{ r : S_r \subseteq \mathfrak{T}, S_r := \{\boldsymbol{x} : \|\boldsymbol{x} - \boldsymbol{x}_0\| < r, \boldsymbol{x}_0 \in \mathfrak{T}\} \right\} .$$

This mesh induces a quasi-uniform mesh $\mathcal{K}_h := \{\mathfrak{T} \cap \Gamma : \mathfrak{T} \in \mathcal{T}_h\}$ of triangles or quadrilaterals on the boundary; we denote by h_F the maximal diameter of a face $F \in \mathcal{K}_h$.

We define by $\mathcal{N}_h(D), \mathcal{E}_h(D), \mathcal{F}_h(D)$ the sets of vertices, edges and faces in $D \subseteq \overline{\Omega}$. If $D = \overline{\Omega}$, for the sake of brevity we will write $\mathcal{N}_h$, $\mathcal{E}_h$, $\mathcal{F}_h$ and denote by $\mathcal{N}_h^{\text{int}}$, $\mathcal{E}_h^{\text{int}}$, $\mathcal{F}_h^{\text{int}}$ and $\mathcal{N}_h^{\Gamma}$, $\mathcal{E}_h^{\Gamma}$, $\mathcal{F}_h^{\Gamma}$ the sets of vertices, edges and faces located in the interior of Ω and on the boundary Γ, respectively.

In the following for an integer $k \geq 0$, $\mathbb{P}_k(\mathfrak{T})$ denotes the linear space of polynomials of degree less or equal to k on $\mathfrak{T}$.

2.1 Nédélec basis functions for the $\mathbf{H}(\mathrm{curl}, \Omega)-$FE space

We consider finite elements which will be used to discretize the electric field in Maxwell's equations. While the elements of lower order were discovered by other authors (e.g. Whitney [77]), the general case is studied initially in Nédélec [63]. For that reason these elements are commonly known as Nédélec elements. The lowest order Nédélec elements are termed **edge elements** because the degrees of freedom are associated with edges of the mesh (see Figures 2.1 and 2.2). The constraint for the $\mathbf{H}(\mathbf{curl}, \Omega)$-conformity is that the tangential component on adjacent elements has to be continuous (see [63, Lemma 6])

Following [63, Definition 6] and [59], we consider initially the definition of the Nédélec finite elements.

2.1.1 Definition on the reference tetrahedron

The element of Nédélec is defined as follows:

(a) The reference tetrahedral is

$$\widehat{\mathfrak{T}} := \{\boldsymbol{x} \in \mathbb{R}^3 : x_1, x_2, x_3 \geq 0,\ x_1 + x_2 + x_3 \leq 1\}$$

with edges e_j, $j = 1, \cdots, 6$.
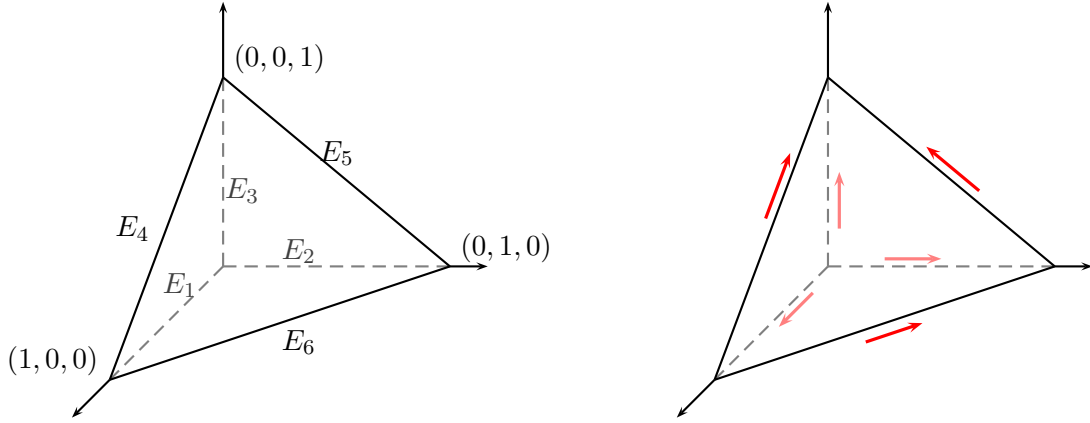
Figure 2.1: Numbering of the edges and a graphical representation of $\Sigma_{\widehat{\mathfrak{T}}}$ (in red) for the edge element lowest-order on the tetrahedron $\widehat{\mathfrak{T}}$.

(b) The local space is defined by

$$\mathcal{ND}_k(\mathfrak{T}) := (\mathbb{P}_{k-1}(\mathfrak{T}))^3 + \left\{ \mathbf{p} \in (\mathbb{P}_k(\mathfrak{T}))^3 : \mathbf{p}(\boldsymbol{x}) \cdot \boldsymbol{x} = 0,\ \forall \boldsymbol{x} \in \mathfrak{T} \right\}.$$

From this, we obtain for the lowest order case $k = 1$ the representation

$$\mathcal{ND}_1(\mathfrak{T}) := \left\{ \boldsymbol{x} \mapsto \alpha + \beta \times \boldsymbol{x} : \alpha, \beta \in \mathbb{R}^3 \right\} \subset (\mathbb{P}_1(\mathfrak{T}))^3.$$

(c) The degrees of freedom $\Sigma_{\widehat{\mathfrak{T}}}$ on $\mathcal{ND}_k(\widehat{\mathfrak{T}})$ are given as follows:

    i. For each edge $E \in \mathcal{E}_h(\widehat{\mathfrak{T}})$ with unit tangent $\boldsymbol{t}$ and $p \in \mathbb{P}_{k-1}(E)$

$$\boldsymbol{u} \mapsto \int_E \boldsymbol{u} \cdot \boldsymbol{t}\, p\, ds,$$

    ii. For each face $F \in \mathcal{F}_h(\widehat{\mathfrak{T}})$ with normal $\boldsymbol{n}$ and $\mathbf{p} \in (\mathbb{P}_{k-2}(F))^2$

$$\boldsymbol{u} \mapsto \int_F \boldsymbol{u} \times \boldsymbol{n} \cdot \mathbf{p}\, d\sigma,$$

iii. For the volume $\widehat{\mathfrak{T}}$ and for all $\boldsymbol{q} \in (\mathbb{P}_{k-3}(\widehat{\mathfrak{T}}))^3$

$$\boldsymbol{u} \mapsto \int_{\widehat{\mathfrak{T}}} \boldsymbol{u} \cdot \boldsymbol{q} \, d\boldsymbol{x}.$$

From this there are k degrees of freedom associated to an edge E, $k(k-1)$ degrees of freedom associated to a face F and $\dfrac{k(k-1)(k-2)}{2}$ degrees of freedom associated to the interior. Hence the total number of degrees of freedom is

$$|\Sigma_{\widehat{\mathfrak{T}}}| = 6k + 4k(k-1) + \frac{k(k-1)(k-2)}{2} = \frac{k(k+2)(k+3)}{2}$$

which is equivalent to $\dim \mathcal{ND}_k(\widehat{\mathfrak{T}})$.

Lemma 2.1.1 ([63, Theorem 1],[59, Theorem 5.37])
A finite element defined by (a) - (c) is $\mathbf{H}(\mathbf{curl}, \Omega)$ *unisolvent and conforming.*

2.1.2 Definition on the reference cube

The element of Nédélec is defined as follows:

(a) The reference cube $\widehat{\mathfrak{T}} = [-1, 1]^3$ with edges e_j, $j = 1, \cdots, 12$.
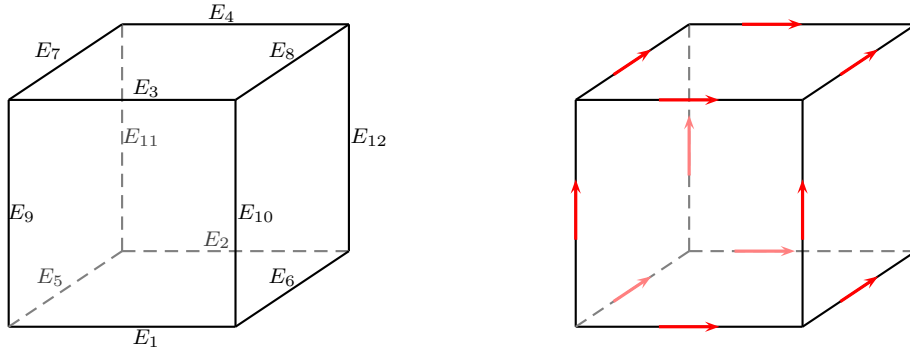
Figure 2.2: Numbering of the edges and a graphical representation of $\Sigma_{\widehat{\mathfrak{T}}}$ (in red) for the edge element lowest-order on the reference cube $\widehat{\mathfrak{T}}$.

(b) The local space is defined by

$$\mathcal{ND}_k(\widehat{\mathfrak{T}}) := \mathsf{Q}_{k-1,k,k}(\widehat{\mathfrak{T}}) \times \mathsf{Q}_{k,k-1,k}(\widehat{\mathfrak{T}}) \times \mathsf{Q}_{k,k,k-1}(\widehat{\mathfrak{T}}).$$

where $\mathsf{Q}_{l,m,n}(\widehat{\mathfrak{T}})$ denotes the space of polynomials in three variables (x, y, z) with maximum degrees l in x, m in y and n in z.

(c) The degrees of freedom $\Sigma_{\widehat{\mathfrak{T}}}$ on $\mathcal{ND}_k(\widehat{\mathfrak{T}})$ are given as follows:

    i. For each edge $E \in \mathcal{E}_h(\widehat{\mathfrak{T}})$ with unit tangent $\boldsymbol{t}$ and $p \in \mathbb{P}_{k-1}(E)$

$$\boldsymbol{u} \mapsto \int_E \boldsymbol{u} \cdot \boldsymbol{t}\, p\, ds,$$

    ii. For each face $F \in \mathcal{F}_h(\widehat{\mathfrak{T}})$ with normal $\boldsymbol{n}$ and $\mathbf{p} = (p_1, p_2) \in \mathsf{Q}_{k-2,k-1} \times \mathsf{Q}_{k-1,k-2}$

$$\boldsymbol{u} \mapsto \int_F \boldsymbol{u} \times \boldsymbol{n} \cdot \mathbf{p}\, d\sigma,$$

    iii. For the volume $\widehat{\mathfrak{T}}$ and for all $\boldsymbol{q} \in \mathsf{Q}_{k-1,k-2,k-2} \times \mathsf{Q}_{k-2,k-1,k-2} \times \mathsf{Q}_{k-2,k-2,k-1}$

$$\boldsymbol{u} \mapsto \int_{\widehat{\mathfrak{T}}} \boldsymbol{u} \cdot \boldsymbol{q}\, dx.$$

Hence, we get k degrees of freedom associated to an edge E, $2k(k-1)$ degrees of freedom associated to a face F and $3k(k-1)^2$ degrees of freedom associated to the interior, i.e., the total number of degrees is

$$12k + 12k(k-1) + 3k(k-1)^2 = 3k(k+1)^2$$

which is also the dimension of the space $\mathcal{ND}_k(\widehat{\mathfrak{T}})$.

Lemma 2.1.2 ([63, Theorem 5], [59, Theorem 6.5])
A finite element defined by the cube $\widehat{\mathfrak{T}}$, the space $\mathcal{ND}_k(\widehat{\mathfrak{T}})$ and the set $\Sigma_{\widehat{\mathfrak{T}}}$ is unisolvent and conforming in $\mathbf{H}(\mathbf{curl}, \Omega)$.

A consequence of the Lemmata 2.1.1 and 2.1.2 is that the space

$$\mathcal{ND}_k(\mathcal{T}_h) := \{\boldsymbol{u} \in \mathbf{H}(\mathbf{curl}, \Omega) : \boldsymbol{u}|_{\mathfrak{T}} \in \mathcal{ND}_k(\widehat{\mathfrak{T}}), \quad \text{for all } \mathfrak{T} \in \mathcal{T}_h\} \tag{2.1}$$

determines the global finite element space on a mesh $\mathcal{T}_h$.

For the sake of brevity we consider for the description of the calculation of the basis functions only the reference cube.

We use the degrees of freedom defined previously to calculate the basis functions. Hence

$$m_j(\boldsymbol{u}) := \begin{cases} \int_E \boldsymbol{u} \cdot \boldsymbol{t}\, p\, ds, & \text{for all } p \in \mathbb{P}_{k-1}(E) \\ \int_F \boldsymbol{u} \times \boldsymbol{n} \cdot \mathbf{p}\, d\sigma, & \text{for all } \mathbf{p} = (p_1, p_2) \in \mathsf{Q}_{k-2,k-1} \times \mathsf{Q}_{k-1,k-2} \\ \int_{\widehat{\mathfrak{T}}} \boldsymbol{u} \cdot \mathbf{p}\, dx, & \text{for all } \mathbf{p} \in \mathsf{Q}_{k-1,k-2,k-2} \times \mathsf{Q}_{k-2,k-1,k-2} \times \mathsf{Q}_{k-2,k-2,k-1} \end{cases}$$

for $j = 1, \ldots, 3k(k+1)^2$.

In general, we require that the basis functions $\boldsymbol{b}_i$ of $\mathcal{ND}_k(\widehat{\mathfrak{T}})$ have to satisfy the conditions

$$m_j(\boldsymbol{b}_i) = \delta_{ij}, \qquad m_j \in \Sigma_{\widehat{\mathfrak{T}}}, \quad i, j = 1, \ldots, 3k(k+1)^2.$$

This leads to a linear system depending on the choice of test and trial functions. One possibility is to use monomials as basis for $\mathcal{ND}_k(\widehat{\mathfrak{T}})$. For computations they are ordered by

$$\boldsymbol{\psi}_i(x, y, z) := \begin{cases} x^r y^s z^t \, \boldsymbol{e}_1, & r \le k-1, \, s \le k, \, t \le k & \text{if } i = 1, \ldots, k(k+1)^2 \\ x^r y^s z^t \, \boldsymbol{e}_2, & r \le k, \, s \le k-1, \, t \le k & \text{if } i = k(k+1)^2 + 1, \ldots, 2k(k+1)^2 \\ x^r y^s z^t \, \boldsymbol{e}_3, & r \le k, \, s \le k, \, t \le k-1 & \text{if } i = 2k(k+1)^2 + 1, \ldots, 3k(k+1)^2 \end{cases}.$$

Here, $\boldsymbol{e}_1$, $\boldsymbol{e}_2$, $\boldsymbol{e}_3$ denote the unit Cartesian vectors. Then, there holds

$$\mathcal{ND}_k(\widehat{\mathfrak{T}}) = \text{span}\{\boldsymbol{\psi}_i, \, i = 1, \ldots, 3k(k+1)^2\},$$

hence the basis functions $\boldsymbol{b}_i$ have a representation

$$\boldsymbol{b}_i = \sum_{l=1}^{3k(k+1)^2} a_{il} \boldsymbol{\psi}_l$$

with the coefficients a_{il} as the solution of the linear system

$$m_j(\boldsymbol{b}_i) = \sum_{l=1}^{3k(k+1)^2} a_{il} m_j(\boldsymbol{\psi}_l) = \delta_{ij}, \quad i, j = 1, \ldots, 3k(k+1)^2.$$

In order to calculate the moments m_j one could use monomials as test functions. It is also possible to use different polynomial basis functions of the polynomial spaces.

For the lowest order $k = 1$ we get the following basis functions associated to the edges of the reference element, see Figure 2.2.

$$\boldsymbol{b}^{(E_1)} = \frac{1}{8}(1-y)(1-z)\boldsymbol{e}_1, \quad \boldsymbol{b}^{(E_2)} = \frac{1}{8}(1+y)(1-z)\boldsymbol{e}_1,$$

$$\boldsymbol{b}^{(E_3)} = \frac{1}{8}(1-y)(1+z)\boldsymbol{e}_1, \quad \boldsymbol{b}^{(E_4)} = \frac{1}{8}(1+y)(1+z)\boldsymbol{e}_1,$$

$$\boldsymbol{b}^{(E_5)} = \frac{1}{8}(1-x)(1-z)\boldsymbol{e}_2, \quad \boldsymbol{b}^{(E_6)} = \frac{1}{8}(1+x)(1-z)\boldsymbol{e}_2,$$

$$\boldsymbol{b}^{(E_7)} = \frac{1}{8}(1-x)(1+z)\boldsymbol{e}_2, \quad \boldsymbol{b}^{(E_8)} = \frac{1}{8}(1+x)(1+z)\boldsymbol{e}_2,$$

$$\boldsymbol{b}^{(E_9)} = \frac{1}{8}(1-x)(1-y)\boldsymbol{e}_3, \quad \boldsymbol{b}^{(E_{10})} = \frac{1}{8}(1+x)(1-y)\boldsymbol{e}_3,$$

$$\boldsymbol{b}^{(E_{11})} = \frac{1}{8}(1-x)(1+y)\boldsymbol{e}_3, \quad \boldsymbol{b}^{(E_{12})} = \frac{1}{8}(1+x)(1+y)\boldsymbol{e}_3.$$

Analogously we get for $k = 1$ on the reference tetrahedral the following basis functions, see Figure 2.1,

$$\boldsymbol{b}^{(E_1)} = (1 - y - z)\boldsymbol{e}_1 + x\boldsymbol{e}_2 + x\boldsymbol{e}_3, \qquad \boldsymbol{b}^{(E_4)} = z\boldsymbol{e}_1 - x\boldsymbol{e}_3,$$
$$\boldsymbol{b}^{(E_2)} = y\boldsymbol{e}_1 + (1 - x - z)\boldsymbol{e}_2 + y\boldsymbol{e}_3, \qquad \boldsymbol{b}^{(E_5)} = z\boldsymbol{e}_2 - y\boldsymbol{e}_3,$$
$$\boldsymbol{b}^{(E_3)} = z\boldsymbol{e}_1 + z\boldsymbol{e}_2 + (1 - x - y)\boldsymbol{e}_3, \qquad \boldsymbol{b}^{(E_6)} = y\boldsymbol{e}_1 - x\boldsymbol{e}_2.$$

We remark that the edge functions are constant on the edge which they are associated to.

2.1.3 Affine transformations for Nédélec functions

An important point in the theory of FE and BE are appropiate mappings from the reference element to an arbitrary local element. In our case this map should ensure that the transformed function has a well-defined curl.

Suppose that $\widehat{\mathfrak{T}}$ is the reference tetrahedron or the reference hexahedron defined in sections 2.1.1 - 2.1.2, and that $\mathfrak{T}$ denotes the image of the reference element $\widehat{\mathfrak{T}}$ under the affine transformation

$$\begin{aligned} \mathcal{M}_{\mathfrak{T}} &: \widehat{\mathfrak{T}} \to \mathfrak{T} \\ \hat{\boldsymbol{x}} &\mapsto \mathcal{B}_{\mathfrak{T}}\,\hat{\boldsymbol{x}} + \mathbf{d} =: \boldsymbol{x}, \end{aligned} \tag{2.2}$$

where $\mathcal{B}_{\mathfrak{T}} \in \mathcal{L}(\widehat{\mathfrak{T}}, \mathbb{R}^3)$ and $\mathbf{d} \in \mathbb{R}^3$. Suppose $\hat{\boldsymbol{u}} \in \mathbf{H}(\mathbf{curl}, \widehat{\mathfrak{T}})$ and $\boldsymbol{u} \in \mathbf{H}(\mathbf{curl}, \mathfrak{T})$, we transform $\hat{\boldsymbol{u}}$ to $\boldsymbol{u}$ via the transformation (2.2) so that

$$\boldsymbol{u} \circ \mathcal{M}_{\mathfrak{T}} = (\mathcal{B}_{\mathfrak{T}}^{\mathsf{T}})^{-1}\hat{\boldsymbol{u}}. \tag{2.3}$$

A consequence of this formula is that the curl of $\boldsymbol{u}$ and the curl of $\hat{\boldsymbol{u}}$ are related by

$$\nabla \times \boldsymbol{u} = \frac{1}{\det(\mathcal{B}_{\mathfrak{T}})}\mathcal{B}_{\mathfrak{T}}\,\widehat{\nabla} \times \hat{\boldsymbol{u}}$$

where $\widehat{\nabla} \times \cdot$ denotes the curl with respect to the coordinate system for $\widehat{\mathfrak{T}}$ (see Monk [59, Corollary 3.58]).

If $\{\hat{\boldsymbol{b}}_j, \ j = 1, \ldots, n_k\}$ is a basis of $\mathcal{N}\mathcal{D}_k(\widehat{\mathfrak{T}})$, then applying the affine transformation $\mathcal{M}_{\mathfrak{T}}$ we obtain a local basis on $\mathfrak{T}$ given by

$$\boldsymbol{b}_j(\boldsymbol{x}) = (\mathcal{B}_{\mathfrak{T}}^{\mathsf{T}})^{-1}\,\hat{\boldsymbol{b}}_j(\hat{\boldsymbol{x}}), \quad j = 1, \ldots, n_k. \tag{2.4}$$

Moreover, the local finite element space $\mathcal{N}\mathcal{D}_k(\mathfrak{T})$ is invariant under this transformation (see [63, Proposition 2], [59, Lemma 5.32]). Thus, we can define the global finite element space $\mathcal{N}\mathcal{D}_k(\mathcal{T}_h)$, if we connect those local basis functions that belong to an edge or a face to a global basis function.

2.1.4 An interpolation operator defined by $\Sigma_{\widehat{\mathfrak{T}}}$ on $\mathcal{ND}_k(\widehat{\mathfrak{T}})$

Considering the degrees of freedom associated to the edges, faces and the volume, $m^E, m^F, m^{\mathfrak{T}}$, respectively, we can define for any $\boldsymbol{u} \in (\mathcal{C}^\infty(\overline{\mathfrak{T}}))^3$ a unique interpolate $\Pi_{\mathfrak{T}}\boldsymbol{u} \in \mathcal{ND}_k(\mathfrak{T})$ such that

$$m_{j_1}^E(\boldsymbol{u} - \Pi_{\mathfrak{T}}\boldsymbol{u}) = m_{j_2}^F(\boldsymbol{u} - \Pi_{\mathfrak{T}}\boldsymbol{u}) = m_{j_3}^{\mathfrak{T}}(\boldsymbol{u} - \Pi_{\mathfrak{T}}\boldsymbol{u}) = 0,$$

with $j_i = \{1, \cdots, J_i\}, i = 1, 2, 3$ and $J_1 + J_2 + J_3 = |\Sigma_{\widehat{\mathfrak{T}}}|$. Here J_1, J_2 and J_3 denote the number of all degree of freedom associated to the edges, faces and volume, respectively.

Using this we can define a global interpolant $\Pi_k^h\boldsymbol{u} \in \mathcal{ND}_k(\mathcal{T}_h)$ element by element by

$$\Pi_k^h\boldsymbol{u}|_{\mathfrak{T}} := \Pi_{\mathfrak{T}}\boldsymbol{u}, \qquad \text{for all } \mathfrak{T} \in \mathcal{T}_h. \tag{2.5}$$

Remark 2.1.1 *The interpolants* $\Pi_{\mathfrak{T}}$ *are not well-defined for all functions* $\boldsymbol{u} \in \mathbf{H}(\mathbf{curl}, \Omega)$. *In fact, Amrouche et al. [2, Lemma 4.7] prove that the interpolants are well-defined for* $\boldsymbol{u} \in \mathbf{L}^p(\mathfrak{T})$, $\mathbf{curl}\,\boldsymbol{u} \in \mathbf{L}^p(\mathfrak{T})$ *and* $\boldsymbol{u} \times \boldsymbol{n} \in (L^p(\partial\mathfrak{T}))^2$ *for some* $p > 2$. *Moreover Monk [59, Lemma 5.38] shows that it is valid also if* $\boldsymbol{u} \in \mathbf{H}^{1/2+\delta}(\mathfrak{T})$, $\delta > 0$ *such that* $\mathbf{curl}\,\boldsymbol{u} \in \mathbf{L}^p(\mathfrak{T})$, $p > 2$.

For the interpolant one can prove the following error estimate .

Lemma 2.1.3 ([59, Theorems 5.41 and 6.6]) *Let* $\mathcal{T}_h$ *be a regular mesh on* Ω. *For* $\boldsymbol{u} \in \mathbf{H}^s(\mathbf{curl}, \Omega)$, $1/2 + \delta \leq s \leq k$, $\delta > 0$, *there exists* $C > 0$, *dependent only on* s, k, *and the shape regularity of* $\mathcal{T}_h$

$$\|\boldsymbol{u} - \Pi_k^h\boldsymbol{u}\|_{\mathbf{H}(\mathbf{curl},\Omega)} \leq Ch^s\|\boldsymbol{u}\|_{\mathbf{H}^s(\mathbf{curl},\Omega)}.$$

Lemma 2.1.4 (Ciarlet & Zou [18], Hiptmair [36], Monk [58], Nédélec[65]) *Let* $\mathcal{T}_h$ *be a regular mesh on* Ω. *For* $s \in]\frac{1}{2}, 1[\cup\mathbb{N}$, $k \in \mathbb{N}_0$, *the interpolation operator* Π_k^h *satisfies*

(a)
$$\|\boldsymbol{u} - \Pi_k^h\boldsymbol{u}\|_{\mathbf{L}^2(\Omega)} \leq Ch^{\min\{s,k+1\}}\|\boldsymbol{u}\|_{\mathbf{H}^s(\mathbf{curl},\Omega)},$$

(b)
$$\|\,\mathbf{curl}\,(\boldsymbol{u} - \Pi_k^h\boldsymbol{u})\,\|_{\mathbf{L}^2(\Omega)} \leq Ch^{\min\{s,k+1\}}\|\,\mathbf{curl}\,\boldsymbol{u}\|_{\mathbf{H}^s(\Omega)}$$

where $C > 0$ *depends only on the shape regularity of the mesh* $\mathcal{T}_h$.

2.2 Raviart-Thomas basis functions on the space $\mathbf{H}(\mathrm{div}, \Omega)$

In this section we analyze the space $\mathbf{H}(\mathrm{div}, \Omega)$. Nédélec [63] extends to three dimensions the divergence conforming elements of Raviart-Thomas. The lowest order $\mathbf{H}(\mathrm{div}, \Omega)$-elements are associated with faces in the mesh and due to that these elements are known also as **face elements**. The constraint for $\mathbf{H}(\mathrm{div}, \Omega)$-conformity is that the normal component, i.e., $\boldsymbol{u} \cdot \boldsymbol{n}$ is continuous between adjacent elements, cf. Nédélec[63].

2.2.1 Divergence conforming elements

Definition on the reference tetrahedron

The element is defined as follows

(a) The reference tetrahedron is

$$\widehat{\mathfrak{T}} := \big\{ \boldsymbol{x} \in \mathbb{R}^3 : x_1, x_2, x_3 \geq 0, \ x_1 + x_2 + x_3 \leq 1 \big\}$$

with edges e_j, $j = 1, \ldots, 6$.
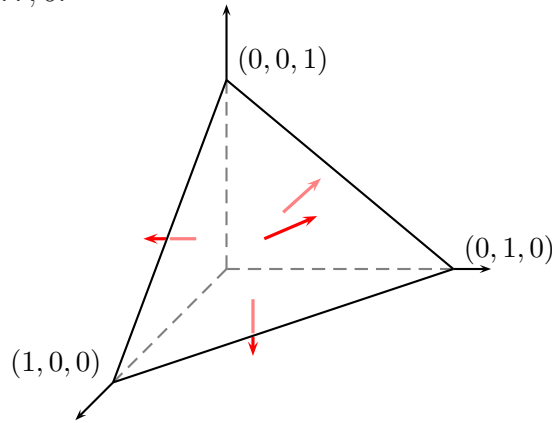
Figure 2.3: Reference tetrahedron $\widehat{\mathfrak{T}}$ and graphical representation of $\Sigma_{\widehat{\mathfrak{T}}}$ (in red) for the face element lowest-order on $\widehat{\mathfrak{T}}$.

(b) The local space is defined by

$$\mathcal{RT}_k(\widehat{\mathfrak{T}}) := \big(\mathbb{P}_{k-1}(\widehat{\mathfrak{T}})\big)^3 \oplus \boldsymbol{x} \, \mathbb{P}_{k-1}^0(\widehat{\mathfrak{T}})$$

where $\mathbb{P}_k^0(\widehat{\mathfrak{T}})$ denotes the space of all homogeneous polynomials of degree k on $\widehat{\mathfrak{T}}$. This space has dimension $\frac{1}{2}k(k+1)(k+3)$ [63, Lemma 5]. We obtain for the lowest order case $k = 1$:

$$\mathcal{RT}_1(\widehat{\mathfrak{T}}) := \big\{ \boldsymbol{x} \mapsto \alpha + \beta \boldsymbol{x} : \alpha \in \mathbb{K}^3, \beta \in \mathbb{K} \big\}$$

where $\mathbb{K}$ can be $\mathbb{R}$ or $\mathbb{C}$.

(c) The degrees of freedom $\Sigma_{\widehat{\mathfrak{T}}}$ on $\mathcal{RT}_k(\widehat{\mathfrak{T}})$ are given as follows:

    i. For each face $F \in \mathcal{F}_h(\widehat{\mathfrak{T}})$ with normal $\hat{\boldsymbol{n}}$ and for all $\hat{p} \in \mathbb{P}_{k-1}(F)$

$$\hat{\boldsymbol{u}} \mapsto \int_F \hat{\boldsymbol{u}} \cdot \hat{\boldsymbol{n}} \, \hat{p} \, d\sigma.$$

    ii. For the volume $\widehat{\mathfrak{T}}$ and for all $\hat{\boldsymbol{q}} \in (\mathbb{P}_{k-2}(\mathfrak{T}))^3$

$$\hat{\boldsymbol{u}} \mapsto \int_{\widehat{\mathfrak{T}}} \hat{\boldsymbol{u}} \cdot \hat{\boldsymbol{q}} \, d\boldsymbol{x}.$$

Remark 2.2.1 *The moments presented above are not well-defined for all functions* $\hat{\boldsymbol{u}} \in \mathbf{H}(\mathrm{div}, \Omega)$, *these moments are well defined for* $\hat{\boldsymbol{u}} \in \mathbf{L}^p(\widehat{\mathfrak{T}})$, $p > 2$ *and* $\widehat{\nabla} \cdot \hat{\boldsymbol{u}} \in L^2(\widehat{\mathfrak{T}})$ *([8], cf. [59, Lemma 5.15]).*

Analogously the Raviart-Thomas space on the reference cube $\widehat{\mathfrak{T}} := [-1, 1]^3$ is given by

$$\mathcal{RT}_k(\widehat{\mathfrak{T}}) := \mathbb{Q}_{k,k-1,k-1} \times \mathbb{Q}_{k-1,k,k-1} \times \mathbb{Q}_{k-1,k-1,k}.$$

The dimension of this space is $3k^2(k+1)$ and the degrees of freedom are defined by

    i. For each face $F \in \mathcal{F}_h(\widehat{\mathfrak{T}})$ with normal $\hat{\boldsymbol{n}}$ and for all $\hat{p} \in \mathbb{Q}_{k-1,k-1}(\widehat{\mathfrak{T}})$

$$\hat{\boldsymbol{u}} \mapsto \int_F \hat{\boldsymbol{u}} \cdot \hat{\boldsymbol{n}} \, \hat{p} \, d\sigma.$$

    ii. For the volume $\widehat{\mathfrak{T}}$ and for all $\hat{\boldsymbol{q}} \in \mathbb{Q}_{k-2,k-1,k-1} \times \mathbb{Q}_{k-1,k-2,k-1} \times \mathbb{Q}_{k-1,k-1,k-2}$

$$\hat{\boldsymbol{u}} \mapsto \int_{\widehat{\mathfrak{T}}} \hat{\boldsymbol{u}} \cdot \hat{\boldsymbol{q}} \, d\boldsymbol{x}.$$

Let $\mathfrak{T} \in \mathcal{T}_h$ be an element with diameter h and $\widehat{\mathfrak{T}}$ the reference element. The affine transformation between these elements is given in (2.2). For functions $\hat{\boldsymbol{q}} : \widehat{\mathfrak{T}} \to \mathbb{R}^3$ and $\boldsymbol{q} : \mathfrak{T} \to \mathbb{R}^3$ the $\mathbf{H}(\mathrm{div})$-conforming Piola transformation is then given by, see e.g. [63],

$$\boldsymbol{q} \circ \mathcal{M}_{\mathfrak{T}} = \frac{1}{\det \mathcal{B}_{\mathfrak{T}}} \mathcal{B}_{\mathfrak{T}} \hat{\boldsymbol{q}} \tag{2.6}$$

As in the case of the Nédélec space the local basis function on T are given by

$$\boldsymbol{b}_j(\boldsymbol{x}) = \frac{1}{\det \mathcal{B}_{\mathfrak{T}}} \mathcal{B}_{\mathfrak{T}} \hat{\boldsymbol{b}}_j(\hat{\boldsymbol{x}}), \quad j = 1, \ldots, n_k.$$

Now, finite elements defined as above are unisolvent on a reference tetrahedron or hexahedron $\widehat{\mathfrak{T}}$ ([59, Lemma 5.21, Theorema 6.2]). This implies that there is a well-defined

interpolation operator $\Pi^{\mathcal{RT}}$ on $\widehat{\mathfrak{T}}$, such that if $\boldsymbol{u}$ satisfies Remark 2.2.1 then there is a unique finite element function $\Pi^{\mathcal{RT}}\boldsymbol{u} \in \mathcal{RT}_k$ such that

$$m_{j_1}^F(\boldsymbol{u} - \Pi^{\mathcal{RT}}\boldsymbol{u}) = m_{j_2}^{\mathfrak{T}}(\boldsymbol{u} - \Pi^{\mathcal{RT}}\boldsymbol{u}) = 0,$$

where $j_i = \{1, \cdots, J_i\}, i = 1, 2$ and $J_1 + J_2 = |\Sigma_{\widehat{\mathfrak{T}}}|$.

Combining together the local basis belonging to a common face we obtain global basis functions. Therefore we can define the space $\mathcal{RT}_k(\mathcal{T}_h)$ which is invariant under the transformation (2.2) if we transform the basis functions by (2.6). As for the $\mathbf{H}(\mathbf{curl}, \Omega)$-conforming space we can define the global interpolation operator $\Pi_h^{\mathcal{RT}_k}$, c.f. (2.5). There holds the following approximation result, see e.g. Hiptmair [33].

Theorem 2.2.1 ([59, Theorems 5.25 and 6.3])
Let $\mathcal{T}_h$ be a regular mesh on Ω, $0 < \delta < \frac{1}{2}$. For $\boldsymbol{u} \in \mathbf{H}^s(\Omega)$, $1/2 + \delta \leq s \leq k$, there is a constant C independent of h and $\boldsymbol{u}$ such that

$$\|\boldsymbol{u} - \Pi_h^{\mathcal{RT}_k}\boldsymbol{u}\|_{\mathbf{L}^2(\Omega)} \leq Ch^s \|\boldsymbol{u}\|_{\mathbf{H}^s(\Omega)}.$$

2.2.2 Raviart-Thomas basis functions for the approximation in $\mathbf{H}_\|^{-1/2}(\mathrm{div}_\Gamma, \Gamma)$

In this section we consider the approximation in $\mathbf{H}_\|^{-1/2}(\mathrm{div}_\Gamma, \Gamma)$. Lemma 1.2.3 shows that $\gamma_D^\times : \mathbf{H}(\mathbf{curl}, \Omega) \to \mathbf{H}_\|^{-1/2}(\mathrm{div}_\Gamma, \Gamma)$ can be extended to a linear, continuous and surjective mapping, i.e., there holds

$$\gamma_D^\times(\mathbf{H}(\mathbf{curl}, \Omega)) = \mathbf{H}_\|^{-1/2}(\mathrm{div}_\Gamma, \Gamma).$$

Moreover, from Section 2.1 we known that the space $\mathbf{H}(\mathbf{curl}, \Omega)$ can be discretized using the Nédélec space $\mathcal{ND}_k(\mathcal{T}_h)$, hence a key to discretize $\mathbf{H}_\|^{-1/2}(\mathrm{div}_\Gamma, \Gamma)$ should be the twisted tangential trace of the space $\mathcal{ND}_k(\mathcal{T}_h)$. Hiptmair [35, Lemma 2.4] shows that the twisted tangential trace of the space $\mathcal{ND}_k(\mathcal{T}_h)$ is exactly the finite element space of Raviart-Thomas functions of order k in two dimensions denoted by $\mathcal{RT}_k(\mathcal{K}_h)$. This space was first considered by Raviart & Thomas [69], see also Brezzi & Fortin [8] and Nédélec [63].

As in the three-dimensional case the constraint for $\mathbf{H}(\mathrm{div}, \Gamma)$-conformity is that the normal component $\boldsymbol{u} \cdot \boldsymbol{n}$ is continuous between adjacent elements.

The definition of the basis functions is again done locally and we use the transformation between different elements to construct the global space in the same way as for the Nédélec functions.

Definition on squares

We first consider the reference square $\widehat{K} = [-1, 1]^2$. Furthermore, $\mathsf{Q}_{l,m}$ denotes all polynomials with maximum degrees l in x- and m in y-direction. The local Raviart-Thomas space of order k is then defined by

$$\mathcal{RT}_k(\widehat{K}) := \mathsf{Q}_{k,k-1} \times \mathsf{Q}_{k-1,k}.$$

The dimension is then $2k(k+1)$. Moreover the divergence free $\mathcal{RT}_k$ elements are defined by

$$\mathcal{RT}_k^0 := \{\boldsymbol{q} \mid \boldsymbol{q} \in \mathcal{RT}_k, \mathrm{div}\,\boldsymbol{q} = 0\}.$$

In literature (e.g. Brezzi & Fortin [8, Section III.3.2]) this space is sometimes denoted by $\mathcal{RT}_{k-1}(\widehat{K})$, but we use the same counting scheme as in Nédélec[63].

In order to ensure continuity of the normal component we can construct basis functions $\boldsymbol{\varphi}_i$ using the following moments.

i. For each edge $E \in \mathcal{E}_h(\widehat{K})$ with unit normal $\boldsymbol{n}$ and for all $p \in \mathbb{P}_{k-1}(E)$

$$\boldsymbol{u} \mapsto \int_E \boldsymbol{u} \cdot \boldsymbol{n}\, p\, ds.$$

ii. On $\widehat{K}$ for all $\mathbf{p} = (p_1, p_2) \in \mathsf{Q}_{k-2,k-1} \times \mathsf{Q}_{k-1,k-2}$

$$\boldsymbol{u} \mapsto \int_{\widehat{K}} \boldsymbol{u} \cdot \mathbf{p}\, d\sigma.$$

The basis functions are calculated in the same way as the Nédélec basis functions (cf. Section 2.1.2), i.e., for the construction of a basis of $\mathcal{RT}_k(\widehat{K})$ we first use monomials and we consider

$$\boldsymbol{\psi}_i(x, y) := \begin{cases} x^r y^s \boldsymbol{e}_1, & r \leq k,\ s \leq k-1, & \text{if } i = 1, \ldots, k(k+1) \\ x^r y^s \boldsymbol{e}_2, & r \leq k-1,\ s \leq k, & \text{if } i = k(k+1)+1, \ldots, 2k(k+1) \end{cases}$$

with the unit Cartesian vectors $\boldsymbol{e}_1$ and $\boldsymbol{e}_2$ and we get the local space by $\mathcal{RT}_k(\widehat{K}) = \mathrm{span}\,\{\boldsymbol{\psi}_i,\ i = 1, \ldots, 2k(k+1)\}$. We get the following basis functions on $\widehat{K}$ for the polynomial degrees $k = 1$. (For the numbering of the edges, see Figure 2.4.)

$$\boldsymbol{\lambda}^{(E_1)} := \frac{1}{4}(y-1)\boldsymbol{e}_2, \quad \boldsymbol{\lambda}^{(E_2)} := \frac{1}{4}(x+1)\boldsymbol{e}_1,$$

$$\boldsymbol{\lambda}^{(E_3)} := \frac{1}{4}(y+1)\boldsymbol{e}_2, \quad \boldsymbol{\lambda}^{(E_4)} := \frac{1}{4}(x-1)\boldsymbol{e}_1.$$

These basis functions are constant on the edge which they are associated to. On the other edges their normal components vanish.
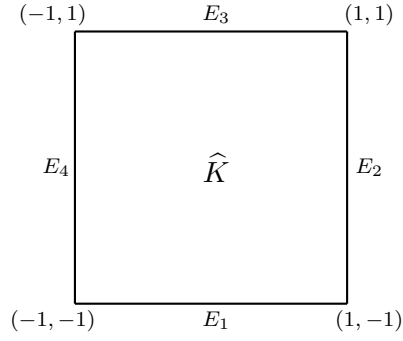
Figure 2.4: Numbering of the edges on the unit square $\widehat{K}$.

Let $\boldsymbol{u} \in \mathbf{H}(\mathrm{div}, \widehat{K})$. Indeed the degrees of freedom previously described always imply the moments of $\boldsymbol{u}$ on the faces (or sides) of an elements. But the functions $q \in \mathcal{RT}_{k-1}(\partial\widehat{K})$ do not belong to $H^{1/2}(\partial\widehat{K})$, and it is not possible in general to compute expressions like $\int_{\partial\widehat{K}} \boldsymbol{u} \cdot \boldsymbol{n}\, p\, ds$ as $\boldsymbol{u} \cdot \boldsymbol{n}$ is only defined in $H^{-1/2}(\partial\widehat{K})$. Such a construction is possible in the following set:

$$W(\widehat{K}) := \{\boldsymbol{u} \in (L^p(\widehat{K}))^2 \,|\, \mathrm{div}\,\boldsymbol{u} \in L^2(\widehat{K})\}, \quad p > 2,$$

and an interpolation operator $\pi_{\widehat{K}} : W(\widehat{K}) \to \mathcal{RT}_k(\widehat{K})$ can be defined by,

$$\int_{\partial\widehat{K}} (\boldsymbol{u} - \pi_{\widehat{K}}\boldsymbol{u}) \cdot \boldsymbol{n}\, q\, ds = 0 \quad \text{for all } q \in \mathcal{RT}_{k-1}(\partial\widehat{K}),$$

$$\int_{\widehat{K}} (\boldsymbol{u} - \pi_{\widehat{K}}\boldsymbol{u}) \cdot \boldsymbol{q}\, d\sigma = 0 \quad \text{for all } \boldsymbol{q} \in \mathsf{Q}_{k-2,k-1} \times \mathsf{Q}_{k-1,k-2}.$$

Let $\widehat{K}$ be associated to the face F_0 ($z = -1$) of the reference cube $\widehat{\mathfrak{T}}$. Comparing the degrees of freedom with the ones of $\mathcal{ND}_k(\widehat{\mathfrak{T}})$ one finds out that there holds

$$\gamma_D^\times\big(\mathcal{ND}_k(\widehat{\mathfrak{T}})\big) = \mathcal{RT}_k(\widehat{\mathfrak{T}}).$$

In general, we can define a global interpolation operator $\pi^{\mathcal{RT}_k}$ which is related to the global interpolation operator $\Pi^{\mathcal{ND}_k}$ by the trace $\gamma_D^\times$. This results is presented in the following lemma.

Lemma 2.2.1 (Hiptmair [35, Lemma 2.4]) *The mapping*

$$\gamma_D^\times : \mathcal{ND}_k(\mathcal{T}_h) \to \mathcal{RT}_k(\mathcal{K}_h), \quad \boldsymbol{u} \mapsto \boldsymbol{u} \times \boldsymbol{n}$$

is continuous and surjective. Furthermore, the degrees of freedom are transformed, i.e.,

$$\gamma_D^\times\Pi^{\mathcal{ND}_k}\boldsymbol{u} = \pi^{\mathcal{RT}_k}\gamma_D^\times\boldsymbol{u} \quad \text{for all } \boldsymbol{u} \in \mathbf{H}(\mathbf{curl}, \Omega).$$

2.2.3 Discretization of $\mathbf{H}_\perp^{-1/2}(\mathrm{curl}_\Gamma, \Gamma)$

Finally, we analyze the approximation in the space $\mathbf{H}_\perp^{-1/2}(\mathrm{curl}_\Gamma, \Gamma)$. This is the tangential trace space of $\mathbf{H}(\mathbf{curl}, \Omega)$ and also the image of $\mathbf{H}_\parallel^{-1/2}(\mathrm{div}_\Gamma, \Gamma)$ under the map $R\boldsymbol{u} := \boldsymbol{n} \times \boldsymbol{u}$. We define the space $\mathcal{TND}_k(\mathcal{K}_h)$ as the tangential trace space of $\mathcal{ND}_k(\mathcal{T}_h)$, see also Teltscher [73],

$$\mathcal{TND}_k(\mathcal{K}_h) := \gamma_D(\mathcal{ND}_k(\mathcal{T}_h|_\Gamma)).$$

Hence, we see that for the reference square $\widehat{K} = [-1, 1]^2$ there holds

$$\mathcal{TND}_k(\widehat{K}) := \mathsf{Q}_{k-1,k} \times \mathsf{Q}_{k,k-1}$$

and that $\dim \mathcal{TND}_k(\widehat{K}) = 2k(k+1)$. The basis functions can easily be calculated from the $\mathcal{ND}_k$-basis functions. For the lowest polynomial degree there holds

$$\boldsymbol{\varphi}_0 := \frac{1}{4}(1-y)\boldsymbol{e}_1, \quad \boldsymbol{\varphi}_1 := \frac{1}{4}(1+x)\boldsymbol{e}_2,$$
$$\boldsymbol{\varphi}_2 := \frac{1}{4}(1+y)\boldsymbol{e}_1, \quad \boldsymbol{\varphi}_3 := \frac{1}{4}(1-x)\boldsymbol{e}_2.$$

2.3 The de Rham diagram

In this subsection we consider the so-called de Rham diagram. It describes the mapping behavior of the differential operators **grad**, **curl** and div in the corresponding Sobolev spaces. Furthermore, we consider further properties of the canonical interpolation operators. Most of the results can be found in the articles of Hiptmair [35, 34, 37, 36].

For $\Omega \subset \mathbb{R}^3$ we consider the following **de Rham diagram**, see e.g. Monk [59]

$$H^1(\Omega) \xrightarrow{\mathbf{grad}} \mathbf{H}(\mathbf{curl}, \Omega) \xrightarrow{\mathbf{curl}} \mathbf{H}(\mathrm{div}, \Omega) \xrightarrow{\mathrm{div}} L^2(\Omega).$$

A similar result holds for homogeneous boundary conditions

$$H_0^1(\Omega) \xrightarrow{\mathbf{grad}} \mathbf{H}_0(\mathbf{curl}, \Omega) \xrightarrow{\mathbf{curl}} \mathbf{H}_0(\mathrm{div}, \Omega) \xrightarrow{\mathrm{div}} L^2(\Omega)/\mathbb{R}.$$

In these diagrams, the range of one operator is contained in the kernel of the following one. The range space of each operator is a closed subspace of the related operator with finite codimension, see Monk [59, Theorem 3.40].

The **discrete de Rham diagram** takes the following form

$$\mathcal{S}_k(\mathcal{T}_h) \xrightarrow{\mathbf{grad}} \mathcal{ND}_k(\mathcal{T}_h) \xrightarrow{\mathbf{curl}} \mathcal{RT}_k(\mathcal{T}_h) \xrightarrow{\mathrm{div}} \mathcal{S}_{k-1}(\mathcal{T}_h).$$

There also holds the following commuting diagram property, see e.g. Hiptmair [35, 34], where I_k^h denotes the canonical interpolation operator for $\mathcal{S}_k(\mathcal{T}_h)$ and $\mathcal{D}(\cdot)$ denotes the domain of the interpolation operators.

Theorem 2.3.1 *For all $k \geq 1$ the following diagram commutes*

$$
\begin{array}{ccccc}
\mathcal{D}(I_k^h) \subset H^1(\Omega) & \xrightarrow{\textbf{grad}} & \mathcal{D}(\Pi_k^h) \subset \mathbf{H}(\textbf{curl}, \Omega) & \xrightarrow{\textbf{curl}} & \mathcal{D}(\pi_k^h) \subset \mathbf{H}(\mathrm{div}, \Omega) \\
\downarrow I_k^h & & \downarrow \Pi_k^h & & \downarrow \pi_k^h \\
\mathcal{S}_k(\mathcal{T}_h) & \xrightarrow{\textbf{grad}} & \mathcal{ND}_k(\mathcal{T}_h) & \xrightarrow{\textbf{curl}} & \mathcal{RT}_k(\mathcal{T}_h)
\end{array} \qquad .
$$

This also holds true if we impose homogeneous boundary conditions.

Thus we have

$$
\textbf{curl}\, \Pi_k^h \boldsymbol{u} = \pi_k^h \,\textbf{curl}\, \boldsymbol{u} \qquad \forall \boldsymbol{u} \in \mathbf{H}(\textbf{curl}, \Omega).
$$

Furthermore, the kernels of the differential operators are preserved:

$$
\begin{aligned}
\boldsymbol{u} \in \mathcal{D}(\Pi_k^h), \textbf{curl}\, \boldsymbol{u} = 0 &\implies \textbf{curl}\, \Pi_k^h \boldsymbol{u} = 0, \\
\boldsymbol{u} \in \mathcal{D}(\pi_k^h), \mathrm{div}\, \boldsymbol{u} = 0 &\implies \mathrm{div}\, \pi_k^h \boldsymbol{u} = 0.
\end{aligned}
$$

2.4 Discrete, time dependent spaces

It is the aim of this section to present suitable spaces and operators needed to obtain the convergence analysis in Theorem 3.3.1.

Initially, we consider a partition $0 = t_0 < t_1 < t_2 < \ldots < t_N = T$ of the time interval $[0, T]$ into subintervals $I_n := (t_{n-1}, t_n]$ of length $k_n := t_n - t_{n-1}$, and associate with each time interval a triangulation $\mathcal{T}_h^n := \mathcal{T}_{h_n}$ (with tetrahedral or hexahedral elements) of Ω and an induced mesh $\mathcal{K}_{h_n}$ of triangles or quadrilaterals on the boundary Γ. We assume that $\mathcal{T}_h^n$ is quasi-uniform with mesh size $h > 0$ and shape-regular (see Ciarlet [19]). In the following we set $\boldsymbol{\mathcal{X}} := \mathbf{H}(\textbf{curl}, \Omega)$, $\boldsymbol{\mathcal{Y}} := \mathbf{H}_\parallel^{-\frac{1}{2}}(\mathrm{div}_\Gamma 0, \Gamma)$.

The spaces $L^2(I_n; \boldsymbol{\mathcal{X}})$ and $L^2(I_n; \boldsymbol{\mathcal{Y}})$ are defined in the sense of the Definition 1.5.1, i.e.,

$$
L^2(I_n; \boldsymbol{\mathcal{X}}) := \left\{ \boldsymbol{u} : I_n \mapsto \boldsymbol{\mathcal{X}}; \left(\int_{I_n} \|\boldsymbol{u}\|_{\boldsymbol{\mathcal{X}}}^2 \, dt \right)^{1/2} < \infty \right\}
$$

and

$$
L^2(I_n; \boldsymbol{\mathcal{Y}}) := \left\{ \boldsymbol{\lambda} : I_n \mapsto \boldsymbol{\mathcal{Y}}; \left(\int_{I_n} \|\boldsymbol{\lambda}\|_{\boldsymbol{\mathcal{Y}}}^2 \, dt \right)^{1/2} < \infty \right\}.
$$

As the Nédélec functions of first order, $\mathcal{ND}_1(\mathcal{T}_h)$, are used to discretize functions $\boldsymbol{u}(., t) \in \boldsymbol{\mathcal{X}}$ (see Section 2.1) and the space of divergence free Raviart-Thomas functions,

$$
\mathcal{RT}_1^0(\mathcal{K}_h) := \{ \boldsymbol{\lambda}_h \in \mathcal{RT}_1(\mathcal{K}_h), \mathrm{div}_\Gamma \boldsymbol{\lambda}_h = 0 \},
$$

are used to discretize functions $\boldsymbol{\lambda}(.,t) \in \boldsymbol{\mathcal{Y}}$ (see Section 2.2.2), the spaces

$$L^2\left(I_n; \mathcal{ND}_1(\mathcal{T}_{h_n})\right) := \left\{\boldsymbol{v} \in L^2\left(I_n; \boldsymbol{\mathcal{X}}\right); \boldsymbol{v}\left(\cdot,t\right) \in \mathcal{ND}_1(\mathcal{T}_{h_n}) \text{ a.e. } t \in I_n\right\} \tag{2.7}$$

$$L^2\left(I_n; \mathcal{RT}_1^0(\mathcal{K}_{h_n})\right) := \left\{\boldsymbol{\psi} \in L^2\left(I_n; \boldsymbol{\mathcal{Y}}\right); \boldsymbol{\psi}\left(\cdot,t\right) \in \mathcal{RT}_1^0(\mathcal{K}_{h_n}) \text{ a.e. } t \in I_n\right\} \tag{2.8}$$

define the global finite element space on $\mathcal{T}_{h_n}$ and boundary element space on $\mathcal{K}_{h_n}$ to discretize the spaces $L^2\left(I_n; \boldsymbol{\mathcal{X}}\right)$ and $L^2\left(I_n; \boldsymbol{\mathcal{Y}}\right)$, respectively.

Now, in order to achieve a fully discrete scheme applying the *discontinuos time stepping method* in Section 3.2.1, we consider the set of polynomial functions of degree l in t with coefficients in the discrete spaces $\mathcal{ND}_1(\mathcal{T}_{h_n})$ and $\mathcal{RT}_1^0(\mathcal{K}_{h_n})$ defined in I_n as

$$\mathbf{V}_h^{n,l} := \left\{\boldsymbol{v} \in L^2\left(I_n; \mathcal{ND}_1(\mathcal{T}_{h_n})\right); \boldsymbol{v}(t) = \sum_{i=0}^{l} t^i \Phi_i, \ \Phi_i \in \mathcal{ND}_1(\mathcal{T}_{h_n}), t \in I_n\right\} \quad \text{and}$$

$$\widetilde{\mathbf{V}}_h^{n,l} := \left\{\boldsymbol{\varphi} \in L^2\left(I_n; \mathcal{RT}_1^0(\mathcal{K}_{h_n})\right); \boldsymbol{\varphi}(t) = \sum_{i=0}^{l} t^i \boldsymbol{\psi}_i, \ \boldsymbol{\psi}_i \in \mathcal{RT}_1^0(\mathcal{K}_{h_n}), t \in I_n\right\}.$$

Moreover, the sets

$$W_{hn}^l := \left\{\boldsymbol{v} \in L^2\left([0,T]; \mathcal{ND}_1(\mathcal{T}_h)\right); \boldsymbol{v}|_{I_n} \in \mathbf{V}_h^{n,l}, \quad n = 1, \dots, N\right\} \quad \text{and}$$

$$\widetilde{W}_{hn}^l := \left\{\boldsymbol{\psi} \in L^2\left([0,T]; \mathcal{RT}_1^0(\mathcal{K}_h)\right); \boldsymbol{\psi}|_{I_n} \in \widetilde{\mathbf{V}}_h^{n,l}, \quad n = 1, \dots, N\right\}$$

extend the definition to the whole interval $(0,T]$. Note that a function $\boldsymbol{v} \in W_{hn}^l$ (resp. $\boldsymbol{\psi} \in \widetilde{W}_{hn}^l$) can be discontinuous at the nodal points, but has to be continuous in the time interval (t_{n-1}, t_n). Besides the initial value $\boldsymbol{v}(0)$ (resp. $\boldsymbol{\psi}(0)$) has to be specified separately since $0 \notin I_1$. In the following we consider only the cases $l = 0, 1$.

Following Eriksson *et al.* [27], we define the L^2-projection in time onto the space $\mathbf{V}^{n,l}$

$$\pi_l: \quad L^2\left(I_n; \mathcal{ND}_1(\mathcal{T}_{h_n})\right) \quad \rightarrow \quad \mathbf{V}_h^{n,l}, \quad l = 0, 1,$$

of a function $\boldsymbol{v}$ as

$$\pi_0 \boldsymbol{v} := \frac{1}{k_n} \int_{I_n} \boldsymbol{v} \, dt, \tag{2.9}$$

$$\pi_1 \boldsymbol{v} := \pi_0 \boldsymbol{v} + \frac{12}{k_n^3}\left(t - t_{n-1} - \frac{k_n}{2}\right) \int_{I_n} \left(s - t_{n-1} - \frac{k_n}{2}\right) \boldsymbol{v} \, ds$$

$$= \boldsymbol{v}_1 + \frac{t - t_{n-1}}{k_n} \boldsymbol{v}_2 \tag{2.10}$$

where

$$\boldsymbol{v}_1(\boldsymbol{x}) := \frac{1}{k_n} \int_{I_n} \left(4 - 6\frac{s - t_{n-1}}{k_n}\right) \boldsymbol{v}(\boldsymbol{x}, s) \, ds$$

$$\boldsymbol{v}_2(\boldsymbol{x}) := \frac{1}{k_n} \int_{I_n} \left(12 \frac{s - t_{n-1}}{k_n} - 6 \right) \boldsymbol{v}(\boldsymbol{x}, s) \, ds.$$

π_0 and π_1 are well-defined, since $\boldsymbol{v} \in L^2 \left(I_n; \mathcal{ND}_1(\mathcal{T}_{h_n}) \right)$ has the form

$$\boldsymbol{v}(\boldsymbol{x}, t) = \sum_{i=1}^{M} c_i(t) \, \Phi_i(\boldsymbol{x}).$$

Thus there holds, e.g.

$$\pi_0 \boldsymbol{v}(\boldsymbol{x}) = \sum_{i=1}^{M} \left(\frac{1}{k_n} \int_{I_n} c_i(t) \, dt \right) \Phi_i(\boldsymbol{x}) \in \mathbf{V}_h^{n,0}$$

where $\{\Phi_i\}_{i=1,\dots,M}$ is a basis of $\mathcal{ND}_1(\mathcal{T}_{h_n})$. In analogous form we define for $l = 0, 1$

$$\tilde{\pi}_l : L^2 \left(I_n; \mathcal{RT}_1^0(\mathcal{K}_h) \right) \to \tilde{\mathbf{V}}_h^{n,l} \quad .$$

The L^2-orthogonal projection in time is proved in the following lemma.

Lemma 2.4.1 *Let be* $\boldsymbol{v} \in L^2(I_n; \mathcal{ND}_1(\mathcal{T}_h))$ *and* $\boldsymbol{\zeta} \in L^2(I_n; \mathcal{RT}_1^0(\mathcal{K}_h))$. *Then for all* $\boldsymbol{w} \in L^2(I_n; \mathbf{L}^2(\Omega))$, $\boldsymbol{w}$ *polynomial of degree* l *in* t, *and for all* $\boldsymbol{\psi} \in L^2(I_n; \mathbf{L}^2(\Gamma))$, $\boldsymbol{\psi}$ *polynomial of degree* l *in* t:

$$\int_{I_n} (\pi_l \, \boldsymbol{v}(t), \boldsymbol{w}(t)) \, dt = \int_{I_n} (\boldsymbol{v}(t), \boldsymbol{w}(t)) \, dt, \tag{2.11}$$

$$\int_{I_n} \langle \tilde{\pi}_l \, \boldsymbol{\zeta}(t), \boldsymbol{\psi}(t) \rangle \, dt = \int_{I_n} \langle \boldsymbol{\zeta}(t), \boldsymbol{\psi}(t) \rangle \, dt \quad and \tag{2.12}$$

$$\int_{I_n} \mathcal{A}(\pi_l \, \boldsymbol{v}(t), \tilde{\pi}_l \, \boldsymbol{\zeta}(t) \, ; \, \boldsymbol{w}(t), \boldsymbol{\psi}(t)) \, dt = \int_{I_n} \mathcal{A}(\boldsymbol{v}(t), \boldsymbol{\zeta}(t) \, ; \, \boldsymbol{w}(t), \boldsymbol{\psi}(t)) \, dt, \tag{2.13}$$

where $\mathcal{A}$ *is an arbitrary bilinear form.*

Proof. In the following we prove only (2.11). For this we consider the cases $l = 0, 1$ separately. The proof of (2.12) and (2.13) is derived using the same arguments.

case $l = 0$. Using (2.9) there holds

$$\int_{I_n} (\pi_0 \, \boldsymbol{v}(t), \boldsymbol{w}(t)) \, dt = k_n \, (\pi_0 \, \boldsymbol{v}(t), \boldsymbol{w}) = k_n \left(\frac{1}{k_n} \int_{I_n} \boldsymbol{v}(t) \, dt, \boldsymbol{w} \right) = \int_{I_n} (\boldsymbol{v}(t), \boldsymbol{w}) \, dt$$

case $l = 1$. Using (2.10) there holds for all $\boldsymbol{w} \in \mathbf{L}^2(\Omega)$:

$$\int_{I_n} (\pi_1 \, \boldsymbol{v}(t), \boldsymbol{w}) \, dt = \int_{I_n} \left(\boldsymbol{v}_1 + \frac{t - t_{n-1}}{k_n} \boldsymbol{v}_2, \boldsymbol{w} \right) dt = \left(k_n \boldsymbol{v}_1 + \frac{k_n}{2} \boldsymbol{v}_2, \boldsymbol{w} \right)$$

$$= \left(\int_{I_n} \boldsymbol{v}(t) \, dt, \boldsymbol{w} \right) = \int_{I_n} (\boldsymbol{v}(t), \boldsymbol{w}) \, dt,$$

and

$$\int_{I_n} \left(\pi_1 \, \boldsymbol{v}(t), \frac{t - t_{n-1}}{k_n} \boldsymbol{w} \right) dt = \int_{I_n} \left(\boldsymbol{v}_1 + \frac{t - t_{n-1}}{k_n} \boldsymbol{v}_2, \frac{t - t_{n-1}}{k_n} \boldsymbol{w} \right) dt = \left(\frac{k_n}{2} \boldsymbol{v}_1 + \frac{k_n}{3} \boldsymbol{v}_2, \boldsymbol{w} \right)$$

$$= \left(\int_{I_n} \frac{t - t_{n-1}}{k_n} \boldsymbol{v}(t) \, dt, \boldsymbol{w} \right) = \int_{I_n} \left(\boldsymbol{v}(t), \frac{t - t_{n-1}}{k_n} \boldsymbol{w} \right) dt.$$

∎

Finally, we prove a theorem which is essential in the proof of Theorem 3.3.1. For the proof we need a duality argument.

2.4.1 A duality argument

In our FE analysis, Ω is assumed to be a simply connected polyhedral domain, not necessarily convex. Note that even for non-convex domains there holds the Helmholtz decompositions (see [36, Lemma 2.4]). In the following, we consider the Helmholtz decomposition (see [24])

$$\mathbf{H}_0(\mathbf{curl}, \Omega) = \boldsymbol{M}_0(\Omega) \oplus \boldsymbol{M}_0^{\perp}(\Omega) \tag{2.14}$$

where

$$\boldsymbol{M}_0(\Omega) := \left\{ \boldsymbol{u} \in \mathbf{L}^2(\Omega), \mathbf{curl} \, \boldsymbol{u} = 0, \boldsymbol{u}|_{\Gamma} \times \boldsymbol{n} = 0 \right\} =: \mathbf{H}_0(\mathbf{curl} \, 0, \Omega)$$

and

$$\boldsymbol{M}_0^{\perp}(\Omega) := \left\{ \boldsymbol{u} \in \mathbf{H}_0(\mathbf{curl}, \Omega), (\boldsymbol{u}, \boldsymbol{v})_{\mathbf{L}^2(\Omega)} = 0 \quad \forall \boldsymbol{v} \in \boldsymbol{M}_0(\Omega) \right\}.$$

Now, with the aim to obtain an estimate for $\|\boldsymbol{u} - \boldsymbol{U}^h\|_{\mathbf{L}^2(\Omega)}$ by using $\|\boldsymbol{u} - \boldsymbol{U}^h\|_{\mathbf{H}(\mathbf{curl}, \Omega)}$ we apply the Aubin-Nitsche trick to an auxiliary problem where $\boldsymbol{u} \in \mathbf{H}_0(\mathbf{curl}, \Omega)$, $\boldsymbol{U}^h \in \mathcal{ND}_1(\mathcal{T}_h)$ satisfies the equations

$$(\boldsymbol{u}, \boldsymbol{v})_{\Omega} + (\mathbf{curl} \, \boldsymbol{u}, \mathbf{curl} \, \boldsymbol{v})_{\Omega} = \left(\tilde{\boldsymbol{f}}, \boldsymbol{v} \right)_{\Omega} \qquad \forall \boldsymbol{v} \in \mathbf{H}_0(\mathbf{curl}, \Omega),$$

$$\left(\boldsymbol{U}^h, \boldsymbol{v}_h \right)_{\Omega} + \left(\mathbf{curl} \, \boldsymbol{U}^h, \mathbf{curl} \, \boldsymbol{v_h} \right)_{\Omega} = \left(\tilde{\boldsymbol{f}}, \boldsymbol{v}_h \right)_{\Omega} \qquad \forall \boldsymbol{v}_h \in \mathcal{ND}_1(\mathcal{T}_h).$$

For this we consider the following lemma, which remains the idea of Hiptmair [36, Theorem 5.8] and allows us to obtain necessary conditions for the proof of the a priori estimates.

Theorem 2.4.1 *For given $\tilde{\boldsymbol{f}} \in \mathbf{H}(\mathrm{div}, \Omega)$ let $\boldsymbol{u} \in \mathbf{H}_0(\mathbf{curl}, \Omega)$ be the solution of the problem*

$$\mathcal{B}(\boldsymbol{u}, \boldsymbol{v}) := (\boldsymbol{u}, \boldsymbol{v})_\Omega + (\mathbf{curl}\,\boldsymbol{u}, \mathbf{curl}\,\boldsymbol{v})_\Omega = (\tilde{\boldsymbol{f}}, \boldsymbol{v})_\Omega \qquad \forall \boldsymbol{v} \in \mathbf{H}_0(\mathbf{curl}, \Omega) \qquad (2.15)$$

and $\boldsymbol{U}^h \in \mathcal{ND}_1(\mathcal{T}_h)$ be the solution of the discrete problem

$$\left(\boldsymbol{U}^h, \boldsymbol{v}_h\right)_\Omega + \left(\mathbf{curl}\,\boldsymbol{U}^h, \mathbf{curl}\,\boldsymbol{v}_h\right)_\Omega = \left(\tilde{\boldsymbol{f}}, \boldsymbol{v}_h\right)_\Omega \qquad \forall \boldsymbol{v}_h \in \mathcal{ND}_1(\mathcal{T}_h). \qquad (2.16)$$

If $\boldsymbol{u} - \boldsymbol{U}^h \in \boldsymbol{M}_0^\perp(\Omega)$ then there exists $\frac{1}{2} < s \leq 1$ such that

$$\|\boldsymbol{u} - \boldsymbol{U}^h\|_{\mathbf{L}^2(\Omega)} \leq C\,h^s\,\|\boldsymbol{u} - \boldsymbol{U}^h\|_{\mathbf{H}(\mathbf{curl}, \Omega)} \qquad (2.17)$$

with $C > 0$ independent of h.

Proof.

We consider the error $\boldsymbol{e} := \boldsymbol{u} - \boldsymbol{U}^h$ and split $\boldsymbol{e} \in \mathbf{H}_0(\mathbf{curl}, \Omega)$ into

$$\boldsymbol{e} = \boldsymbol{e}^\perp + \boldsymbol{e}^0 \qquad (2.18)$$

where $\boldsymbol{e}^\perp \in \boldsymbol{M}_0^\perp(\Omega)$ and $\boldsymbol{e}^0 \in \boldsymbol{M}_0(\Omega)$. As the error is assumed in $\boldsymbol{M}_0^\perp(\Omega)$ we analyze the first component of the error.

Estimate for $\boldsymbol{e}^\perp$:   Define $\boldsymbol{g} \in \boldsymbol{M}_0^\perp(\Omega)$ as the solution of

$$\mathcal{B}\left(\boldsymbol{g}, \boldsymbol{v}\right) = \left(\boldsymbol{e}^\perp, \boldsymbol{v}\right)_\Omega \qquad \forall \boldsymbol{v} \in \boldsymbol{M}_0^\perp(\Omega)\,. \qquad (2.19)$$

As $\mathrm{div}\,\boldsymbol{g} = 0$, from Amrouche *et al.* [2, Proposition 3.7] we get that for some $\tilde{s} > \frac{1}{2}$ that $\boldsymbol{g} \in \mathbf{H}^{\tilde{s}}(\Omega)$, and that

$$\|\boldsymbol{g}\|_{\mathbf{H}^{\tilde{s}}(\Omega)} \leq \|\boldsymbol{g}\|_{\mathbf{H}(\mathbf{curl}, \Omega)}. \qquad (2.20)$$

Furthermore, the equation (2.19) means that $\boldsymbol{g}$ satisfies, in the sense of distributions,

$$\mathbf{curl}\,\mathbf{curl}\,\boldsymbol{g} + \boldsymbol{g} = \boldsymbol{e}^\perp \qquad \text{in } \Omega.$$

Thus, $\boldsymbol{w} = \mathbf{curl}\,\boldsymbol{g}$ fulfils $\mathbf{curl}\,\boldsymbol{w} = \boldsymbol{e}^\perp - \boldsymbol{g} \in \mathbf{L}^2(\Omega), \mathrm{div}\,\boldsymbol{w} = 0$ and $\gamma_{\boldsymbol{n}}\boldsymbol{w} = 0$. From Hiptmair [36, Lemma 4.2], we obtain that $\boldsymbol{w} \in \mathbf{H}^{s'}(\Omega)$ for some $\frac{1}{2} < s' \leq 1$ and

$$\begin{aligned}
\|\boldsymbol{w}\|_{\mathbf{H}^{s'}(\Omega)} &\leq C\left(\|\boldsymbol{w}\|_{\mathbf{L}^2(\Omega)} + \|\mathbf{curl}\,\boldsymbol{w}\|_{\mathbf{L}^2(\Omega)} + \|\mathrm{div}\,\boldsymbol{w}\|_{\mathbf{L}^2(\Omega)}\right) \\
&\leq C\left(\|\boldsymbol{g}\|_{\mathbf{H}(\mathbf{curl}, \Omega)} + \|\boldsymbol{e}^\perp\|_{\mathbf{L}^2(\Omega)}\right)\,.
\end{aligned} \qquad (2.21)$$

In the following we take $s := \min\{\tilde{s}, s'\}$.

The coercitivity and continuity of $\mathcal{B}$ guarantees the existence and uniqueness of the solution of (2.19). Then the following inf-sup condition is valid

$$\sup_{\boldsymbol{v} \in \mathbf{H}_0(\mathbf{curl}, \Omega)} \frac{|\mathcal{B}(\boldsymbol{u}, \boldsymbol{v})|}{\|\boldsymbol{v}\|_{\mathbf{H}(\mathbf{curl}, \Omega)}} \geq C'\|\boldsymbol{u}\|_{\mathbf{H}(\mathbf{curl}, \Omega)} \qquad \forall \boldsymbol{u} \in \mathbf{H}_0(\mathbf{curl}, \Omega)$$

with $C' > 0$. From this and (2.19) it follows that

$$\|\boldsymbol{g}\|_{\mathbf{H}(\mathbf{curl},\Omega)} \leq C'^{-1}\|\boldsymbol{e}^{\perp}\|_{\mathbf{L}^2(\Omega)}.$$

Combined with (2.20) and (2.21), this yields

$$\|\boldsymbol{g}\|_{\mathbf{H}^s(\Omega)} + \|\mathbf{curl}\,\boldsymbol{g}\|_{\mathbf{H}^s(\Omega)} \leq C\,\|\boldsymbol{e}^{\perp}\|_{\mathbf{L}^2(\Omega)} \tag{2.22}$$

where $C = C(\Omega) > 0$.

Due to the Galerkin orthogonality $\mathcal{B}(\boldsymbol{u} - \boldsymbol{U}^h, \boldsymbol{v}_h) = 0$, for all $\boldsymbol{v}_h \in \mathcal{ND}_1(\mathcal{T}_h)$ it follows that

$$\begin{aligned}
\|\boldsymbol{e}^{\perp}\|_{\mathbf{L}^2(\Omega)}^2 &= \mathcal{B}(\boldsymbol{g}, \boldsymbol{e}^{\perp}) = \mathcal{B}(\boldsymbol{g}, \boldsymbol{e}^{\perp} + \boldsymbol{e}^0) \\
&= \mathcal{B}(\boldsymbol{g}, \boldsymbol{u} - \boldsymbol{U}^h) \\
&= \mathcal{B}(\boldsymbol{g} - \Pi^h \boldsymbol{g}\,, \boldsymbol{u} - \boldsymbol{U}^h) \\
&\lesssim \|\boldsymbol{g} - \Pi^h \boldsymbol{g}\|_{\mathbf{H}(\mathbf{curl},\Omega)}\|\boldsymbol{u} - \boldsymbol{U}^h\|_{\mathbf{H}(\mathbf{curl},\Omega)}.
\end{aligned} \tag{2.23}$$

Due to $s > \frac{1}{2}$, the operator Π^h is well defined (c.f. Remark 2.1.1), moreover it is valid from Lemma 2.1.4 that

$$\begin{aligned}
\|\boldsymbol{g} - \Pi^h \boldsymbol{g}\|_{\mathbf{L}^2(\Omega)} &\lesssim h^s\big(\|\boldsymbol{g}\|_{\mathbf{H}^s(\Omega)} + \|\mathbf{curl}\,\boldsymbol{g}\|_{\mathbf{H}^s(\Omega)}\big), \\
\|\mathbf{curl}\,\big(\boldsymbol{g} - \Pi^h \boldsymbol{g}\big)\|_{\mathbf{L}^2(\Omega)} &\lesssim h^s\|\mathbf{curl}\,\boldsymbol{g}\|_{\mathbf{H}^s(\Omega)}.
\end{aligned}$$

Combining this with (2.22) we obtain

$$\|\boldsymbol{g} - \Pi^h \boldsymbol{g}\|_{\mathbf{H}(\mathbf{curl},\Omega)} \leq C h^s\,\|\boldsymbol{e}^{\perp}\|_{\mathbf{L}^2(\Omega)}.$$

Finally, this and (2.23) give the result for $\boldsymbol{e}^{\perp}$, i.e.,

$$\|\boldsymbol{e}^{\perp}\|_{\mathbf{L}^2(\Omega)} \lesssim h^s\|\boldsymbol{u} - \boldsymbol{U}^h\|_{\mathbf{H}(\mathbf{curl},\Omega)}. \tag{2.24}$$

∎

Remark 2.4.1 *In particular, if $\boldsymbol{u}$ is an irrotational function and $\boldsymbol{u} - \boldsymbol{U}^h \in \boldsymbol{M}_0(\Omega)$ we just get*

$$\|\boldsymbol{u} - \boldsymbol{U}^h\|_{\mathbf{H}(\mathbf{curl},\Omega)} \approx \|\boldsymbol{u} - \boldsymbol{U}^h\|_{\mathbf{L}^2(\Omega)}.$$

Thus the convergence of $\|\boldsymbol{u} - \boldsymbol{U}^h\|_{\mathbf{L}^2(\Omega)}$ is expected of the same order as $\|\boldsymbol{u} - \boldsymbol{U}^h\|_{\mathbf{H}(\mathbf{curl},\Omega)}$. In the other case the **curl** *plays a strong role and we expect a better order of convergence of $\|\boldsymbol{u} - \boldsymbol{U}^h\|_{\mathbf{L}^2(\Omega)}$ with regard to $\|\boldsymbol{u} - \boldsymbol{U}^h\|_{\mathbf{H}(\mathbf{curl},\Omega)}$.*

3 The eddy current problem

This chapter discusses a mathematical analysis for the time dependent eddy current problem. In Section 3.1 we derive a symmetric FE/BE coupling formulation for the unknowns $\boldsymbol{u} \in W^1(0, T; \mathbf{H}(\mathbf{curl}, \Omega))$, which represents the electric field in the domain Ω, and $\boldsymbol{\lambda} := \mathbf{curl}\, \boldsymbol{u} \times \boldsymbol{n} \in L^2(0, T; \mathbf{H}_\parallel^{-\frac{1}{2}}(\mathrm{div}_\Gamma 0, \Gamma))$, the twisted tangential trace of the magnetic field on the boundary. Moreover, we obtain a semi-discrete scheme using Nédélec functions of first order to approximate the electric field $\boldsymbol{u}$ in the interior of the domain and divergence free Raviart-Thomas functions to approximate the unknown $\boldsymbol{\lambda}$. Section 3.2 gives a full discretization of the problem using the *discontinuous time stepping Galerkin method* with piecewise linear test and trial functions in time. Finally, in Section 3.3 we prove an a priori estimate in Theorem 3.3.1 and an a posteriori error estimate in Theorem 3.3.2. The residual based local error indicators allow us to introduce an adaptive feedback algorithm for the mesh refinement of the coupling procedure, which is presented in Algorithm 1, Page 66.

3.1 The time dependent eddy current problem

Let $\Omega \subset \mathbb{R}^3$ be a bounded, open polyhedral domain with a Lipschitz continuous boundary $\Gamma := \partial\Omega$. We assume Ω and Γ to be simply connected and denote by $\Omega_e := \mathbb{R}^3 \setminus \overline{\Omega}$ the exterior domain and by $\boldsymbol{n}$ the unit normal vector on Γ pointing into Ω_e.
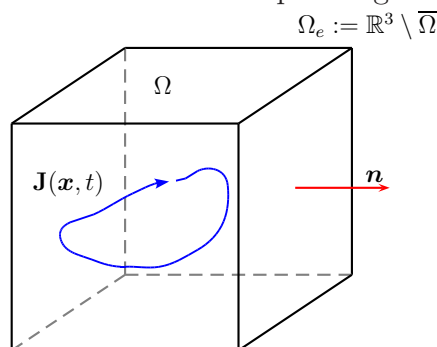
Figure 3.1: Model configuration for eddy current problem.

We consider the eddy current problem induced by a given current density $\mathbf{J}(t, \boldsymbol{x})$ in a conductor represented by the bounded domain Ω. The problem describes a submodel of

3 The eddy current problem

Maxwell's equations obtained by neglecting the displacement currents, where the electric and magnetic fields $\mathbf{E}(t, \boldsymbol{x})$ and $\mathbf{H}(t, \boldsymbol{x})$ are solutions of the following problem:

$$\mu\,\partial_t \mathbf{H} + \mathbf{curl}\,\mathbf{E} = 0 \qquad \text{in} \quad (0,T) \times \mathbb{R}^3 \,, \qquad (3.1)$$

$$\mathbf{curl}\,\mathbf{H} = \mathbf{J} + \sigma\,\mathbf{E} \qquad \text{in} \quad (0,T) \times \mathbb{R}^3 \,, \qquad (3.2)$$

$$\operatorname{div}\,\varepsilon\,\mathbf{E} = 0 \qquad \text{in} \quad \mathbb{R}^3 \setminus \overline{\Omega}\,, \qquad (3.3)$$

$$\int_\Gamma (\varepsilon\,\mathbf{E})^+ \cdot \boldsymbol{n}\,ds = 0 \qquad \text{on} \quad \Gamma, \qquad (3.4)$$

$$\mathbf{H}(0, \boldsymbol{x}) = \mathbf{H}_0(\boldsymbol{x}), \quad \mathbf{E}(0, \boldsymbol{x}) = \mathbf{E}_0(\boldsymbol{x}) \qquad \text{in} \quad \mathbb{R}^3 \,, \qquad (3.5)$$

$$[\mathbf{E} \times \boldsymbol{n}]_\Gamma = [\mathbf{H} \times \boldsymbol{n}]_\Gamma = 0 \qquad \text{on} \quad \Gamma, \qquad (3.6)$$

$$\mathbf{H}(t, \boldsymbol{x}) = \mathbf{E}(t, \boldsymbol{x}) = \mathcal{O}\left(|\boldsymbol{x}|^{-1}\right) \quad |\boldsymbol{x}| \to \infty \,. \qquad (3.7)$$

In (3.4) $(\varepsilon\,\mathbf{E})^+$ denotes the trace of $\varepsilon\,\mathbf{E}$ from Ω_e to Γ. Here, the permeability $\mu = \mu(\boldsymbol{x}) \in L^\infty(\mathbb{R}^3)$, the permittivity $\varepsilon = \varepsilon(\boldsymbol{x}) \in L^\infty(\mathbb{R}^3)$ and the conductivity $\sigma = \sigma(\boldsymbol{x}) \in L^\infty(\mathbb{R}^3)$ are real valued, bounded functions, and

$$\mu_1 \geq \mu(\boldsymbol{x}) \geq \mu_0 > 0 \quad \text{for a.e. } \boldsymbol{x} \in \Omega \text{ with} \quad \mu(\boldsymbol{x}) = \mu_0 \quad \text{in} \quad \mathbb{R}^3 \setminus \overline{\Omega}$$

$$\varepsilon_1 \geq \varepsilon(\boldsymbol{x}) \geq \varepsilon_0 > 0 \quad \text{for a.e. } \boldsymbol{x} \in \Omega \text{ with} \quad \varepsilon(\boldsymbol{x}) = \varepsilon_0 \quad \text{in} \quad \mathbb{R}^3 \setminus \overline{\Omega}$$

$$\sigma_1 \geq \sigma(\boldsymbol{x}) \geq \sigma_0 > 0 \quad \text{for a.e. } \boldsymbol{x} \in \Omega \text{ with} \quad \sigma(\boldsymbol{x}) = 0 \quad \text{in} \quad \mathbb{R}^3 \setminus \overline{\Omega}$$

where μ_i, σ_i, and ε_i $(i = 0, 1)$, are positive constants.

We assume that $\operatorname{supp}(\mathbf{J}) \subset \Omega$. Thus, there holds $\mathbf{J} = 0$ in Ω_e and $\mathbf{J} \cdot \boldsymbol{n} = 0$ on Γ, i.e., no current flows through Γ. In Ω_e, as $\sigma \equiv 0$ equation (3.2) becomes $\mathbf{curl}\,\mathbf{H} = 0$. Hence, $\mathbf{E}$ cannot be uniquely determined in Ω_e and requires the further gauging condition $\operatorname{div}(\varepsilon\,\mathbf{E}) = 0$, known as **Coulomb gauge condition**. The transmission conditions (3.6) result from requiring $\mathbf{E}, \mathbf{H} \in \mathbf{L}^2_{loc}(\mathbb{R}^3)$ and the radiation condition (3.7) follows from the Silver Müller conditions (see [20, (6.19)]).

Remark 3.1.1 *If Γ is connected, the condition (3.4) is changed by*

$$\int_{\Gamma_i} (\varepsilon\,\mathbf{E}) \cdot \boldsymbol{n}\,ds = 0 \quad \forall \Gamma_i, \quad i = 1, \cdots, N,$$

where Γ_i, $i = 1, \cdots, N$, are the connected components of Γ.

3.1.1 Symmetric FE/BE Coupling

In the following we obtain an $\mathbf{E}$-based symmetric FE/BE coupling for the problem (3.1) - (3.7). For this we set $\mathcal{X} := \mathbf{H}(\mathbf{curl}, \Omega)$, $\mathcal{Y} := \mathbf{H}_\|^{-\frac{1}{2}}(\operatorname{div}_\Gamma 0, \Gamma)$ and $\boldsymbol{u} := \mathbf{E} \in W^1(0, T; \mathbf{H}(\mathbf{curl}, \Omega))$.

By taking the rotational of equation (3.1) in the bounded domain Ω, we obtain

$$\partial_t\left(\mathbf{curl\,H}\right) + \mathbf{curl}\left(\mu^{-1}\,\mathbf{curl\,}u\right) = 0 \qquad \text{in} \quad (0,T) \times \Omega. \tag{3.8}$$

Now, inserting (3.2) in (3.8) and testing with a function $v \in \mathbf{H}(\mathbf{curl},\Omega)$ yields

$$(\partial_t\mathbf{J}, v)_\Omega + (\sigma\partial_t u, v)_\Omega + \left(\mathbf{curl}\left(\mu^{-1}\,\mathbf{curl\,}u\right), v\right)_\Omega = 0. \tag{3.9}$$

Integration by parts of the third term on the left hand side leads to

$$(\sigma\partial_t u, v)_\Omega + \left(\mu^{-1}\,\mathbf{curl\,}u, \mathbf{curl\,}v\right)_\Omega - \left\langle \gamma_N^- u, \gamma_D^- v\right\rangle_\Gamma = -\left(\partial_t\mathbf{J}, v\right)_\Omega, \tag{3.10}$$

where $\gamma_D{}^-$ and $\gamma_N{}^-$ are the traces on Γ from Ω defined in (1.2) and (1.8), respectively.

In the exterior domain Ω_e, we observe from (3.1), (3.2) and (3.3) that $\mathbf{curl\,curl\,}u = 0$ and $\mathrm{div}\ u = 0$ gives

$$\Delta u = \mathbf{grad}\,\mathrm{div}\ u - \mathbf{curl\,curl\,}u = 0 \quad \text{in } \Omega_e, \text{ for a.e. } t \in (0,T).$$

Therefore, u is given by the Stratton-Chu representation formula, see (1.29),

$$\begin{aligned}
u(x) = \ &\mathbf{curl}\int_\Gamma (n \times u)(y)\Phi(x,y)ds(y) + \int_\Gamma (n \times \mathbf{curl\,}u)(y)\Phi(x,y)ds(y) \\
&- \mathbf{grad}\int_\Gamma (n \cdot u)(y)\Phi(x,y)dS(y), \qquad x \in \Omega_e,
\end{aligned} \tag{3.11}$$

where $\Phi(x,y) = \dfrac{1}{4\pi}\|x - y\|^{-1}$ denotes the Laplace kernel.

Then, taking traces, we obtain for x tending to Γ the jump relations

$$\gamma_D^+ u = \mathcal{K}(\gamma_D^+ u) - \mathcal{V}(\gamma_N^+ u) - \gamma_D^+\mathbf{grad}\int_\Gamma (n \cdot u)(y)\Phi(x,y)ds(y), \tag{3.12}$$

$$\gamma_N^+ u = \mathcal{W}\left(\gamma_D^+ u\right) - \widetilde{\mathcal{K}}\left(\gamma_N^+ u\right), \tag{3.13}$$

with the limits $\gamma_D^+ u$ and $\gamma_N^+ u$ from Ω_e onto Γ of the traces $\gamma_D u$ and $\gamma_N u$, and the integral operators $\mathcal{K}$, $\widetilde{\mathcal{K}}$, $\mathcal{V}$ and $\mathcal{W}$ defined in (1.16) - (1.19).

(1.4) yields for the third term of the right hand side of (3.12):

$$\mathbf{grad}_\Gamma V(\gamma_n^+ u) = \gamma_D^+\mathbf{grad}\int_\Gamma (n \cdot u)(y)\Phi(x,y)ds(y),$$

and applying to this the duality between the surface gradient and the surface divergence (see Page 5) with $\vartheta \in \mathcal{Y}$ we get

$$\left\langle \mathbf{grad}_\Gamma V(\gamma_n u), \vartheta\right\rangle_\Gamma = -\left\langle V(\gamma_n u), \mathrm{div}_\Gamma\,\vartheta\right\rangle_\Gamma = 0.$$

Thus, testing (3.12) with a function $\zeta \in \mathcal{Y}$ we obtain

$$\left\langle (I - \mathcal{K})\gamma_D^+ u, \zeta\right\rangle_\Gamma + \left\langle \mathcal{V}\gamma_N^+ u, \zeta\right\rangle_\Gamma = 0. \tag{3.14}$$

Choosing $\boldsymbol{u}_\Gamma := \gamma_D \boldsymbol{u}$ and $\boldsymbol{\lambda} := \gamma_N \boldsymbol{u} = \mathbf{curl}\,\boldsymbol{u} \times \boldsymbol{n}$, we consider the interface conditions (3.6), i.e., $[\gamma_N \boldsymbol{u}] = [\gamma_D \boldsymbol{u}] = 0$ on Γ, and inserting the integral equation (3.13) into (3.10), and adding the integral equation (3.14) there follows the **weak formulation**:

Find $\boldsymbol{u} \in W^1(0, T; \boldsymbol{\mathcal{X}}), \boldsymbol{\lambda} \in L^2(0, T; \boldsymbol{\mathcal{Y}})$ *such that*

$$(\sigma \partial_t \boldsymbol{u}, \boldsymbol{v})_\Omega + \left(\mu^{-1}\,\mathbf{curl}\,\boldsymbol{u}, \mathbf{curl}\,\boldsymbol{v}\right)_\Omega - \langle \mathcal{W}\boldsymbol{u}_\Gamma, \boldsymbol{v}_\Gamma \rangle_\Gamma + \left\langle \widetilde{\mathcal{K}}\boldsymbol{\lambda}, \boldsymbol{v}_\Gamma \right\rangle_\Gamma = -\,(\partial_t \mathbf{J}, \boldsymbol{v})_\Omega\,,$$

$$\langle (I - \mathcal{K})\boldsymbol{u}_\Gamma, \boldsymbol{\zeta} \rangle_\Gamma + \langle \mathcal{V}\boldsymbol{\lambda}, \boldsymbol{\zeta} \rangle_\Gamma = 0, \tag{3.15}$$

$$\boldsymbol{u}(\cdot, 0) = \boldsymbol{u}_0|_\Omega, \ \ \boldsymbol{\lambda}(\cdot, 0) = \boldsymbol{n} \times \mathbf{curl}\,\boldsymbol{u}_0|_\Gamma$$

for all $\boldsymbol{v} \in \boldsymbol{\mathcal{X}}$ *and* $\boldsymbol{\zeta} \in \boldsymbol{\mathcal{Y}}$ *and almost all* $t \in (0, T)$.

Remark 3.1.2 *Lemma 1.5.2 shows that the initial condition* $\boldsymbol{u}(\cdot, 0) = \boldsymbol{u}_0|_\Omega$ *is appropriate due to the continuous embedding*

$$W^1(0, T; \mathbf{H}(\mathbf{curl}, \Omega)) \hookrightarrow \mathcal{C}^0(0, T \,;\, \mathbf{L}^2(\Omega))\,.$$

In order to obtain a coercive bilinear form, we now add a penalty function term $\tilde{\lambda}\,(\boldsymbol{u}, \boldsymbol{v})_\Omega$ to the left-hand side of (3.15), for arbitrary $\tilde{\lambda} \in \mathbb{R}^+$. Introducing the bilinear form

$$\mathcal{B}(\boldsymbol{u}, \boldsymbol{\lambda}; \boldsymbol{v}, \boldsymbol{\zeta}) := \tilde{\lambda}\,(\boldsymbol{u}, \boldsymbol{v})_\Omega + \left(\mu^{-1}\,\mathbf{curl}\,\boldsymbol{u}, \mathbf{curl}\,\boldsymbol{v}\right)_\Omega - \langle \mathcal{W}\boldsymbol{u}_\Gamma, \boldsymbol{v}_\Gamma \rangle_\Gamma + \left\langle \widetilde{\mathcal{K}}\boldsymbol{\lambda}, \boldsymbol{v}_\Gamma \right\rangle_\Gamma$$
$$+ \langle (I - \mathcal{K})\boldsymbol{u}_\Gamma, \boldsymbol{\zeta} \rangle_\Gamma + \langle \mathcal{V}\boldsymbol{\lambda}, \boldsymbol{\zeta} \rangle_\Gamma\,, \tag{3.16}$$

and the linear form

$$\mathcal{L}(\boldsymbol{v}) = \mathcal{L}(t, \boldsymbol{v}) := -\,(\partial_t \mathbf{J}, \boldsymbol{v})_\Omega \tag{3.17}$$

we obtain the **penalty weak formulation**:

Find $\boldsymbol{u} \in W^1(0, T; \boldsymbol{\mathcal{X}}), \boldsymbol{\lambda} \in L^2(0, T; \boldsymbol{\mathcal{Y}})$ *such that*

$$(\sigma\,\dot{\boldsymbol{u}}, \boldsymbol{v})_\Omega + \mathcal{B}(\boldsymbol{u}, \boldsymbol{\lambda}; \boldsymbol{v}, \boldsymbol{\zeta}) = \mathcal{L}(\boldsymbol{v}), \tag{3.18a}$$

$$\boldsymbol{u}(\cdot, 0) = \boldsymbol{u}_0|_\Omega, \quad \boldsymbol{\lambda}(\cdot, 0) = \boldsymbol{n} \times \mathbf{curl}\,\boldsymbol{u_0}|_\Gamma\,. \tag{3.18b}$$

for all $\boldsymbol{v} \in \boldsymbol{\mathcal{X}}$ *and* $\boldsymbol{\zeta} \in \boldsymbol{\mathcal{Y}}$, *almost all* $t \in (0, T)$ *and* $\tilde{\lambda} > 0$ *given.*

Lemma 3.1.1 ([37, Theorem 7.1]) *The bilinear form* $\mathcal{B}$ *is elliptic and continuous in* $\boldsymbol{\mathcal{X}} := \mathbf{H}(\mathbf{curl}, \Omega) \times \mathbf{H}_\|^{-\frac{1}{2}}(\mathrm{div}_\Gamma 0, \Gamma).$

Proof. The continuity is an immediate consequence of the continuity of the boundary integral operators (see Lemma 1.3.2), and the uniform boundedness of μ and σ in the

domain Ω. Lemma 1.3.3 shows that the operators $\mathcal{V}$ and $\mathcal{W}$ are elliptic, and that the operator $\widetilde{\mathcal{K}}$ is adjoint to $\mathcal{K} - \mathcal{I}$. Therefore we get

$$
\begin{aligned}
|\mathcal{B}(\boldsymbol{u}, \boldsymbol{\lambda}; \boldsymbol{u}, \boldsymbol{\lambda})| &= \left| \tilde{\lambda} \left(\boldsymbol{u}, \boldsymbol{u}\right)_\Omega + \left(\mu^{-1} \operatorname{\mathbf{curl}} u, \operatorname{\mathbf{curl}} u\right)_\Omega - \langle \mathcal{W} u_\Gamma, u_\Gamma \rangle_\Gamma \right. \\
&\quad \left. + \left\langle \widetilde{\mathcal{K}} \boldsymbol{\lambda}, \boldsymbol{u}_\Gamma \right\rangle_\Gamma + \langle (I - \mathcal{K}) u_\Gamma, \boldsymbol{\lambda} \rangle_\Gamma + \langle \mathcal{V} \boldsymbol{\lambda}, \boldsymbol{\lambda} \rangle_\Gamma \right| \\
&= \left| \tilde{\lambda} \left(\boldsymbol{u}, \boldsymbol{u}\right)_\Omega + \left(\mu^{-1} \operatorname{\mathbf{curl}} u, \operatorname{\mathbf{curl}} u\right)_\Omega - \langle \mathcal{W} u_\Gamma, u_\Gamma \rangle_\Gamma + \langle \mathcal{V} \boldsymbol{\lambda}, \boldsymbol{\lambda} \rangle_\Gamma \right| \\
&\gtrsim \left(\boldsymbol{u}, \boldsymbol{u}\right)_\Omega + \left(\operatorname{\mathbf{curl}} u, \operatorname{\mathbf{curl}} u\right)_\Omega + \| \operatorname{curl}_\Gamma u_\Gamma \|^2_{H^{-1/2}(\Gamma)} + \| \boldsymbol{\lambda} \|^2_{\mathbf{H}_\|^{-\frac{1}{2}}(\operatorname{div}_\Gamma, \Gamma)} \\
&\gtrsim \| \boldsymbol{u} \|^2_{\mathbf{H}(\operatorname{\mathbf{curl}}, \Omega)} + \| \boldsymbol{\lambda} \|^2_{\mathbf{H}_\|^{-\frac{1}{2}}(\operatorname{div}_\Gamma, \Gamma)} \quad .
\end{aligned}
$$

∎

3.1.2 A semi-discrete Galerkin method

Let $\mathcal{T}_h$ be a triangulation (with tetrahedral or hexahedral elements) of the domain Ω. We assume that $\mathcal{T}_h$ is quasi-uniform with mesh size $h > 0$ and shape-regular in the sense of Ciarlet [19], i.e., there exists a positive constant c_1 such that

$$
\frac{h_\mathfrak{T}}{\rho_\mathfrak{T}} \leq c_1 \qquad \forall \mathfrak{T} \in \mathcal{T}_h
$$

where $h_\mathfrak{T}$ is diameter of element $\mathfrak{T} \in \mathcal{T}_h$ and

$$
\rho_\mathfrak{T} := \max \left\{ r : S_r \subseteq \mathfrak{T}, S_r := \{ \boldsymbol{x} : \| \boldsymbol{x} - \boldsymbol{x}_0 \| < r, \boldsymbol{x}_0 \in \mathfrak{T} \} \right\} \quad .
$$

This mesh induces a mesh $\mathcal{K}_h := \{ \mathfrak{T} \cap \Gamma : \mathfrak{T} \in \mathcal{T}_h \}$ of triangles or quadrilaterals on the boundary. On these meshes we define our polynomial spaces.

We consider Nédélec functions of first order $\mathcal{ND}_1(\mathcal{T}_h)$, a conforming finite element space of $\mathbf{H}(\operatorname{\mathbf{curl}}, \Omega)$, for the discretization of the unknown $\boldsymbol{u} := \boldsymbol{u}(t, \boldsymbol{x})$ with $\boldsymbol{u} \in W^1(0, T; \mathbf{H}(\operatorname{\mathbf{curl}}, \Omega))$, see Section 2.1. Furthermore for the discretization of $\boldsymbol{\lambda} := \boldsymbol{\lambda}(t, \boldsymbol{x}) = \operatorname{\mathbf{curl}} u \times n$, with $\boldsymbol{\lambda} \in L^2(0, T; \mathbf{H}_\|^{-\frac{1}{2}}(\operatorname{div}_\Gamma 0, \Gamma))$, we use the space of divergence free Raviart-Thomas functions $\mathcal{RT}_1^0(\mathcal{K}_h) := \{ \boldsymbol{\lambda}_h \in \mathcal{RT}_1(\mathcal{K}_h), \operatorname{div}_\Gamma \boldsymbol{\lambda}_h = 0 \}$ a conforming finite element space of $\mathbf{H}_\|^{-\frac{1}{2}}(\operatorname{div}_\Gamma 0, \Gamma)$, see Section 2.2.2.

Then the semi-discrete Galerkin system reads:

Find $\boldsymbol{U}^h(t) \in \mathcal{ND}_1(\mathcal{T}_h)$, $\boldsymbol{\lambda}^h(t) \in \mathcal{RT}_1^0(\mathcal{K}_h)$ such that

$$
\left(\sigma \dot{\boldsymbol{U}}^h, \boldsymbol{v}^h \right)_\Omega + \mathcal{B}(\boldsymbol{U}^h, \boldsymbol{\lambda}^h; \boldsymbol{v}^h, \boldsymbol{\zeta}^h) = - \left(\partial_t \mathbf{J}, \boldsymbol{v}^h \right)_\Omega \tag{3.19}
$$

for all $\boldsymbol{v}^h \in \mathcal{ND}_1(\mathcal{T}_h)$, $\boldsymbol{\zeta}^h \in \mathcal{RT}_1^0(\mathcal{K}_h)$, $0 < t \leq T$ subject to the initial conditions

$$
\boldsymbol{U}^h(\cdot, 0) = \boldsymbol{u}_0 \in \mathcal{ND}_1(\mathcal{T}_h) \quad \text{and} \quad \boldsymbol{\lambda}^h(\cdot, 0) = \boldsymbol{\lambda}_0 \in \mathcal{RT}_1^0(\mathcal{K}_h) \quad .
$$

Here $\boldsymbol{u}_0$ and $\boldsymbol{\lambda}_0$ are the L^2-projections of $\boldsymbol{u}(\boldsymbol{x}, 0)$ and $\boldsymbol{\lambda}(\boldsymbol{x}, 0)$ into the spaces $\mathcal{ND}_1(\mathcal{T}_h)$ and $\mathcal{RT}_1^0(\mathcal{K}_h)$, respectively.

3.2 A fully-discrete coupling method

In order to obtain a fully-discrete scheme for (3.18), we consider a piecewise polynomial approximation in time for the unknowns using the discontinuos Galerkin method.

Let $\mathcal{X}_T := \left(W^1(0, T; \mathbf{H}(\mathbf{curl}, \Omega)), L^2(0, T; \mathbf{H}_{\parallel}^{-\frac{1}{2}}(\mathrm{div}_\Gamma 0, \Gamma)) \right)$. The discontinuous Galerkin method is based on an approximation of the solution $(\boldsymbol{u}, \boldsymbol{\lambda}) \in \mathcal{X}_T$ of (3.18a) sought as a piecewise polynomial test and trial function in t of degree at most l, which is not necessarily continuous at the nodes of the chosen partition of the time interval $[0, T]$, $T > 0$.

3.2.1 The discontinuous Galerkin method

In the following we denote by $\{\Phi_k\}_{k=1,\ldots,M}$ a basis of $\mathcal{ND}_1(\mathcal{T}_h)$ and by $\{\boldsymbol{\psi}_k\}_{k=1,\ldots,m}$ a basis of $\mathcal{RT}_1^0(\mathcal{K}_h)$. Then the discrete function $\boldsymbol{U}^h(\boldsymbol{x}) \in \mathcal{ND}_1(\mathcal{T}_h)$ can be represented as a linear combination of the basis functions, i.e., $\boldsymbol{U}^h = \boldsymbol{U}^h(\boldsymbol{x}) := \sum_{i=1}^{M} \boldsymbol{U}_i^h \Phi_i(\boldsymbol{x}) \in \mathcal{ND}_1(\mathcal{T}_h)$. Without loss of generality we identify the function $\boldsymbol{U}^h$ with the vector $\boldsymbol{U}^h := (\boldsymbol{U}_i^h)_{i=1,\ldots,M}$. Analogously we identify the function $\boldsymbol{\lambda}^h = \boldsymbol{\lambda}^h(\boldsymbol{x}) := \sum_{i=1}^{M} \boldsymbol{\lambda}_i^h \boldsymbol{\psi}_i(\boldsymbol{x}) \in \mathcal{RT}_1^0(\mathcal{K}_h)$ with the vector $\boldsymbol{\lambda}^h = (\boldsymbol{\lambda}_i^h)_{i=1,\ldots,m}$.

We consider a partition $0 = t_0 < t_1 < t_2 < \ldots < t_N = T$ of the time interval $[0, T]$ into subintervals $I_n := (t_{n-1}, t_n]$ of length $k_n := t_n - t_{n-1}$, and associate with each time interval a triangulation $\mathcal{T}_h^n := \mathcal{T}_{h_n}$ (with tetrahedral or hexahedral elements) of Ω and an induced mesh $\mathcal{K}_{h_n}$ of triangles or quadrilaterals on the boundary Γ. We assume that $\mathcal{T}_h^n$ is quasi-uniform with mesh size $h > 0$ and shape-regular.

For the fully-discrete scheme we use the following finite dimensional subspaces (see Section 2.4)

$$\mathbf{V}_h^{n,l} = \left\{ \boldsymbol{v} : I_n \to \mathcal{ND}_1(\mathcal{T}_{h_n}) \,,\, \boldsymbol{v}(t) = \sum_{i=0}^{l} t^i \Phi_i \,,\, \Phi_i \in \mathcal{ND}_1(\mathcal{T}_{h_n}), \, t \in I_n \right\},$$

$$\widetilde{\mathbf{V}}_h^{n,l} = \left\{ \boldsymbol{\varphi} : I_n \to \mathcal{RT}_1^0(\mathcal{K}_{h_n}) \,,\, \boldsymbol{\varphi}(t) = \sum_{i=0}^{l} t^i \boldsymbol{\psi}_i \,,\, \boldsymbol{\psi}_i \in \mathcal{RT}_1^0(\mathcal{K}_{h_n}), \, t \in I_n \right\},$$

and

$$W_{hn}^l = \{ \boldsymbol{v} \,;\, \boldsymbol{v}|_{I_n} \in \mathbf{V}_h^{n,l} \text{ for } n = 1, \ldots, N \},$$

$$\widetilde{W}_{hn}^l = \{\boldsymbol{\psi} \,;\, \boldsymbol{\psi}|_{I_n} \in \widetilde{\mathbf{V}}_h^{n,l} \text{ for } n = 1, \dots, N\}\,.$$

Note that a function $\boldsymbol{v} \in W_{hn}^l$ (resp. $\boldsymbol{\psi} \in \widetilde{W}_{hn}^l$) can be discontinuous at the nodal points, but has to be continuous in the time interval (t_{n-1}, t_n). Besides the initial value $\boldsymbol{v}(0)$ (resp. $\boldsymbol{\psi}(0)$) has to be specified separately since $0 \notin I_1$.

Now, defining

$$\boldsymbol{v}_n^+ := \lim_{t\to 0+} \boldsymbol{v}(t_n + t)\,, \quad \boldsymbol{v}_n^- := \lim_{t\to 0-} \boldsymbol{v}(t_n + t) \quad \text{and} \quad [\boldsymbol{v}]_n := \boldsymbol{v}_n^+ - \boldsymbol{v}_n^-$$

the **discontinuous Galerkin method** reads

Find $\boldsymbol{U}^h \in W_{hn}^l$ and $\boldsymbol{\lambda}^h \in \widetilde{W}_{hn}^l$ such that

$$\int_0^T \left\{ (\sigma \dot{\boldsymbol{U}}^h, \boldsymbol{v}) + \mathcal{B}(\boldsymbol{U}^h, \boldsymbol{\lambda}^h; \boldsymbol{v}, \boldsymbol{\zeta}) \right\} dt + \sum_{n=2}^N ([\sigma \boldsymbol{U}^h]_{n-1}, \boldsymbol{v}_{n-1}^+) + (\sigma \boldsymbol{U}_0^{h^+}, \boldsymbol{v}_0^+)$$

$$= (\sigma \boldsymbol{U}_0^{h^-}, \boldsymbol{v}_0^+) + \int_0^T \mathcal{L}(\boldsymbol{v})\, dt$$

for all $\boldsymbol{v} \in W_{hn}^l$ and all $\boldsymbol{\zeta} \in \widetilde{W}_{hn}^l$, where $\boldsymbol{U}_0^{h^-} := \boldsymbol{u}_0$.

This formulation is equivalent to:

For $n = 1, \dots, N$, find $\boldsymbol{U}_n^h \in \mathbf{V}_h^{n,l}$ and $\boldsymbol{\lambda}_n^h \in \widetilde{\mathbf{V}}_h^{n,l}$ such that

$$\int_{I_n} \left\{ (\sigma \dot{\boldsymbol{U}}_n^h, \boldsymbol{v}) + \mathcal{B}(\boldsymbol{U}^h, \boldsymbol{\lambda}_n^h; \boldsymbol{v}, \boldsymbol{\zeta}) \right\} dt + (\sigma [\boldsymbol{U}^h]_{n-1}, \boldsymbol{v}_{n-1}^+) = \int_{I_n} \mathcal{L}(\boldsymbol{v})\, dt\,. \qquad (3.20)$$

for all $\boldsymbol{v} \in \mathbf{V}_h^{n,l}$ and all $\boldsymbol{\zeta} \in \widetilde{\mathbf{V}}_h^{n,l}$.

In the following we consider the case of constant ($l = 0$) and linear ($l = 1$) basis functions in time.

Piecewise constant in time ($l = 0$)

Here the test and trial functions are piecewise constant in the time intervall I_n, $n = 1, \dots, N$. Thus $\dot{\boldsymbol{U}}_n^h \equiv 0$, $\boldsymbol{U}_{n-1}^{h^+} = \boldsymbol{U}_n^h$, $\boldsymbol{U}_{n-1}^{h^-} = \boldsymbol{U}_{n-1}^h$, $\boldsymbol{v}_{n-1}^+ = \boldsymbol{v}$ and (3.20) reduces to:

For $n = 1, \dots, N$, find $\boldsymbol{U}_n^h \in \mathcal{ND}_1(\mathcal{T}_{h_n})$ and $\boldsymbol{\lambda}_n^h \in \mathcal{RT}_1^0(\mathcal{K}_{h_n})$ such that

$$k_n\, \mathcal{B}(\boldsymbol{U}_n^h, \boldsymbol{\lambda}_n^h; \boldsymbol{v}, \boldsymbol{\zeta}) + (\sigma \boldsymbol{U}_n^h, \boldsymbol{v}) = (\sigma \boldsymbol{U}_{n-1}^h, \boldsymbol{v}) + \int_{I_n} \mathcal{L}(\boldsymbol{v})\, dt, \qquad (3.21)$$

for all $\boldsymbol{v} \in \mathcal{ND}_1(\mathcal{T}_{h_n})$ and all $\boldsymbol{\zeta} \in \mathcal{RT}_1^0(\mathcal{K}_{h_n})$.

This is a variant of the backward Euler method (see Luskin[42]). In matrix form this is equivalent to:

$$\begin{pmatrix} (\tilde{\lambda} + \frac{\sigma}{k_n})\mathcal{M} + \mathcal{R}^* - \mathcal{W} & \mathcal{C} \\ \mathcal{B} & \mathcal{V} \end{pmatrix} \begin{pmatrix} \boldsymbol{U}_n^h \\ \boldsymbol{\lambda}_n^h \end{pmatrix} = \begin{pmatrix} \widetilde{F}_1 \\ 0 \end{pmatrix} \tag{3.22}$$

with

$$\widetilde{F}_1 := \frac{\sigma}{k_n}\mathcal{M}\,\boldsymbol{U}_{n-1}^{h^-} + \frac{1}{k_n}\mathcal{F}$$

and

$$\mathcal{M}_{ij} := (\Phi_i, \Phi_j), \qquad\qquad \mathcal{R}_{ij}^* := (\mu^{-1}\,\mathbf{curl}\,\Phi_i, \mathbf{curl}\,\Phi_j),$$

$$\mathcal{F}_i := \left(\int_{I_n} -\partial_t \mathbf{J}\, dt, \Phi_i\right), \qquad\qquad \mathcal{W}_{ij} := \langle \mathcal{W}(\gamma_D \Phi_i), \gamma_D \Phi_j\rangle,$$

$$\mathcal{B}_{ij} := \langle (I - \mathcal{K})\gamma_D \Phi_i, \boldsymbol{\psi}_j\rangle, \qquad\qquad \mathcal{C}_{ij} := \langle \widetilde{\mathcal{K}}(\gamma_N \boldsymbol{\psi}_i), \gamma_D \Phi_j\rangle,$$

$$\mathcal{V}_{ij} := \langle \mathcal{V}\boldsymbol{\psi}_i, \boldsymbol{\psi}_j\rangle,$$

where $\{\Phi_k\}_{k=1,\dots,M}$ is a basis of $\mathcal{ND}_1(\mathcal{T}_{h_n})$ and $\{\boldsymbol{\psi}_k\}_{k=1,\dots,m}$ a basis of $\mathcal{RT}_1^0(\mathcal{K}_{h_n})$.

Piecewise linear in time ($l = 1$)

In this case we consider piecewise linear test and trial functions on the time intervall I_n. We may write the trial functions $\boldsymbol{U}_n^h(\boldsymbol{x}, t)$ and $\boldsymbol{\lambda}_n^h(\boldsymbol{x}, t)$ as

$$\boldsymbol{U}_n^h(\boldsymbol{x}, t) := \boldsymbol{U}_{n,1}^h(\boldsymbol{x}) + \frac{t - t_{n-1}}{k_n}\boldsymbol{U}_{n,2}^h(\boldsymbol{x}),$$

$$\boldsymbol{\lambda}_n^h(\boldsymbol{x}, t) := \boldsymbol{\lambda}_{n,1}^h(\boldsymbol{x}) + \frac{t - t_{n-1}}{k_n}\boldsymbol{\lambda}_{n,2}^h(\boldsymbol{x})$$

for some $\boldsymbol{U}_{n,1}^h, \boldsymbol{U}_{n,2}^h \in \mathcal{ND}_1(\mathcal{T}_{h_n})$ and $\boldsymbol{\lambda}_{n,1}^h, \boldsymbol{\lambda}_{n,2}^h \in \mathcal{RT}_1^0(\mathcal{K}_{h_n})$.

Let $\Phi(\boldsymbol{x})$ denote an arbitrary basis function of $\mathcal{ND}_1(\mathcal{T}_{h_n})$, thus our test functions are defined by

$$\Phi_1(\boldsymbol{x}, t) := \Phi(\boldsymbol{x}) \qquad \text{and} \qquad \Phi_2(\boldsymbol{x}, t) := \frac{t_n - t}{k_n}\Phi(\boldsymbol{x})$$

and respectively for $\boldsymbol{\psi}$, an arbitrary basis function of $\mathcal{RT}_1^0(\mathcal{K}_{h_n})$.

Considering the test and trial functions above defined, we get

$$\begin{aligned}
\frac{1}{k_n}\int_{I_n}(\boldsymbol{U}_n^h, \Phi_1)\,dt &= \frac{1}{k_n}\int_{I_n}\left(\boldsymbol{U}_{n,1}^h(\boldsymbol{x}) + \frac{t - t_{n-1}}{k_n}\boldsymbol{U}_{n,2}^h(\boldsymbol{x}), \Phi\right)dt \\
&= \frac{1}{k_n}\int_{I_n}\left(\boldsymbol{U}_{n,1}^h(\boldsymbol{x}), \Phi\right)dt + \frac{1}{k_n}\int_{I_n}\frac{t - t_{n-1}}{k_n}\left(\boldsymbol{U}_{n,2}^h(\boldsymbol{x}), \Phi\right)dt \\
&= \frac{1}{k_n}\left(\boldsymbol{U}_{n,1}^h(\boldsymbol{x}), \Phi\right)\int_{I_n}dt + \frac{1}{k_n}\left(\boldsymbol{U}_{n,2}^h(\boldsymbol{x}), \Phi\right)\int_{I_n}\frac{t - t_{n-1}}{k_n}\,dt \\
&= (\boldsymbol{U}_{n,1}^h, \Phi) + \frac{1}{2}(\boldsymbol{U}_{n,2}^h, \Phi)
\end{aligned}$$

and

$$\frac{1}{k_n}\int_{I_n}(\boldsymbol{U}_n^h, \Phi_2)\,dt = \frac{1}{k_n}\int_{I_n}\left(\boldsymbol{U}_{n,1}^h(\boldsymbol{x}) + \frac{t - t_{n-1}}{k_n}\boldsymbol{U}_{n,2}^h(\boldsymbol{x}), \frac{t_n - t}{k_n}\Phi(\boldsymbol{x})\right)dt$$

$$= \frac{1}{k_n}\int_{I_n}\frac{t_n - t}{k_n}\left(\boldsymbol{U}_{n,1}^h(\boldsymbol{x}), \Phi\right)dt + \frac{1}{k_n}\int_{I_n}\left(\frac{t - t_{n-1}}{k_n}\right)\left(\frac{t_n - t}{k_n}\right)\left(\boldsymbol{U}_{n,2}^h(\boldsymbol{x}), \Phi\right)dt$$

$$= \frac{1}{k_n^2}\left(\boldsymbol{U}_{n,1}^h(\boldsymbol{x}), \Phi\right)\int_{I_n}(t_n - t)\,dt + \frac{1}{k_n^3}\left(\boldsymbol{U}_{n,2}^h(\boldsymbol{x}), \Phi\right)\int_{I_n}(t - t_{n-1})(t_n - t)\,dt$$

$$= \frac{1}{2}(\boldsymbol{U}_{n,1}^h, \Phi) + \frac{1}{6}(\boldsymbol{U}_{n,2}^h, \Phi)\,.$$

Analogously, we obtain the following identities

$$\int_{I_n}(\dot{\boldsymbol{U}}^h, \Phi_1)\,dt = (\boldsymbol{U}_{n,2}^h, \Phi)\,, \qquad \int_{I_n}(\dot{\boldsymbol{U}}^h, \Phi_2)\,dt = \frac{1}{2}(\boldsymbol{U}_{n,2}^h, \Phi)$$

$$\text{and} \qquad (\boldsymbol{U}_{n-1}^{h^+}, \Phi_{1,n-1}^+) = (\boldsymbol{U}_{n-1}^{h^+}, \Phi_{2,n-1}^+) = (\boldsymbol{U}_{n,1}^h, \Phi)\,.$$

Then (3.20) reduces to

For $n = 1, \ldots, N$, find $\boldsymbol{U}_{n,1}^h, \boldsymbol{U}_{n,2}^h \in \mathcal{ND}_1(\mathcal{T}_{h_n})$ and $\boldsymbol{\lambda}_{n,1}^h, \boldsymbol{\lambda}_{n,2}^h \in \mathcal{RT}_1^0(\mathcal{K}_{h_n})$, such that

$$\mathcal{B}(\boldsymbol{U}_{n,1}^h, \boldsymbol{\lambda}_{n,1}^h; \boldsymbol{v}, \boldsymbol{\zeta}) + \frac{1}{k_n}(\sigma\boldsymbol{U}_{n,1}^h, \boldsymbol{v}) + \frac{1}{2}\mathcal{B}(\boldsymbol{U}_{n,2}^h, \boldsymbol{\lambda}_{n,2}^h; \boldsymbol{v}, \boldsymbol{\zeta}) + \frac{1}{k_n}(\sigma\boldsymbol{U}_{n,2}^h, \boldsymbol{v}) =$$

$$= \frac{1}{k_n}(\sigma\boldsymbol{U}_{n-1}^{h^-}, \boldsymbol{v}) + \frac{1}{k_n}\int_{I_n}\mathcal{L}(\boldsymbol{v})\,dt \tag{3.23}$$

and

$$\frac{1}{2}\mathcal{B}(\boldsymbol{U}_{n,1}^h, \boldsymbol{\lambda}_{n,1}^h; \boldsymbol{v}, \boldsymbol{\zeta}) + \frac{1}{k_n}(\sigma\boldsymbol{U}_{n,1}^h, \boldsymbol{v}) + \frac{1}{6}\mathcal{B}(\boldsymbol{U}_{n,2}^h, \boldsymbol{\lambda}_{n,2}^h; \boldsymbol{v}, \boldsymbol{\zeta}) + \frac{1}{2k_n}(\sigma\boldsymbol{U}_{n,2}^h, \boldsymbol{v}) =$$

$$= \frac{1}{k_n}(\sigma\boldsymbol{U}_{n-1}^{h^-}, \boldsymbol{v}) + \frac{1}{k_n}\int_{I_n}\frac{t_n - t}{k_n}\mathcal{L}(\boldsymbol{v})\,dt \tag{3.24}$$

for all $\boldsymbol{v} \in \mathcal{ND}_1(\mathcal{T}_{h_n})$ and all $\boldsymbol{\zeta} \in \mathcal{RT}_1^0(\mathcal{K}_{h_n})$.

We observe that (3.23) and (3.24) are equivalent to the following linear system of equations:

$$\left(\begin{array}{cc|cc} \left(\tilde{\lambda}+\frac{\sigma}{k_n}\right)\mathcal{M}+\mathcal{R}^*-\mathcal{W} & \mathcal{C} & \left(\frac{\tilde{\lambda}}{2}+\frac{\sigma}{k_n}\right)\mathcal{M}+\frac{1}{2}\mathcal{R}^*-\frac{1}{2}\mathcal{W} & \frac{1}{2}\mathcal{C} \\ \mathcal{B} & \mathcal{V} & \frac{1}{2}\mathcal{B} & \frac{1}{2}\mathcal{V} \\ \hline \left(\frac{\tilde{\lambda}}{2}+\frac{\sigma}{k_n}\right)\mathcal{M}+\frac{1}{2}\mathcal{R}^*-\frac{1}{2}\mathcal{W} & \frac{1}{2}\mathcal{C} & \left(\frac{\tilde{\lambda}}{6}+\frac{\sigma}{2k_n}\right)\mathcal{M}+\frac{1}{6}\mathcal{R}^*-\frac{1}{6}\mathcal{W} & \frac{1}{6}\mathcal{C} \\ \frac{1}{2}\mathcal{B} & \frac{1}{2}\mathcal{V} & \frac{1}{6}\mathcal{B} & \frac{1}{6}\mathcal{V} \end{array}\right)\left(\begin{array}{c} \boldsymbol{U}_{n,1}^h \\ \boldsymbol{\lambda}_{n,1}^h \\ \boldsymbol{U}_{n,2}^h \\ \boldsymbol{\lambda}_{n,2}^h \end{array}\right) = \left(\begin{array}{c} \widetilde{F}_1 \\ 0 \\ \widetilde{F}_2 \\ 0 \end{array}\right) \tag{3.25}$$

where

$$\widetilde{F}_1 := \frac{\sigma}{k_n}\mathcal{M}\,\boldsymbol{U}_{n-1}^{h^-} + \frac{1}{k_n}\mathcal{F}_1\,, \qquad \widetilde{F}_2 := \frac{\sigma}{k_n}\mathcal{M}\,\boldsymbol{U}_{n-1}^{h^-} + \frac{1}{k_n^2}\mathcal{F}_2\,,$$

3 The eddy current problem

$$(\mathcal{F}_1)_i := \left(\int_{I_n} -\partial_t \mathbf{J}\, dt, \Phi_i\right), \qquad (\mathcal{F}_2)_i := \left(\int_{I_n} (t_n - t)\partial_t \mathbf{J}\, dt, \Phi_i\right), \qquad i = 1, \dots, M,$$

and the matrices $\mathcal{M}$, $\mathcal{R}^*$, $\mathcal{W}$, $\mathcal{V}$, $\mathcal{C}$ and $\mathcal{B}$ are defined on Page 42.

Furthermore, Lemma 1.3.3 shows that $\widetilde{\mathcal{K}}$ is adjoint to $\mathcal{K} - I$, hence this is equivalent to:

$$\left(\begin{array}{cc|cc} \left(\tilde\lambda + \frac{\sigma}{kn}\right)\mathcal{M} + \mathcal{R}^* - \mathcal{W} & -\mathcal{B}^\top & \left(\frac{\tilde\lambda}{2} + \frac{\sigma}{kn}\right)\mathcal{M} + \frac{1}{2}\mathcal{R}^* - \frac{1}{2}\mathcal{W} & -\frac{1}{2}\mathcal{B}^\top \\ \mathcal{B} & \mathcal{V} & \frac{1}{2}\mathcal{B} & \frac{1}{2}\mathcal{V} \\ \hline \left(\frac{\tilde\lambda}{2} + \frac{\sigma}{kn}\right)\mathcal{M} + \frac{1}{2}\mathcal{R}^* - \frac{1}{2}\mathcal{W} & -\frac{1}{2}\mathcal{B}^\top & \left(\frac{\tilde\lambda}{6} + \frac{\sigma}{2kn}\right)\mathcal{M} + \frac{1}{6}\mathcal{R}^* - \frac{1}{6}\mathcal{W} & -\frac{1}{6}\mathcal{B}^\top \\ \frac{1}{2}\mathcal{B} & \frac{1}{2}\mathcal{V} & \frac{1}{6}\mathcal{B} & \frac{1}{6}\mathcal{V} \end{array}\right) \left(\begin{array}{c} \boldsymbol{U}_{n,1}^h \\ \boldsymbol{\lambda}_{n,1}^h \\ \boldsymbol{U}_{n,2}^h \\ \boldsymbol{\lambda}_{n,2}^h \end{array}\right) = \left(\begin{array}{c} \widetilde{F}_1 \\ 0 \\ \widetilde{F}_2 \\ 0 \end{array}\right).$$

Rearranging the variables, we finally obtain

$$\left(\begin{array}{cc|cc} \left(\tilde\lambda + \frac{\sigma}{kn}\right)\mathcal{M} + \mathcal{R}^* - \mathcal{W} & \left(\frac{\tilde\lambda}{2} + \frac{\sigma}{kn}\right)\mathcal{M} + \frac{1}{2}\mathcal{R}^* - \frac{1}{2}\mathcal{W} & -\mathcal{B}^\top & -\frac{1}{2}\mathcal{B}^\top \\ \left(\frac{\tilde\lambda}{2} + \frac{\sigma}{kn}\right)\mathcal{M} + \frac{1}{2}\mathcal{R}^* - \frac{1}{2}\mathcal{W} & \left(\frac{\tilde\lambda}{6} + \frac{\sigma}{2kn}\right)\mathcal{M} + \frac{1}{6}\mathcal{R}^* - \frac{1}{6}\mathcal{W} & -\frac{1}{2}\mathcal{B}^\top & -\frac{1}{6}\mathcal{B}^\top \\ \hline \mathcal{B} & \frac{1}{2}\mathcal{B} & \mathcal{V} & \frac{1}{2}\mathcal{V} \\ \frac{1}{2}\mathcal{B} & \frac{1}{6}\mathcal{B} & \frac{1}{2}\mathcal{V} & \frac{1}{6}\mathcal{V} \end{array}\right) \left(\begin{array}{c} \boldsymbol{U}_{n,1}^h \\ \boldsymbol{U}_{n,2}^h \\ \boldsymbol{\lambda}_{n,1}^h \\ \boldsymbol{\lambda}_{n,2}^h \end{array}\right) = \left(\begin{array}{c} \widetilde{F}_1 \\ \widetilde{F}_2 \\ 0 \\ 0 \end{array}\right).$$
$$(3.26)$$

Lemma 3.2.1 *The fully-discrete system in* (3.20) *has a unique solution.*

Proof. Let us define the Galerkin matrix as

$$\mathcal{A} := \begin{pmatrix} \widehat{\mathcal{M}} & -\widehat{\mathcal{B}}^\top \\ \widehat{\mathcal{B}} & \widehat{\mathcal{V}} \end{pmatrix}$$

where $\widehat{\mathcal{M}} \in \mathbb{R}^{2M \times 2M}$, $\widehat{\mathcal{V}} \in \mathbb{R}^{2m \times 2m}$, $-\widehat{\mathcal{B}}^\top \in \mathbb{R}^{2M \times 2m}$ and $\widehat{\mathcal{B}} \in \mathbb{R}^{2m \times 2M}$.

Notice that $\boldsymbol{u} \in \mathbf{H}(\mathbf{curl}, \Omega)$ yields

$$(\boldsymbol{u}, \boldsymbol{u})_\Omega \geq 0, \quad (\mathbf{curl}\,\boldsymbol{u}, \mathbf{curl}\,\boldsymbol{u})_\Omega \geq 0 \quad , (\boldsymbol{u}, \boldsymbol{u})_\Omega + (\mathbf{curl}\,\boldsymbol{u}, \mathbf{curl}\,\boldsymbol{u})_\Omega \geq c\|\boldsymbol{u}\|_{\mathbf{H}(\mathbf{curl}, \Omega)},$$

and from Lemma 1.3.3 there exists $c_\mathcal{V} > 0$ and $c_\mathcal{W} > 0$ such that

$$\langle \mathcal{V}\boldsymbol{u}, \boldsymbol{u}\rangle_\Gamma \geq c_\mathcal{V} \|\boldsymbol{u}\|_{\mathbf{H}_\parallel^{-1/2}(\mathrm{div}_\Gamma, \Gamma)}^2 \quad \forall\, \boldsymbol{u} \in \mathbf{H}_\parallel^{-1/2}(\mathrm{div}_\Gamma\, 0, \Gamma)\,,$$

$$-\langle \mathcal{W}\boldsymbol{u}, \boldsymbol{u}\rangle_\Gamma \geq c_\mathcal{W} \|\mathrm{curl}_\Gamma\,\boldsymbol{u}\|_{H^{-1/2}(\Gamma)}^2 \quad \forall\, \boldsymbol{u} \in \mathbf{H}_\perp^{-1/2}(\mathrm{curl}_\Gamma, \Gamma)\,.$$

We obtain that the mass matrix $\mathcal{M}$ is positive definite, the stiffness matrix $\mathcal{R}^*$ and the matrix $-\mathcal{W}$ are positive semi-definite and $\mathcal{V}$ is positive definite, hence $\widehat{\mathcal{M}}$ and $\widehat{\mathcal{V}}$ are positive definite. Then, the Galerkin matrix $\mathcal{A}$ is positive definite and thus the linear system (3.26) has a unique solution. ∎

3.3 Error analysis

3.3.1 A priori estimate

The following Lemma gives us a necessary outcome for the proof of the convergence analysis of the fully-discrete system (3.20).

Lemma 3.3.1 *Given $\boldsymbol{u} \in \mathbf{H}^s(\Omega)$ and $\operatorname{\mathbf{curl}} \boldsymbol{u} \in \mathbf{H}^s(\Omega)$ for $s > \frac{1}{2}$. Let $\boldsymbol{z}_1 \in \mathcal{ND}_1(\mathcal{T}_h)$ and $\boldsymbol{z}_2 \in \mathcal{RT}_1^0(\mathcal{K}_h)$ be defined by the elliptic projection, i.e.,*

$$\mathcal{B}(\boldsymbol{u}, \boldsymbol{\lambda}; \boldsymbol{v}_h, \boldsymbol{\psi}_h) = \mathcal{B}(\boldsymbol{z}_1, \boldsymbol{z}_2; \boldsymbol{v}_h, \boldsymbol{\psi}_h) \qquad \forall\, \boldsymbol{v}_h \in \mathcal{ND}_1(\mathcal{T}_h)\,,\, \boldsymbol{\psi}_h \in \mathcal{RT}_1^0(\mathcal{K}_h)\,.$$

Then, there are positive constants γ_1 and γ_2 depending only on the geometry and the material parameters σ and μ, such that

$$\|\boldsymbol{u} - \boldsymbol{z}_1\|_{\mathbf{L}^2(\Omega)} \leq \gamma_1\, h^r \left[\|\boldsymbol{u}\|_{\mathbf{H}^s(\Omega)} + \|\operatorname{\mathbf{curl}} \boldsymbol{u}\|_{\mathbf{H}^s(\Omega)}\right], \tag{3.27}$$

$$\|\boldsymbol{\lambda} - \boldsymbol{z}_2\|_{\mathbf{H}_\parallel^{-\frac{1}{2}}(\operatorname{div}_\Gamma,\Gamma)} \leq \gamma_2\, h^{r_0} \left[\|\operatorname{\mathbf{curl}} \boldsymbol{u}\|_{\mathbf{H}^s(\Omega)} + \|\operatorname{\mathbf{curl}}\operatorname{\mathbf{curl}} \boldsymbol{u}\|_{\mathbf{H}^s(\Omega)}\right] \tag{3.28}$$

where $r_0 := \min\{s, 1\}$, $r := \alpha + r_0$, $\alpha \in \left(\frac{1}{2}, 1\right]$, if $\boldsymbol{u} - \boldsymbol{z}_1 \in \boldsymbol{M}_0^\perp(\Omega)$ (see (2.17)), else $\alpha = 0$.

Proof. Since $\boldsymbol{z}_1$ is an orthogonal projection of $\boldsymbol{u}$ in $\mathcal{ND}_1(\mathcal{T}_h)$ relative to the bilinear form $\mathcal{B}$ defined in (3.16), it follows that

$$\|\boldsymbol{u} - \boldsymbol{z}_1\|_{\mathbf{H}(\operatorname{\mathbf{curl}},\Omega)} \leq \|\boldsymbol{u} - \Pi^h \boldsymbol{u}\|_{\mathbf{H}(\operatorname{\mathbf{curl}},\Omega)} \tag{3.29}$$

where Π^h is the canonical interpolation operator for the space $\mathcal{ND}_1(\mathcal{T}_h)$ presented in Section 2.1.4. The operator Π^h is well defined on the space

$$\left\{\boldsymbol{v} \in (L^p(K))^3; \operatorname{curl} \boldsymbol{v} \in (L^p(K))^3; \boldsymbol{v} \times \boldsymbol{n} \in (L^p(K))^2, K \in \mathcal{T}_h\right\},$$

for any $p > 2$, see Amrouche *et al.* [2, Lemma 4.7]. For Π^h there holds the estimate (see Lemma 2.1.4)

$$\|\boldsymbol{u} - \Pi^h \boldsymbol{u}\|_{\mathbf{H}(\operatorname{\mathbf{curl}},\Omega)} \leq \tilde{\gamma}\, h^{\min\{s,1\}} \left\{\|\boldsymbol{u}\|_{\mathbf{H}^s(\Omega)} + \|\operatorname{\mathbf{curl}} \boldsymbol{u}\|_{\mathbf{H}^s(\Omega)}\right\} \tag{3.30}$$

where $\tilde{\gamma}$ is a positive constant depending only on the shape-regularity of the mesh. Now if $\boldsymbol{u} - \boldsymbol{z}_1 \in \boldsymbol{M}_0^\perp(\Omega)$, due to the Theorem 2.4.1 there exist $C > 0$ and $\frac{1}{2} < \alpha \leq 1$ such that

$$\|\boldsymbol{u} - \boldsymbol{z}_1\|_{\mathbf{L}^2(\Omega)} \leq Ch^\alpha \|\boldsymbol{u} - \boldsymbol{z}_1\|_{\mathbf{H}(\operatorname{\mathbf{curl}},\Omega)}\,. \tag{3.31}$$

Combining the inequalities (3.29),(3.30) and (3.31) proves (3.27).

The inequality (3.28) follows by

$$
\begin{aligned}
\left\|\boldsymbol{\lambda} - \boldsymbol{z}_2\right\|_{\mathbf{H}_{\|}^{-\frac{1}{2}}(\mathrm{div}_\Gamma, \Gamma)}
&= \left\|\gamma_D^\times \operatorname{\mathbf{curl}} \boldsymbol{u} - \boldsymbol{z}_2\right\|_{\mathbf{H}_{\|}^{-\frac{1}{2}}(\mathrm{div}_\Gamma, \Gamma)} \\
&\leq \left\|\gamma_D^\times \operatorname{\mathbf{curl}} \boldsymbol{u} - \gamma_D^\times \Pi^h \operatorname{\mathbf{curl}} \boldsymbol{u}\right\|_{\mathbf{H}_{\|}^{-\frac{1}{2}}(\mathrm{div}_\Gamma, \Gamma)} \\
&\leq \left\|\operatorname{\mathbf{curl}} \boldsymbol{u} - \Pi^h \operatorname{\mathbf{curl}} \boldsymbol{u}\right\|_{\mathbf{H}(\mathbf{curl}, \Omega)} \\
&\lesssim h^{r_0} \left[\| \operatorname{\mathbf{curl}} \boldsymbol{u}\|_{\mathbf{H}^s(\Omega)} + \| \operatorname{\mathbf{curl}} \operatorname{\mathbf{curl}} \boldsymbol{u}\|_{\mathbf{H}^s(\Omega)}\right] ,
\end{aligned}
\tag{3.32}
$$

with $r_0 := \min\{s, 1\}$. The second inequality is due to Hiptmair [37, p. 58] ∎

Remark 3.3.1 *In our examples in chapter 4 we get different convergence rates depending on whether the function is divergence-free or not. In example 4.2.1 we consider a non divergence-free function, and in example 4.2.2 we have a divergence-free function. As predicted in (3.27) the convergence rate in the first example is less than in the second example.*

Now, we can proof a converge theorem for our fully-discrete system. The ideas of the proof are similar to the ideas of Theorem 4.4 in Mund [60].

Theorem 3.3.1 *For some time interval $[0, T]$, with $(0, T] := \bigcup_{n=1}^N (t_{n-1}, t_n]$ and $t_n := nk = n\frac{T}{N}$, let $(\boldsymbol{u}, \boldsymbol{\lambda})$ denote the solution of (3.15) and $(\boldsymbol{U}^h, \boldsymbol{\lambda}^h)$ the solution of (3.20). Then there holds for $\boldsymbol{u} \in C^1([0, T]; \mathbf{H}^s(\mathbf{curl}, \Omega)) \cap C^3([0, T]; \mathbf{L}^2(\Omega))$, $s > \frac{1}{2}$*

$$
\max_{1 \leq n \leq N} \|(\boldsymbol{U}^h - \boldsymbol{u})(t_n^-)\|_{L^2(\Omega)} = \mathcal{O}(h^r + k^{l+1}) ,
\tag{3.33}
$$

$$
\left\|\boldsymbol{U}^h - \boldsymbol{u}\right\|_{L^2(0,T\,;\,\mathbf{H}(\mathbf{curl},\Omega))} = \mathcal{O}(h^{r_0} + k^{l+1}) ,
\tag{3.34}
$$

$$
\left\|\boldsymbol{\lambda} - \boldsymbol{\lambda}^h\right\|_{L^2(0,T\,;\,\mathbf{H}_{\|}^{-\frac{1}{2}}(\mathrm{div}_\Gamma, \Gamma))} = \mathcal{O}(h^{r_0} + k^{l+1}) ,
\tag{3.35}
$$

where $l = 0, 1$ and $r := \alpha + \min\{s, 1\}$, $r_0 := \min\{s, 1\}$ with $\alpha > \frac{1}{2}$.

Proof.

Throughout this proof we use for brevity $\| \cdot \| := \| \cdot \|_{\mathbf{L}^2(\Omega)}$ and $\| \cdot \|_{\sigma, \Omega}^2 := (\sigma \cdot, \cdot)$.

We define $\boldsymbol{z}_1 \in L^2([0, T]; \mathcal{N}\mathcal{D}_1(\mathcal{T}_h))$ and $\boldsymbol{z}_2 \in L^2([0, T]; \mathcal{R}\mathcal{T}_1^0(\mathcal{K}_h))$ through the elliptic projection

$$
\mathcal{B}(\boldsymbol{u}(t), \boldsymbol{\lambda}(t)\,;\,\boldsymbol{w}, \boldsymbol{\psi}) = \mathcal{B}(\boldsymbol{z}_1(t), \boldsymbol{z}_2(t)\,;\,\boldsymbol{w}, \boldsymbol{\psi})
\tag{3.36}
$$

for all $\boldsymbol{w} \in \mathcal{N}\mathcal{D}_1(\mathcal{T}_h)$, $\boldsymbol{\psi} \in \mathcal{R}\mathcal{T}_1^0(\mathcal{K}_h)$, $t \in [0, T]$ and the bilinear form $\mathcal{B}$ defined in (3.16).

As $\boldsymbol{u} \in C^3([0, T], \mathbf{L}^2(\Omega))$, we note that $\boldsymbol{z}_1 \in C^3([0, T], \mathcal{N}\mathcal{D}_1(\mathcal{T}_h))$. Moreover, for $i = 1, 2, 3$ and for all $t \in [0, T]$ there holds

$$
\mathcal{B}(\frac{\partial^i}{\partial t^i}\,\boldsymbol{u}(t), \boldsymbol{\lambda}(t)\,;\,\boldsymbol{w}, \boldsymbol{\psi}) = \mathcal{B}(\frac{\partial^i}{\partial t^i}\,\boldsymbol{z}_1(t), \boldsymbol{z}_2(t)\,;\,\boldsymbol{w}, \boldsymbol{\psi})
\tag{3.37}
$$

for all $\boldsymbol{w} \in \mathcal{ND}_1(\mathcal{T}_h)$, $\boldsymbol{\psi} \in \mathcal{RT}_1^0(\mathcal{K}_h)$ and $t \in [0,T]$. Let $I_n := (t_{n-1}, t_n]$ denote the nth-time subinterval, and $\pi_l \, \boldsymbol{z}_1|_{I_n}$ and $\widetilde{\pi}_l \, \boldsymbol{z}_2|_{I_n}$ the L^2-orthogonal projections of z_i into the discrete spaces $\mathbf{V}_h^{n,l}$ and $\widetilde{\mathbf{V}}_h^{n,l}$. For all $\boldsymbol{w} \in \mathbf{V}_h^{n,l}$, $\boldsymbol{\psi} \in \widetilde{\mathbf{V}}_h^{n,l}$, (2.13) and (3.36) yield

$$\int_{I_n} \mathcal{B}(\pi_l \, \boldsymbol{z}_1 - \boldsymbol{u}, \widetilde{\pi}_l \, \boldsymbol{z}_2 - \boldsymbol{\lambda} \, ; \, \boldsymbol{w}, \boldsymbol{\psi}) \, dt$$

$$= \int_{I_n} \mathcal{B}(\pi_l \, \boldsymbol{z}_1 - \boldsymbol{z}_1, \widetilde{\pi}_l \, \boldsymbol{z}_2 - \boldsymbol{z}_2 \, ; \, \boldsymbol{w}, \boldsymbol{\psi}) \, dt + \int_{I_n} \mathcal{B}(\boldsymbol{z}_1 - \boldsymbol{u}, \boldsymbol{z}_2 - \boldsymbol{\lambda} \, ; \, \boldsymbol{w}, \boldsymbol{\psi}) \, dt = 0 \, . \quad (3.38)$$

Choosing $\boldsymbol{\xi} := \left(\boldsymbol{U}^h - \pi_l \, \boldsymbol{z}_1\right)|_{I_n}$ and $\boldsymbol{\eta} := \left(\pi_l \, \boldsymbol{z}_1 - \boldsymbol{u}\right)|_{I_n}$, the error $\boldsymbol{e} := \left(\boldsymbol{U}^h - \boldsymbol{u}\right)|_{I_n}$ can be written as $\boldsymbol{e} = \boldsymbol{\xi} + \boldsymbol{\eta}$, and we observe that

$$\|(\boldsymbol{U}^h - \boldsymbol{u})(t_n^-)\| \le \|\boldsymbol{\xi}_n^-\| + \|\boldsymbol{\eta}_n^-\| \, . \quad (3.39)$$

Furthermore,

$$\int_{I_n} \left((\sigma \, \dot{\boldsymbol{\xi}}, \boldsymbol{w}) + \mathcal{B}(\boldsymbol{\xi}, \boldsymbol{\lambda}^h - \widetilde{\pi}_l \, \boldsymbol{z}_2 \, ; \, \boldsymbol{w}, \boldsymbol{\psi}) \right) dt + (\sigma \, \boldsymbol{\xi}_{n-1}^+, \boldsymbol{w}_{n-1}^+)$$

$$= \int_{I_n} \left((\sigma \, \dot{\boldsymbol{U}}^h, \boldsymbol{w}) + \mathcal{B}(\boldsymbol{U}^h, \boldsymbol{\lambda}^h; \boldsymbol{w}, \boldsymbol{\psi}) \right) dt + (\sigma \, \boldsymbol{U}_{n-1}^{h+}, \boldsymbol{w}_{n-1}^+)$$

$$- \int_{I_n} \left((\sigma \, \frac{\partial}{\partial t} \pi_l \, \boldsymbol{z}_1, \boldsymbol{w}) + \mathcal{B}(\pi_l \, \boldsymbol{z}_1, \widetilde{\pi}_l \, \boldsymbol{z}_2 \, ; \, \boldsymbol{w}, \boldsymbol{\psi}) \right) dt - (\sigma \, \pi_l \, \boldsymbol{z}_{1,n-1}^+, \boldsymbol{w}_{n-1}^+).$$

From this we get using (3.20), (3.38) and (3.18a)

$$\int_{I_n} \left((\sigma \, \dot{\boldsymbol{\xi}}, \boldsymbol{w}) + \mathcal{B}(\boldsymbol{\xi}, \boldsymbol{\lambda}^h - \widetilde{\pi}_l \, \boldsymbol{z}_2 \, ; \, \boldsymbol{w}, \boldsymbol{\psi}) \right) dt + (\sigma \, \boldsymbol{\xi}_{n-1}^+, \boldsymbol{w}_{n-1}^+)$$

$$= (\sigma \, \boldsymbol{U}_{n-1}^{h-}, \boldsymbol{w}_{n-1}^+) + \int_{I_n} \mathcal{L}(\boldsymbol{w}) \, dt$$

$$- \int_{I_n} \left((\sigma \, \frac{\partial}{\partial t} \pi_l \, \boldsymbol{z}_1, \boldsymbol{w}) + \mathcal{B}(\boldsymbol{u}, \boldsymbol{\lambda}; \boldsymbol{w}, \boldsymbol{\psi}) \right) dt - (\sigma \, \pi_l \, \boldsymbol{z}_{1,n-1}^+, \boldsymbol{w}_{n-1}^+)$$

$$= \left(\sigma \, (\boldsymbol{U}^h - \boldsymbol{u})_{n-1}^-, \boldsymbol{w}_{n-1}^+ \right) + \int_{I_n} \left((\sigma \, \dot{\boldsymbol{u}}, \boldsymbol{w}) + \mathcal{B}(\boldsymbol{u}, \boldsymbol{\lambda}; \boldsymbol{w}, \boldsymbol{\psi}) \right) dt + (\sigma \, \boldsymbol{u}_{n-1}^+, \boldsymbol{w}_{n-1}^+)$$

$$- \int_{I_n} \left((\sigma \, \frac{\partial}{\partial t} \pi_l \, \boldsymbol{z}_1, \boldsymbol{w}) + \mathcal{B}(\boldsymbol{u}, \boldsymbol{\lambda}; \boldsymbol{w}, \boldsymbol{\psi}) \right) dt - (\sigma \, \pi_l \, \boldsymbol{z}_{1,n-1}^+, \boldsymbol{w}_{n-1}^+)$$

$$= - \int_{I_n} (\sigma \, \dot{\boldsymbol{\eta}}, \boldsymbol{w}) \, dt - (\sigma \, \boldsymbol{\eta}_{n-1}^+, \boldsymbol{w}_{n-1}^+) + \left(\sigma \, (\boldsymbol{U}^h - \boldsymbol{u})_{n-1}^-, \boldsymbol{w}_{n-1}^+ \right)$$

$$= - \int_{I_n} (\sigma \, \dot{\boldsymbol{\eta}}, \boldsymbol{w}) \, dt - (\sigma \, [\boldsymbol{\eta}]_{n-1}, \boldsymbol{w}_{n-1}^+) + (\sigma \, \boldsymbol{\xi}_{n-1}^-, \boldsymbol{w}_{n-1}^+) \, .$$

Now, choosing $\boldsymbol{w} := \boldsymbol{\xi}$ and $\boldsymbol{\psi} := \boldsymbol{\lambda}^h|_{I_n} - \widetilde{\pi}_l \, \boldsymbol{z}_2|_{I_n}$ it follows

$$\int_{I_n} (\sigma \, \dot{\boldsymbol{\xi}}, \boldsymbol{\xi}) \, dt + (\sigma \, \boldsymbol{\xi}_{n-1}^+, \boldsymbol{\xi}_{n-1}^+) + \int_{I_n} \mathcal{B}(\boldsymbol{\xi}, \boldsymbol{\lambda}^h - \widetilde{\pi}_l \, \boldsymbol{z}_2 \, ; \, \boldsymbol{\xi}, \boldsymbol{\lambda}^h - \widetilde{\pi}_l \, \boldsymbol{z}_2) \, dt$$

$$\le - \int_{I_n} (\sigma \, \dot{\boldsymbol{\eta}}, \boldsymbol{\xi}) \, dt - (\sigma \, [\boldsymbol{\eta}]_{n-1}, \boldsymbol{\xi}_{n-1}^+) + (\sigma \, \boldsymbol{\xi}_{n-1}^-, \boldsymbol{\xi}_{n-1}^+) \, .$$

3 The eddy current problem

From this and the identities

$$\int_{I_n} (\sigma\,\dot{\boldsymbol{\xi}}, \boldsymbol{\xi})\,dt = \frac{1}{2}\|\boldsymbol{\xi}_n^-\|_{\sigma,\Omega}^2 - \frac{1}{2}\|\boldsymbol{\xi}_{n-1}^+\|_{\sigma,\Omega}^2,$$

$$(\sigma\,\boldsymbol{\xi}_{n-1}^+, \boldsymbol{\xi}_{n-1}^+) - (\sigma\,\boldsymbol{\xi}_{n-1}^-, \boldsymbol{\xi}_{n-1}^+) = \frac{1}{2}\|\boldsymbol{\xi}_{n-1}^+\|_{\sigma,\Omega}^2 + \frac{1}{2}\|[\boldsymbol{\xi}]_{n-1}\|_{\sigma,\Omega}^2 - \frac{1}{2}\|\boldsymbol{\xi}_{n-1}^-\|_{\sigma,\Omega}^2$$

(3.40)

we get

$$\frac{1}{2}\|\boldsymbol{\xi}_n^-\|_{\sigma,\Omega}^2 - \frac{1}{2}\|\boldsymbol{\xi}_{n-1}^-\|_{\sigma,\Omega}^2 + \frac{1}{2}\|[\boldsymbol{\xi}]_{n-1}\|_{\sigma,\Omega}^2 + \int_{I_n} \mathcal{B}(\boldsymbol{\xi}, \boldsymbol{\lambda}^h - \widetilde{\pi}_l\,\boldsymbol{z}_2\,;\, \boldsymbol{\xi}, \boldsymbol{\lambda}^h - \widetilde{\pi}_l\,\boldsymbol{z}_2)\,dt$$

$$\leq -\int_{I_n} (\sigma\,\dot{\boldsymbol{\eta}}, \boldsymbol{\xi})\,dt - (\sigma\,[\boldsymbol{\eta}]_{n-1}, \boldsymbol{\xi}_{n-1}^+)\,.$$

(3.41)

Note that $\mathcal{B}(\boldsymbol{\xi}, \boldsymbol{\lambda}^h - \widetilde{\pi}_l\,\boldsymbol{z}_2\,;\, \boldsymbol{\xi}, \boldsymbol{\lambda}^h - \widetilde{\pi}_l\,\boldsymbol{z}_2) \geq 0$. From this we obtain

$$\frac{1}{2}\|\boldsymbol{\xi}_n^-\|_{\sigma,\Omega}^2 - \frac{1}{2}\|\boldsymbol{\xi}_{n-1}^-\|_{\sigma,\Omega}^2 + \frac{1}{2}\|[\boldsymbol{\xi}]_{n-1}\|_{\sigma,\Omega}^2 \leq -\int_{I_n} (\sigma\,\dot{\boldsymbol{\eta}}, \boldsymbol{\xi})\,dt - (\sigma\,[\boldsymbol{\eta}]_{n-1}, \boldsymbol{\xi}_{n-1}^+)\,.$$

(3.42)

Next we consider two different cases of polynomial degree l.

Case $l = 0$

As $\boldsymbol{\xi}$ is constant on I_n there holds $\boldsymbol{\xi} = \boldsymbol{\xi}_n = \boldsymbol{\xi}_{n-1}^+$, and due to (3.42) we obtain

$$\frac{1}{2}\|\boldsymbol{\xi}_n\|_{\sigma,\Omega}^2 - \frac{1}{2}\|\boldsymbol{\xi}_{n-1}\|_{\sigma,\Omega}^2 \leq -\left(\int_{I_n} \sigma\,\dot{\boldsymbol{\eta}}\,dt + \sigma\,[\boldsymbol{\eta}]_{n-1}\,,\, \boldsymbol{\xi}_n\right)$$

$$= -(\sigma\,\boldsymbol{\eta}_n^- - \sigma\,\boldsymbol{\eta}_{n-1}^-, \boldsymbol{\xi}_n)$$

$$\leq \|\boldsymbol{\eta}_n^- - \boldsymbol{\eta}_{n-1}^-\|_{\sigma,\Omega} \left(\|\boldsymbol{\xi}_n\|_{\sigma,\Omega} + \|\boldsymbol{\xi}_{n-1}\|_{\sigma,\Omega}\right)\,.$$

Hence,

$$\|\boldsymbol{\xi}_n\|_{\sigma,\Omega} - \|\boldsymbol{\xi}_{n-1}\|_{\sigma,\Omega} \leq 2\|\boldsymbol{\eta}_n^- - \boldsymbol{\eta}_{n-1}^-\|_{\sigma,\Omega}\,.$$

Summing over the first J time intervals now leads to

$$\|\boldsymbol{\xi}_J\|_{\sigma,\Omega} \leq \|\boldsymbol{\xi}_0\|_{\sigma,\Omega} + 2\sum_{n=1}^{J} \|\boldsymbol{\eta}_n^- - \boldsymbol{\eta}_{n-1}^-\|_{\sigma,\Omega}\,.$$

(3.43)

Here $\boldsymbol{\xi}_0 := \boldsymbol{u}_0(\boldsymbol{x}) - \boldsymbol{z}_{1,0}$ where $\boldsymbol{u}_0(\boldsymbol{x})$ is the projection of the electric initial data $\boldsymbol{u}(\cdot, 0)$ on $\mathcal{ND}_1(\mathcal{T}_h)$ and $\boldsymbol{z}_{1,0}$ the L^2-projection of $\boldsymbol{u}_0(.)$ on $\mathcal{ND}_1(\mathcal{T}_h)$ with respect to $\mathcal{B}(\cdot\,;\,\cdot)$. Then, due to (3.27) we have

$$\|\boldsymbol{\xi}_0\| \lesssim h^r \left[\|\boldsymbol{u}_0\|_{\mathbf{H}^s(\Omega)} + \|\operatorname{\mathbf{curl}}\boldsymbol{u}_0\|_{\mathbf{H}^s(\Omega)}\right] = \mathcal{O}(h^r),$$

with $r = \min\{s, 1\}$, and from the triangle inequality and the continuity in time of $\boldsymbol{z}_1$ and $\boldsymbol{u}$ it holds

$$\|\boldsymbol{\eta}_n^- - \boldsymbol{\eta}_{n-1}^-\|_{\sigma,\Omega} \leq \|(\pi_0\boldsymbol{z}_1 - \boldsymbol{z}_1)_n^- - (\pi_0\boldsymbol{z}_1 - \boldsymbol{z}_1)_{n-1}^-\|_{\sigma,\Omega} + \|(\boldsymbol{z}_1 - \boldsymbol{u})(t_n) - (\boldsymbol{z}_1 - \boldsymbol{u})(t_{n-1})\|_{\sigma,\Omega}\,.$$

(3.44)

48

Considering (3.27) and taking $\boldsymbol{u} \in C^1([0,T], \mathbf{H}^s(\mathbf{curl}, \Omega))$ it follows

$$
\begin{aligned}
\sum_{n=1}^{J} \|(\boldsymbol{z}_1 - \boldsymbol{u})(t_n) - (\boldsymbol{z}_1 - \boldsymbol{u})(t_{n-1})\|_{\sigma,\Omega} &= \sum_{n=1}^{J} \left\| \int_{I_n} \frac{\partial}{\partial t}(\boldsymbol{z}_1 - \boldsymbol{u}) \, dt \right\|_{\sigma,\Omega} \\
&\leq \sum_{n=1}^{J} \int_{I_n} \left\| \frac{\partial}{\partial t}(\boldsymbol{z}_1 - \boldsymbol{u}) \right\| dt \\
&\lesssim \sum_{n=1}^{J} \int_{I_n} h^r \left[\|\partial_t \boldsymbol{u}\|_{\mathbf{H}^s(\Omega)} + \|\mathbf{curl}\, \partial_t \boldsymbol{u}\|_{\mathbf{H}^s(\Omega)} \right] dt \\
&\lesssim h^r \int_0^T \left[\|\partial_t \boldsymbol{u}\|_{\mathbf{H}^s(\Omega)} + \|\mathbf{curl}\, \partial_t \boldsymbol{u}\|_{\mathbf{H}^s(\Omega)} \right] dt \\
&= \mathcal{O}(h^r) \, .
\end{aligned} \tag{3.45}
$$

Next we consider the first term in (3.44). Using the definition of π_0 yields

$$
\begin{aligned}
(\pi_0 \boldsymbol{z}_1 - \boldsymbol{z}_1)_n^- - (\pi_0 \boldsymbol{z}_1 - \boldsymbol{z}_1)_{n-1}^- &= \frac{1}{k} \int_{I_n} \boldsymbol{z}_1(t) \, dt - \frac{1}{k} \int_{I_{n-1}} \boldsymbol{z}_1(t) \, dt - (\boldsymbol{z}_1(t_n) - \boldsymbol{z}_1(t_{n-1})) \\
&= \int_{I_n} \left(\frac{\boldsymbol{z}_1(t) - \boldsymbol{z}_1(t - k)}{k} - \dot{\boldsymbol{z}}_1(t) \right) dt \, ,
\end{aligned}
$$

and using the Taylor expansion of $\|\ddot{\boldsymbol{z}}_1(\tau)\|_{\sigma,\Omega}$

$$
\begin{aligned}
\sum_{n=1}^{J} \|(\pi_0 \boldsymbol{z}_1 - \boldsymbol{z}_1)_n^- - (\pi_0 \boldsymbol{z}_1 - \boldsymbol{z}_1)_{n-1}^-\|_{\sigma,\Omega} &\leq \int_0^T \left\| \frac{\boldsymbol{z}_1(t) - \boldsymbol{z}_1(t-k)}{k} - \dot{\boldsymbol{z}}_1(t) \right\|_{\sigma,\Omega} dt \\
&\leq T \frac{k}{2} \max_{0 \leq \tau \leq T} \|\ddot{\boldsymbol{z}}_1(\tau)\|_{\sigma,\Omega} = \mathcal{O}(k) \, .
\end{aligned}
$$

Combining this with (3.43), (3.44) and (3.45) we obtain

$$
\|\boldsymbol{\xi}_J\| = \mathcal{O}(h^r + k) \, . \tag{3.46}
$$

Furthermore for the second term on the right hand side of (3.39) there holds

$$
\|\boldsymbol{\eta}_J^-\| \leq \|\boldsymbol{u}(t_J) - \boldsymbol{z}_1(t_J)\| + \|\pi_0 \boldsymbol{z}_1(t_J^-) - \boldsymbol{z}_1(t_J)\| \, .
$$

The first term behaves like $\mathcal{O}(h^r)$. For the second term we apply the mean value theorem for integrals to $\pi_0 \boldsymbol{z}_1$ and Taylor's expansion of $\boldsymbol{z}_1$ to get

$$
\begin{aligned}
\|\pi_0 \boldsymbol{z}_1(t_J^-) - \boldsymbol{z}_1(t_J)\| &= \left\| \frac{1}{k} \int_{I_J} \boldsymbol{z}_1(t) \, dt - \boldsymbol{z}_1(t_J) \right\| \\
&\leq k \max_{\tau \in I_J} \|\dot{\boldsymbol{z}}_1(\tau)\| = \mathcal{O}(k)
\end{aligned}
$$

and thus

$$
\|\boldsymbol{\eta}_J\| = \mathcal{O}(h^r + k) \, . \tag{3.47}
$$

Combining (3.39), (3.46) and (3.47) we obtain for $J = 1, 2, \ldots, N$ the final result

$$
\|(\boldsymbol{U}^h - \boldsymbol{u})_J^-\| = \mathcal{O}(h^r + k) \, .
$$

Case $l = 1$

As $\boldsymbol{\xi}$ is linear on I_n, the first term of the right hand side of (3.42) becomes

$$-\int_{I_n} (\sigma\,\dot{\boldsymbol{\eta}}(t), \boldsymbol{\xi}(t))\, dt = -\int_{I_n} \left(\sigma\,\dot{\boldsymbol{\eta}}(t)\,, \boldsymbol{\xi}_{n-1}^+ + \frac{t - t_{n-1}}{k}(\boldsymbol{\xi}_n^- - \boldsymbol{\xi}_{n-1}^+)\right) dt$$

$$= -\left(\int_{I_n} \sigma\,\dot{\boldsymbol{\eta}}(t)\, dt\,,\, \boldsymbol{\xi}_{n-1}^+\right) - \left(\int_{I_n} \frac{t - t_{n-1}}{k}\sigma\,\dot{\boldsymbol{\eta}}(t)\, dt\,,\, (\boldsymbol{\xi}_n^- - \boldsymbol{\xi}_{n-1}^+)\right)$$

$$\leq \left(\left\|\int_{I_n} \dot{\boldsymbol{\eta}}(t)\, dt\right\|_{\sigma,\Omega} + \left\|\int_{I_n} \frac{t - t_{n-1}}{k}\dot{\boldsymbol{\eta}}(t)\, dt\right\|_{\sigma,\Omega}\right)\left(\|\boldsymbol{\xi}_n^-\|_{\sigma,\Omega} + \|\boldsymbol{\xi}_{n-1}^+\|_{\sigma,\Omega}\right).$$

Using $\|\boldsymbol{\xi}_{n-1}^+\|_{\sigma,\Omega} \leq \|\boldsymbol{\xi}_{n-1}^-\|_{\sigma,\Omega} + \|[\boldsymbol{\xi}]_{n-1}\|_{\sigma,\Omega}$ and (3.42) this results in

$$\frac{1}{2}\|\boldsymbol{\xi}_n^-\|_{\sigma,\Omega}^2 - \frac{1}{2}\|\boldsymbol{\xi}_{n-1}^-\|_{\sigma,\Omega}^2 + \frac{1}{2}\|[\boldsymbol{\xi}]_{n-1}\|_{\sigma,\Omega}^2 \leq \left(\|\boldsymbol{\xi}_n^-\|_{\sigma,\Omega} + \|\boldsymbol{\xi}_{n-1}^-\|_{\sigma,\Omega} + \|[\boldsymbol{\xi}]_{n-1}\|_{\sigma,\Omega}\right)$$

$$\times \left(\left\|\int_{I_n} \dot{\boldsymbol{\eta}}(t)\, dt\right\|_{\sigma,\Omega} + \left\|\int_{I_n} \frac{t - t_{n-1}}{k}\dot{\boldsymbol{\eta}}(t)\, dt\right\|_{\sigma,\Omega} + \|[\boldsymbol{\eta}]_{n-1}\|_{\sigma,\Omega}\right).$$

There exist $\gamma_1 \geq \frac{1}{2}$ and $\gamma_2 \geq 0$, such that

$$\|\boldsymbol{\xi}_n^-\|_{\sigma,\Omega}^2 - \|\boldsymbol{\xi}_{n-1}^-\|_{\sigma,\Omega}^2 + \|[\boldsymbol{\xi}]_{n-1}\|_{\sigma,\Omega}^2 \geq \gamma_1 \left(\|\boldsymbol{\xi}_n^-\|_{\sigma,\Omega} - \|\boldsymbol{\xi}_{n-1}^-\|_{\sigma,\Omega} + \gamma_2\|[\boldsymbol{\xi}]_{n-1}\|_{\sigma,\Omega}\right)$$

$$\times \left(\|\boldsymbol{\xi}_n^-\|_{\sigma,\Omega} + \|\boldsymbol{\xi}_{n-1}^-\|_{\sigma,\Omega} + \|[\boldsymbol{\xi}]_{n-1}\|_{\sigma,\Omega}\right).$$

Thus we obtain

$$\|\boldsymbol{\xi}_n^-\|_{\sigma,\Omega} - \|\boldsymbol{\xi}_{n-1}^-\|_{\sigma,\Omega} + \gamma_2\|[\boldsymbol{\xi}]_{n-1}\|_{\sigma,\Omega}$$

$$\leq \frac{2}{\gamma_1}\left(\|[\boldsymbol{\eta}]_{n-1}\|_{\sigma,\Omega} + \left\|\int_{I_n} \dot{\boldsymbol{\eta}}(t)\, dt\right\|_{\sigma,\Omega} + \left\|\int_{I_n} \frac{t - t_{n-1}}{k}\dot{\boldsymbol{\eta}}(t)\, dt\right\|_{\sigma,\Omega}\right).$$

Choosing $\gamma_1 = \frac{1}{2}$ and $\gamma_2 = 0$ the summing this expression from $n = 1$ to J for $n = 1, \ldots, J$ it follows that

$$\|\boldsymbol{\xi}_J^-\|_{\sigma,\Omega} \leq \|\boldsymbol{\xi}_0\|_{\sigma,\Omega} + 4\sum_{n=1}^{J}\|[\boldsymbol{\eta}]_{n-1}\|_{\sigma,\Omega} + 4\sum_{n=1}^{J}\left\|\int_{I_n}\dot{\boldsymbol{\eta}}(t)\, dt\right\|_{\sigma,\Omega} + 4\sum_{n=1}^{J}\left\|\int_{I_n}\frac{t - t_{n-1}}{k}\dot{\boldsymbol{\eta}}(t)\, dt\right\|_{\sigma,\Omega}. \tag{3.48}$$

From the first case we know that $\|\boldsymbol{\xi}_0\|_{\sigma,\Omega} = \mathcal{O}(h^r)$. Now we proceed to estimate the remaining terms on the right hand side. First using the definition of π_1 for fixed $\boldsymbol{x} \in \Omega$ gives

$$[\boldsymbol{\eta}]_{n-1} = (\pi_1 \boldsymbol{z}_1)_{n-1}^+ - (\pi_1 \boldsymbol{z}_1)_{n-1}^-$$

$$= \frac{1}{k}\int_{I_n}\left(4 - 6\frac{s - t_{n-1}}{k}\right)\boldsymbol{z}_1(s)\, ds$$

$$-\frac{1}{k}\int_{I_{n-1}}\left(4-6\frac{s-t_{n-2}}{k}\right)z_1(s)\,ds-\frac{1}{k}\int_{I_{n-1}}\left(12\frac{s-t_{n-2}}{k}-6\right)z_1(s)\,ds$$

$$=\frac{1}{k}\int_{I_n}\left(4-6\frac{s-t_{n-1}}{k}\right)z_1(s)\,ds-\frac{1}{k}\int_{I_{n-1}}\left(6\frac{s-t_{n-2}}{k}-2\right)z_1(s)\,ds$$

$$=\frac{1}{k}\int_0^k\left(4-6\frac{t}{k}\right)z_1(t_{n-1}+t)\,dt-\frac{1}{k}\int_0^k\left(6\frac{k-t}{k}-2\right)z_1(t_{n-1}-t)\,dt$$

$$=\frac{1}{k}\int_0^k\left(4-6\frac{t}{k}\right)(z_1(t_{n-1}+t)-z_1(t_{n-1}-t))\,dt$$

$$=\frac{1}{k}\int_0^k\left(4-6\frac{t}{k}\right)\left(2t\dot{z}_1(t_{n-1})+\frac{1}{3}t^3\frac{\partial^3 z_1(\tau)}{\partial t^3}\right)dt$$

for $\tau=\tau(t)\in I_n\cup I_{n-1}$.

$$\int_0^k\left(4-6\frac{t}{k}\right)t\,dt=0\qquad\text{and}\qquad\int_0^k\frac{1}{3}\left|4-6\frac{t}{k}\right|t^3\,dt<\frac{1}{5}k^4,$$

yield

$$[\boldsymbol{\eta}]_{n-1}<\frac{k^3}{5}\max_{\tau\in I_n\cup I_{n-1}}\left|\frac{\partial^3 z_1(\tau)}{\partial t^3}\right|.$$

Thus the second term on the right hand side of (3.48) can be estimated by

$$\begin{aligned}4\sum_{n=1}^J\|[\boldsymbol{\eta}]_{n-1}\|_{\sigma,\Omega}&\le\frac{4}{5}k^2\sum_{n=1}^J k\max_{t\in I_n}\left\|\frac{\partial^3 z_1(t)}{\partial t^3}\right\|_{\sigma,\Omega}\\&\le\frac{4}{5}k^2\,T\max_{0\le t\le T}\left\|\frac{\partial^3 z_1(t)}{\partial t^3}\right\|_{\sigma,\Omega}=\mathcal{O}(k^2).\end{aligned}\tag{3.49}$$

For the third term on the right hand side of (3.48) there holds

$$\sum_{n=1}^J\left\|\int_{I_n}\dot{\boldsymbol{\eta}}(t)\,dt\right\|_{\sigma,\Omega}=\sum_{n=1}^J\|\boldsymbol{\eta}_n^--\boldsymbol{\eta}_{n-1}^+\|_{\sigma,\Omega}$$

$$\le\sum_{n=1}^J\left(\|(\boldsymbol{u}-\boldsymbol{z}_1)(t_n)-(\boldsymbol{u}-\boldsymbol{z}_1)(t_{n-1})\|_{\sigma,\Omega}+\left\|(\pi_1\boldsymbol{z}_1-\boldsymbol{z}_1)_n^--(\pi_1\boldsymbol{z}_1-\boldsymbol{z}_1)_{n-1}^+\right\|_{\sigma,\Omega}\right).$$

The first term does not depend on l due to continuity of $\boldsymbol{u}$ and $\boldsymbol{z}_1$. Therefore we can use (3.45) to get

$$\sum_{n=1}^J\|(\boldsymbol{u}-\boldsymbol{z}_1)(t_n)-(\boldsymbol{u}-\boldsymbol{z}_1)(t_{n-1})\|_{\sigma,\Omega}=\mathcal{O}(h^r).$$

Again, due to the definition of π_1 there holds for $\tau_1\in I_n$

$$(\pi_1\boldsymbol{z}_1-\boldsymbol{z}_1)_n^--(\pi_1\boldsymbol{z}_1-\boldsymbol{z}_1)_{n-1}^+=$$

$$=\frac{1}{k}\int_{I_n}\left(12\frac{s-t_{n-1}}{k}-6\right)z_1(s)\,ds-(z_1(t_n)-z_1(t_{n-1}))$$

$$= \frac{1}{k} \int_{I_n} \left(12 \frac{s - t_{n-1}}{k} - 6 \right) \cdot \left(z_1(t_{n-1}) + (s - t_{n-1}) \dot{z}_1(t_{n-1}) \right.$$

$$\left. + \frac{1}{2} (s - t_{n-1})^2 \ddot{z}_1(t_{n-1}) + \frac{1}{6} (s - t_{n-1})^3 \frac{\partial^3 z_1(\tau_1)}{\partial t^3} \right) ds$$

$$- k \dot{z}_1(t_{n-1}) - \frac{1}{2} k^2 \ddot{z}_1(t_{n-1}) - \frac{1}{6} k^3 \frac{\partial^3 z_1(\tau_2)}{\partial t^3}$$

$$\leq \left(\frac{1}{6k} \int_{I_n} \left| 12 \frac{s - t_{n-1}}{k} - 6 \right| (s - t_{n-1})^3 \, ds + \frac{1}{6} k^3 \right) \max_{\tau \in I_n} \left| \frac{\partial^3 z_1(\tau)}{\partial t^3} \right|$$

$$= \frac{31}{96} k^3 \max_{\tau \in I_n} \left| \frac{\partial^3 z_1(\tau)}{\partial t^3} \right| .$$

Here was used that

$$\frac{1}{k} \int_{I_n} \left(12 \frac{s - t_{n-1}}{k} - 6 \right) ds = 0 ,$$

$$\frac{1}{k} \int_{I_n} \left(12 \frac{s - t_{n-1}}{k} - 6 \right) (s - t_{n-1}) \, ds = k ,$$

$$\frac{1}{k} \int_{I_n} \left(12 \frac{s - t_{n-1}}{k} - 6 \right) (s - t_{n-1})^2 \, ds = k^2 ,$$

and $$\frac{1}{k} \int_{I_n} \left| 12 \frac{s - t_{n-1}}{k} - 6 \right| (s - t_{n-1})^3 \, ds = \frac{15}{16} k^3 .$$

Hence

$$4 \sum_{n=1}^{J} \left\| \int_{I_n} \dot{\boldsymbol{\eta}}(t) \, dt \right\|_{\sigma, \Omega} \leq \frac{31}{24} k^2 \sum_{n=1}^{J} k \max_{t \in I_n} \left\| \frac{\partial^3 z_1(t)}{\partial t^3} \right\|_{\sigma, \Omega} + \mathcal{O}(h^r) \tag{3.50}$$

$$= \mathcal{O}(h^r + k^2) .$$

Analogously, for the last term in (3.48) there holds

$$4 \sum_{n=1}^{N} \left\| \int_{I_n} \frac{t - t_{n-1}}{k} \dot{\boldsymbol{\eta}}(t) \, dt \right\|_{\sigma, \Omega} = \mathcal{O}(h^r + k^2) \tag{3.51}$$

and therefore

$$\left\| \boldsymbol{\xi}_J^- \right\|_{\sigma, \Omega} = \mathcal{O}(h^r + k^2) . \tag{3.52}$$

As in the first case there holds

$$\left\| \boldsymbol{\eta}_J^- \right\|_{\sigma, \Omega} \leq \underbrace{\left\| \boldsymbol{u}(t_J) - \boldsymbol{z}_1(t_J) \right\|_{\sigma, \Omega}}_{= \mathcal{O}(h^r)} + \left\| \pi_1 \boldsymbol{z}_1(t_J^-) - \boldsymbol{z}_1(t_J) \right\|_{\sigma, \Omega}$$

and

$$\pi_1 \boldsymbol{z}_1(t_J^-) - \boldsymbol{z}_1(t_J) = \frac{1}{k} \int_{I_J} \left(6 \frac{s - t_{J-1}}{k} - 2 \right) \boldsymbol{z}_1(s) \, ds - \boldsymbol{z}_1(t_J)$$

$$= \frac{1}{k} \int_0^k \left(4 - 6 \frac{t}{k} \right) \boldsymbol{z}_1(t_J - t) \, dt - \boldsymbol{z}_1(t_J) \tag{3.53}$$

$$\leq \frac{1}{2k} \max_{t \in I_n} |\ddot{\boldsymbol{z}}_1(t)| \int_0^k \left| 4 - 6 \frac{t}{k} \right| t^2 \, dt = \mathcal{O}(k^2) .$$

Thus,

$$\left\|\boldsymbol{\eta}_J^-\right\|_{\sigma,\Omega} = \mathcal{O}(h^r + k^2). \tag{3.54}$$

Since the norms $\|\cdot\|$ and $\|\cdot\|_{\sigma,\Omega}$ are equivalent, we can estimate (3.39) for $J = 1, \ldots, N$ to get the final result

$$\left\|(\boldsymbol{U}^h - \boldsymbol{u})_J^-\right\| = \mathcal{O}(h^r + k^2)$$

which is the assertion (3.33). This finishes the proof of the $\mathbf{L}^2$-estimate for the cases $l = 0$ and $l = 1$.

Next, we show (3.34). In the following we only consider the case $l = 1$. The case $l = 0$ is proven analogously.

As the bilinear form $\mathcal{B}$ is coercive in $\boldsymbol{\mathcal{X}} := \mathbf{H}(\mathbf{curl}, \Omega) \times \mathbf{H}_\|^{-\frac{1}{2}}(\mathrm{div}_\Gamma 0, \Gamma)$, we get from (3.41):

$$\frac{1}{2}\|\boldsymbol{\xi}_n^-\|_{\sigma,\Omega}^2 - \frac{1}{2}\|\boldsymbol{\xi}_{n-1}^-\|_{\sigma,\Omega}^2 + \frac{1}{2}\|[\boldsymbol{\xi}]_{n-1}\|_{\sigma,\Omega}^2 + \left\|(\boldsymbol{\xi}, \boldsymbol{\lambda}^h - \widetilde{\pi}_l \, \boldsymbol{z}_2)\right\|_{L^2(I_n \, ; \, \boldsymbol{\mathcal{X}})}^2$$
$$\leq -\int_{I_n} (\sigma \, \dot{\boldsymbol{\eta}}, \boldsymbol{\xi}) \, dt - (\sigma \, [\boldsymbol{\eta}]_{n-1}, \boldsymbol{\xi}_{n-1}^+) \,. \tag{3.55}$$

Let $\boldsymbol{\xi} := \boldsymbol{\xi}_{n-1}^+ + \frac{t-t_{n-1}}{k}\left(\boldsymbol{\xi}_n^- - \boldsymbol{\xi}_{n-1}^+\right)$, from the triangle inequality we obtain

$$2\int_{I_n} \|\boldsymbol{\xi}\|_{\sigma,\Omega} \, dt \leq k\left(\left\|\boldsymbol{\xi}_n^-\right\|_{\sigma,\Omega} + \left\|\boldsymbol{\xi}_{n-1}^+\right\|_{\sigma,\Omega}\right).$$

Combining this with (3.49), (3.50) and (3.55) we obtain

$$-\int_{I_n} (\sigma \, \dot{\boldsymbol{\eta}}, \boldsymbol{\xi}) \, dt - (\sigma \, [\boldsymbol{\eta}]_{n-1}, \boldsymbol{\xi}_{n-1}^+) \lesssim (h^r k + k^3)\left(\left\|\boldsymbol{\xi}_n^-\right\|_{\sigma,\Omega} + \left\|\boldsymbol{\xi}_{n-1}^+\right\|_{\sigma,\Omega}\right).$$

The sum over all time intervalls I_n now leads to

$$\frac{1}{2}\|\boldsymbol{\xi}_N^-\|_{\sigma,\Omega}^2 - \frac{1}{2}\|\boldsymbol{\xi}_0^-\|_{\sigma,\Omega}^2 + \left\|(\boldsymbol{\xi}, \boldsymbol{\lambda}^h - \widetilde{\pi}_l \, \boldsymbol{z}_2)\right\|_{L^2(0,T; \, \boldsymbol{\mathcal{X}})}^2$$
$$\leq C(h^r + k^2)\sum_{n=1}^N k\left(\left\|\boldsymbol{\xi}_n^-\right\|_{\sigma,\Omega} + \left\|\boldsymbol{\xi}_{n-1}^+\right\|_{\sigma,\Omega}\right)$$
$$\leq 2C(h^r + k^2)\int_0^T \|\boldsymbol{\xi}(t)\|_{\sigma,\Omega} \, dt$$
$$\lesssim (h^r + k^2)\int_0^T \|\boldsymbol{\xi}(t)\|_{\mathbf{H}(\mathbf{curl},\Omega)} \, dt$$
$$\lesssim (h^r + k^2)\sqrt{T}\,\|\boldsymbol{\xi}\|_{L^2(0,T \, ; \, \mathbf{H}(\mathbf{curl},\Omega))}\,.$$

Using that $\|\boldsymbol{\xi}_N^-\|_{\sigma,\Omega}^2 \geq 0$, $\|\boldsymbol{\xi}_0^-\|_{\sigma,\Omega}^2 = \mathcal{O}(h^r)$ and the Cauchy-Schwarz inequality, we obtain

$$\left\|(\boldsymbol{\xi}, \boldsymbol{\lambda}^h - \widetilde{\pi}_l \, \boldsymbol{z}_2)\right\|_{L^2(0,T; \, \boldsymbol{\mathcal{X}})} = O(h^r + k^2). \tag{3.56}$$

Furthermore, from Lemma 3.3.1 and (3.53) it follows that

$$\|\boldsymbol{\eta}\|_{L^2(0,T\,;\,\mathbf{H}(\mathbf{curl},\Omega))} \leq \|\boldsymbol{u} - \boldsymbol{z}_1\|_{L^2(0,T\,;\,\mathbf{H}(\mathbf{curl},\Omega))} + \|\boldsymbol{z}_1 - \pi_1\,\boldsymbol{z}_1\|_{L^2(0,T\,;\,\mathbf{H}(\mathbf{curl},\Omega))} \\ = \mathcal{O}(h^{r_0} + k^2)\,, \tag{3.57}$$

and finally we obtain

$$\left\|\boldsymbol{U}^h - \boldsymbol{u}\right\|_{L^2(0,T\,;\,\mathbf{H}(\mathbf{curl},\Omega))} \leq \|\boldsymbol{\xi}\|_{L^2(0,T\,;\,\mathbf{H}(\mathbf{curl},\Omega))} + \|\boldsymbol{\eta}\|_{L^2(0,T\,;\,\mathbf{H}(\mathbf{curl},\Omega))} = \mathcal{O}(h^{r_0} + k^2)\,.$$

Analogously to the proof of (3.35), from (3.28) and (3.53) it follows

$$\left\|\boldsymbol{\lambda} - \widetilde{\pi}_1\,\boldsymbol{z}_2\right\|_{L^2(0,T\,;\,\mathbf{H}_{\parallel}^{-\frac{1}{2}}(\mathrm{div}_\Gamma,\Gamma))} \leq \|\boldsymbol{\lambda} - \boldsymbol{z}_2\|_{L^2(0,T\,;\,\mathbf{H}_{\parallel}^{-\frac{1}{2}}(\mathrm{div}_\Gamma,\Gamma))} + \|\boldsymbol{z}_2 - \widetilde{\pi}_1\,\boldsymbol{z}_2\|_{L^2(0,T\,;\,\mathbf{H}_{\parallel}^{-\frac{1}{2}}(\mathrm{div}_\Gamma,\Gamma))} \\ = \mathcal{O}(h^{r_0} + k^2)$$

and combining this with (3.56) we obtain

$$\left\|\boldsymbol{\lambda} - \boldsymbol{\lambda}^h\right\|_{L^2(0,T\,;\,\mathbf{H}_{\parallel}^{-\frac{1}{2}}(\mathrm{div}_\Gamma,\Gamma))} \leq \|\boldsymbol{\lambda} - \widetilde{\pi}_1\,\boldsymbol{z}_2\|_{L^2(0,T\,;\,\mathbf{H}_{\parallel}^{-\frac{1}{2}}(\mathrm{div}_\Gamma,\Gamma))} + \left\|\widetilde{\pi}_1\,\boldsymbol{z}_2 - \boldsymbol{\lambda}^h\right\|_{L^2(0,T\,;\,\mathbf{H}_{\parallel}^{-\frac{1}{2}}(\mathrm{div}_\Gamma,\Gamma))} \\ = \mathcal{O}(h^{r_0} + k^2)\,.$$

∎

3.3.2 A posteriori estimate

In order to derive the a posteriori error estimate in Theorem 3.3.2 we define the set of faces $\mathcal{F}_h$ of $\mathcal{T}_h$, the set of exterior faces $\mathcal{F}_h^\Gamma := \{F \in \mathcal{F}_h : F \subset \Gamma\}$ and the set of interior faces $\mathcal{F}_h^C := \mathcal{F}_h \setminus \mathcal{F}_h^\Gamma$ and $\mathcal{F}_h(\mathfrak{T})$ as the set of faces of the element $\mathfrak{T} \in \mathcal{T}_h$. Let $h_{\mathfrak{T}}$ denote the maximal diameter of an element $\mathfrak{T} \in \mathcal{T}_h$ and h_F the maximal diameter of a face $F \in \mathcal{F}_h$. Furthermore we assume that the mesh is regular, i.e., there holds

$$h_{\mathfrak{T}'} \lesssim h_{\mathfrak{T}} \quad \forall \mathfrak{T}, \mathfrak{T}' \in \mathcal{T}_h,\ \mathfrak{T} \cap \mathfrak{T}' \neq \emptyset,$$
$$h_F \lesssim h_{\mathfrak{T}} \quad \forall F \in \mathcal{F}_h(\mathfrak{T}).$$

For a common face $F \in \mathcal{F}_h^C$ of two elements $\mathfrak{T}_1, \mathfrak{T}_2$ and the normal $\boldsymbol{n}$ pointing into $\mathfrak{T}_2$ we define the jump of a function $\boldsymbol{q}$ by

$$[\boldsymbol{n} \cdot \boldsymbol{q}]_F := \boldsymbol{n} \cdot \boldsymbol{q}_{|F \subset \mathfrak{T}_1} - \boldsymbol{n} \cdot \boldsymbol{q}_{|F \subset \mathfrak{T}_2}.$$

For $F \in \mathcal{F}_h^\Gamma$ we define

$$[\boldsymbol{n} \cdot \boldsymbol{q}]_F := \boldsymbol{n} \cdot \boldsymbol{q}_{|F}.$$

Analogously,

$$[\boldsymbol{n} \times \boldsymbol{q}]_F := \boldsymbol{n} \times \boldsymbol{q}_{|F \subset \mathfrak{T}_1} - \boldsymbol{n} \times \boldsymbol{q}_{|F \subset \mathfrak{T}_2}, \qquad\qquad F \in \mathcal{F}_h^C,$$
$$[\boldsymbol{n} \times \boldsymbol{q}]_F := \boldsymbol{n} \times \boldsymbol{q}_{|F}, \qquad\qquad F \in \mathcal{F}_h^\Gamma.$$

Let $D_{\mathfrak{T}}$ and D_F denote the set of elements containing at least one vertex of the element $\mathfrak{T}$ or of the face F, resp. and let $D_{\mathfrak{T}}^1$ and D_F^1 denote the set of elements containing at least one edge of the element $\mathfrak{T}$ or the face F, respectively (see [6]). Then for all $\psi \in H^1$, $\boldsymbol{q} \in \mathbf{H}^1$ and $\phi \in H^{1/2}(\Gamma)$ the following approximation properties hold

$$
\begin{aligned}
|P_h^1\psi|_{H^1(\mathfrak{T})} &\lesssim |\psi|_{H^1(D_{\mathfrak{T}})}, & \|\mathfrak{P}_h^1\boldsymbol{q}\|_{\mathbf{L}^2(\mathfrak{T})} &\lesssim \|\boldsymbol{q}\|_{\mathbf{H}^1(D_{\mathfrak{T}}^1)}, \\
\|P_h^1\psi\|_{L^2(\mathfrak{T})}, &\lesssim h_{\mathfrak{T}}\|\psi\|_{H^1(D_{\mathfrak{T}})}, & \|\boldsymbol{q} - \mathfrak{P}_h^1\boldsymbol{q}\|_{\mathbf{L}^2(\mathfrak{T})} &\lesssim h_{\mathfrak{T}}|\boldsymbol{q}|_{\mathbf{H}^1(D_{\mathfrak{T}}^1)}, \\
\|\psi - P_h^1\psi\|_{L^2(\mathfrak{T})} &\lesssim h_{\mathfrak{T}}|\psi|_{H^1(D_{\mathfrak{T}})}, & \|\boldsymbol{q} - \mathfrak{P}_h^1\boldsymbol{q}\|_{\mathbf{L}^2(F)} &\lesssim h_F^{1/2}|\boldsymbol{q}|_{\mathbf{H}^1(D_F^1)}, \\
\|\psi - P_h^1\psi\|_{L^2(F)} &\lesssim h_F^{1/2}|\psi|_{H^1(D_F)}, & \|\phi - p_h^1\phi\|_{L^2(F)} &\lesssim h_F^{1/2}|v|_{H^1(D_F)},
\end{aligned}
\tag{3.58}
$$

where

$$
P_h^1 : H^1(\Omega) \to \mathcal{S}_1(\mathcal{T}_h), \quad \mathfrak{P}_h^1 : \mathbf{H}(\mathbf{curl}, \Omega) \to \mathcal{ND}_1(\mathcal{T}_h), \quad \text{and} \quad p_h^1 : H^{1/2}(\Gamma) \to \mathcal{S}_1(\mathcal{K}_h)
$$

are the interpolation operators analyzed in Beck et. al. [6, Sections 4 and 5], Monk [59, Section 5.6] and Teltscher [73, Theorem 3.3.3].

The following theorem is devoted to derive a residual based a posteriori error estimate. The ideas of the proof can be found in Teltscher [73] and Mund & Stephan [61]. The derived error indicators are used later for the implementation of adaptive algorithms.

Theorem 3.3.2 *Let $\partial_t \boldsymbol{J}(\boldsymbol{x}, t) \in C^2([0, T]; \mathbf{L}^2(\Omega))$, $(\boldsymbol{u}, \boldsymbol{\lambda})$ be the solution of (3.15) with $\boldsymbol{u} \in \mathcal{C}^1([0, T]; \Omega)$ and $(\boldsymbol{U}^h, \boldsymbol{\lambda}^h)$ be the solution of (3.20). Then there exists a constant $c > 0$, such that*

$$
\left\|(\boldsymbol{U}^h - \boldsymbol{u}, \boldsymbol{\lambda}^h - \boldsymbol{\lambda})\right\|_{L^2(I_n; \boldsymbol{\mathcal{X}})} \leq c \left[\left(\sum_{i=1}^{11} R_{i,n}\right) + T_{1,n} + T_{2,n} + \left\|(\boldsymbol{U}^h - \boldsymbol{u})_{n-1}^-\right\|_{\mathbf{L}^2(\Omega)} \right]
\tag{3.59}
$$

where $\boldsymbol{\mathcal{X}} := \mathbf{H}(\mathbf{curl}, \Omega) \times \mathbf{H}_{\|}^{-\frac{1}{2}}(\mathrm{div}_\Gamma 0, \Gamma)$,

$$
R_{1,n}^2 := k_n \max_{t \in I_n} \sum_{\mathfrak{T} \in \mathcal{T}_h} h_{\mathfrak{T}}^2 \left\|\sqrt{\mu}\left(\partial_t \boldsymbol{J} + \tilde{\lambda}\boldsymbol{U}^h + \sigma\dot{\boldsymbol{U}}^h + \mathbf{curl}\left(\mu^{-1}\mathbf{curl}\,\boldsymbol{U}^h\right)\right)\right\|_{0,\mathfrak{T}}^2,
$$

$$
R_{2,n}^2 := k_n \max_{t \in I_n} \sum_{F \in \mathcal{F}_h^C} h_F \left\|\sqrt{\mu_A}[\mu^{-1}\mathbf{curl}\,\boldsymbol{U}^h \times \boldsymbol{n}]_F\right\|_{0,F}^2,
$$

$$
R_{3,n}^2 := k_n \max_{t \in I_n} \sum_{F \in \mathcal{F}_h^\Gamma} h_F \left\|\sqrt{\mu^{-1}}\mathbf{curl}\,\boldsymbol{U}^h \times \boldsymbol{n} - \sqrt{\mu}\mathcal{W}\boldsymbol{U}_\Gamma^h + \sqrt{\mu}\widetilde{\mathcal{K}}\boldsymbol{\lambda}^h\right\|_{0,F}^2,
$$

$$
R_{4,n}^2 := k_n \max_{t \in I_n} \sum_{\mathfrak{T} \in \mathcal{T}_h} h_{\mathfrak{T}}^2 \left\|\sqrt{\sigma^{-1}}\left(\mathrm{div}\,\partial_t \boldsymbol{J} + \tilde{\lambda}\,\mathrm{div}\,\boldsymbol{U}^h + \mathrm{div}\,\sigma\dot{\boldsymbol{U}}^h\right)\right\|_{0,\mathfrak{T}}^2,
$$

$$
R_{5,n}^2 := k_n \max_{t \in I_n} \sum_{F \in \mathcal{F}_h^C} h_F \left\|\sqrt{\sigma_A}^{-1}[(\sigma\dot{\boldsymbol{U}}^h + \tilde{\lambda}\boldsymbol{U}^h) \cdot \boldsymbol{n}]_F\right\|_{0,F}^2,
$$

$$R_{6,n}^2 := k_n \max_{t \in I_n} \sum_{F \in \mathcal{F}_h^\Gamma} h_F \left\| \left(\sqrt{\sigma}\, \dot{\boldsymbol{U}}^h + \sqrt{\sigma^{-1}}\, \tilde{\lambda}\, \boldsymbol{U}^h \right) \cdot \boldsymbol{n} \right\|_{0,F}^2,$$

$$R_{7,n}^2 := k_n \max_{t \in I_n} \sum_{F \in \mathcal{F}_h^\Gamma} h_F \left\| \mathrm{curl}_\Gamma \left(\mathcal{K} - I \right) \boldsymbol{U}_\Gamma^h - \mathrm{curl}_\Gamma\, \mathcal{V} \boldsymbol{\lambda}^h \right\|_{0,F}^2,$$

$$R_{8,n}^2 := \frac{1}{k_n} \sum_{\mathfrak{T} \in \mathcal{T}_h} h_\mathfrak{T}^2 \left\| \left[\sigma\, \boldsymbol{U}^h \right]_{n-1} \right\|_{0,\mathfrak{T}}^2,$$

$$R_{9,n}^2 := \frac{1}{k_n} \sum_{\mathfrak{T} \in \mathcal{T}_h} h_\mathfrak{T}^2 \left\| \sqrt{\sigma^{-1}}\, \mathrm{div} \left[\sigma\, \boldsymbol{U}^h \right]_{n-1} \right\|_{0,\mathfrak{T}}^2,$$

$$R_{10,n}^2 := \frac{1}{k_n} \sum_{F \in \mathcal{F}_h^C} h_F \left\| \sqrt{\sigma_A}^{-1} \left[\left[\sigma\, \boldsymbol{U}^h \right]_{n-1} \cdot \boldsymbol{n} \right]_F \right\|_{0,F}^2,$$

$$R_{11,n}^2 := \frac{1}{k_n} \sum_{F \in \mathcal{F}_h^\Gamma} h_F \left\| \sqrt{\sigma} \left[\boldsymbol{U}^h \right]_{n-1} \cdot \boldsymbol{n} \right\|_{0,F}^2,$$

and

$$T_{1,n} := \sqrt{k_n}^{-1} \left\| \left[\sigma\, \boldsymbol{U}^h \right]_{n-1} \right\|_{0,\Omega},$$

$$T_{2,n}^2 := k_n^5 \max_{t \in I_n} \| \partial_t^3 \mathbf{J} \|_{\mathbf{L}^2(\Omega)}^2.$$

Proof.

Let $\mathcal{B}$ and $\mathcal{L}$ be the bilinear and linear forms defined in (3.16) and (3.17), respectively . Since $(\boldsymbol{u}, \boldsymbol{\lambda})$ is the solution of (3.15), $(\boldsymbol{u}(t), \boldsymbol{\lambda}(t)) \in \mathcal{X}$ and analogously we have $\left(\boldsymbol{U}^h(t), \boldsymbol{\lambda}^h(t) \right) \in \mathcal{X}_h^{n,1} := \mathbf{V}_h^{n,1} \times \widetilde{\mathbf{V}}_h^{n,1}$.

Let $\boldsymbol{e} = \boldsymbol{e}(t) := \left(\boldsymbol{u} - \boldsymbol{U}^h \right)(t)$, $\boldsymbol{\varepsilon} = \boldsymbol{\varepsilon}(t) := \left(\boldsymbol{\lambda} - \boldsymbol{\lambda}^h \right)(t)$, and define $\| \cdot \|_{\sigma,\tau} := \| \sigma \cdot \|_{\mathbf{L}^2(\tau)}$ and $\| \cdot \|_{0,\tau} := \| \cdot \|_{\mathbf{L}^2(\tau)}$.

Now, as Ω is assumed to be convex, we use the Helmholtz decomposition

$$\mathbf{H}(\mathbf{curl}, \Omega) = \boldsymbol{M}(\Omega) \oplus \mathbf{grad}\, H^1(\Omega)/\mathbb{C}$$

with $\boldsymbol{M}(\Omega) = \mathbf{H}_0(\mathrm{div}\, 0, \Omega) \cap \mathbf{H}(\mathbf{curl}, \Omega)$. This follows from the $\mathbf{L}^2$-orthogonal decomposition

$$\mathbf{L}^2(\Omega) := \mathbf{H}_0(\mathrm{div}\, 0, \Omega) \oplus \mathbf{grad}\, H^1(\Omega)/\mathbb{C}$$

for connected Lipschitz domains, see Dautray and Lions [24, Chap. IX, §1, Prop. 1] .

We split the error $\boldsymbol{e} \in \mathbf{H}(\mathbf{curl}, \Omega)$ into

$$\boldsymbol{e} = \boldsymbol{e}^\perp + \boldsymbol{e}^0 \tag{3.60}$$

where $\boldsymbol{e}^\perp \in \boldsymbol{M}(\Omega)$, $\boldsymbol{e}^0 = \mathbf{grad}\, \psi$, for $\psi \in H^1(\Omega)$ and there holds

$$\| \boldsymbol{e}^\perp \|_{\mathbf{H}^1(\Omega)} \lesssim \| \mathbf{curl}\, \boldsymbol{e} \|_{\mathbf{L}^2(\Omega)}, \qquad \| \mathbf{grad}\, \psi \|_{\mathbf{L}^2(\Omega)} \le \| \boldsymbol{e} \|_{\mathbf{H}(\mathbf{curl}, \Omega)} . \tag{3.61}$$

The first estimate is due to the fact that $\mathbf{M}(\Omega)$ is continuously embedded in $\mathbf{H}^1(\Omega)$, see Amrouche *et al.* [2, Theorem 2.17]. The second one follows from the definition of the $\mathbf{H}(\mathbf{curl}, \Omega)$-norm.

Set

$$\boldsymbol{e}_h := \boldsymbol{\mathfrak{P}}_h^1 \boldsymbol{e}^\perp + \mathbf{grad}\, P_h^1 \psi \in \mathcal{ND}_1(\mathcal{T}_h) \tag{3.62}$$

where $\boldsymbol{e}^\perp, \psi$ as from (3.60).

Since $\boldsymbol{\varepsilon} \in \mathbf{H}_\parallel^{-\frac{1}{2}}(\mathrm{div}_\Gamma\, 0, \Gamma) = \mathbf{curl}_\Gamma\, H^{\frac{1}{2}}(\Gamma)/\mathbb{C}$, there exists a $\phi \in H^{\frac{1}{2}}(\Gamma)$ such that $\boldsymbol{\varepsilon} = \mathbf{curl}_\Gamma\, \phi$. Now, choose $\phi_h = p_h^1 \phi$ and $\boldsymbol{\varepsilon}_h = \mathbf{curl}_\Gamma\, \phi_h$ and take

$$\boldsymbol{\mathcal{E}} := \pi_1 \boldsymbol{e}_h \quad \text{and} \quad \widetilde{\boldsymbol{\mathcal{E}}} := \tilde{\pi}_1 \boldsymbol{\varepsilon}_h \tag{3.63}$$

as the orthogonal L^2 - projection (defined in (2.10)) of $\boldsymbol{e}_h := \boldsymbol{e}_h(t)$ and $\boldsymbol{\varepsilon}_h := \boldsymbol{\varepsilon}_h(t)$ into the space $\mathbf{V}_h^{n,1}$ and $\widetilde{\mathbf{V}}_h^{n,1}$, respectively.

From the equality (cf. (3.40))

$$\int_{I_n} (\sigma\, \dot{\boldsymbol{e}}, \boldsymbol{e})\, dt + \left([\sigma\, \boldsymbol{e}]_{n-1}, \boldsymbol{e}_{n-1}^+\right) = \frac{1}{2}\|\boldsymbol{e}_n^-\|_{\sigma,\Omega}^2 - \frac{1}{2}\|\boldsymbol{e}_{n-1}^-\|_{\sigma,\Omega}^2 + \frac{1}{2}\|\,[\boldsymbol{e}]_{n-1}\,\|_{\sigma,\Omega}^2$$

and the fact that the operator $\mathcal{B}(\boldsymbol{u}, \boldsymbol{\lambda}; \boldsymbol{w}, \boldsymbol{\zeta})$ is coercive, we obtain that there exists a constant $\alpha_1 > 0$, such that

$$\begin{aligned}
\alpha_1\, \|(\boldsymbol{e}, \boldsymbol{\varepsilon})\|_{\mathbf{L}^2(I_n;\mathcal{X})}^2 &+ \frac{1}{2}\|\boldsymbol{e}_n^-\|_{\sigma,\Omega}^2 - \frac{1}{2}\|\boldsymbol{e}_{n-1}^-\|_{\sigma,\Omega}^2 + \frac{1}{2}\|\,[\boldsymbol{e}]_{n-1}\,\|_{\sigma,\Omega}^2 \\
&\leq \int_{I_n} \left((\sigma\, \dot{\boldsymbol{e}}, \boldsymbol{e}) + \mathcal{B}\,(\boldsymbol{e}, \boldsymbol{\varepsilon}; \boldsymbol{e}, \boldsymbol{\varepsilon})\right) dt + \left([\sigma\, \boldsymbol{e}]_{n-1}, \boldsymbol{e}_{n-1}^+\right) \\
&= \int_{I_n} \left((\sigma\, \dot{\boldsymbol{u}}, \boldsymbol{e}) + \mathcal{B}\,(\boldsymbol{u}, \boldsymbol{\lambda}; \boldsymbol{e}, \boldsymbol{\varepsilon})\right) dt \\
&\quad - \int_{I_n} \left((\sigma\, \dot{\boldsymbol{U}}^h, \boldsymbol{e}) + \mathcal{B}\,(\boldsymbol{U}^h, \boldsymbol{\lambda}^h; \boldsymbol{e}, \boldsymbol{\varepsilon})\right) dt - \left([\sigma\, \boldsymbol{U}^h]_{n-1}, \boldsymbol{e}_{n-1}^+\right),
\end{aligned} \tag{3.64}$$

since $[\boldsymbol{u}]_{n-1} = 0$. From (3.18a) and (3.20) we obtain:

$$\int_{I_n} \left((\sigma\, \dot{\boldsymbol{u}}, \boldsymbol{e}) + \mathcal{B}\,(\boldsymbol{u}, \boldsymbol{\lambda}; \boldsymbol{e}, \boldsymbol{\varepsilon})\right) dt = \int_{I_n} \mathcal{L}(\boldsymbol{e})\, dt,$$

$$\int_{I_n} \left\{(\sigma\, \dot{\boldsymbol{U}}^h, \boldsymbol{\mathcal{E}}) + \mathcal{B}(\boldsymbol{U}^h, \boldsymbol{\lambda}^h; \boldsymbol{\mathcal{E}}, \widetilde{\boldsymbol{\mathcal{E}}})\right\} dt + (\sigma\,[\boldsymbol{U}^h]_{n-1}, \boldsymbol{\mathcal{E}}_{n-1}^+) = \int_{I_n} \mathcal{L}(\boldsymbol{\mathcal{E}})\, dt. \tag{3.65}$$

Inserting (3.65) into (3.64) yields

$$\alpha_1\, \|(\boldsymbol{e}, \boldsymbol{\varepsilon})\|_{\mathbf{L}^2(I_n;\mathcal{X})}^2 + \frac{1}{2}\|\boldsymbol{e}_n^-\|_{\sigma,\Omega}^2 - \frac{1}{2}\|\boldsymbol{e}_{n-1}^-\|_{\sigma,\Omega}^2 + \frac{1}{2}\|\,[\boldsymbol{e}]_{n-1}\,\|_{\sigma,\Omega}^2 \tag{3.66}$$

$$\leq \int_{I_n} \mathcal{L}(\boldsymbol{e})\, dt - \int_{I_n} \left((\sigma\, \dot{\boldsymbol{U}}^h, \boldsymbol{e}) + \mathcal{B}\,(\boldsymbol{U}^h, \boldsymbol{\lambda}^h; \boldsymbol{e}, \boldsymbol{\varepsilon})\right) dt - \left([\sigma\, \boldsymbol{U}^h]_{n-1}, \boldsymbol{e}_{n-1}^+\right)$$

$$
= \int_{I_n} \mathcal{L}(e - \mathcal{E}) \, dt - \int_{I_n} \left((\sigma \dot{U}^h, e - \mathcal{E}) + \mathcal{B}(U^h, \lambda^h; e - \mathcal{E}, \varepsilon - \widetilde{\mathcal{E}}) \right) dt
$$

$$
- \left([\sigma U^h]_{n-1}, (e - \mathcal{E})^+_{n-1} \right)
$$

$$
= \int_{I_n} \mathcal{L}(e - e_h) \, dt + \int_{I_n} \mathcal{L}(e_h - \mathcal{E}) \, dt - \int_{I_n} \mathcal{B}(U^h, \lambda^h; e - e_h, \varepsilon - \varepsilon_h) \, dt
$$

$$
- \int_{I_n} \mathcal{B}(U^h, \lambda^h; e_h - \mathcal{E}, \varepsilon_h - \widetilde{\mathcal{E}}) \, dt - \left([\sigma U^h]_{n-1}, (e - \mathcal{E})^+_{n-1} \right)
$$

$$
- \int_{I_n} (\sigma \dot{U}^h, e - e_h) \, dt - \int_{I_n} (\sigma \dot{U}^h, e_h - \mathcal{E}) \, dt
$$

$$
= \int_{I_n} \mathcal{L}(e - e_h) \, dt + \int_{I_n} \mathcal{L}(e_h - \mathcal{E}) \, dt - \int_{I_n} \mathcal{B}(U^h, \lambda^h; e - e_h, \varepsilon - \varepsilon_h) \, dt
$$

$$
- \left([\sigma U^h]_{n-1}, (e - \mathcal{E})^+_{n-1} \right) - \int_{I_n} (\sigma \dot{U}^h, e - e_h) \, dt, \tag{3.67}
$$

where we have used that for the projection properties of P_h^1, $\mathfrak{P}_h^1$, p_h^1, $\mathcal{E} := \pi_1 e_h$ and $\widetilde{\mathcal{E}} := \tilde{\pi}_1 \varepsilon_h$ there holds:

$$
\int_{I_n} \mathcal{B}(U^h, \lambda^h; e_h - \mathcal{E}, \varepsilon_h - \widetilde{\mathcal{E}}) \, dt = 0 \ ,
$$

$$
\int_{I_n} (\sigma \dot{U}^h, e_h - \mathcal{E}) \, dt = 0 \ . \tag{3.68}
$$

For the left hand side of (3.67), there exists $\gamma_1 \geq \frac{1}{4}$ such that

$$
\alpha_1 \|(e, \varepsilon)\|^2_{\mathbf{L}^2(I_n; \boldsymbol{\mathcal{X}})} + \frac{1}{2} \|e_n^-\|^2_{\sigma, \Omega} - \frac{1}{2} \|e_{n-1}^-\|^2_{\sigma, \Omega} + \frac{1}{2} \| [e]_{n-1} \|^2_{\sigma, \Omega}
$$

$$
\geq \gamma_1 \left(\sqrt{2\alpha_1} \|(e, \varepsilon)\|_{\mathbf{L}^2(I_n; \boldsymbol{\mathcal{X}})} + \|e_{n-1}^-\|_{\sigma, \Omega} + \sqrt{\|e_n^-\|^2_{\sigma, \Omega} + \| [e]_{n-1} \|^2_{\sigma, \Omega}} \right) \tag{3.69}
$$

$$
\times \left(\sqrt{2\alpha_1} \|(e, \varepsilon)\|_{\mathbf{L}^2(I_n; \boldsymbol{\mathcal{X}})} - \|e_{n-1}^-\|_{\sigma, \Omega} \right) \ .
$$

Combining (3.67) and (3.69) we see that

$$
\left(\sqrt{2\alpha_1} \|(e, \varepsilon)\|_{\mathbf{L}^2(I_n; \boldsymbol{\mathcal{X}})} + \|e_{n-1}^-\|_{\sigma, \Omega} + \sqrt{\|e_n^-\|^2_{\sigma, \Omega} + \| [e]_{n-1} \|^2_{\sigma, \Omega}} \right)
$$

$$
\times \left(\sqrt{2\alpha_1} \|(e, \varepsilon)\|_{\mathbf{L}^2(I_n; \boldsymbol{\mathcal{X}})} - \|e_{n-1}^-\|_{\sigma, \Omega} \right) \tag{3.70}
$$

$$
\lesssim \int_{I_n} \mathcal{L}(e - e_h) \, dt - \int_{I_n} \left((\sigma \dot{U}^h, e - e_h) + \mathcal{B}(U^h, \lambda^h; e - e_h, \varepsilon - \varepsilon_h) \right) dt
$$

$$
- \left([\sigma U^h]_{n-1}, (e - \mathcal{E})^+_{n-1} \right)
$$

$$
+ \int_{I_n} \mathcal{L}(e_h - \mathcal{E}) \, dt \tag{3.71}
$$

$$
=: S_1 + S_2 + S_3.
$$

The estimates of S_1, S_2 and S_3 are discussed in the Lemmas 3.3.2, 3.3.3 and 3.3.4. The proof of Theorem 3.3.2 is finished on page 65.

Lemma 3.3.2 (estimate of S_1)

$$S_1 := \int_{I_n} \left\{ \mathcal{L}(e - e_h) - \left(\sigma \dot{U}^h, e - e_h \right) - \mathcal{B}\left(U^h, \lambda^h; e - e_h, \varepsilon - \varepsilon_h \right) \right\} dt \tag{3.72}$$
$$\lesssim (R_{1,n} + R_{2,n} + R_{3,n} + R_{4,n} + R_{5,n} + R_{6,n} + R_{7,n}) \, \|(e, \varepsilon)\|_{\mathbf{L}^2(I_n, \mathcal{X})}$$

where $R_{1,n}, \cdots, R_{7,n}$ are defined in Theorem 3.3.2.

Proof.

$$\mathcal{L}(e - e_h) - \left(\sigma \dot{U}^h, e - e_h \right) - \mathcal{B}\left(U^h, \lambda^h; e - e_h, \varepsilon - \varepsilon_h \right)$$

$$= - \left(\partial_t J + \tilde{\lambda} U^h + \sigma \dot{U}^h, e - e_h \right)_\Omega - \left(\mu^{-1} \operatorname{\mathbf{curl}} U^h, \operatorname{\mathbf{curl}} (e - e_h) \right)_\Omega$$

$$+ \left\langle \mathcal{W} U^h_\Gamma, (e - e_h)_\Gamma \right\rangle_\Gamma - \left\langle \widetilde{\mathcal{K}} \lambda^h, (e - e_h)_\Gamma \right\rangle_\Gamma - \left\langle (I - \mathcal{K}) U^h, \varepsilon - \varepsilon_h \right\rangle_\Gamma - \left\langle \mathcal{V} \lambda^h, \varepsilon - \varepsilon_h \right\rangle_\Gamma$$

$$\leq \left| \left(\partial_t J + \tilde{\lambda} U^h + \sigma \dot{U}^h, \tilde{e}^\perp \right)_\Omega + \left(\mu^{-1} \operatorname{\mathbf{curl}} U^h, \operatorname{\mathbf{curl}} \tilde{e}^\perp \right)_\Omega - \left\langle \mathcal{W} U^h_\Gamma - \widetilde{\mathcal{K}} \lambda^h, (\tilde{e}^\perp)_\Gamma \right\rangle_\Gamma \right|$$

$$+ \left| \left(\partial_t J + \tilde{\lambda} U^h + \sigma \dot{U}^h, \operatorname{\mathbf{grad}} \psi - \operatorname{\mathbf{grad}} P^1_h \psi \right)_\Omega - \left\langle \mathcal{W} U^h_\Gamma - \widetilde{\mathcal{K}} \lambda^h, \operatorname{\mathbf{grad}}_\Gamma \psi - \operatorname{\mathbf{grad}}_\Gamma P^1_h \psi \right\rangle_\Gamma \right|$$

$$+ \left| \left\langle (\mathcal{K} - I) U^h_\Gamma + \mathcal{V} \lambda^h, \operatorname{\mathbf{curl}}_\Gamma \phi - \operatorname{\mathbf{curl}}_\Gamma p^1_h \phi \right\rangle_\Gamma \right|, \tag{3.73}$$

where $\tilde{e}^\perp := e^\perp - \mathfrak{P}^1_h e^\perp$, $(\tilde{e}^\perp)_\Gamma := \gamma_D \tilde{e}^\perp$ and $U^h_\Gamma := \gamma_D U^h$. First, we consider the term $\left(\mu^{-1} \operatorname{\mathbf{curl}} U^h, \operatorname{\mathbf{curl}} \tilde{e}^\perp \right)_\Omega$. Since U^h is only elementwise in $\mathbf{H}(\operatorname{\mathbf{curl}}\mathbf{curl}, \Omega)$ we use the Green's formula to obtain

$$\left(\mu^{-1} \operatorname{\mathbf{curl}} U^h, \operatorname{\mathbf{curl}} \tilde{e}^\perp \right)_\Omega = \sum_{\mathfrak{T} \in \mathcal{T}_h} \left(\mu^{-1} \operatorname{\mathbf{curl}} U^h, \operatorname{\mathbf{curl}} \tilde{e}^\perp \right)_\mathfrak{T}$$

$$= \sum_{\mathfrak{T} \in \mathcal{T}_h} \left(\left(\operatorname{\mathbf{curl}} \left(\mu^{-1} \operatorname{\mathbf{curl}} U^h \right), \tilde{e}^\perp \right)_\mathfrak{T} + \left\langle \mu^{-1} \gamma_N U^h, \tilde{e}^\perp_\Gamma \right\rangle_{\partial \mathfrak{T}} \right)$$

$$= \sum_{\mathfrak{T} \in \mathcal{T}_h} \left\{ \left(\operatorname{\mathbf{curl}} \left(\mu^{-1} \operatorname{\mathbf{curl}} U^h \right), \tilde{e}^\perp \right)_\mathfrak{T} + \left\langle \mu^{-1} \operatorname{\mathbf{curl}} U^h \times n, \tilde{e}^\perp_\Gamma \right\rangle_{\partial \mathfrak{T}} \right\}$$

$$= \sum_{\mathfrak{T} \in \mathcal{T}_h} \left(\operatorname{\mathbf{curl}} \left(\mu^{-1} \operatorname{\mathbf{curl}} U^h \right), \tilde{e}^\perp \right)_\mathfrak{T} + \sum_{F \in \mathcal{F}_h} \left\langle [\mu^{-1} \operatorname{\mathbf{curl}} U^h \times n]_F, \tilde{e}^\perp_\Gamma \right\rangle_F . \tag{3.74}$$

Here we have used that the terms $\mu^{-1} \operatorname{\mathbf{curl}} U^h \times n \in \mathbf{L}^2(\partial \mathfrak{T})$ and $(e^\perp - \mathfrak{P}^1_h e^\perp)_\Gamma \in \mathbf{L}^2(\partial \mathfrak{T})$ (as $U^h_{|\mathfrak{T}}$ is a polynomial and $e^\perp, \mathfrak{P}^1_h e^\perp \in \mathbf{H}^1(\mathfrak{T})$), such that we can consider the $\mathbf{H}^{-\frac{1}{2}}_\| (\operatorname{div}_\Gamma, \partial \mathfrak{T}) - \mathbf{H}^{-\frac{1}{2}}_\perp (\operatorname{curl}_\Gamma, \partial \mathfrak{T})$-duality $\langle \cdot, \cdot \rangle_{\partial \mathfrak{T}}$ as a $\mathbf{L}^2(\partial \mathfrak{T})$-duality.

Next, we consider the term $\left(\partial_t J + \tilde{\lambda} U^h + \sigma \dot{U}^h, \operatorname{\mathbf{grad}} \psi - \operatorname{\mathbf{grad}} P^1_h \psi \right)_\Omega$ and Green's formula to obtain:

$$\left(\partial_t J + \tilde{\lambda} U^h + \sigma \dot{U}^h, \operatorname{\mathbf{grad}} \psi - \operatorname{\mathbf{grad}} P^1_h \psi \right)_\Omega \tag{3.75}$$

$$= \sum_{F \in \mathcal{F}_h} \left\langle [(\sigma \dot{U}^h + \tilde{\lambda} U^h) \cdot n]_F, \psi - P^1_h \psi \right\rangle_F - \left(\operatorname{div} \partial_t J + \tilde{\lambda} \operatorname{div} U^h + \operatorname{div} \sigma \dot{U}^h, \psi - P^1_h \psi \right)_\Omega .$$

3 The eddy current problem

In (3.75) due to the regularity of $\boldsymbol{U}^h$ we have interpreted the $H^{-\frac{1}{2}}(\partial\mathfrak{T}) - H^{\frac{1}{2}}(\partial\mathfrak{T})$-duality as a $\mathbf{L}^2(\partial\mathfrak{T})$-duality. Furthermore, we use the fact that there is no jump of $\partial_t\boldsymbol{J}\cdot\boldsymbol{n}$ over Γ due to the assumption that there is no flow of $\mathbf{J}$ through Γ and the continuity of $\mathbf{J}$ in Ω (see Page 36).

In the following we examine the terms with the boundary integral operators. First we analyze the term $\left\langle \mathcal{W}\boldsymbol{U}_\Gamma^h - \widetilde{\mathcal{K}}\boldsymbol{\lambda}^h, \mathbf{grad}_\Gamma\psi - \mathbf{grad}_\Gamma P_h^1\psi \right\rangle_\Gamma$, which represents an $\mathbf{H}_\|^{-\frac{1}{2}}(\mathrm{div}_\Gamma,\Gamma)-$ $\mathbf{H}_\perp^{-\frac{1}{2}}(\mathrm{curl}_\Gamma,\Gamma)$-duality pairing (the first term is in $\mathbf{H}_\|^{-\frac{1}{2}}(\mathrm{div}_\Gamma,\Gamma)$ as a result of (1.18) and (1.19), and the second term as tangential trace of $\mathbf{H}(\mathbf{curl},\Omega)$-functions is in $\mathbf{H}_\perp^{-\frac{1}{2}}(\mathrm{curl}_\Gamma,\Gamma)$). We use the facts that for functions $\Phi = \mathbf{curl}_\Gamma\varphi_1 + \mathbf{grad}_\Gamma\varphi_2 \in \mathbf{H}_\|^{-\frac{1}{2}}(\mathrm{div}_\Gamma,\Gamma)$ and $\Psi = \mathbf{grad}_\Gamma\psi_1 + \mathbf{curl}_\Gamma\psi_2 \in \mathbf{H}_\perp^{-\frac{1}{2}}(\mathrm{curl}_\Gamma,\Gamma)$ it follows

$$
\begin{aligned}
\langle\Phi,\Psi\rangle_\Gamma &= -\langle\varphi_1,\Delta_\Gamma\psi_2\rangle_\Gamma - \langle\Delta_\Gamma\varphi_2,\psi_1\rangle_\Gamma \\
&= \langle\varphi_1,\mathrm{curl}_\Gamma\Psi\rangle_\Gamma - \langle\mathrm{div}_\Gamma\Phi,\psi_1\rangle_\Gamma .
\end{aligned} \tag{3.76}
$$

Moreover, Lemma 1.3.5 provides that for $\boldsymbol{v}\in\mathbf{H}(\mathbf{curl},\Omega_e)$ and $\widetilde{\boldsymbol{\lambda}}\in\mathbf{H}_\|^{-\frac{1}{2}}(\mathrm{div}\,0_\Gamma,\Gamma)$ there holds

$$
\mathrm{div}_\Gamma\mathcal{W}\gamma_D\boldsymbol{v} = 0 \quad\text{and}\quad \mathrm{div}_\Gamma\widetilde{\mathcal{K}}\widetilde{\boldsymbol{\lambda}} = 0 \quad\text{in}\quad H^{-1/2}(\Gamma) . \tag{3.77}
$$

Then, from (3.77) and (3.76) we deduce

$$
\begin{aligned}
\left\langle \mathcal{W}\gamma_D\boldsymbol{U}^h - \widetilde{\mathcal{K}}\boldsymbol{\lambda}^h, \mathbf{grad}_\Gamma\psi - \mathbf{grad}_\Gamma P_h^1\psi \right\rangle_\Gamma & \\
= -\left\langle \mathrm{div}_\Gamma\mathcal{W}\gamma_D\boldsymbol{U}^h - \mathrm{div}_\Gamma\widetilde{\mathcal{K}}\boldsymbol{\lambda}^h, \psi - P_h^1\psi \right\rangle_\Gamma &= 0.
\end{aligned} \tag{3.78}
$$

Finally, we examine the term $\left\langle (\mathcal{K}-I)\boldsymbol{U}_\Gamma^h - \mathcal{V}\boldsymbol{\lambda}^h, \mathbf{curl}_\Gamma\,\phi - \mathbf{curl}_\Gamma\,p_h^1\phi \right\rangle_\Gamma$ which constitutes an $\mathbf{H}_\perp^{-\frac{1}{2}}(\mathrm{curl}_\Gamma,\Gamma) - \mathbf{H}_\|^{-\frac{1}{2}}(\mathrm{div}_\Gamma,\Gamma)$-duality pairing (the left hand side is in $\mathbf{H}_\perp^{-\frac{1}{2}}(\mathrm{curl}_\Gamma,\Gamma)$ as a result of (1.16) and (1.17) , and the right hand side as vectorial surface rotation on Γ is in $\mathbf{H}_\|^{-\frac{1}{2}}(\mathrm{div}_\Gamma,\Gamma)$). This and (3.76) gives

$$
\left\langle (\mathcal{K}-I)\boldsymbol{U}_\Gamma^h - \mathcal{V}\boldsymbol{\lambda}^h, \mathbf{curl}_\Gamma\,\phi - \mathbf{curl}_\Gamma\,p_h^1\phi \right\rangle_\Gamma = \left\langle \mathrm{curl}_\Gamma(\mathcal{K}-I)\boldsymbol{U}_\Gamma^h - \mathrm{curl}_\Gamma\mathcal{V}\boldsymbol{\lambda}^h, \phi - p_h^1\phi \right\rangle_\Gamma . \tag{3.79}
$$

Combining the equations (3.73), (3.74), (3.75), (3.78) and (3.79) yields

$$
\begin{aligned}
\mathcal{L}(\boldsymbol{e}-\boldsymbol{e}_h) &- \left(\sigma\dot{\boldsymbol{U}}^h, \boldsymbol{e}-\boldsymbol{e}_h\right) - \mathcal{B}\left(\boldsymbol{U}^h,\boldsymbol{\lambda}^h;\boldsymbol{e}-\boldsymbol{e}_h,\boldsymbol{\varepsilon}-\boldsymbol{\varepsilon}_h\right) \\
&\lesssim \sum_{\mathfrak{T}\in\mathcal{T}_h}\left| (\partial_t\boldsymbol{J} + \tilde{\lambda}\boldsymbol{U}^h + \sigma\dot{\boldsymbol{U}}^h + \mathbf{curl}\left(\mu^{-1}\mathbf{curl}\,\boldsymbol{U}^h\right), \tilde{\mathbf{e}}^\perp)_{\mathfrak{T}} \right| \\
&+ \sum_{F\in\mathcal{F}_h^C}\left| \left\langle [\mu^{-1}\mathbf{curl}\,\boldsymbol{U}^h\times\boldsymbol{n}]_F, \tilde{\mathbf{e}}_\Gamma^\perp \right\rangle_F \right| \\
&+ \sum_{F\in\mathcal{F}_h^\Gamma}\left| \left\langle \mu^{-1}\mathbf{curl}\,\boldsymbol{U}^h\times\boldsymbol{n} - \mathcal{W}\boldsymbol{U}_\Gamma^h + \widetilde{\mathcal{K}}\boldsymbol{\lambda}^h, \tilde{\mathbf{e}}_\Gamma^\perp \right\rangle_F \right|
\end{aligned}
$$

$$+ \sum_{\mathfrak{T} \in \mathcal{T}_h} \left| \left(\operatorname{div} \partial_t \boldsymbol{J} + \tilde{\lambda} \operatorname{div} \boldsymbol{U}^h + \operatorname{div} \sigma \dot{\boldsymbol{U}}^h, \psi - P_h^1 \psi \right)_{\mathfrak{T}} \right|$$

$$+ \sum_{F \in \mathcal{F}_h^C} \left| \left\langle [(\sigma \dot{\boldsymbol{U}}^h + \tilde{\lambda} \boldsymbol{U}^h) \cdot \boldsymbol{n}]_F, \psi - P_h^1 \psi \right\rangle_F \right| \qquad (3.80)$$

$$+ \sum_{F \in \mathcal{F}_h^\Gamma} \left| \left\langle (\sigma \dot{\boldsymbol{U}}^h + \tilde{\lambda} \boldsymbol{U}^h) \cdot \boldsymbol{n}, \psi - P_h^1 \psi \right\rangle_F \right|$$

$$+ \sum_{F \in \mathcal{F}_h^\Gamma} \left| \left\langle \operatorname{curl}_\Gamma (\mathcal{K} - I) \boldsymbol{U}_\Gamma^h - \operatorname{curl}_\Gamma \mathcal{V} \boldsymbol{\lambda}^h, \phi - p_h^1 \phi \right\rangle_F \right|.$$

Integrating over I_n and applying the Cauchy-Schwarz inequality, where all scalar products are interpreted as $\mathbf{L}^2$-products, the continuity of the integral operators (see [73, Lemma 4.3.3]) and the estimates properties in (3.58) we get

$$\int_{I_n} \left\{ \mathcal{L}(\boldsymbol{e} - \boldsymbol{e}_h) - (\sigma \dot{\boldsymbol{U}}^h, \boldsymbol{e} - \boldsymbol{e}_h) - \mathcal{B}\left(\boldsymbol{U}^h, \boldsymbol{\lambda}^h; \boldsymbol{e} - \boldsymbol{e}_h, \boldsymbol{\varepsilon} - \boldsymbol{\varepsilon}_h\right) \right\} dt$$

$$\leq \left\{ \left(\int_{I_n} \sum_{\mathfrak{T} \in \mathcal{T}_h} h_{\mathfrak{T}}^2 \left\| \sqrt{\mu} \left(\partial_t \boldsymbol{J} + \sigma \dot{\boldsymbol{U}}^h + \operatorname{\mathbf{curl}} \left(\mu^{-1} \operatorname{\mathbf{curl}} \boldsymbol{U}^h \right) \right) \right\|_{0,\mathfrak{T}}^2 dt \right)^{1/2} \right.$$

$$+ \left(\int_{I_n} \sum_{F \in \mathcal{F}_h^C} h_F \left\| \sqrt{\mu_A} [\mu^{-1} \operatorname{\mathbf{curl}} \boldsymbol{U}^h \times \boldsymbol{n}]_F \right\|_{0,F}^2 dt \right)^{1/2}$$

$$\left. + \left(\int_{I_n} \sum_{F \in \mathcal{F}_h^\Gamma} h_F \left\| \sqrt{\mu^{-1}} \operatorname{\mathbf{curl}} \boldsymbol{U}^h \times \boldsymbol{n} - \sqrt{\mu} \,\mathcal{W} \boldsymbol{U}_\Gamma^h + \sqrt{\mu} \,\widetilde{\mathcal{K}} \boldsymbol{\lambda}^h \right\|_{0,F}^2 dt \right)^{1/2} \right\} \left| \frac{1}{\sqrt{\mu}} \boldsymbol{e}^\perp \right|_{\mathbf{L}^2(I_n, \mathbf{H}^1(\Omega))}$$

$$+ \left\{ \left(\int_{I_n} \sum_{\mathfrak{T} \in \mathcal{T}_h} h_{\mathfrak{T}}^2 \left\| \sqrt{\sigma^{-1}} \left(\operatorname{div} \partial_t \boldsymbol{J} + \operatorname{div} \sigma \dot{\boldsymbol{U}}^h \right) \right\|_{0,\mathfrak{T}}^2 dt \right)^{1/2} \right. \qquad (3.81)$$

$$+ \left(\int_{I_n} \sum_{F \in \mathcal{F}_h^C} h_F \left\| \sqrt{\sigma_A}^{-1} [\sigma \dot{\boldsymbol{U}}^h \cdot \boldsymbol{n}]_F \right\|_{0,F}^2 dt \right)^{1/2}$$

$$\left. + \left(\int_{I_n} \sum_{F \in \mathcal{F}_h^\Gamma} h_F \left\| \sqrt{\sigma} \dot{\boldsymbol{U}}^h \cdot \boldsymbol{n} \right\|_{0,F}^2 dt \right)^{1/2} \right\} \| \sqrt{\sigma} \operatorname{\mathbf{grad}} \psi \|_{\mathbf{L}^2(I_n, \mathbf{L}^2(\Omega))}$$

$$+ \left\{ \left(\int_{I_n} \sum_{F \in \mathcal{F}_h^\Gamma} h_F \left\| \operatorname{curl}_\Gamma (\mathcal{K} - I) \boldsymbol{U}_\Gamma^h - \operatorname{curl}_\Gamma \mathcal{V} \boldsymbol{\lambda}^h \right\|_{0,F}^2 dt \right)^{1/2} \right\} \| \operatorname{\mathbf{curl}}_\Gamma \phi \|_{\mathbf{L}^2(I_n, \mathbf{H}^{-1/2}(\Gamma))},$$

where σ, μ on Γ are always refering to the interior σ, μ, i.e., the trace from Ω, and σ_A and μ_A denote the average of σ and μ on a face F.

We conclude the proof of estimate (3.72) due to $\| \sqrt{\sigma} \operatorname{\mathbf{grad}} \psi \|_{\mathbf{L}^2(\Omega)} \lesssim \| \boldsymbol{e}^0 \|_{\mathbf{H}(\operatorname{\mathbf{curl}}, \Omega)}$, $\| \operatorname{\mathbf{curl}}_\Gamma \phi \|_{\mathbf{H}^{-1/2}(\Gamma)} = \| \boldsymbol{\varepsilon} \|_{\mathbf{H}^{-1/2}(\Gamma)}$, and $\left| \frac{1}{\sqrt{\mu}} \boldsymbol{e}^\perp \right|_{\mathbf{H}^1(\Omega)}$ can be estimated from above by $\| \boldsymbol{e} \|_{\mathbf{H}(\operatorname{\mathbf{curl}}, \Omega)}$ due to (3.61). $\square$

61

Lemma 3.3.3 (estimate of S_2)

$$S_2 := \left(\left[\sigma \, U^h \right]_{n-1}, (\mathcal{E} - e)^+_{n-1} \right)$$

$$\lesssim \left(\left(\sum_{i=8}^{11} R_{i,n}^2 \right) + T_{1,n} \right) \left(\left\| e_{n-1}^- \right\|_{0,\Omega} + \left\| [e]_{n-1} \right\|_{0,\Omega} + \left\| e \right\|_{L^2(I_n \,;\mathbf{H(curl,\Omega)})} \right) \tag{3.82}$$

where $R_{8,n}, \cdots, R_{11,n}$ and $T_{1,n}$ are defined in Theorem 3.3.2

Proof. The definition of the orthogonal L^2-projection in (2.10) leads to the following representation formula for $\mathcal{E}$:

$$\mathcal{E}(\boldsymbol{x}, t) := \pi_1 e_h(\boldsymbol{x}, t) = \mathcal{E}_1(\boldsymbol{x}) + \frac{t - t_{n-1}}{k_n} \mathcal{E}_2(\boldsymbol{x}) \tag{3.83}$$

with

$$\mathcal{E}_1(\boldsymbol{x}) := \frac{1}{k_n} \int_{I_n} \left(4 - 6 \frac{s - t_{n-1}}{k_n} \right) e_h(\boldsymbol{x}, s) ds \,, \tag{3.84}$$

$$\mathcal{E}_2(\boldsymbol{x}) := \frac{1}{k_n} \int_{I_n} \left(12 \frac{s - t_{n-1}}{k_n} - 6 \right) e_h(\boldsymbol{x}, s) ds \,. \tag{3.85}$$

From $\int_0^1 (4 - 6s)\, ds = 1$ we obtain

$$
\begin{aligned}
(\mathcal{E} - e)^+_{n-1} &= \frac{1}{k_n} \int_{I_n} \left(4 - 6 \frac{s - t_{n-1}}{k_n} \right) \left(e_h(s) - e_{n-1}^+ \right) ds \\
&= \frac{1}{k_n} \int_{I_n} \left(4 - 6 \frac{s - t_{n-1}}{k_n} \right) \left((e_h(s) - e) + (e - e_{n-1}^+) \right) ds \\
&= \frac{1}{k_n} \int_{I_n} \left(4 - 6 \frac{s - t_{n-1}}{k_n} \right) \left((\mathfrak{P}_h^1 e^\perp - e^\perp) + \mathbf{grad}(P_h^1 \psi - \psi) + (e - e_{n-1}^+) \right) ds
\end{aligned}
\tag{3.86}
$$

Inserting (3.86) in S_2 it follows that

$$\left(\left[\sigma \, U^h \right]_{n-1}, (\mathcal{E} - e)^+_{n-1} \right) := S_{2,1} + S_{2,2} + S_{2,3} \tag{3.87}$$

where

$$
\begin{aligned}
S_{2,1} &:= \left(\left[\sigma \, U^h \right]_{n-1}, \frac{1}{k_n} \int_{I_n} \left(4 - 6 \frac{s - t_{n-1}}{k_n} \right) (\mathfrak{P}_h^1 e^\perp - e^\perp)\, ds \right) , \\
S_{2,2} &:= \left(\left[\sigma \, U^h \right]_{n-1}, \frac{1}{k_n} \int_{I_n} \left(4 - 6 \frac{s - t_{n-1}}{k_n} \right) (\mathbf{grad}(P_h^1 \psi - \psi))\, ds \right) , \\
S_{2,3} &:= \left(\left[\sigma \, U^h \right]_{n-1}, \frac{1}{k_n} \int_{I_n} \left(4 - 6 \frac{s - t_{n-1}}{k_n} \right) (e - e_{n-1}^+)\, ds \right) .
\end{aligned}
\tag{3.88}
$$

We start with the term $S_{2,1}$. By applying Cauchy's inequality and the approximation properties cited in (3.58) we obtain

$$
\begin{aligned}
S_{2,1} &\leq \sum_{\mathfrak{T}\in\mathcal{T}_h} \left\| \left[\sigma\, \boldsymbol{U}^h\right]_{n-1} \right\|_{0,\mathfrak{T}} \left\| \frac{1}{k_n} \int_{I_n} \left(4 - 6\frac{s - t_{n-1}}{k_n}\right) \left(\boldsymbol{\mathfrak{P}}_h^1 \boldsymbol{e}^\perp - \boldsymbol{e}^\perp\right) ds \right\|_{0,\mathfrak{T}} \\
&\leq \sum_{\mathfrak{T}\in\mathcal{T}_h} \left\| \left[\sigma\, \boldsymbol{U}^h\right]_{n-1} \right\|_{0,\mathfrak{T}} \frac{2}{\sqrt{k_n}} \left\| \boldsymbol{\mathfrak{P}}_h^1 \boldsymbol{e}^\perp - \boldsymbol{e}^\perp \right\|_{L^2(I_n;\mathbf{L}^2(\mathfrak{T}))} \\
&\lesssim \sum_{\mathfrak{T}\in\mathcal{T}_h} \left\| \left[\sigma\, \boldsymbol{U}^h\right]_{n-1} \right\|_{0,\mathfrak{T}} \frac{h_{\mathfrak{T}}}{\sqrt{k_n}} |\boldsymbol{e}^\perp|_{L^2\left(I_n;\mathbf{H}^1(D_{\mathfrak{T}}^1)\right)} \\
&\lesssim \left(\frac{1}{k_n} \sum_{\mathfrak{T}\in\mathcal{T}_h} h_{\mathfrak{T}}^2 \left\| \left[\sigma\, \boldsymbol{U}^h\right]_{n-1} \right\|_{0,\mathfrak{T}}^2 \right)^{1/2} |\boldsymbol{e}^\perp|_{L^2\left(I_n;\mathbf{H}^1(\Omega)\right)}\;.
\end{aligned}
\tag{3.89}
$$

Next, we consider the term $S_{2,2}$. Since $\left[\boldsymbol{U}^h\right]$ is only elementwise in $\mathbf{H}(\mathrm{div},\Omega)$ we use Green's formula for a fixed t to obtain

$$
\begin{aligned}
&\left(\left[\sigma\, \boldsymbol{U}^h\right]_{n-1}, \mathbf{grad}\, P_h^1\psi - \mathbf{grad}\,\psi\right)_\Omega \\
&= -\left(\mathrm{div}\left[\sigma\, \boldsymbol{U}^h\right]_{n-1}, P_h^1\psi - \psi\right)_\Omega + \sum_{F\in\mathcal{F}_h} \left\langle \left[\left[\sigma\, \boldsymbol{U}^h\right]_{n-1} \cdot \boldsymbol{n}\right]_F, P_h^1\psi - \psi \right\rangle_F \;.
\end{aligned}
\tag{3.90}
$$

Combining (3.90) and the definition of $S_{2,2}$ yields

$$
\begin{aligned}
S_{2,2} &\lesssim \sum_{\mathfrak{T}\in\mathcal{T}_h} \left| \left(\mathrm{div}\left[\sigma\, \boldsymbol{U}^h\right]_{n-1}, \frac{1}{k_n}\int_{I_n}\left(4 - 6\frac{s - t_{n-1}}{k_n}\right)\left(P_h^1\psi - \psi\right) ds\right)_{\mathfrak{T}} \right| \\
&\quad + \sum_{F\in\mathcal{F}_h^C} \left| \left\langle \left[\left[\sigma\, \boldsymbol{U}^h\right]_{n-1} \cdot \boldsymbol{n}\right]_F, \frac{1}{k_n}\int_{I_n}\left(4 - 6\frac{s - t_{n-1}}{k_n}\right)\left(P_h^1\psi - \psi\right) ds\right\rangle_F \right| \\
&\quad + \sum_{F\in\mathcal{F}_h^\Gamma} \left| \left\langle \left[\sigma\, \boldsymbol{U}^h\right]_{n-1} \cdot \boldsymbol{n}, \frac{1}{k_n}\int_{I_n}\left(4 - 6\frac{s - t_{n-1}}{k_n}\right)\left(P_h^1\psi - \psi\right) ds\right\rangle_F \right| \;.
\end{aligned}
\tag{3.91}
$$

We apply to (3.91) the Cauchy-Schwarz inequality (here all scalar products are interpreted as $\mathbf{L}^2$-products) and the estimate properties in (3.58) to obtain

$$
\begin{aligned}
S_{2,2} &\lesssim \left\{ \left(\frac{1}{k_n}\sum_{\mathfrak{T}\in\mathcal{T}_h} h_{\mathfrak{T}}^2 \left\| \sqrt{\sigma^{-1}}\,\mathrm{div}\left[\sigma\, \boldsymbol{U}^h\right]_{n-1} \right\|_{0,\mathfrak{T}}^2\right)^{1/2} \right. \\
&\quad + \left(\frac{1}{k_n}\sum_{F\in\mathcal{F}_h^C} h_F \left\| \sqrt{\sigma_A}^{-1}\left[\left[\sigma\, \boldsymbol{U}^h\right]_{n-1} \cdot \boldsymbol{n}\right]_F \right\|_{0,F}^2\right)^{1/2} \\
&\quad \left. + \left(\frac{1}{k_n}\sum_{F\in\mathcal{F}_h^\Gamma} h_F \left\| \sqrt{\sigma}\,\left[\boldsymbol{U}^h\right]_{n-1} \cdot \boldsymbol{n} \right\|_{0,F}^2\right)^{1/2} \right\} \left\|\sqrt{\sigma}\,\mathbf{grad}\,\psi\right\|_{\mathbf{L}^2(I_n,\mathbf{L}^2(\Omega))} \;.
\end{aligned}
\tag{3.92}
$$

Finally, we consider the term $S_{2,3}$ and use the Cauchy-Schwarz inequality to get

$$
\begin{aligned}
S_{2,3} &:= \left([\sigma\, \boldsymbol{U}^h]_{n-1}, \frac{1}{k_n} \int_{I_n} \left(4 - 6\frac{s - t_{n-1}}{k_n} \right) \left(\boldsymbol{e} - \boldsymbol{e}_{n-1}^+ \right) ds \right) \\
&\leq \sum_{\mathfrak{T}\in\mathcal{T}_h} \left\| [\sigma\, \boldsymbol{U}^h]_{n-1} \right\|_{0,\mathfrak{T}} \left\| \frac{1}{k_n} \int_{I_n} \left(4 - 6\frac{s - t_{n-1}}{k_n} \right) \left(\boldsymbol{e} - \boldsymbol{e}_{n-1}^+ \right) ds \right\|_{0,\mathfrak{T}} \\
&\leq \sum_{\mathfrak{T}\in\mathcal{T}_h} \left\| [\sigma\, \boldsymbol{U}^h]_{n-1} \right\|_{0,\mathfrak{T}} \frac{2}{\sqrt{k_n}} \left\| \left(\boldsymbol{e} - \boldsymbol{e}_{n-1}^+ \right) \right\|_{L^2(I_n;\mathbf{L}^2(\mathfrak{T}))} \\
&\leq \left\| [\sigma\, \boldsymbol{U}^h]_{n-1} \right\|_{0,\Omega} \left(\frac{1}{\sqrt{k_n}} \|\boldsymbol{e}\|_{L^2(I_n;\mathbf{L}^2(\Omega))} + \left\| \boldsymbol{e}_{n-1}^+ \right\|_{\mathbf{L}^2(\Omega)} \right).
\end{aligned}
\tag{3.93}
$$

We conclude the proof of estimate (3.82) combining the inequalities (3.89), (3.92) and (3.93) and the fact that $\|\sqrt{\sigma}\,\mathbf{grad}\,\psi\|_{\mathbf{L}^2(\Omega)} \lesssim \|\boldsymbol{e}\|_{\mathbf{H}(\mathbf{curl},\Omega)}$ and that $\left|\frac{1}{\sqrt{\mu}}\boldsymbol{e}^\perp\right|_{\mathbf{H}^1(\Omega)}$ can be estimated from above by $\|\boldsymbol{e}\|_{\mathbf{H}(\mathbf{curl},\Omega)}$ due to (3.61). $\square$

Lemma 3.3.4 (estimate of S_3)

$$
S_3 := \int_{I_n} \mathcal{L}(\boldsymbol{e}_h - \boldsymbol{\mathcal{E}})\, dt \lesssim k_n^{5/2} \max_{t\in I_n} \|\ddot{f}\|_{\mathbf{L}^2(\Omega)} \|\boldsymbol{e}\|_{L^2(I_n;\mathbf{H}(\mathbf{curl},\Omega))}
\tag{3.94}
$$

where $f = f(\boldsymbol{x},t) := -\partial_t \mathbf{J}(\boldsymbol{x},t)$ and $\mathcal{L}(\boldsymbol{e}_h - \boldsymbol{\mathcal{E}}) = (f, \boldsymbol{e}_h - \boldsymbol{\mathcal{E}})_\Omega$.

Proof.

Define the linear interpolate of the function f at t_{n-1} and t_n

$$
\overline{f} := f_{n-1}^+ + \frac{t - t_{n-1}}{k_n} \left(f_n^- - f_{n-1}^+ \right) \quad t \in I_n
\tag{3.95}
$$

Then from Lemma 2.4.1 we obtain that $\int_{I_n} (\overline{f}, \boldsymbol{e}_h - \boldsymbol{\mathcal{E}})_\Omega\, dt = 0$. Hence

$$
\begin{aligned}
\int_{I_n} (f, \boldsymbol{e}_h - \boldsymbol{\mathcal{E}})_\Omega\, dt &:= \int_{I_n} (f - \overline{f}, \boldsymbol{e}_h - \boldsymbol{\mathcal{E}})_\Omega\, dt \\
&\leq \|f - \overline{f}\|_{L^2(I_n;\mathbf{L}^2(\Omega))} \|\boldsymbol{e}_h - \boldsymbol{\mathcal{E}}\|_{L^2(I_n;\mathbf{L}^2(\Omega))} \\
&\lesssim k_n^2 \|\ddot{f}\|_{L^2(I_n;\mathbf{L}^2(\Omega))} \|\boldsymbol{e}_h\|_{L^2(I_n;\mathbf{L}^2(\Omega))} \\
&\lesssim k_n^{5/2} \max_{t\in I_n} \|\ddot{f}\|_{\mathbf{L}^2(\Omega)} \|\boldsymbol{e}_h\|_{L^2(I_n;\mathbf{L}^2(\Omega))}.
\end{aligned}
\tag{3.96}
$$

Now, from the definition of $\boldsymbol{e}_h$ and the properties in (3.58) we obtain

$$
\begin{aligned}
\|\boldsymbol{e}_h\|_{\mathbf{L}^2(\Omega)} &= \|\boldsymbol{\mathfrak{P}}_h^1 \boldsymbol{e}^\perp + \mathbf{grad}\, P_h^1 \psi\|_{\mathbf{L}^2(\Omega)} \leq \|\boldsymbol{\mathfrak{P}}_h^1 \boldsymbol{e}^\perp\|_{\mathbf{L}^2(\Omega)} + \|\mathbf{grad}\, P_h^1 \psi\|_{\mathbf{L}^2(\Omega)} \\
&\lesssim \|\boldsymbol{e}^\perp\|_{\mathbf{H}^1(\Omega)} + \|\mathbf{grad}\,\psi\|_{\mathbf{L}^2(\Omega)} \lesssim \|\boldsymbol{e}\|_{\mathbf{H}(\mathbf{curl},\Omega)}.
\end{aligned}
\tag{3.97}
$$

From (3.97) and (3.96) it follows that

$$\int_{I_n} (f, \boldsymbol{e}_h - \boldsymbol{\mathcal{E}})_\Omega \, dt \lesssim k_n^{5/2} \max_{t \in I_n} \|\ddot{f}\|_{\mathbf{L}^2(\Omega)} \|e\|_{L^2(I_n;\mathbf{H}(\mathbf{curl},\Omega))} . \tag{3.98}$$

□

Conclusion of the proof of Theorem 3.3.2: Finally, the assertion follows immediately by inserting (3.72), (3.82) and (3.94) in the inequality (3.70). ■

From the global error indicators $R_{i,n}$ we can derive local error indicators $\eta_{i,n}(\mathfrak{T})$ for each $\mathfrak{T} \in \mathcal{T}_h$. These local error indicators are defined as follows:

$$(\eta_{1,n}(\mathfrak{T}))^2 := k_n \max_{t \in I_n} h_{\mathfrak{T}}^2 \left\| \sqrt{\mu} \big(\partial_t \boldsymbol{J} + \tilde{\lambda} \boldsymbol{U}^h + \sigma \dot{\boldsymbol{U}}^h + \mathbf{curl} \left(\mu^{-1} \mathbf{curl} \, \boldsymbol{U}^h \right) \big) \right\|_{0,\mathfrak{T}}^2 ,$$

$$(\eta_{2,n}(\mathfrak{T}))^2 := k_n \max_{t \in I_n} \sum_{F \in \mathcal{F}_h^C(\mathfrak{T})} h_F \left\| \sqrt{\mu_A} [\mu^{-1} \mathbf{curl} \, \boldsymbol{U}^h \times \boldsymbol{n}]_F \right\|_{0,F}^2 ,$$

$$(\eta_{3,n}(\mathfrak{T}))^2 := k_n \max_{t \in I_n} \sum_{F \in \mathcal{F}_h^\Gamma(\mathfrak{T})} h_F \left\| \sqrt{\mu^{-1}} \, \mathbf{curl} \, \boldsymbol{U}^h \times \boldsymbol{n} - \sqrt{\mu} \, \mathcal{W} \boldsymbol{U}_\Gamma^h + \sqrt{\mu} \, \widetilde{\mathcal{K}} \boldsymbol{\lambda}^h \right\|_{0,F}^2 ,$$

$$(\eta_{4,n}(\mathfrak{T}))^2 := k_n \max_{t \in I_n} h_{\mathfrak{T}}^2 \left\| \sqrt{\sigma^{-1}} \big(\mathrm{div} \, \partial_t \boldsymbol{J} + \tilde{\lambda} \, \mathrm{div} \, \boldsymbol{U}^h + \mathrm{div} \, \sigma \dot{\boldsymbol{U}}^h \big) \right\|_{0,\mathfrak{T}}^2 ,$$

$$(\eta_{5,n}(\mathfrak{T}))^2 := k_n \max_{t \in I_n} \sum_{F \in \mathcal{F}_h^C(\mathfrak{T})} h_F \left\| \sqrt{\sigma_A}^{-1} [(\sigma \dot{\boldsymbol{U}}^h + \tilde{\lambda} \boldsymbol{U}^h) \cdot \boldsymbol{n}]_F \right\|_{0,F}^2 ,$$

$$(\eta_{6,n}(\mathfrak{T}))^2 := k_n \max_{t \in I_n} \sum_{F \in \mathcal{F}_h^\Gamma(\mathfrak{T})} h_F \left\| \big(\sqrt{\sigma} \dot{\boldsymbol{U}}^h + \sqrt{\sigma^{-1}} \tilde{\lambda} \boldsymbol{U}^h \big) \cdot \boldsymbol{n} \right\|_{0,F}^2 ,$$

$$(\eta_{7,n}(\mathfrak{T}))^2 := k_n \max_{t \in I_n} \sum_{F \in \mathcal{F}_h^\Gamma(\mathfrak{T})} h_F \left\| \mathrm{curl}_\Gamma \, (\mathcal{K} - I) \boldsymbol{U}_\Gamma^h - \mathrm{curl}_\Gamma \, \mathcal{V} \boldsymbol{\lambda}^h \right\|_{0,F}^2 ,$$

$$(\eta_{8,n}(\mathfrak{T}))^2 := \frac{1}{k_n} h_{\mathfrak{T}}^2 \left\| [\sigma \boldsymbol{U}^h]_{n-1} \right\|_{0,\mathfrak{T}} ,$$

$$(\eta_{9,n}(\mathfrak{T}))^2 := \frac{1}{k_n} h_{\mathfrak{T}}^2 \left\| \sqrt{\sigma^{-1}} \, \mathrm{div} \, [\sigma \boldsymbol{U}^h]_{n-1} \right\|_{0,\mathfrak{T}}^2 ,$$

$$(\eta_{10,n}(\mathfrak{T}))^2 := \frac{1}{k_n} \sum_{F \in \mathcal{F}_h^C(\mathfrak{T})} h_F \left\| \sqrt{\sigma_A}^{-1} \left[[\sigma \boldsymbol{U}^h]_{n-1} \cdot \boldsymbol{n} \right]_F \right\|_{0,F}^2 ,$$

$$(\eta_{11,n}(\mathfrak{T}))^2 := \frac{1}{k_n} \sum_{F \in \mathcal{F}_h^\Gamma(\mathfrak{T})} h_F \left\| \sqrt{\sigma} \, [\boldsymbol{U}^h]_{n-1} \cdot \boldsymbol{n} \right\|_{0,F}^2 .$$

The local mesh size and the length of the time steps are determined by the following adaptive feedback algorithm. A version of this algorithm is implemented by Mund & Stephan [61].

Algorithm 1 Adaptive feedback algorithm

Require: *Initial mesh $\mathcal{T}_h^0$, error tolerance $\vartheta > 0$, percentage of refined elements denoted by $\delta \in [0,1]$, initial time step $k_1 > 0$*

  for $n = 1, 2, \cdots$ **do**

  1. Compute the Galerkin solution $(\boldsymbol{U}^h, \boldsymbol{\lambda}^h)$ of the fully-discrete system (3.26) in the time intervall $(t_{n-1}, t_n]$.

  2. Compute for each $\mathfrak{T} \in \mathcal{T}_h$ the local error indicators $\eta_{i,n}, i = 1, \dots, 11$ and set

$$
\eta^n(\mathfrak{T}) := \sum_{i=1}^{11} \eta_{i,n}(\mathfrak{T}), \qquad \eta^n_{\max} := \max_{\mathfrak{T}' \in \mathcal{T}_h} \eta^n(\mathfrak{T}').
$$

  3. Refine any $\mathfrak{T} \in \mathcal{T}_h$ where $\delta \cdot \eta^n_{\max} \leq \eta^n(\mathfrak{T})$. If necessary refine adjacent elements.

  4. If

$$
\eta^{\mathfrak{T}}_n := \sum_{i=1}^{11} \left(\sum_{\mathfrak{T}' \in \mathcal{T}_h} \eta^2_{i,n}(\mathfrak{T}') \right)^{\frac{1}{2}} \leq \vartheta
$$

  go to step 5. Otherwise repeat the step 1-4 for the refined mesh.

  5. Choose k_{n+1} such that

$$
\left(\frac{k_{n+1}}{k_n} \right)^{\frac{5}{2}} (T_{1,n} + T_{2,n}) = \eta^{\mathfrak{T}}_n.
$$

  Stop if $t_{n+1} = t_n + k_{n+1} \geq T$.

The implementation of this algorithm was performed using the program package MAI-PROGS (see [50]). The corresponding results are given in Chapter 4. For the implementation we allow hanging nodes and start the refinements at each time level with the initial triangulation $\mathcal{T}_h^0$.
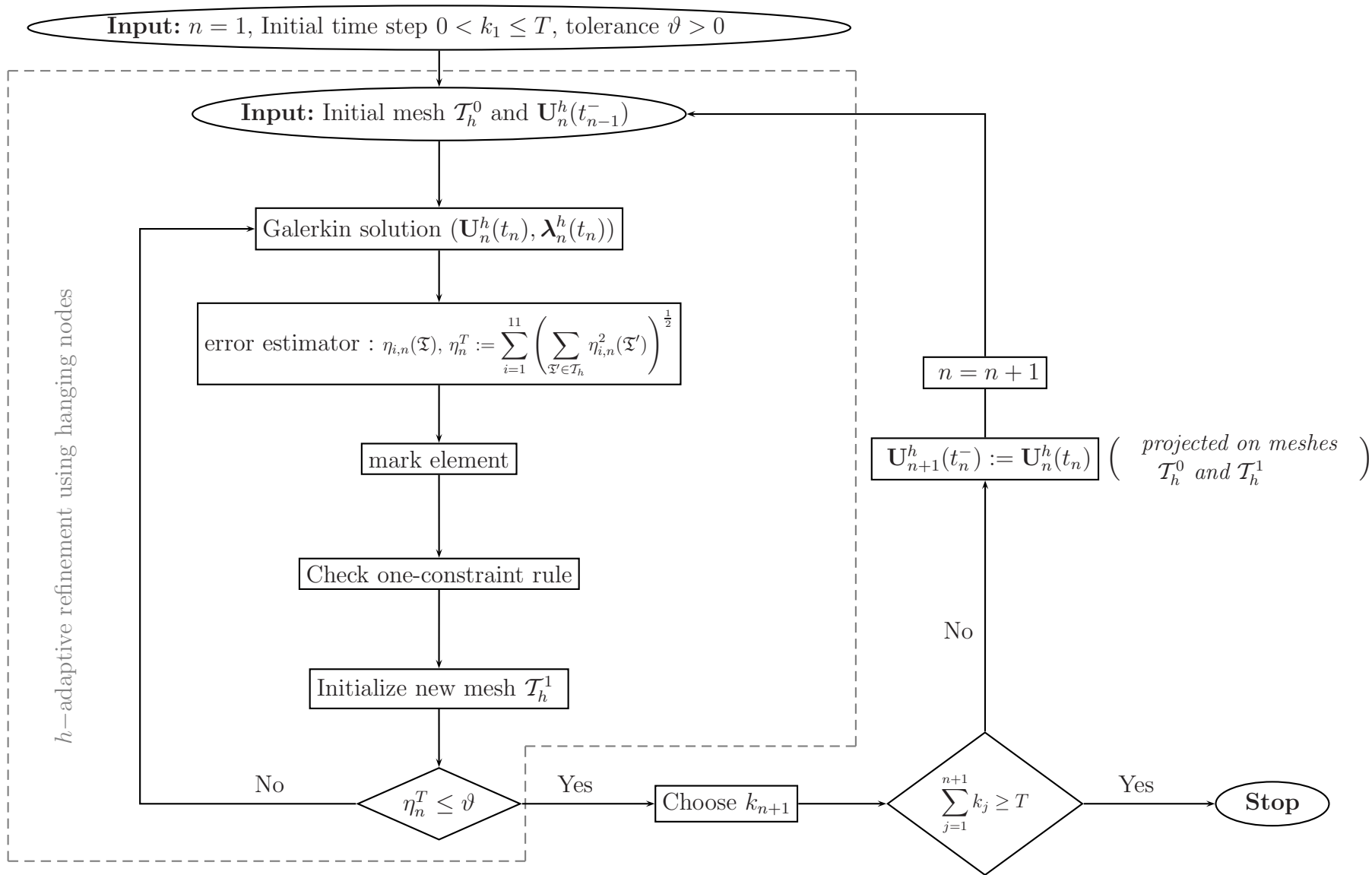
4 Numerical experiments

In this Chapter we will present numerical experiments underlining the theoretical results derived in Chapter 3. For this purpose we compare the numerical approximation obtained by (4.2) with the exact solution of Problem (4.1).

All numerical experiments were performed using the scientific program package MAI-PROGS [50],[49], which is a Fortran-based program package used for various kinds of numerical simulations [51]. Initially developed by M. Maischak, MAIPROGS has been extended for electromagnetics problem by Teltscher [73] and Leydecker [39].

We realized the fully-discrete system (4.2) within MAIPROGS. Moreover, we extended MAIPROGS by the error estimator presented in Theorem 3.3.2, the Newton scheme as presented in Chapter 5 and the inverses block and multigrid preconditioners presented in Section 4.2.1.

For the implementation of the FE and BE matrices we follow the guidelines contained in [49]:

1. The (global) basis functions are based on a mesh.

2. On every mesh element we have a given set of local basis functions.

3. The local basis functions are generated by mapping a reference element to the mesh element.

4. Basis functions are a linear combination of local basis functions.

5. Every local basis functions belongs only to one and only one global basis function.

which gives the implementation scheme for MAIPROGS. Now, using these fundamental assumptions we have the following objects to deal with:

- The mesh consisting of mesh elements: $\mathfrak{T}_i$.

- The mappings $\varphi_i : Q \mapsto \mathfrak{T}_i$ from the reference element to the mesh elements.

- The set of basis function on the reference element: $\phi_k^{\mathrm{ref}} : Q \mapsto R$.

- The local basis functions on every element: $\phi_{i,k}(x) = \phi_k^{\mathrm{ref}}(\varphi_i^{-1}(x)) : \mathfrak{T}_i \mapsto R$.

Then every global basis function can be represented in the following way:

$$\phi_j(x) = \sum_{j=r_{i,k}} w_{i,k}\phi_{i,k}(x).$$

Here $w_{i,k}$ are weights belonging to every local basis functions and $r_{i,k}$ denotes the global basis functions to which every local basis function belongs to.

Every local basis function has a representation consisting of monomials and transformation factors, e.g., for Raviart-Thomas function of degree p we get

$$\boldsymbol{\varphi} = \mathbf{e}^{(1)} \sum_{m=0}^{p} \sum_{n=0}^{p-1} c_{mn}^{(1)} x_1^m x_2^n + \mathbf{e}^{(2)} \sum_{m=0}^{p-1} \sum_{n=0}^{p} c_{mn}^{(2)} x_1^m x_2^n$$

on the reference square $[-1,1]^2$.

The implementation of the integrals in the Galerkin system (3.25) leads to integrals over monomials. Using suitable transformations (see Leydecker [39] and Teltscher [73]) we get integrals of the form

$$\sum_{k,l,m,n} \sum_{s=1,2,3} c_{k,l}^{(s)} c_{m,n}^{(s)} \mathbf{e}^{(s)} \int_Q \int_Q \Phi(\boldsymbol{x}, \boldsymbol{y}) x_1^k x_2^l y_1^m y_2^n \, d\boldsymbol{x} \, d\boldsymbol{y},$$

with kernel Φ. Those integrals can be evaluated analytically, see Maischak [47, 48].

For our numerical experiments we have implemented functions of the form $\boldsymbol{w} = f(t)\boldsymbol{v}(\boldsymbol{x})$, a general transient function is not implemented. In the implementation of all examples we use the special property that the right hand side $\mathbf{J}$ has the form $\mathbf{J}(\boldsymbol{x},t) = f(t)\boldsymbol{u}(\boldsymbol{x})$, which allows us to calculate the right hand side in the linear system (4.2), e.g., as

$$(\mathcal{F}_1)_i = \left(\int_{I_n} -\partial_t \mathbf{J} \, dt, \Phi_i \right) = -\int_{I_n} f'(t) \, dt \int_\Omega \boldsymbol{u}(\boldsymbol{x}) \Phi_i(\boldsymbol{x}) \, d\boldsymbol{x}$$

$$= -\int_{I_n} f'(t) \, dt \sum_{k,l,m} \sum_{s=1,2,3} c_{k,l,m}^{(s)} \mathbf{e}^{(s)} \int_Q x_1^k x_2^l x_3^m \boldsymbol{u}^{(s)}(\boldsymbol{x}) \, d\boldsymbol{x} \, d\boldsymbol{y}.$$

In the following we analyze the a priori estimate of the Section 3.3.1, the residual error estimate of the Section 3.3.2 and present an analysis for the fast solvers and preconditioners used for solving the linear system.

4.1 Framework

Let $\mathcal{T}_h$ be a regular mesh (with tetrahedral or hexahedral elements) of the domain Ω and $\mathcal{K}_h := \{\mathfrak{T} \cap \Gamma : \mathfrak{T} \in \mathcal{T}_h\}$ the induced mesh on Γ (c.f. Page 15). To perform our experiments we consider a simply connected polyhedral domain Ω represented by a cube using only hexahedral elements.

We consider Nédélec functions of first order $\mathcal{ND}_1(\mathcal{T}_h)$, a conforming finite element space of $\mathbf{H}(\mathbf{curl}, \Omega)$, for the discretization of the unknown $\boldsymbol{u} := \boldsymbol{u}(t, \boldsymbol{x})$ with $\boldsymbol{u} \in W^1(0, T; \mathbf{H}(\mathbf{curl}, \Omega))$. Furthermore the divergence free Raviart-Thomas functions space

$$\mathcal{RT}_1^0(\mathcal{K}_h) := \left\{ \boldsymbol{\lambda}^h \in \mathcal{RT}_1(\mathcal{K}_h), \ \mathrm{div}_\Gamma \, \boldsymbol{\lambda}^h = 0 \right\} \subset \mathcal{RT}_1(\mathcal{K}_h),$$

a conforming finite element space of $\mathbf{H}_{\parallel}^{-\frac{1}{2}}(\mathrm{div}_\Gamma \, 0, \Gamma)$, is used for the discretization of the boundary unknown $\boldsymbol{\lambda} := \boldsymbol{\lambda}(t, \boldsymbol{x}) = \mathbf{curl} \, \boldsymbol{u} \times \boldsymbol{n}$, with $\boldsymbol{\lambda} \in L^2(0, T; \mathbf{H}_{\parallel}^{-\frac{1}{2}}(\mathrm{div}_\Gamma 0, \Gamma))$. As Γ is simply connected there holds

$$\mathcal{RT}_1^0(\mathcal{K}_h) = \mathbf{curl}_\Gamma \mathcal{S}_1(\mathcal{K}_h),$$

where $\mathcal{S}_1(\mathcal{K}_h)$ denotes the space of piecewise polynomials on the triangulation $\mathcal{K}_h$ (see Hiptmair [34]).

Thus, instead of seeking $\boldsymbol{\lambda}^h \in \mathcal{RT}_1^0(\mathcal{K}_h)$, we now seek a function $\varphi_h \in \mathcal{S}_1(\mathcal{K}_h)/\mathbb{C}$ such that $\boldsymbol{\lambda}^h := \mathbf{curl}_\Gamma \varphi_h$. In order to ensure a unique φ_h we require that $\int_\Gamma \varphi_h(\boldsymbol{x}) dS_{\boldsymbol{x}} = 0$. This can be reformulated in a weak sense and used for computations by

$$\mathcal{P}(\varphi_h, \tau_h) := \left(\int_\Gamma \varphi_h(\boldsymbol{x}) \, dS_{\boldsymbol{x}} \right) \overline{\left(\int_\Gamma \tau_h(\boldsymbol{x}) \, dS_{\boldsymbol{x}} \right)} = 0 \quad \text{for all } \tau_h \in \mathcal{S}_1(\mathcal{K}_h).$$

Note that the bilinear form $\mathcal{P}(\varphi, \tau)$ is positive semidefinite $(\mathcal{P}(\varphi, \varphi) = |\int_\Gamma \varphi(\boldsymbol{x}) \, dS_{\boldsymbol{x}}|^2)$ and that the corresponding matrix has rank 1. Then the Galerkin system (3.19) becomes:

Find $\boldsymbol{U}^h(t) \in \mathcal{ND}_1(\mathcal{T}_h), \varphi_h(t) \in \mathcal{S}_1(\mathcal{K}_h)$ such that

$$\left(\sigma \dot{\boldsymbol{U}}^h, \boldsymbol{v}_h \right)_\Omega + \mathcal{A}^h \left(\boldsymbol{U}^h \ ; \ \boldsymbol{v}_h \right) + \mathcal{B}_1^h \left(\boldsymbol{U}^h, \varphi_h \ ; \ \boldsymbol{v}_h \right) = - \left(\partial_t \mathbf{J}, \boldsymbol{v}_h \right)_\Omega,$$
$$\mathcal{B}_2^h \left(\boldsymbol{U}^h, \varphi_h \ ; \ \tau_h \right) = 0$$

$$(4.1)$$

for all $\boldsymbol{v}_h \in \mathcal{ND}_1(\mathcal{T}_h), \tau_h \in \mathcal{S}_1(\mathcal{K}_h)$, where

$$\mathcal{A}^h \left(\boldsymbol{U}^h; \boldsymbol{v}_h \right) := \tilde{\lambda} \left(\boldsymbol{U}^h, \boldsymbol{v}_h \right)_\Omega + \left(\mu^{-1} \, \mathbf{curl} \, \boldsymbol{U}^h, \mathbf{curl} \, \boldsymbol{v}_h \right)_\Omega,$$
$$\mathcal{B}_1^h \left(\boldsymbol{U}^h, \varphi_h; \boldsymbol{v}_h \right) := - \left\langle \mathcal{W} \gamma_D \boldsymbol{U}^h, \gamma_D \boldsymbol{v_h} \right\rangle_\Gamma + \left\langle \tilde{\mathcal{K}} \mathbf{curl}_\Gamma \varphi_h, \gamma_D \boldsymbol{v_h} \right\rangle_\Gamma,$$
$$\mathcal{B}_2^h \left(\boldsymbol{U}^h, \varphi_h; \tau_h \right) := \left\langle (I - \mathcal{K}) \gamma_D \boldsymbol{U}^h, \mathbf{curl}_\Gamma \tau_h \right\rangle_\Gamma + \left\langle \mathcal{V} \mathbf{curl}_\Gamma \varphi_h, \mathbf{curl}_\Gamma \tau_h \right\rangle_\Gamma + \mathcal{P}(\varphi_h, \tau_h).$$

Moreover, applying the discontinuous Galerkin method and taking piecewice linear functions in time we obtain the following linear system (see Section 3.2.1)

$$
\left(
\begin{array}{cc|cc}
\left(\tilde{\lambda}+\frac{\sigma}{kn}\right)\mathcal{M}+\mathcal{R}^{*}-\mathcal{W} & \left(\frac{\tilde{\lambda}}{2}+\frac{\sigma}{kn}\right)\mathcal{M}+\frac{1}{2}\mathcal{R}^{*}-\frac{1}{2}\mathcal{W} & \mathcal{B}^{\top} & \frac{1}{2}\mathcal{B}^{\top} \\
\left(\frac{\tilde{\lambda}}{2}+\frac{\sigma}{kn}\right)\mathcal{M}+\frac{1}{2}\mathcal{R}^{*}-\frac{1}{2}\mathcal{W} & \left(\frac{\tilde{\lambda}}{6}+\frac{\sigma}{2kn}\right)\mathcal{M}+\frac{1}{6}\mathcal{R}^{*}-\frac{1}{6}\mathcal{W} & \frac{1}{2}\mathcal{B}^{\top} & \frac{1}{6}\mathcal{B}^{\top} \\
\hline
-\mathcal{B} & -\frac{1}{2}\mathcal{B} & \mathcal{V} & \frac{1}{2}\mathcal{V} \\
-\frac{1}{2}\mathcal{B} & -\frac{1}{6}\mathcal{B} & \frac{1}{2}\mathcal{V} & \frac{1}{6}\mathcal{V}
\end{array}
\right)
\left(
\begin{array}{c}
\mathbf{U}^{h}_{n,1} \\
\mathbf{U}^{h}_{n,2} \\
\boldsymbol{\lambda}^{h}_{n,1} \\
\boldsymbol{\lambda}^{h}_{n,2}
\end{array}
\right)
=
\left(
\begin{array}{c}
\widetilde{F}_{1} \\
\widetilde{F}_{2} \\
0 \\
0
\end{array}
\right),
\qquad (4.2)
$$

which is equivalent to the fully discrete system (3.20). Here the matrices $\mathcal{M}$, $\mathcal{R}^{*}$, $\mathcal{W}$, $\widetilde{F}_{1}$ and $\widetilde{F}_{2}$ are defined on Pages 42 and 44, and

$$
\mathcal{V} := [\langle \mathcal{V}\mathbf{curl}_{\Gamma}\boldsymbol{\psi}_{i}, \mathbf{curl}_{\Gamma}\boldsymbol{\psi}_{k}\rangle + \mathcal{P}(\boldsymbol{\psi}_{i}, \boldsymbol{\psi}_{k})]^{i=1,\ldots,m}_{k=1,\ldots,m}
$$

$$
\mathcal{B} := [\langle (\mathcal{K}-I)\gamma_{D}\Phi_{i}, \mathbf{curl}_{\Gamma}\boldsymbol{\psi}_{k}\rangle]^{i=1,\ldots,m}_{k=1,\ldots,M}
$$

where $\{\Phi_{k}\}_{k=1,\ldots,M}$ is a basis of $\mathcal{ND}_{1}(\mathcal{T}_{h})$ and $\{\boldsymbol{\psi}_{k}\}_{k=1,\ldots,m}$ is a basis of $\mathcal{S}_{1}(\mathcal{K}_{h})$.

We compute the approximate solution $(\boldsymbol{U}^{h}, \boldsymbol{\lambda}^{h})$ at each time step k on a series of uniform meshes in space and define the approximation errors

$$
e_{1} = \max_{1\leq n\leq N} \|(\boldsymbol{U}^{h}-\boldsymbol{u})(t^{-}_{n})\|_{L^{2}(\Omega)}, \qquad (4.3)
$$

$$
e_{2} = \|\boldsymbol{U}^{h}-\boldsymbol{u}\|_{L^{2}(0,T\,;\,\mathbf{H}(\mathbf{curl},\Omega))}, \qquad (4.4)
$$

$$
e_{3} = \|\boldsymbol{\lambda}-\boldsymbol{\lambda}^{h}\|_{L^{2}(0,T\,;\,\mathbf{H}^{-\frac{1}{2}}_{\parallel}(\mathrm{div}_{\Gamma},\Gamma))} \qquad (4.5)
$$

(cf. Theorem 3.3.1). In most of our examples we compare the error in the energy norm

$$
e := \sqrt{\|\boldsymbol{u}-\boldsymbol{U}^{h}\|^{2}_{\mathbf{H}(\mathbf{curl},\Omega)} + \|\boldsymbol{\lambda}-\boldsymbol{\lambda}^{h}\|^{2}_{\mathbf{H}^{-1/2}_{\parallel}(\mathrm{div}_{\Gamma},\Gamma)}} \qquad (4.6)
$$

with the value of the residual error estimator $\eta^{n}(\mathfrak{T}) := \sum_{i=1}^{11} \eta_{i,n}(\mathfrak{T})$, where $\eta_{i,n}$ represent the local error indicator for each $\mathfrak{T} \in \mathcal{T}_{h}$ defined on Page 65.

The experimental convergence rate α_{h} is obtained by evaluating the errors and the degrees of freedom of two successive meshes by

$$
\alpha_{h} = \frac{\log(e_{i,j}/e_{i,j+1})}{\log(h_{i,j}/h_{i,j+1})} = 3\frac{\log(e_{i,j}/e_{i,j+1})}{\log(N_{i,j+1}/N_{i,j})}, \quad i = 1, 2, 3.
$$

Here we use that $h \sim N^{-1/3}$; and define $e_{i,j}$ and $N_{i,j}$ as the error e_{i} and the degree of freedom for the mesh $\mathcal{T}_{h_{j}}$, respectively.

The effectivity index q is the quotient of the error estimator η and the error e,

$$
q := \frac{\eta}{e}.
$$

The time interval $(0, T]$ is divided into N subintervals of uniform length $k = \frac{T}{N}$, thus the Galerkin matrix of (4.2) is independent of the choosen subintervall $I_{n} := ((n-1)k, nk]$.

4.1.1 Analysis of the unpreconditioned system

The fully discrete scheme (4.2) can be written as

$$\underbrace{\begin{pmatrix} \widehat{\mathcal{M}} & \widehat{\mathcal{B}}^\top \\ -\widehat{\mathcal{B}} & \widehat{\mathcal{V}} \end{pmatrix}}_{\mathcal{A}} \begin{pmatrix} \boldsymbol{U}^h \\ \boldsymbol{\lambda}^h \end{pmatrix} = \begin{pmatrix} \mathfrak{F} \\ 0 \end{pmatrix} \tag{4.7}$$

or

$$\underbrace{\begin{pmatrix} \widehat{\mathcal{M}} & \widehat{\mathcal{B}}^\top \\ \widehat{\mathcal{B}} & -\widehat{\mathcal{V}} \end{pmatrix}}_{\mathcal{A}_H} \begin{pmatrix} \boldsymbol{U}^h \\ \boldsymbol{\lambda}^h \end{pmatrix} = \begin{pmatrix} \mathfrak{F} \\ 0 \end{pmatrix}, \tag{4.8}$$

where

$$\widehat{\mathcal{M}} := \begin{pmatrix} \mathcal{M}_{11} & \mathcal{M}_{12} \\ \mathcal{M}_{21} & \mathcal{M}_{22} \end{pmatrix} = \begin{pmatrix} \left(\tilde{\lambda}+\frac{\sigma}{k_n}\right)\mathcal{M}+\mathcal{R}^*-\mathcal{W} & \left(\frac{\tilde{\lambda}}{2}+\frac{\sigma}{k_n}\right)\mathcal{M}+\frac{1}{2}\mathcal{R}^*-\frac{1}{2}\mathcal{W} \\ \left(\frac{\tilde{\lambda}}{2}+\frac{\sigma}{k_n}\right)\mathcal{M}+\frac{1}{2}\mathcal{R}^*-\frac{1}{2}\mathcal{W} & \left(\frac{\tilde{\lambda}}{6}+\frac{\sigma}{2k_n}\right)\mathcal{M}+\frac{1}{6}\mathcal{R}^*-\frac{1}{6}\mathcal{W} \end{pmatrix},$$

$$\widehat{\mathcal{B}} := \begin{pmatrix} \mathcal{B} & \frac{1}{2}\mathcal{B} \\ \frac{1}{2}\mathcal{B} & \frac{1}{6}\mathcal{B} \end{pmatrix}, \qquad \widehat{\mathcal{B}}^\top := \begin{pmatrix} \mathcal{B}^\top & \frac{1}{2}\mathcal{B}^\top \\ \frac{1}{2}\mathcal{B}^\top & \frac{1}{6}\mathcal{B}^\top \end{pmatrix},$$

$$\widehat{\mathcal{V}} := \begin{pmatrix} \mathcal{V} & \frac{1}{2}\mathcal{V} \\ \frac{1}{2}\mathcal{V} & \frac{1}{6}\mathcal{V} \end{pmatrix}, \qquad \boldsymbol{U}^h = \begin{pmatrix} \mathbf{U}_1^h \\ \mathbf{U}_2^h \end{pmatrix}, \qquad \mathfrak{F} = \begin{pmatrix} \mathcal{F}_1 \\ \mathcal{F}_2 \end{pmatrix}.$$

In the following the given CPU times refer to the computation of the Galerkin matrix $\mathcal{A}$ and the solution of the linear system (4.7) (or the equivalent system (4.8)) for the Example 4.2.1

Table 4.1 shows that for small linear systems up to 3280 degrees of freedom the assembling of the Galerkin matrix is more expensive than solving the linear system with the Gauss's algorithm. For more degrees of freedom, iterative solvers seem to be most appropriate. Their order of convergence, however, depends strongly on the spectrum of the Galerkin matrix. Initially we consider for the unpreconditioned system two iterative solvers: the Generalized Minimal Residual Method (GMRES) and the Hybrid Modified Conjugate Residual method (HMCR).

The GMRES method was originally introduced by Saad and Schultz [70] and is an extension of MINRES to nonsymmetric systems, hence we apply this iterative solver to the matrix $\mathcal{A}$ in the linear system (4.7).

HMCR, a stable variant of MINRES [26], can be applied to linear systems of equations with symmetric, indefinite matrices [71]. Hence we apply this method to (4.8) in which the system matrix $\mathcal{A}_H$ is symmetric and indefinite.

Degree of freedom			Solution		
$N = N_{U^h} + N_{\lambda^h}$	$\kappa(\mathcal{A})$	Matrix assembling	GAUSS	GMRES	HMCR
$160 = 108 + 52$	783	35.71	0.44	0.26	0.29
$400 = 288 + 112$	1536	92.61	3.24	4.38	1.73
$796 = 600 + 196$	3120	219.79	17.24	34.56	7.99
$1384 = 1080 + 304$	5788	460.48	68.98	391.44	28.08
$2200 = 1764 + 436$	9822	881.72	234.90	753.95	99.79
$3280 = 2688 + 592$	15460	1531.97	658.84	2472.36	256.78
$4660 = 3888 + 772$	23000	2470.22	1908.22	8011.43	826.70
$6376 = 5400 + 976$	32670	3866.40	3907.34	12540.05	1513.33
$8464 = 7260 + 1204$	44760	5659.13	7258.46	25785.11	2659.70
$10960 = 9504 + 1456$	59520	8147.21	13860.23	48060.22	6332.32

Table 4.1: Condition number ($\kappa(\mathcal{A})$) and cpu time (in seconds) for the solution of example 4.2.1 using the cube $(-1, 1)^3$ and time $t = 0.2$.

In Table 4.1 one observes growing condition numbers and cpu-times for the matrix assembling compared to the solvers times for Gauss, GMRES and HMCR.

Figure 4.16 shows that for refined space discretizations the condition number $\kappa(\mathcal{A})$ of the matrix $\mathcal{A}$ increases like $\mathcal{O}(N)$, i.e., the Galerkin matrix is ill-conditioned. Thus, the unpreconditioned GMRES does not work properly. However, the HMCR solver behaves well for the unpreconditioned system.

As for unpreconditioned systems the condition number $\kappa(\mathcal{A})$ deteriorates on very fine space meshes, we need efficient preconditioners. This is discussed in Section 4.2.1.

4.2 Examples

Example 4.2.1 *In $\Omega := (-1, 1)^3$, we choose $\mu = \sigma = \varepsilon = 1$ and consider the irrotational function*

$$\boldsymbol{u}(t, \boldsymbol{x}) = g(t)\, \boldsymbol{v}(x) = \sin t \, \mathbf{grad} \int_\Omega \frac{1}{\|\boldsymbol{x} - \boldsymbol{y}\|} \rho(\boldsymbol{y})\, d\boldsymbol{y}, \quad t \in [0, \pi] \tag{4.9}$$

with density function

$$\rho(\boldsymbol{x}) = ((1 - x_1^2)(1 - x_2^2)(1 - x_3^2))^2 x_1 x_2 x_3, \quad \boldsymbol{x} \in \Omega$$

as exact solution of the system of equations (3.1)-(3.7) .

For a fixed time t, $\boldsymbol{v}$ is both divergence free and irrotational in the exterior domain Ω_e, hence $\boldsymbol{u}$ is harmonic. In Ω there holds $\mathbf{curl}\, \boldsymbol{u} = 0$ and $\mathrm{div}\, \boldsymbol{u} = -4\pi \sin t\, \rho(\boldsymbol{x})$. Combining

this with (3.9) we obtain for the right hand function:

$$-\partial_t \mathbf{J} = \sigma\, \partial_t \boldsymbol{u} + \mathbf{curl}\, \mu^{-1}\, \mathbf{curl}\, \boldsymbol{u} = \begin{cases} \sigma\, \cos t\, \boldsymbol{v}(x) & in\ \Omega \\ 0 & in\ \Omega_e. \end{cases}$$

Moreover it is valid that for the boundary unknown $\boldsymbol{\lambda} = \mu^{-1}\, \mathbf{curl}\, \boldsymbol{u} \times \boldsymbol{n} = 0$. We remark that the exact energy norm of $\boldsymbol{\lambda}$ is extrapolated using the sequence of uniformly refined meshes.

As a consequence of this analysis, we observe in the experimental results that the norms $\|\boldsymbol{\lambda} - \boldsymbol{\lambda}^h\|_{\mathbf{H}_\parallel^{-1/2}(\mathrm{div}_\Gamma,\Gamma)}$ and $\|\mathbf{curl}\, \boldsymbol{u} - \mathbf{curl}\, \boldsymbol{U}^h\|_{\mathbf{L}^2(\Omega)}$ are considerably smaller than the norm of $\|\boldsymbol{u} - \boldsymbol{U}^h\|_{\mathbf{L}^2(\Omega)}$, e.g. for $t = 1.0$ and $h = \frac{1}{6}$ (i.e., 13900 total degree of freedom) we obtain

$$\|\boldsymbol{u} - \boldsymbol{U}^h\|_{\mathbf{L}^2(\Omega)} = 6.514 \times 10^{-3},$$
$$\|\mathbf{curl}\, \boldsymbol{u} - \mathbf{curl}\, \boldsymbol{U}^h\|_{\mathbf{L}^2(\Omega)} = 3.609 \times 10^{-5},$$
$$\|\boldsymbol{\lambda} - \boldsymbol{\lambda}^h\|_{\mathbf{H}_\parallel^{-1/2}(\mathrm{div}_\Gamma,\Gamma)} = \|\boldsymbol{\lambda}^h\|_{\mathbf{H}_\parallel^{-1/2}(\mathrm{div}_\Gamma,\Gamma)} = 3.969 \times 10^{-11}$$

and hence

$$e \approx \|\boldsymbol{u} - \boldsymbol{U}^h\|_{\mathbf{L}^2(\Omega)}.$$

For uniform meshes in time we calculate the errors e_1, e_2 and e defined in (4.3) - (4.6) using piecewise linear polynomials in time and analyze the experimental convergence rates proved in Theorem 3.3.1. As the exact solution is an irrotational function we expect a convergence of order $O(h + k^2)$ (see Remark 2.4.1), i.e., choosing $k = \sqrt{h}$ we look for convergence rates $\alpha_{h1} = 1$ and $\alpha_{h2} = 1$, for the errors e_1 and e_2, respectively. Table 4.2 shows the computed rates α_h. In Figure 4.1 the $\mathbf{L}^2$-norm of the error is plotted for different meshes of length h taking a constant time step $k_n = 0.2$ for the time interval $[0, 3.2]$, which shows that the $\mathbf{L}^2$-norm of the error is monotone with respect to h.

Next, in Figures 4.2 - 4.5 the error in the energy norm and the error estimator $\eta = \sum_{i=1}^{11} R_{i,n}$ (obtained in Theorem 3.3.2) are plotted versus the degrees of freedom for the time intervals (0,0.2], (0.4,0.6], (1.0,1.2] and (1.4,1.6]. We remark that in the subinterval (1.4,1.6] the maximum of the error occurs (cf. Figure 4.1). One can see that the residual error estimator behaves like the error. Moreover, the tables below show the convergence rates of the error in the energy norm α, which have the same behavior, independent of the time intervals, and the effectivity indices q, which are stable, but depend on the time interval.
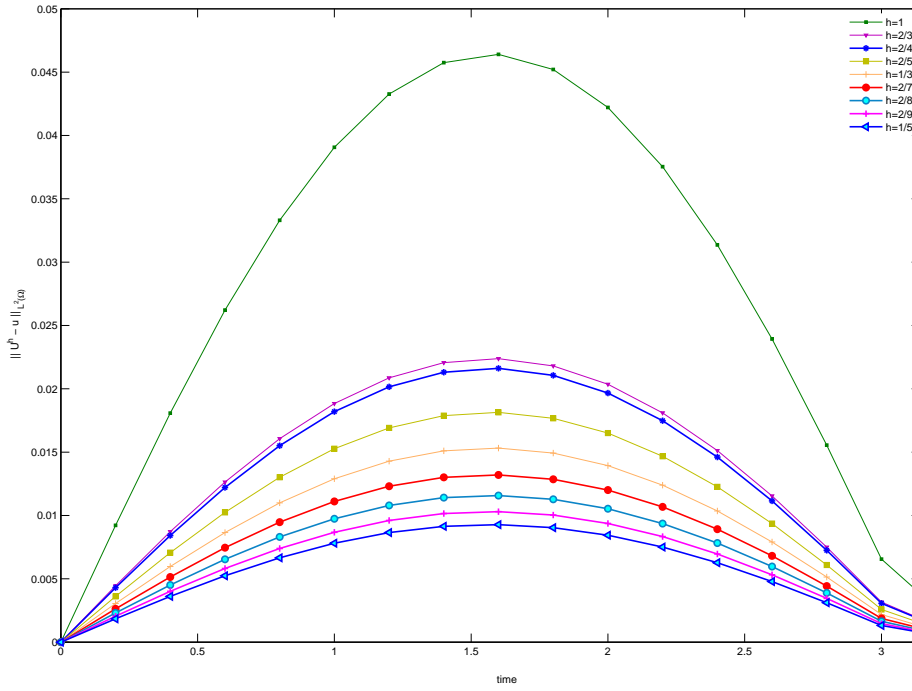
Figure 4.1: $\|(\boldsymbol{u} - \boldsymbol{U}^h)(t_n)\|_{\mathbf{L}^2(\Omega)}$ calculated on $t_n = n \cdot 0.2, n = 1, 16$ for diverse meshes of length $h = 2/J, J = 2, \cdots, 10$.

h	DOF	e_1	α_{h1}	e_2	α_{h2}
2/2	108	0.0464	-	0.0578	-
2/4	600	0.0216	1.1031	0.0256	1.3508
2/5	1080	0.0181	0.8945	0.0267	1.1119
2/6	1764	0.0153	1.0320	0.0215	0.7148
2/7	2688	0.0132	1.0630	0.0191	1.2219
2/8	3888	0.0116	1.0674	0.0161	0.8618
2/9	5400	0.0103	1.0646	0.0128	1.1184
2/10	7260	0.0093	1.0601	0.0114	1.2138

Table 4.2: Error e_1, e_2 and convergence rates α_{h1}, α_{h2} for Example 4.2.1.

	Degree of freedom									
	160	400	796	1384	2200	3280	4660	6376	8464	10960
η	0.1407	0.1288	0.1053	0.0889	0.0767	0.0673	0.0600	0.0542	0.0494	0.0455
e	0.0092	0.0045	0.0043	0.0036	0.0031	0.0026	0.0023	0.0020	0.0018	0.0017
$q = \frac{\eta}{e}$	15.252	28.948	24.4891	24.616	25.130	25.628	26.063	26.441	26.777	27.082
α	-	2.3414	0.1982	1.2103	0.9679	1.3212	1.0474	1.3373	1.1158	0.6635

Figure 4.2: Error in energy norm, value of the residual indicators and effectivity indices calculated in time intervall $(0.0, 0.2]$ for Example 4.2.1.

	Degree of freedom									
	160	400	796	1384	2200	3280	4660	6376	8464	10960
η	0.1185	0.1101	0.0903	0.0763	0.0659	0.0579	0.0516	0.0466	0.0425	0.0391
e	0.0262	0.0126	0.0122	0.0102	0.0087	0.0075	0.0065	0.0058	0.0052	0.0048
$q = \frac{\eta}{e}$	4.5205	8.7116	7.3958	7.4508	7.6126	7.7658	7.8979	8.0128	8.1144	8.2068
α	-	2.3968	0.1406	0.9711	1.0296	1.1149	1.2225	1.0903	1.1564	0.92918

Figure 4.3: Error in energy norm, value of the residual indicators and effectivity indices calculated in time intervall $(0.4, 0.6]$ for Example 4.2.1.

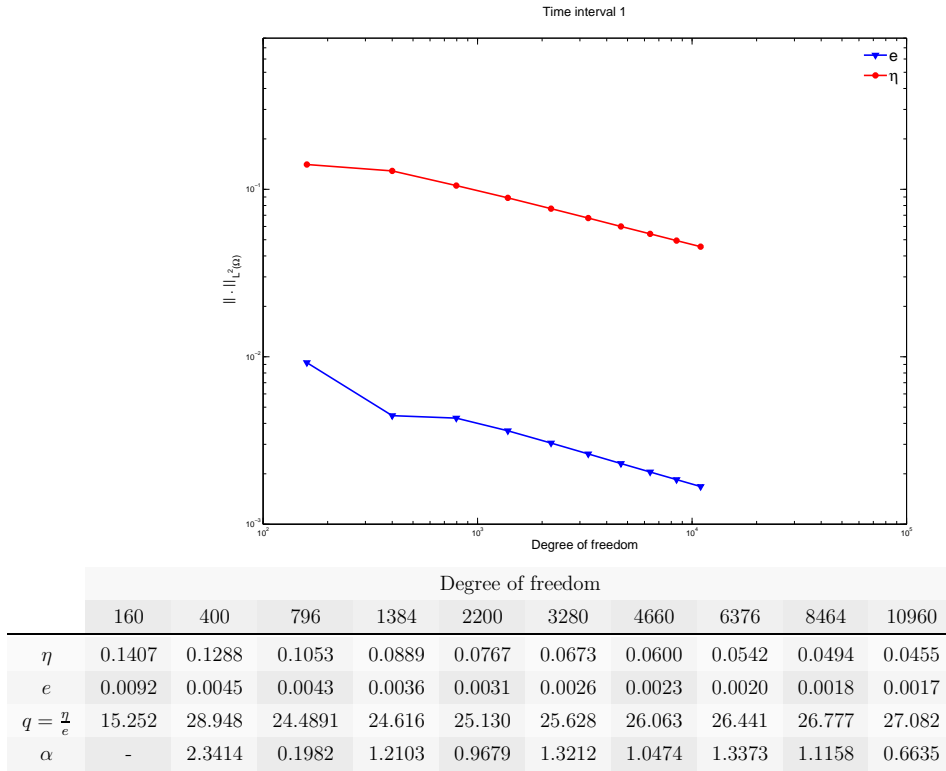|	Degree of freedom									
	160	400	796	1384	2200	3280	4660	6376	8464	10960
η	0.0521	0.0514	0.0425	0.0361	0.0313	0.0275	0.0246	0.0222	0.0203	0.0187
e	0.0433	0.0209	0.0202	0.0169	0.0143	0.0123	0.0108	0.0096	0.0087	0.0079
$q = \frac{\eta}{e}$	1.2040	2.4621	2.1075	2.1352	2.1887	2.2373	2.2786	2.3141	2.3453	2.3735
α	-	2.3848	0.1485	0.9674	1.0813	1.1317	1.1114	1.1270	1.0425	1.1198

Figure 4.4: Error in energy norm, value of the residual indicators and effectivity indices calculated in time intervall $(1.0, 1.2]$ for Example 4.2.1.
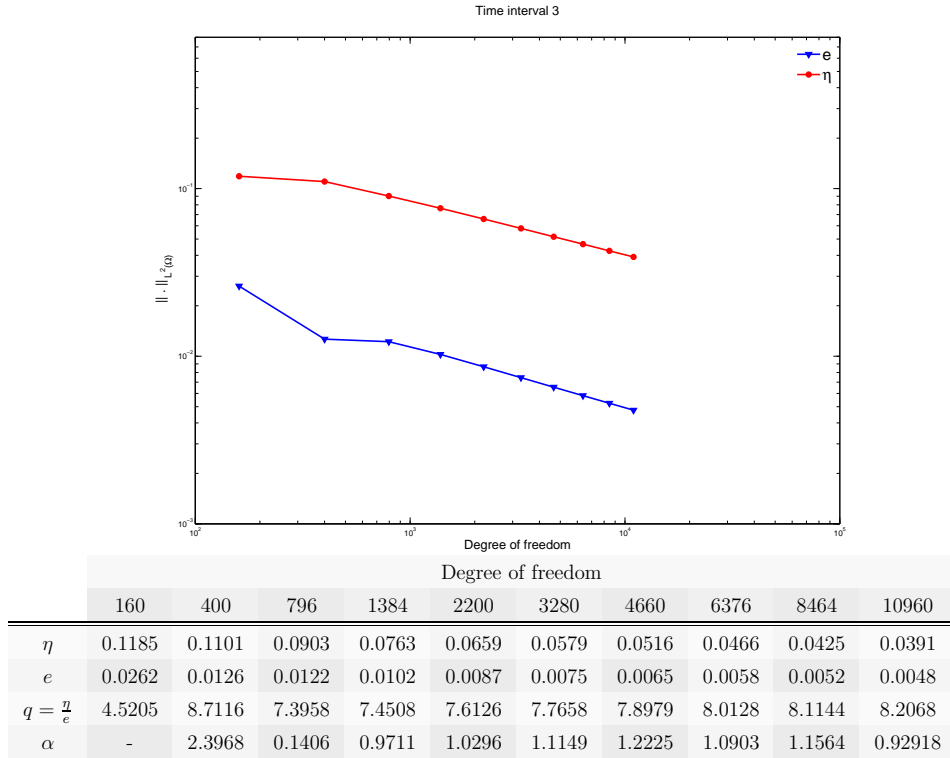

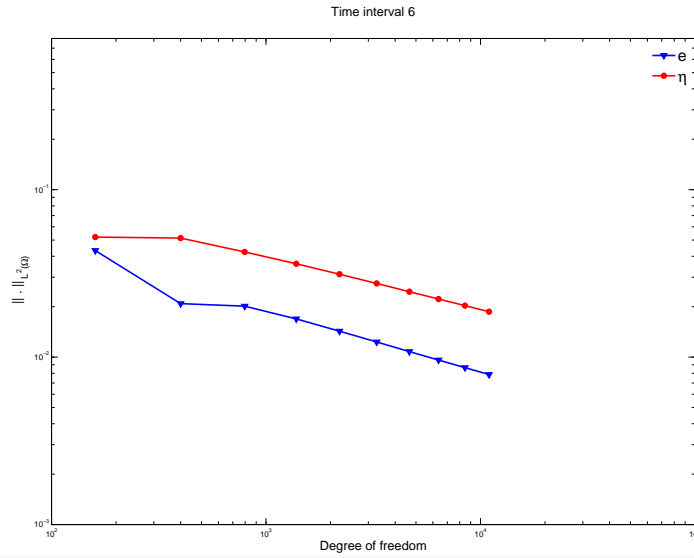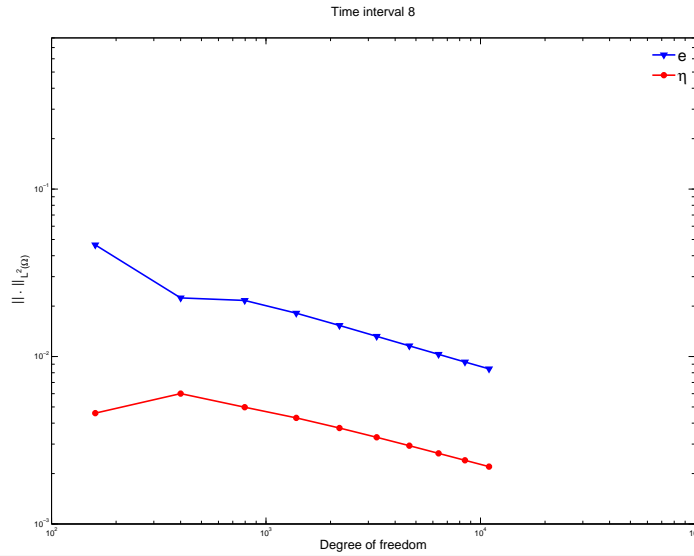|	Degree of freedom									
	160	400	796	1384	2200	3280	4660	6376	8464	10960
η	0.0046	0.0060	0.0050	0.0043	0.0037	0.0033	0.0029	0.0026	0.0024	0.0022
e	0.0464	0.0224	0.0216	0.0181	0.0153	0.0132	0.0116	0.0103	0.0093	0.0084
$q = \frac{\eta}{e}$	0.0989	0.2682	0.2305	0.2371	0.2441	0.2495	0.2534	0.2564	0.2587	0.2606
α	-	2.3843	0.1586	0.9588	1.0878	1.1091	1.1038	1.1373	1.0816	1.1815

Figure 4.5: Error in energy norm, value of the residual indicators and effectivity indices calculated in time intervall $(1.4, 1.6]$ for Example 4.2.1.

Example 4.2.2 *We define* $\Omega := (-1, 1)^3$ *and consider for* $t \in [0, 6]$ *the function*

$$\boldsymbol{u}(t, \boldsymbol{x}) = g(t)\boldsymbol{v}(\boldsymbol{x}) = te^{-\frac{1}{3}t}\,\mathbf{curl}\,\mathfrak{I}_\Omega(\boldsymbol{\rho}(\boldsymbol{y}))(\boldsymbol{x}), \quad \boldsymbol{x} \in \Omega,$$

as solution of (3.1) - (3.7), *where*

$$\mathfrak{I}_\Omega(\boldsymbol{\rho}(\boldsymbol{y}))(\boldsymbol{x}) = \int_\Omega \frac{1}{\|\boldsymbol{x} - \boldsymbol{y}\|}\boldsymbol{\rho}(\boldsymbol{y})\,d\boldsymbol{y}$$

with

$$\boldsymbol{\rho}(\boldsymbol{x}) := ((1 - x_1^2)(1 - x_2^2)(1 - x_3^2))^2 x_1 x_2 x_3 (1, 1, 1)^\mathsf{T}, \quad \boldsymbol{x}\ in\ \Omega.$$

As $\boldsymbol{\rho} = 0$ *and* $\partial_{x_j}\boldsymbol{\rho} = 0 \quad (j = 1, 2, 3)$ *on* Γ, *we obtain using partial integration*

$$\boldsymbol{v} = \mathbf{curl}\,\mathfrak{I}_\Omega(\boldsymbol{\rho}(\boldsymbol{y}))(\boldsymbol{x}) = \mathfrak{I}_\Omega(\mathbf{curl}\,\boldsymbol{\rho}(\boldsymbol{y}))(\boldsymbol{x}).$$

Moreover,

$$\mathbf{curl}\,\boldsymbol{v} = \mathbf{curl}\,\mathbf{curl}\,\mathfrak{I}_\Omega(\boldsymbol{\rho})$$

$$= (\mathbf{grad}\,\mathrm{div} - \Delta)\mathfrak{I}_\Omega(\boldsymbol{\rho}) = \begin{cases} \mathbf{grad}\,\mathfrak{I}_\Omega(\mathrm{div}\,\boldsymbol{\rho}) + 4\pi\boldsymbol{\rho} & in \quad \Omega, \\ \mathbf{grad}\,\mathfrak{I}_\Omega(\mathrm{div}\,\boldsymbol{\rho}) & in \quad \Omega_e. \end{cases}$$

Note that the exact solution $\boldsymbol{u}$ *has a non-vanishing* $\mathbf{curl}$. *Now, as* $\boldsymbol{\rho} = 0$ *on* Γ *it holds that* $\mathbf{curl}\,\boldsymbol{u}$ *is continuous on* Γ, *and we set*

$$\boldsymbol{\lambda} := \mathbf{curl}\,\boldsymbol{u} \times \boldsymbol{n} = g(t)\,\mathbf{grad}\,\mathfrak{I}_\Omega(\mathrm{div}\,\boldsymbol{\rho}) \times \boldsymbol{n} \quad on\ \Gamma.$$

Furthermore,

$$\mathbf{curl}\,\mathbf{curl}\,\boldsymbol{v} = \begin{cases} \mathbf{curl}\,4\pi\boldsymbol{\rho} & in \quad \Omega \\ 0 & in \quad \Omega_e \end{cases},$$

and $\mathrm{div}\,\boldsymbol{v} = 0 \in \mathbb{R}^3$, *hence* $\boldsymbol{u}$ *is harmonic in the exterior domain* Ω_e. *Therefore, choosing* $\sigma = \mu = \varepsilon = 1$ *we define the function* $-\partial_t \mathbf{J}$ *(used in the right side) by*

$$-\partial_t \mathbf{J} = \partial_t \boldsymbol{u} + \mathbf{curl}\,\mathbf{curl}\,\boldsymbol{u} = g'(t)\boldsymbol{v} + 4\pi g(t)\,\mathbf{curl}\,\boldsymbol{\rho}.$$

Here, $g'(t)$ *means the first derivative of the function* $g(t)$ *w.r.t. the time variable.*

For a uniform time step k_n, *we calculate* e_1, e_2, e_3 *and* e *(see Page 72) using piecewise linear polynomials in time and analyze the experimental convergence rates of the solution for the fully-discrete system* (4.2). *The exact energy norm of* $\boldsymbol{\lambda}$ *is extrapolated using the sequence of uniformly refined meshes.*

We choose $k = \sqrt{h}$ *and study the convergence rate for* e_1, e_2 *and* e_3. *From Theorem 3.3.1 we expect convergence rates* $1 < \alpha_{h1} \leq 2$ *and* $\alpha_{h2} = \alpha_{h3} = 1$. *Table 4.3 shows that the computed rates* α_h *are bounded and have average values* $\alpha_{h1} = 1.33, \alpha_{h2} = 1.13$ *and* $\alpha_{h3} = 1.13$. *Figure 4.6 shows the* $\mathbf{L}^2(\Omega)-$*error for different meshes of length* h, *we take*
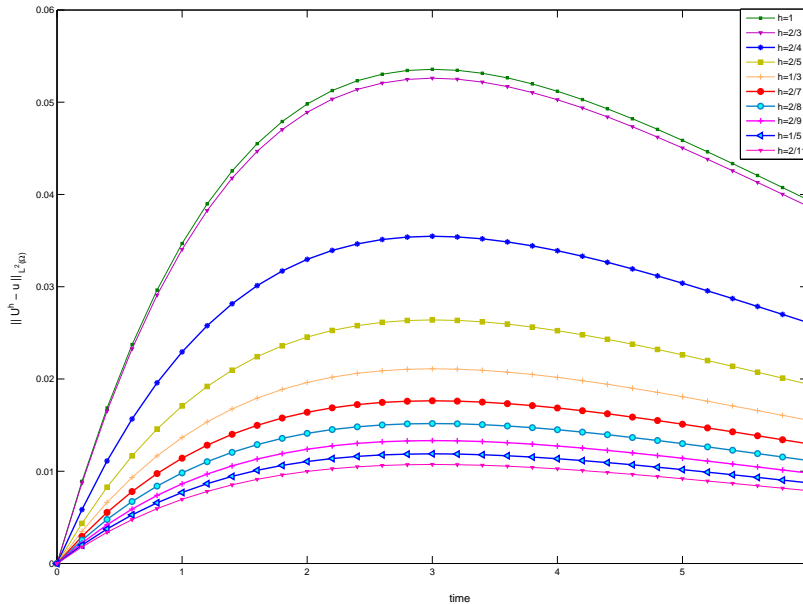
Figure 4.6: Error in $\mathbf{L}^2(\Omega)$ for $h = 2/J, J = 2, \ldots, 11$ vs time.

a constant time step $k_n = 0.2$ for the time interval $[0, 6]$, here we note the monotonicity of the error w.r.t. the mesh length h.

In Figures 4.7 - 4.10 we plot the error in the energy norm e, the error estimator $\eta = \sum_{i=1}^{11} R_{i,n}$ and the error indicators $R_{1,n}$, $R_{2,n}$, $R_{3,n}$, $R_{5,n}$, $R_{6,n}$, $R_{7,n}$, $R_{8,n}$, $R_{10,n}$, $R_{11,n}$ (obtained by Theorem 3.3.2) versus the degrees of freedom for the time intervals (0,0.2], (0.4,0.6], (1.4,1.6] and (3.0,3.2]. The latter is just the subinterval, in which the maximum of the error occurs (cf. Figure 4.6). The indicators $R_{4,n}$ and $R_{9,n}$ are not indicated because they are of order 10^{-8}. The plots show a similar behavior of the error e, the indicators and the error estimator η on all four time intervals. The tables below the figures list the values of e, η, the effectivity indices $q = \frac{\eta}{e}$ and the convergence rates α. In every time interval the effectivity index is quite constant, and the convergence rates are approximately 1 (as expected in Theorem 3.3.1)

h	DOF	e_1	α_{h1}	e_2	α_{h2}	e_3	α_{h3}
2/3	400	0.0526	-	0.1709	-	0.0093	-
2/4	796	0.0355	1.6108	0.1224	1.3656	0.0083	0.4939
2/5	1384	0.0264	1.5070	0.0952	1.2806	0.0070	0.9042
2/6	2200	0.0211	1.3690	0.0787	1.1635	0.0061	0.9400
2/7	3280	0.0176	1.2803	0.0676	1.0870	0.0052	1.1896
2/8	4660	0.0152	1.2240	0.0595	1.0360	0.0045	1.1920
2/9	6376	0.0133	1.1857	0.0533	1.0102	0.0035	2.4800
2/10	8464	0.0119	1.1823	0.0483	0.9866	0.0033	0.7101

Table 4.3: Convergence rate analysis for Example 4.2.2.
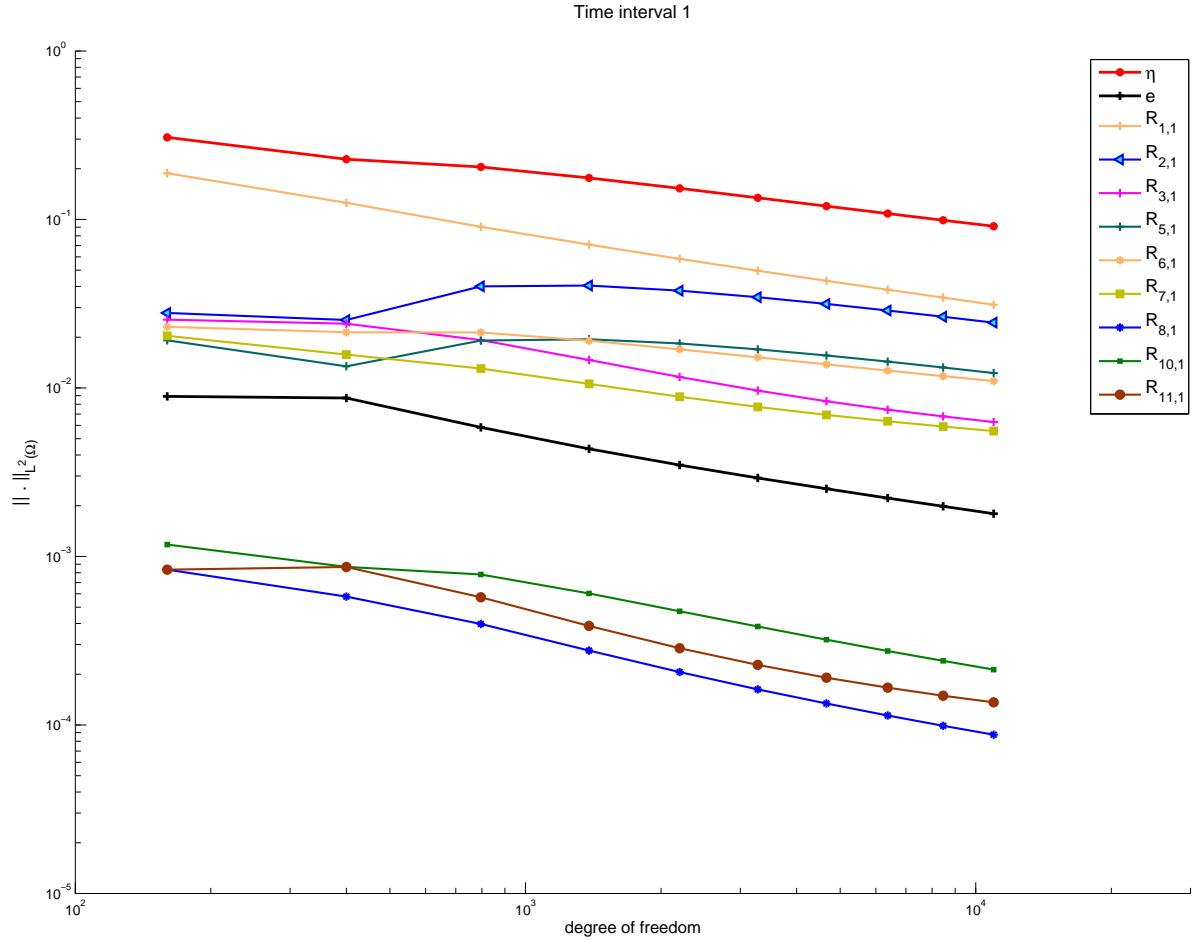
DOF	η	e	$q = \frac{\eta}{e}$	α
160	0.3069	0.0579	5.2988	-
400	0.2279	0.0569	4.0076	0.0562
796	0.2051	0.0441	4.6495	1.0379
1384	0.1764	0.0356	4.9594	1.0974
2200	0.1529	0.0298	5.1231	1.0735
3280	0.1345	0.0257	5.2251	1.0531
4660	0.1201	0.0227	5.3004	1.0414
6376	0.1085	0.0202	5.3631	1.0349
8464	0.0990	0.0183	5.4190	1.0312
10960	0.0911	0.0167	5.4708	1.0314

Figure 4.7: Error in energy norm, value of the residual indicators and effectivity indices calculated in time intervall $(0.0, 0.2]$ for Example 4.2.2.
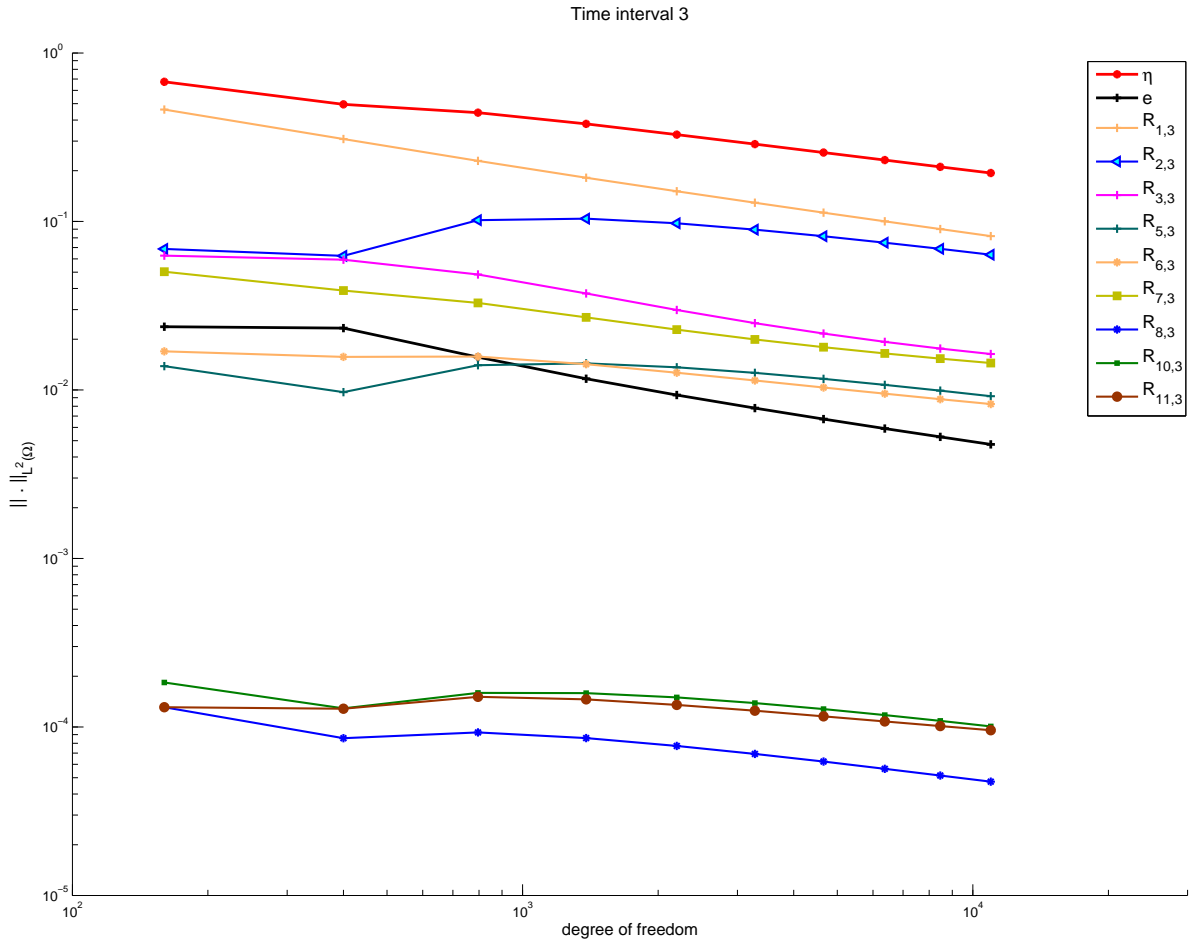
DOF	η	e	$q = \frac{\eta}{e}$	α
160	0.6742	0.1521	4.4317	-
400	0.4952	0.1492	3.3202	0.0604
796	0.4422	0.1157	3.8234	1.0396
1384	0.3792	0.0933	4.0648	1.0969
2200	0.3279	0.0783	4.1883	1.0728
3280	0.2878	0.0675	4.2628	1.0525
4660	0.2564	0.0594	4.3166	1.0410
6376	0.2313	0.0530	4.3612	1.0347
8464	0.2109	0.0479	4.4010	1.031
10960	0.1939	0.0437	4.4378	1.030

Figure 4.8: Error in energy norm, value of the residual indicators and effectivity indices calculated in time intervall $(0.4, 0.6]$ for Example 4.2.2.

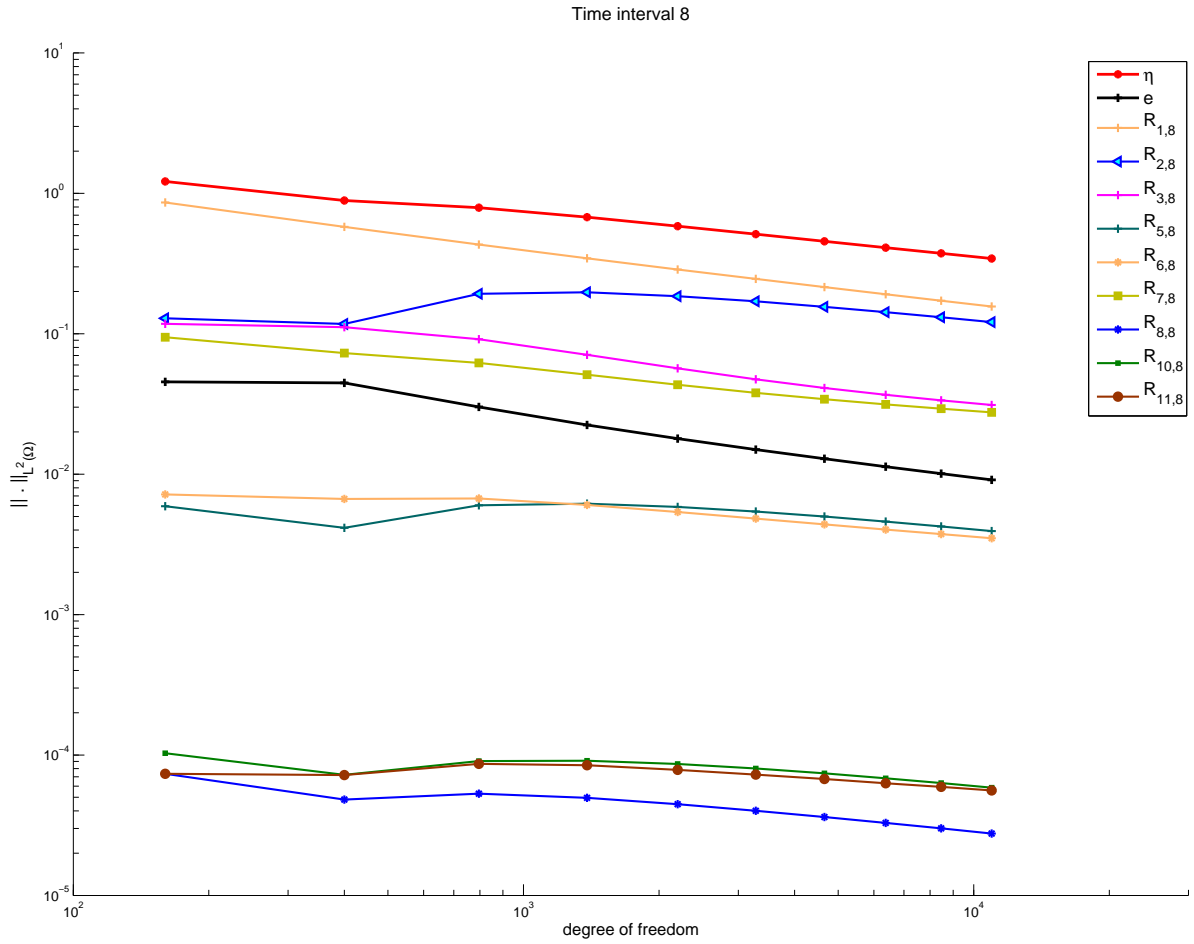| DOF	η	e	$q = \frac{\eta}{e}$	α
160	1.2160	0.2908	4.1817	-
400	0.8899	0.2850	3.1225	0.0614
796	0.7911	0.2210	3.5798	1.0398
1384	0.6767	0.1782	3.7964	1.0969
2200	0.5840	0.1496	3.9049	1.0728
3280	0.5121	0.1290	3.9690	1.0525
4660	0.4557	0.1135	4.0149	1.0410
6376	0.4108	0.1014	4.0529	1.0347
8464	0.3741	0.0915	4.0870	1.0312
10960	0.3438	0.0835	4.1186	1.0301

Figure 4.9: Error in energy norm, value of the residual indicators and effectivity indices calculated in time intervall $(1.4, 1.6]$ for Example 4.2.2.

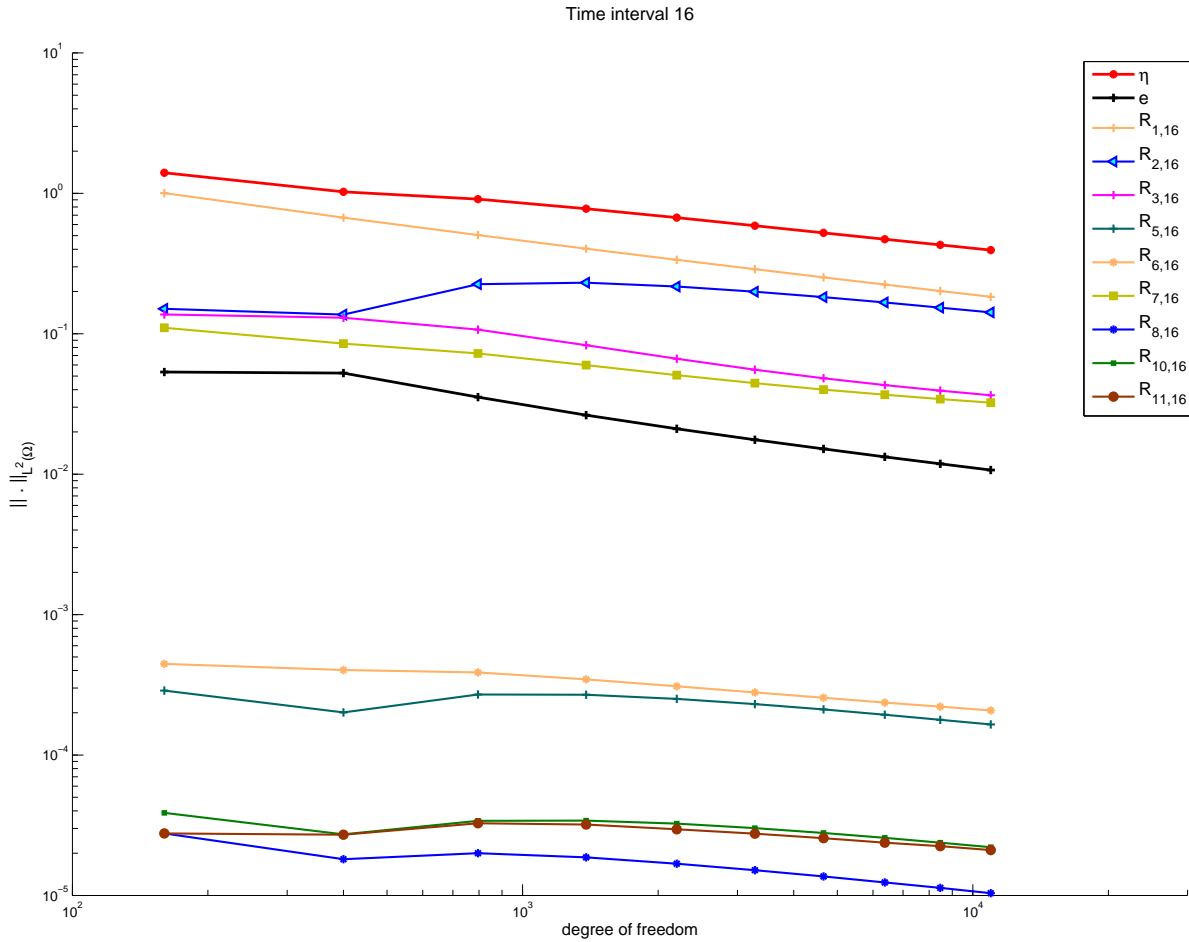| DOF	η	e	$q = \frac{\eta}{e}$	α
160	1.4027	0.3412	4.1111	-
400	1.0256	0.3344	3.0669	0.0616
796	0.9106	0.2593	3.5118	1.0399
1384	0.7784	0.2091	3.7218	1.0970
2200	0.6714	0.1755	3.8262	1.0728
3280	0.5885	0.1514	3.8875	1.0525
4660	0.5236	0.1332	3.9314	1.0410
6376	0.4718	0.1189	3.9676	1.0347
8464	0.4297	0.1074	4.0001	1.0312
10960	0.3947	0.0979	4.0303	1.0301

Figure 4.10: Error in energy norm, value of the residual indicators and effectivity indices calculated in time intervall $(3.0, 3.2]$ for Example. 4.2.2

Example 4.2.3 *In this example we use the L-block* $\Omega = [-1,1]^3 \setminus ([0,1]^2 \times [-1,1])$. *As given current we take the singularity function (r and ϕ polar coordinates)*

$$\mathbf{J}(\boldsymbol{x}, t) = t^{\frac{4}{3}} \, \mathbf{grad}(r^{\frac{2}{3}} \sin \frac{2}{3} \phi), \qquad t \in [0, 0.5].$$

We start by computing the Galerkin solution for the uniform mesh with 6 hexahedrons. The refinement algorithm then proceeds by first refining the 10% of the elements on which the local contributions of the residual error estimator are the greatest and then by further refining in order to eliminate hanging nodes that violate the **one-constraint rule**, *i.e., only one edge has at most two smaller neighboring edges on the other element (see e.g. Demkowicz et al. [25], Oestmann[67] and Leydecker [39]).*

We extrapolate the error using a sequence of uniform meshes and compare the error of the adaptive and uniform sequences in Figure 4.11. After several refinements the error of the adaptive algorithm is less than the error in the uniform refinement.

Our adaptive algorithm produces a sequence of refined meshes, which is shown in Figure 4.12. As expected our algorithm refines towards the singular edge.
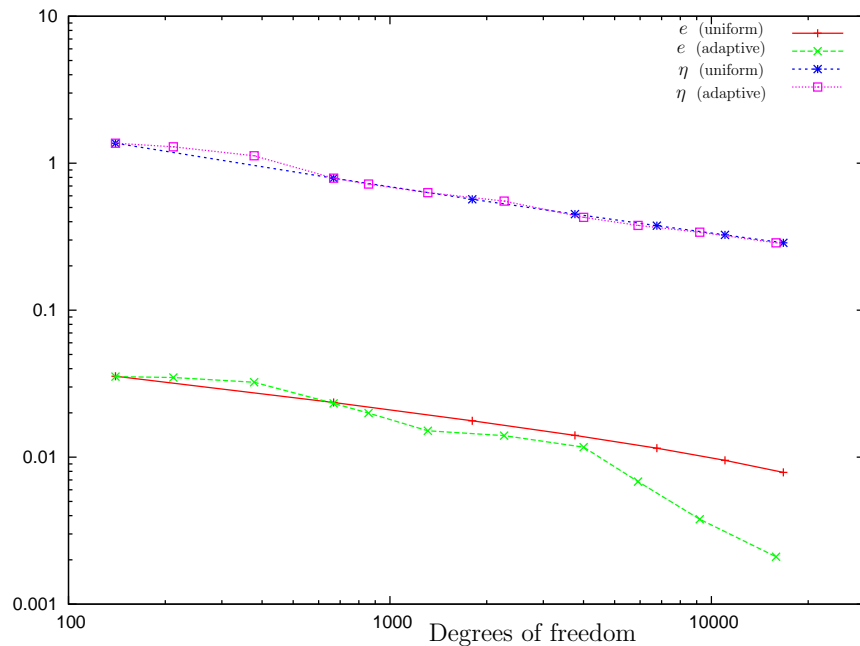
Figure 4.11: Error in the energy norm *e* and error estimators for adaptive and uniform refinement for the Example 4.2.3.

The complete implementation of the adaptive feedback Algorithm 1, Page 66, requires not only the use of the hanging nodes for Nédélec elements but also the use of certain interpolation techniques for Nédélec elements between different meshes and splines with hanging nodes, which has to be done in the future. Therefore, the adaptive algorithm was just tested for one time step.

$N = 140$

$N = 378$

$N = 1312$

$N = 4006$

$N = 9200$

$N = 15886$

Figure 4.12: The adaptive meshes (levels of refinement: 1, 3, 6, 8, 9, 10,11) for Example 4.2.3 with N degrees of freedom using the residual error estimator

Example 4.2.4 *In this example we use the residual error estimator to construct an adaptive mesh. We use hexahedral elements with hanging nodes on $\Omega = (-1,0)^3$ and for $t \in [0, 0.2]$ we choose the right-hand side function*
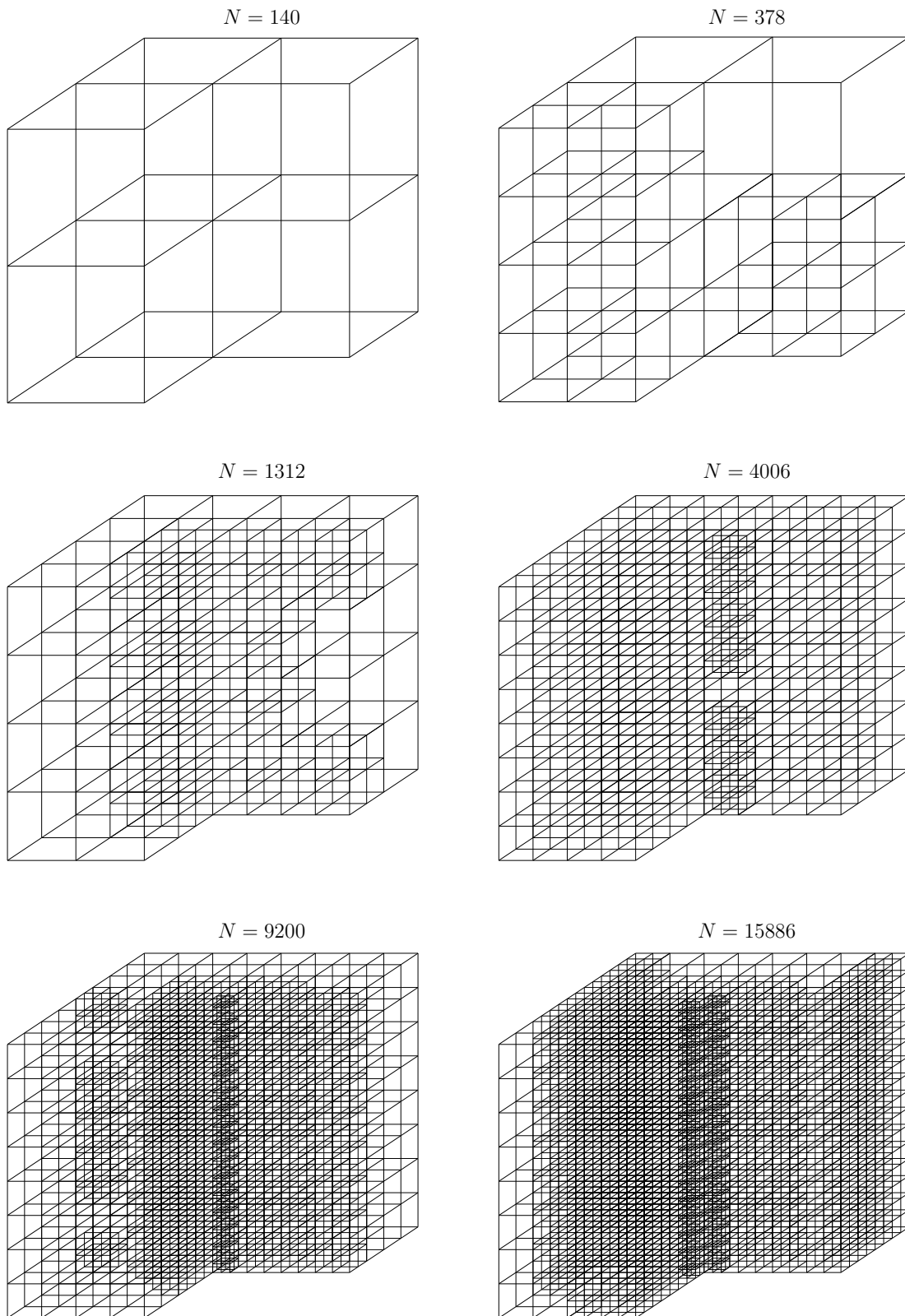
$$-\partial_t \mathbf{J} = \sigma \partial_t \mathbf{u} + \mathbf{curl}\,(\mathbf{curl}\,\mathbf{u}) + 0.001\,\mathbf{u} \tag{4.10}$$

such that the exact solution is

$$\mathbf{u}(t, \mathbf{x}) = g(t)\,\mathbf{v}(\mathbf{x}) := \sin t\,(f_1(\mathbf{x}), f_2(\mathbf{x}), f_3(\mathbf{x}))^\top = \sin t \begin{pmatrix} x_2 x_3 (1 - x_2)(1 - x_3) \\ x_1 x_2 (1 - x_1)(1 - x_3) \\ x_1 x_2 (1 - x_1)(1 - x_2) \end{pmatrix}.$$

Note, that we violate the (physical but not technical) assumption $\partial_t \mathbf{J} \cdot \mathbf{n} = 0$ on Γ. But
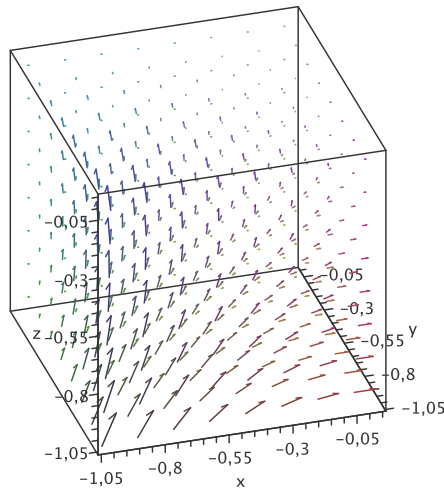
Figure 4.13: Vector field of the function $\mathbf{u}$ of Example 4.2.4.

this creates no difficulty, we must only consider in the error estimators $r_{6,n}$ and $r_{11,n}$ the corresponding term $\partial_t \mathbf{J}$, i.e., we substitute

$$r_6^{F,\Gamma} = r_{6,n} := \sqrt{k_n h_F}\, \max_{t \in I_n} \left\| \left(\sqrt{\sigma}\,\dot{\mathbf{U}}^h + \sqrt{\sigma^{-1}}\,\tilde{\lambda}\,\mathbf{U}^h \right) \cdot \mathbf{n} \right\|_{0,F}$$

by

$$\tilde{r}_6^{F,\Gamma} = \sqrt{k_n h_F}\, \max_{t \in I_n} \left\| \left(\sqrt{\sigma}\,\dot{\mathbf{U}}^h + \sqrt{\sigma^{-1}}\,\tilde{\lambda}\,\mathbf{U}^h + \partial_t \mathbf{J} \right) \cdot \mathbf{n} \right\|_{0,F}.$$

Also in Example 4.2.3 we perform an adaptive refinement starting with a uniform mesh with 8 hexahedrons. We also compute the same problem with uniform refinement. The comparison between the residual error estimator obtained by using uniform and adaptive refinement is displayed in Figure 4.14.

We compare the meshes in figure 4.15 with the vector field in figure 4.13 and note that, as expected, the mesh is refined in places where the function $\mathbf{u}$ possesses a large variation.
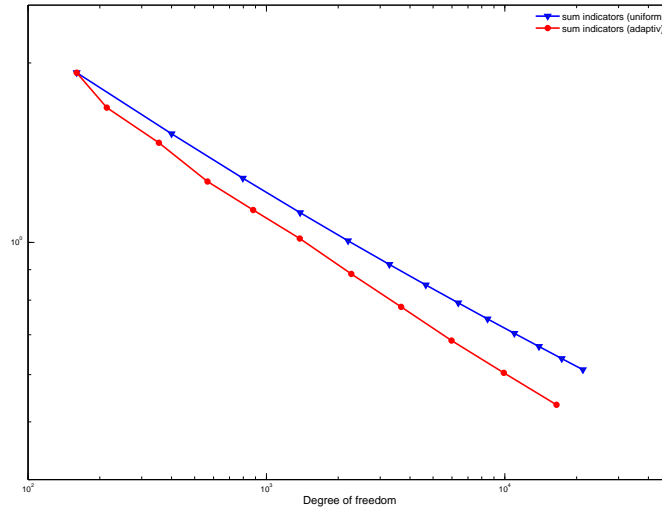
Figure 4.14: Residual error estimator using uniform and adaptive refinement, Example 4.2.4.

Adaptive		Uniform	
DOF	η	DOF	η
160	1.9263	160	1.9263
214	1.6831	400	1.5212
354	1.4692	796	1.2814
566	1.2650	1384	1.1216
880	1.1332	2200	1.0062
1380	1.0152	3280	0.9182
2270	0.8852	4660	0.8485
3672	0.7796	6376	0.7916
5978	0.6845	8464	0.7441
9900	0.6043	10960	0.7037
16472	0.5341	13900	0.6689

Table 4.4: Degrees of freedom and residual error estimator for Figure 4.14.
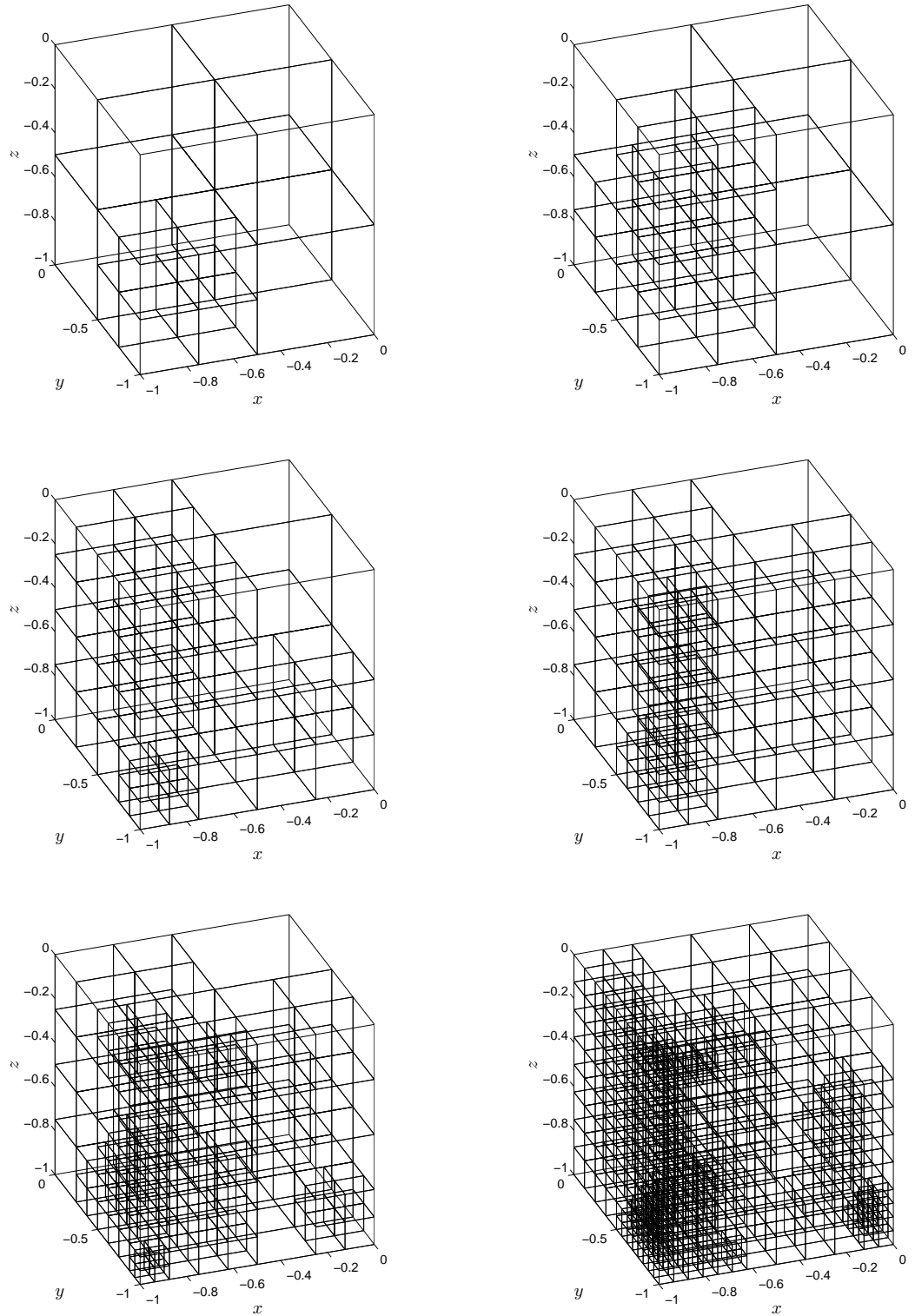
Figure 4.15: The adaptive meshes (levels of refinement: 2, 3, 4, 5, 6, 8) for Example 4.2.4 using the residual error estimator.

4.2.1 Preconditioned system

Inverse-Block preconditioner

Maischak & Tran [52] analyse a diagonal block preconditioner for a symmetric coupling of finite elements and boundary elements for the time harmonic eddy current problem. The authors apply successfully a diagonal preconditioner as follows

$$\mathcal{P} = \begin{pmatrix} (\mathcal{M} + \widetilde{\mathcal{R}})^{-1} & \\ & (\mathcal{V} + \mathcal{P}_h)^{-1} \end{pmatrix} \tag{4.11}$$

to the matrix

$$\mathcal{A}_{\mathcal{MT}} = \begin{pmatrix} \mathcal{M} + \widetilde{\mathcal{R}} - \mathcal{W} & \mathcal{B}^\top \\ \mathcal{B} & -\mathcal{V} - \mathcal{P}_h \end{pmatrix}, \tag{4.12}$$

where $\widetilde{\mathcal{R}} := [(\mathbf{curl}\,\Phi_i, \mathbf{curl}\,\Phi_j)]_{j=1,\dots,M}^{i=1,\dots,M}$ and the matrices $\mathcal{M}, \mathcal{R}^*, \mathcal{B}, \mathcal{V}$ are the one defined on page 42 and 72. Correspondingly, we consider the preconditioners

$$P_A = (\frac{1}{k_n}\mathcal{M} + \widetilde{\mathcal{R}})^{-1} \qquad \text{and} \qquad P_B = (\mathcal{V} + \mathcal{P}_h)^{-1} \tag{4.13}$$

for the matrix

$$A = \frac{1}{k_n}\mathcal{M} + \widetilde{\mathcal{R}} - \mathcal{W} \qquad \text{and} \qquad B = \mathcal{V} + \mathcal{P}_h,$$

respectively, and apply to the Galerkin matrix $\mathcal{A}$ in (4.7) the block diagonal preconditioner

$$\mathcal{P} = \begin{pmatrix} P_{\mathcal{MR}} & \\ & P_{\mathcal{V}} \end{pmatrix} \tag{4.14}$$

where

$$P_{\mathcal{MR}} = \begin{pmatrix} -2P_A & 6P_A \\ 6P_A & -12P_A \end{pmatrix}, \qquad P_{\mathcal{V}} = \begin{pmatrix} 2P_B & -6P_B \\ -6P_B & 12P_B \end{pmatrix}.$$

For the FEM matrix P_A, we obtain this inverse by solving an auxiliary problem with CG and the inverse for the BEM matrix B is obtained using LR decomposition.

Table 4.5 and Table 4.6 give the condition number for the block-diagonal preconditioner using the solvers GMRES and HMCR. Note that $\kappa(\mathcal{A})$ is bounded and does not depend on the time step.

		Solver time(Sec.)		Number of iterations	
DOF	$\kappa(\mathcal{A})$	GMRES	HMCR	GMRES	HMCR
160	37.22	0.013	0.012	2	2
400	37.22	0.182	0.187	6	6
796	37.22	0.810	0.964	8	9
1384	37.22	2.920	2.523	11	11
2200	37.22	8.993	6.656	14	13
3280	37.22	9.484	13.962	15	14
4660	37.22	35.377	28.635	16	18
6376	37.22	62.404	53.025	17	18
8464	37.22	91.410	79.412	17	19
10960	37.22	141.581	127.977	16	20
13900	37.22	191.428	164.690	16	19
17320	37.22	278.700	226.032	17	18
21256	37.22	359.180	301.520	16	18

Table 4.5: Condition number $\kappa(\mathcal{A})$ for preconditioned sytem ($k_n = 0.20$).

time step k_n	$\kappa(\mathcal{A})$
0.500	37.217
0.250	37.217
0.167	37.215
0.125	37.214
0.100	37.214
0.083	37.213
0.055	37.213

Table 4.6: Condition number $\kappa(\mathcal{A})$ for preconditioned sytem for time step k_n.

Multigrid preconditioner

Multigrid methods are used very often, because (if they work) their convergence rate can be independent of the problem size, in contrast to the classical iterative methods. As a consequence, their complexity is optimal, since the computational work is proportional to the number of unknowns [31]. Usually a multigrid method is constructed, based on the following recursive algorithm:

Algorithm 2   Multigrid algorithm for solving $\mathcal{A}_l \boldsymbol{x} = \mathfrak{b}_l$

Require: $\boldsymbol{r}, \mathfrak{b}$
Ensure: $\mathfrak{r}$

    PROCEDURE MG$(l, \boldsymbol{r}, \mathfrak{b})$
    if $l = 0$ **then**
        $\boldsymbol{r} \leftarrow \mathcal{A}_0^{-1}\mathfrak{b}_0$
    else
        for $i = 1, \nu_1$ **do**
            $\boldsymbol{r} \leftarrow \mathcal{S}_l(\boldsymbol{r}, \mathfrak{b})$ {presmoothing}
        $\boldsymbol{\sigma} \leftarrow \mathcal{R}(\mathcal{A}_l \boldsymbol{r} - \mathfrak{b})$ {Restriction}
        $\boldsymbol{\eta} \leftarrow 0$
        for $i = 1, \gamma$ **do**
            MG$(l - 1, \boldsymbol{\eta}, \boldsymbol{\sigma})$
        $\boldsymbol{r} \leftarrow \boldsymbol{r} + \mathcal{P}\boldsymbol{\eta}$ {Correction}
        for $i = 1, \nu_2$ **do**
            $\boldsymbol{r} \leftarrow \mathcal{S}_l(\boldsymbol{r}, \mathfrak{b})$ {postsmoothing}
        $\mathfrak{r} \leftarrow \boldsymbol{r}$

Following Hiptmair [35] for the FEM part, we assume a nested sequence of quasi-uniform triangulations $\mathcal{T}_l$, $l \in \{0, \cdots, L\} \subset \mathbb{N}$, with mesh size $h_l > 0$ of the domain Ω, created by regular refinement of an initial mesh $\mathcal{T}_0$. The mesh size $h_l > 0$ of $\mathcal{T}_l$ is considered to decrease in a geometric progression $h_l \approx 2^l h_0$. The meshes generated in this way are nested, and so are the finite element spaces, i.e., $\mathcal{ND}_1^0(\mathcal{T}_{l-1}) \subset \mathcal{ND}_1^0(\mathcal{T}_l)$, $l \in \mathbb{N}$.

The prolongation operator $\mathcal{P} : \mathcal{ND}_1^0(\mathcal{T}_{l-1}) \rightarrow \mathcal{ND}_1^0(\mathcal{T}_l)$ and the restriction operator $\mathcal{R} : \mathcal{ND}_1^0(\mathcal{T}_l) \rightarrow \mathcal{ND}_1^0(\mathcal{T}_{l-1})$ designate the canonical intergrid tranfers in the Nédélec spaces, induced by the natural embedding of these spaces [32].

The algorithm with $\gamma = 1$ corresponds to the V-cycle and the algorithm with $\gamma = 2$ corresponds to the W-cycle. ν_1 and ν_2 are the number of pre- and postsmoothing steps using the smoothing procedure $\mathcal{S}_l$, respectively. For the implementation is used a smoother $\mathcal{S}_l$ like the hybrid smoother used in [35] and described by the Algorithm 3. Note that the iterative solver (e.g. Gauss-Seidel, Jacobi) used in this algorithm carries out smoothing sweeps in both the space of edge elements and the scalar potential spaces $\mathcal{S}_1^0(\mathcal{T}_l)$. Aditionally, Δ_l stands for the stiffness matrix related to the bilinear form in $\mathcal{S}_1^0(\mathcal{T}_l)$, namely

$$(\phi_l, \psi_l) \rightarrow (\mathbf{grad}\,\phi_l, \mathbf{grad}\,\psi_l)_{\mathbf{L}^2(\Omega)}$$

and $\mathcal{T}_l : \mathcal{S}_1^0(\mathcal{T}_l) \rightarrow \mathcal{ND}_1^0(\mathcal{T}_l)$ is the transfer operator defined by the embeddings $\mathbf{grad}\,\mathcal{S}_1^0(\mathcal{T}_l) \subset \mathcal{ND}_1^0(\mathcal{T}_l)$ (see Section 2.3).

Algorithm 3   Hybrid smoother $\mathcal{S}_l$

Require: $r, \mathfrak{b}$

Ensure: $\mathfrak{r}$

   PROCEDURE $\mathcal{S}_l(r, \mathfrak{b})$

   Damped Iterative Solver sweep on $\mathcal{A}_l r = \mathfrak{b}$

   $\boldsymbol{\rho} \leftarrow \mathfrak{b} - \mathcal{A}_l r$

   $\rho \leftarrow \mathcal{T}_l^* \boldsymbol{\rho}$

   $\psi \leftarrow 0$

   Damped Iterative Solver sweep on $\Delta_l \psi = \rho$

   $\mathfrak{r} \leftarrow \mathfrak{b} + \mathcal{T}_l \psi$

Now, since there holds for $\mathcal{W} : \mathbf{H}_{\parallel}^{-1/2}(\mathrm{div}_\Gamma, \Gamma) \to \mathbf{H}_{\perp}^{-1/2}(\mathrm{curl}_\Gamma, \Gamma)$ (see Lemma 1.3.3) :

$$\langle \mathcal{W}\boldsymbol{u}, \boldsymbol{v} \rangle_\Gamma = -\langle V_0(\mathrm{curl}_\Gamma \, \boldsymbol{u}), \mathrm{curl}_\Gamma \, \boldsymbol{v} \rangle_{-1/2,\Gamma},$$

we can use the multigrid method development by Stephan & von Petersdorff, for the implementation of the hypersingular operator for the Laplace operator [75, 76]. We assume $\mathcal{K}_l$ (induced mesh by $\mathcal{T}_l$ on $\Gamma = \partial\Omega$) to posses a mesh size $h_l \approx 2^l h_0$ and consider the standard Algorithm 2 with damped Jacobi as the smoothing procedure $\mathcal{S}_l$.

Our goal is to calculate the inverses P_A and P_B on (4.13) for the implementation of the preconditioner (4.14) using preconditioned GMRES and preconditioned HMCR as iterative solvers. For this purpose we approximate it using a multigrid preconditioner $V(\nu_1, \nu_2)$-cycle, where ν_1 and ν_2 are the presmoothing and postsmoothing step, respectively. A $W(\nu_1, \nu_2)$-cycle was also used, but the results are very similar to those obtained by applying a $V(\nu_1, \nu_2)$-cycle, because this we present only results using $V(\nu_1, \nu_2)$-cycle.

Table 4.7 shows the condition number $\kappa(\mathcal{A})$ of the preconditioned matrix, the solver time and the number of iterations for $V(\nu, \nu)$-cycle with $\nu = 1, 2, 3, 4$ using as smoother for both the FEM matrix P_A and the BEM matrix P_B the damped Jacobi with $\omega = \frac{1}{2}$.

Table 4.8 gives a comparation of the condition number, the solver time and the number of iterations for the $V(\nu, \nu)$-Cycle with $\nu = 1, 2$ using as smoothers for the FEM matrix P_A damped Gauss-Seidel or damped Jacobi with $\omega = \frac{1}{2}$ and for both cases we use the dampened Jacobi with $\omega = \frac{1}{2}$ for the BEM matrix P_B . The iteration stops if the last relative change of the iterate is less than 10^{-7} and the preconditioned GMRES was set to restart after maximal 1100 iterations.

| | | | $V(1,1)$−cycle | |
| | | | Solver time(Number of iterations) | |
h	DOF	$\kappa(\mathcal{A})$	GMRES	HMCR
2/2	160	87.73	0.08 (2)	0.08 (2)
2/4	796	164.69	5.25 (120)	2.90 (63)
2/8	4660	584.37	304.62 (544)	96.10 (156)

| | | | $V(2,2)$−cycle | |
| | | | Solver time(Number of iterations) | |
h	DOF	$\kappa(\mathcal{A})$	GMRES	HMCR
2/2	160	55.80	0.08 (2)	0.07 (2)
2/4	796	83.83	3.80 (68)	2.97 (52)
2/8	4660	293.65	166.14 (250)	85.59 (109)

| | | | $V(3,3)$−cycle | |
| | | | Solver time(Number of iterations) | |
h	DOF	$\kappa(\mathcal{A})$	GMRES	HMCR
2/2	160	46.12	0.07 (2)	0.08 (2)
2/4	796	56.88	3.32 (49)	2.97 (43)
2/8	4660	196.75	134.22 (175)	73.73 (90)

| | | | $V(4,4)$−cycle | |
| | | | Solver time(Number of iterations) | |
h	DOF	$\kappa(\mathcal{A})$	GMRES	HMCR
2/2	160	41.91	0.08 (2)	0.09 (2)
2/4	796	43.42	3.33 (42)	2.85 (35)
2/8	4660	148.29	129.52 (149)	73.86 (79)

Table 4.7: Estimated condition number $\kappa(\mathcal{A})$, solver time and number of GM-RES and HMCR iterations (in parentheses) for Example 4.2.1 using multi-grid preconditioner with $V(i,i)$-cycle, $i = 1, \cdots, 4$, and the damped Jacobi with $\omega = \frac{1}{2}$ as smoother. Time step $k_n = 0.25$.

	V(1,1)−cycle			
	$\kappa(\mathcal{A})$		Solver time(Number of iterations)	
DOF	D. Jacobi	D. Gauss-Seidel	D. Jacobi	D. Gauss-Seidel
160	94.76	91.41	0.07 (2)	0.87 (89)
796	304.61	81.46	7.04 (165)	36.63 (275)
4660	1144.10	264.00	528.98 (943)	4775.34 (995)

	V(2,2)−cycle			
	$\kappa(\mathcal{A})$		Solver time(Number of iterations)	
DOF	D. Jacobi	D. Gauss-Seidel	D. Jacobi	D. Gauss-Seidel
160	55.80	56.19	0.07 (2)	1.03 (73)
796	153.78	52.20	4.75 (87)	44.32 (198)
4660	573.51	132.1	274.62 (416)	4523.55 (500)

Table 4.8: Estimated condition number $\kappa(\mathcal{A})$, solver time and number of GM-RES iterations (in parentheses) for Example 4.2.1 using multigrid preconditioner with smoother damped Jacobi and damped Gauss-Seidel for $V(i,i)$ cycle, $i = 1, 2$ and time step $k_n = 0.5$.

In Table 4.9 we see that the condition number $\kappa(\mathcal{A})$, obtained by applying our multigrid preconditioner, is in general depending on the time step k_n, but for small time step k_n is bounded.

time step k_n	$\kappa(\mathcal{A})$	Solver time(N. of iterations)
0.500	304.608	7.59 (155)
0.250	164.686	6.05 (123)
0.167	118.053	4.91 (99)
0.125	94.740	4.39 (88)
0.083	78.450	3.73 (77)
0.071	78.454	3.46 (68)
0.063	78.450	3.33 (65)
0.056	78.450	3.16 (65)
0.050	78.450	3.17 (62)

Table 4.9: Estimated condition number $\kappa(\mathcal{A})$, solver time and number of GM-RES iterations (in parentheses) for Example 4.2.1 using multigrid preconditioner with smoother damped Jacobi for $h = 1/2$ (DOF=796), time step k_n and $V(1,1)$-cycle.
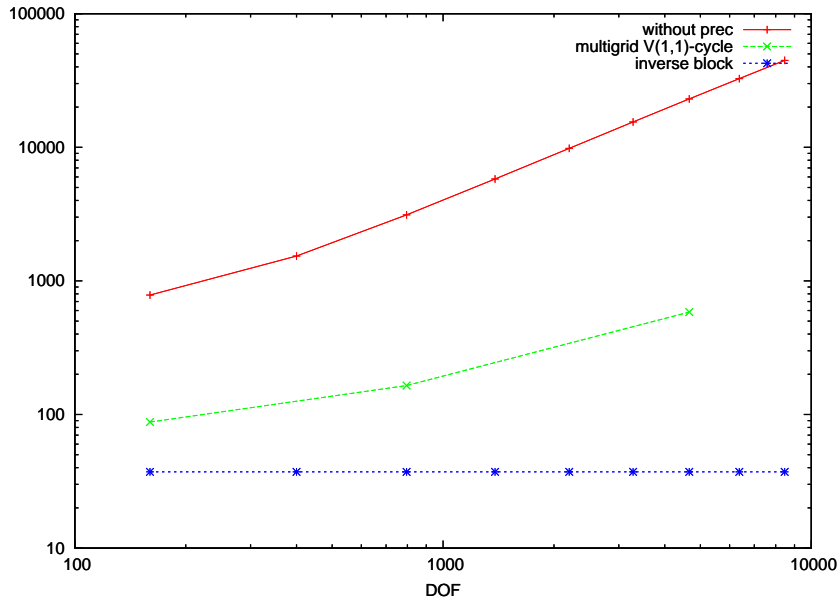
Figure 4.16: Condition numbers for unpreconditioned system, multigrid
precondicioner $(V(1,1)-$cycle) and inverse block preconditioner
vs. degrees of freedom.

Figure 4.16 shows a comparison of the condition numbers $\kappa(\mathcal{A})$ for different solution
procedures: no preconditioning, multigrid $V(1,1)-$cycle and inverse block preconditioner
collecting the results from Tables 4.1, 4.5 and 4.7. For the unpreconditioned system the
condition number $\kappa(\mathcal{A})$ behaves like $\mathcal{O}(N)$. While the multigrid preconditioner is not
optimal in this case the inverse block preconditioner results in a constant condition
number.

4.2.2 Concluding remarks

As we have seen in the last two sections the observed convergence rates in space and time
are not quite the ones predicted in Theorem 3.3.1, see e.g. Example 4.2.2, where we get
an average rate of 1.33 instead of at least 1.5. We fix the space and time discretization for
the time and space converge analysis, respectively. Due to the enormous computational
demands of three dimensional MOT (Marching on in time) algorithms (cf. Table 4.1)
we were not able to fix the time or space discretization on a sufficiently fine level for
the space or time convergence analysis, respectively. Therefore, the approximation errors
in time and space could not be studied separately but the approximation error in time
influenced the converge analysis in space and vice versa.

5 A nonlinear, time dependent eddy current problem

5.1 Problem description

Let $\Omega \subset \mathbb{R}^3$ be a bounded, simply connected polyhedral domain with a Lipschitz continuous and simply connected boundary $\Gamma_c = \partial\Omega$, $\Omega_e := \mathbb{R}^3 \setminus \overline{\Omega}$ the exterior domain and $\boldsymbol{n}$ be the unit normal vector on Γ pointing into Ω_e.

Eddy current problems describe very low-frequency electromagnetic problems. For these problems the displacement currents may be neglected and the problem is modeled by quasi-static Maxwell's equations. In constrast to the eddy current problem given in Chapter 3 here we examine a nonlinear variant where the magnetic permeability μ depends on the magnetic field and on the time.

We consider the eddy current induced by a given current density $\mathbf{J}(t, \boldsymbol{x})$ in a conductor represented by the bounded domain Ω (see Figure 3.1), where the electric and magnetic fields $\mathbf{E}(t, \boldsymbol{x})$ and $\mathbf{H}(t, \boldsymbol{x})$ fulfill

$$\mathbf{curl\,E} = -\partial_t \mathbf{B} \quad \text{in} \quad (0, T) \times \mathbb{R}^3 \, , \tag{5.1}$$

$$\mathbf{curl\,H} = \mathbf{J} + \sigma \, \mathbf{E} \quad \text{in} \quad (0, T) \times \mathbb{R}^3 \, , \tag{5.2}$$

$$\operatorname{div} \varepsilon \, \mathbf{E} = 0 \quad \text{in} \quad \Omega_e \, , \tag{5.3}$$

$$\int_\Gamma (\varepsilon \, \mathbf{E}) \cdot \boldsymbol{n} \, ds = 0 \quad \text{on} \quad \Gamma \, , \tag{5.4}$$

$$\mathbf{H}(0, \boldsymbol{x}) = \mathbf{H}_0(\boldsymbol{x}), \quad \mathbf{E}(0, \boldsymbol{x}) = \mathbf{E}_0(\boldsymbol{x}) \quad \text{in} \quad \mathbb{R}^3 \, , \tag{5.5}$$

$$[\mathbf{E} \times \boldsymbol{n}]_\Gamma = [\mathbf{H} \times \boldsymbol{n}]_\Gamma = 0 \quad \text{on} \quad \Gamma \, , \tag{5.6}$$

$$\mathbf{H}(t, \boldsymbol{x}) = \mathbf{E}(t, \boldsymbol{x}) = \mathcal{O}\left(|\boldsymbol{x}|^{-1}\right) \quad \text{uniformly for } |\boldsymbol{x}| \to \infty \tag{5.7}$$

where $\mathbf{B}$ denotes the magnetic flux density, the permeability $\mu = \mu(t, \boldsymbol{x}) \in L^\infty((0, T) \times \mathbb{R}^3)$, the permittivity $\varepsilon = \varepsilon(\boldsymbol{x}) \in L^\infty(\mathbb{R}^3)$ and the conductivity $\sigma = \sigma(\boldsymbol{x}) \in L^\infty(\mathbb{R}^3)$ are real valued and bounded functions, which satisfy

$$\mu_1 \geq \mu(t, \boldsymbol{x}) \geq \mu_0 > 0 \quad \text{a.e. in } (0, T) \times \Omega \text{ with} \quad \mu(t, \boldsymbol{x}) = \mu_0 \text{ a.e. in } (0, T) \times \Omega_e \, ,$$

$$\varepsilon_1 \geq \varepsilon(\boldsymbol{x}) \geq \varepsilon_0 > 0 \quad \text{a.e. } \boldsymbol{x} \in \Omega \text{ with} \quad \varepsilon(\boldsymbol{x}) = \varepsilon_0 \quad \text{in } \Omega_e \, ,$$

$$\sigma_1 \geq \sigma(\boldsymbol{x}) \geq \sigma_0 > 0 \quad \text{a.e. } \boldsymbol{x} \in \Omega \text{ with} \quad \sigma(\boldsymbol{x}) = 0 \quad \text{in } \Omega_e.$$

5 A nonlinear, time dependent eddy current problem

Here μ_i, σ_i and ε_i $(i = 0, 1)$ are positive contants.

Additionaly we consider the material relations

$$\mathbf{B} = \mu \mathbf{H} \ . \tag{5.8}$$

Note that in general μ, σ and ε can depend on many factors (i. e., position, the frequency of the field applied, magnetic field, electric field,...). Disregarding the effects of hysteresis, we assume that the magnetic permeability depends on the magnetic field (see e.g. [5, Chapter 2]) , i.e., $\mu := \mu(|\mathbf{H}|)$. Considering the nonlinear relation (5.8) between $\mathbf{B}$ and $\mathbf{H}$, the magnetic reluctivity is defined by $\nu = \nu(|\mathbf{B}|) := \frac{1}{\mu(|\mathbf{H}|)}$ and satisfies

$$\mathbf{H} = \nu(|\mathbf{B}|) \mathbf{B} \ . \tag{5.9}$$

ν is assumed to be a continuous function $\nu : \mathbb{R}_0^+ \to \mathbb{R}_0^+$, which due to the physical background satisfies

$$0 < \nu_1 \leq \nu(s) \leq \nu_0, \quad \forall s \in \mathbb{R}_0^+$$
$$s \mapsto \nu(s)s \text{ is strictly monotone and Lipschitz continuous,}$$

where ν_0 is the reluctivity in vacuum.

We assume that $\text{supp}(\mathbf{J}) \subset \Omega$. Then, $\mathbf{J} = 0$ in Ω_e and $\mathbf{J} \cdot \boldsymbol{n} = 0$ on Γ. Moreover, since $\sigma \equiv 0$ in Ω_e it follows from (5.2) that $\mathbf{curl}\, \mathbf{H} = 0$ in Ω_e. Hence, $\mathbf{E}$ cannot be uniquely determined in Ω_e and requires the further gauging condition $\text{div}\,(\varepsilon \mathbf{E}) = 0$, known as **Coulomb gauge**.

In the bounded domain Ω we denote by

$$\boldsymbol{u}(t, \boldsymbol{x}) := \int_0^t \mathbf{E}(s, \boldsymbol{x}) \, ds$$

the time primitive of the electric field and obtain by the integration of (5.1) with respect to t on the time intervall $[0, t]$ that

$$\mathbf{curl}\, \boldsymbol{u} = \mathbf{B}(0, \boldsymbol{x}) - \mathbf{B}(t, \boldsymbol{x})$$
$$= \mathbf{B}(0, \boldsymbol{x}) - \mu(t, \boldsymbol{x}) \mathbf{H}(t, \boldsymbol{x}) \ .$$

We assume that $\mathbf{B}(0, \boldsymbol{x}) = 0$. From this and (5.2) it follows that

$$\sigma \frac{\partial \boldsymbol{u}}{\partial t} + \mathbf{curl}(\mu^{-1}\, \mathbf{curl}\, \boldsymbol{u}) = -\mathbf{J}(t, \boldsymbol{x}) =: \boldsymbol{f}(t, \boldsymbol{x}) \ . \tag{5.10}$$

Now, using the definition of the magnetic reluctivity we obtain

$$\sigma \frac{\partial \boldsymbol{u}}{\partial t} + \mathbf{curl}(\nu(|\mathbf{curl}\, \boldsymbol{u}|)\, \mathbf{curl}\, \boldsymbol{u}) = \boldsymbol{f} \ . \tag{5.11}$$

Procceding as in Chapter 3, testing this with a function $\boldsymbol{v} \in \mathbf{H}(\mathbf{curl}\,, \Omega)$ yields

$$\left(\sigma\,\frac{\partial \boldsymbol{u}}{\partial t}, \boldsymbol{v}\right)_{\Omega} + \left(\mathbf{curl}\big(\nu\,(|\mathbf{curl}\,\boldsymbol{u}|)\,\mathbf{curl}\,\boldsymbol{u}\big), \boldsymbol{v}\right)_{\Omega} = (\boldsymbol{f}, \boldsymbol{v})_{\Omega}\ .$$

Integration by parts of the second term on the left hand side leads to

$$\left(\sigma\,\frac{\partial \boldsymbol{u}}{\partial t}, \boldsymbol{v}\right)_{\Omega} + \big(\nu\,(|\mathbf{curl}\,\boldsymbol{u}|)\,\mathbf{curl}\,\boldsymbol{u}, \mathbf{curl}\,\boldsymbol{v}\big)_{\Omega} - \big\langle \gamma_N^- \boldsymbol{u}, \gamma_D^- \boldsymbol{v}\big\rangle_{\Gamma} = (\boldsymbol{f}, \boldsymbol{v})_{\Omega} \tag{5.12}$$

where $\gamma_D{}^-$ and $\gamma_N{}^-$ are the traces on Γ from Ω defined in (1.2) and (1.8).

In the exterior domain Ω_e, we observe from (5.2), (5.1) and (5.3) that $\mathbf{curl}\,\mathbf{curl}\,\boldsymbol{u} = 0$ and div $\boldsymbol{u} = 0$ gives

$$\Delta \boldsymbol{u} = \mathbf{grad}\,\mathrm{div}\,\boldsymbol{u} - \mathbf{curl}\,\mathbf{curl}\,\boldsymbol{u} = 0 \quad \text{in} \quad \Omega_e$$

for a.e. $t \in (0, T)$. Therefore, $\boldsymbol{u}$ is given via the Stratton-Chu representation formula

$$\begin{aligned} \boldsymbol{u}(\boldsymbol{x}) =\ &\mathbf{curl}_{\boldsymbol{x}} \int_{\Gamma} (\boldsymbol{n} \times \boldsymbol{u})(\boldsymbol{y})\Phi(\boldsymbol{x}, \boldsymbol{y})ds(\boldsymbol{y}) + \int_{\Gamma} (\boldsymbol{n} \times \mathbf{curl}\,\boldsymbol{u})(\boldsymbol{y})\Phi(\boldsymbol{x}, \boldsymbol{y})ds(\boldsymbol{y}) \\ &- \mathbf{grad}_{\boldsymbol{x}} \int_{\Gamma} (\boldsymbol{n} \cdot \boldsymbol{u})(\boldsymbol{y})\Phi(\boldsymbol{x}, \boldsymbol{y})dS(\boldsymbol{y}), \qquad \boldsymbol{x} \in \Omega_e \end{aligned} \tag{5.13}$$

with Laplace kernel $\Phi(\boldsymbol{x}, \boldsymbol{y}) = \dfrac{1}{4\pi}\|\boldsymbol{x} - \boldsymbol{y}\|^{-1}$.

Taking traces, we obtain for $\boldsymbol{x} \longrightarrow \Gamma$ the jump relations

$$\gamma_D^+ \boldsymbol{u} = \mathcal{K}(\gamma_D^+ \boldsymbol{u}) - \mathcal{V}(\gamma_N^+ \boldsymbol{u}) - \mathbf{grad}_{\Gamma}\,V(\gamma_n^+ \boldsymbol{u})\ , \tag{5.14}$$

$$\gamma_N^+ \boldsymbol{u} = \mathcal{W}\left(\gamma_D^+ \boldsymbol{u}\right) - \widetilde{\mathcal{K}}\left(\gamma_N^+ \boldsymbol{u}\right) \tag{5.15}$$

with the limits $\gamma_D^+ \boldsymbol{u}$ and $\gamma_N^+ \boldsymbol{u}$ from Ω_e onto Γ of the traces $\gamma_D \boldsymbol{u}$ and $\gamma_N \boldsymbol{u}$, and the integral operators defined in (1.20) .

Now, we test (5.14) with a function $\boldsymbol{\zeta} \in \mathbf{H}_{\|}^{-\frac{1}{2}}(\mathrm{div}_{\Gamma}0, \Gamma)$ and as for the third term of the right hand side yields

$$\big\langle \mathbf{grad}_{\Gamma}\,V(\gamma_n \boldsymbol{u}), \boldsymbol{\zeta}\big\rangle_{\Gamma} = -\big\langle V(\gamma_n \boldsymbol{u}), \mathrm{div}_{\Gamma}\,\boldsymbol{\zeta}\big\rangle_{\Gamma} = 0$$

we obtain

$$\big\langle (I - \mathcal{K})\boldsymbol{u}_{\Gamma}, \boldsymbol{\zeta}\big\rangle_{\Gamma} + \big\langle \mathcal{V}\boldsymbol{\lambda}, \boldsymbol{\zeta}\big\rangle_{\Gamma} = 0\ . \tag{5.16}$$

Choosing $\boldsymbol{u}_{\Gamma} := \gamma_D \boldsymbol{u}$ and $\boldsymbol{\lambda} := \mathbf{curl}\,\boldsymbol{u} \times \boldsymbol{n}$, we consider the interface conditions (5.6), i.e., $[\gamma_N \boldsymbol{u}] = [\gamma_D \boldsymbol{u}] = 0$ on Γ, and replacing the integral equation (5.15) into (5.12), and adding the integral equation (5.16) it follows the weak formulation:

5 A nonlinear, time dependent eddy current problem

Find $\boldsymbol{u} \in W^1(0, T; \mathbf{H}(\mathbf{curl}, \Omega)), \boldsymbol{\lambda} \in L^2(0, T; \mathbf{H}_{\|}^{-\frac{1}{2}}(\mathrm{div}_\Gamma 0, \Gamma))$ *such that*

$$(\sigma \partial_t \boldsymbol{u}, \boldsymbol{v})_\Omega + (\nu(|\mathbf{curl}\,\boldsymbol{u}|)\,\mathbf{curl}\,\boldsymbol{u}, \mathbf{curl}\,\boldsymbol{v})_\Omega - \langle \mathcal{W}\boldsymbol{u}_\Gamma, \boldsymbol{v}_\Gamma \rangle_\Gamma + \left\langle \widetilde{\mathcal{K}}\boldsymbol{\lambda}, \boldsymbol{v}_\Gamma \right\rangle_\Gamma = (\boldsymbol{f}, \boldsymbol{v})_\Omega,$$

$$\langle (I - \mathcal{K})\boldsymbol{u}_\Gamma, \boldsymbol{\zeta} \rangle_\Gamma + \langle \mathcal{V}\boldsymbol{\lambda}, \boldsymbol{\zeta} \rangle_\Gamma = 0, \tag{5.17}$$

$$\boldsymbol{u}(\cdot, 0) = \boldsymbol{u}_0|_\Omega = 0, \quad \boldsymbol{\lambda}(\cdot, 0) = \boldsymbol{n} \times \mathbf{curl}\,\boldsymbol{u}_0|_\Gamma$$

for all $\boldsymbol{v} \in \mathbf{H}(\mathbf{curl}, \Omega)$ *and* $\boldsymbol{\zeta} \in \mathbf{H}_{\|}^{-\frac{1}{2}}(\mathrm{div}_\Gamma 0, \Gamma)$.

Notice that the initial condition $\boldsymbol{u}(\cdot, 0) = \boldsymbol{u}_0|_\Omega$ is meaningful, due to the continuous enbeddding $W^1(0, T; \mathbf{H}(\mathbf{curl}, \Omega)) \hookrightarrow \mathcal{C}^0(0, T ; \mathbf{L}^2(\Omega, \sigma))$ (cf. page 38).

To obtain coercitivity, we now add a penalty function term $\tilde{\lambda}(\boldsymbol{u}, \boldsymbol{v})_\Omega$ to the left-hand side of (5.17), where $\tilde{\lambda}$ ist an arbitrary positive real constant. Then, considering

$$\mathcal{A}(\boldsymbol{u}, \boldsymbol{\lambda}; \boldsymbol{v}, \boldsymbol{\zeta}) := \tilde{\lambda}(\boldsymbol{u}, \boldsymbol{v})_\Omega - \langle \mathcal{W}\boldsymbol{u}_\Gamma, \boldsymbol{v}_\Gamma \rangle_\Gamma + \langle \widetilde{\mathcal{K}}\boldsymbol{\lambda}, \boldsymbol{v}_\Gamma \rangle + \langle (I - \mathcal{K})\boldsymbol{u}_\Gamma, \boldsymbol{\zeta} \rangle_\Gamma + \langle \mathcal{V}\boldsymbol{\lambda}, \boldsymbol{\zeta} \rangle_\Gamma \ ,$$

$$\mathcal{A}_\nu(\boldsymbol{u}, \boldsymbol{v}) := (\nu(|\mathbf{curl}\,\boldsymbol{u}|)\,\mathbf{curl}\,\boldsymbol{u}, \mathbf{curl}\,\boldsymbol{v})_\Omega \quad \text{and}$$

$$\mathcal{C}_\nu(\boldsymbol{u}, \boldsymbol{\lambda}; \boldsymbol{v}, \boldsymbol{\zeta}) := \mathcal{A}_\nu(\boldsymbol{u}, \boldsymbol{v}) + \mathcal{A}(\boldsymbol{u}, \boldsymbol{\lambda}; \boldsymbol{v}, \boldsymbol{\zeta}) \ ,$$

$$\tag{5.18}$$

the formulation can be rewritten as:

Find $\boldsymbol{u} \in W^1(0, T; \mathbf{H}(\mathbf{curl}, \Omega)), \boldsymbol{\lambda} \in L^2(0, T; \mathbf{H}_{\|}^{-\frac{1}{2}}(\mathrm{div}_\Gamma 0, \Gamma))$ *such that*

$$(\sigma\,\dot{\boldsymbol{u}}, \boldsymbol{v})_\Omega + \mathcal{C}_\nu(\boldsymbol{u}, \boldsymbol{\lambda}; \boldsymbol{v}, \boldsymbol{\zeta}) = (\boldsymbol{f}, \boldsymbol{v})_\Omega, \tag{5.19a}$$

$$\boldsymbol{u}(0) = \boldsymbol{u}_0|_\Omega = 0, \quad \boldsymbol{\lambda}_0 := \boldsymbol{n} \times \mathbf{curl}\,\boldsymbol{u}_0|_\Gamma \tag{5.19b}$$

for all $\boldsymbol{v} \in \mathbf{H}(\mathbf{curl}, \Omega)$ *and* $\boldsymbol{\zeta} \in \mathbf{H}_{\|}^{-\frac{1}{2}}(\mathrm{div}_\Gamma 0, \Gamma)$.

The existence and uniqueness of solution is provided by the following theorem.

Theorem 5.1.1 *We assume* $\boldsymbol{u}_0 \in \mathbf{L}^2(\Omega)$, $\boldsymbol{\lambda}_0 \in \mathbf{L}^2(\Gamma)$ *and* $\boldsymbol{f} \in \mathbf{L}^2((0, T), \mathbf{H}(\mathbf{curl}, \Omega)')$. *Let* $s \to \nu(s)$ *be a continuous function with* $0 < \nu_1 \leq \nu(s) \leq \nu_0$ *for all* $s \in \mathbb{R}_0^+$, *and the function* $s \to \nu(s)\,s$ *be monotone. Then we have unique* $\boldsymbol{u} \in W^1(0, T; \mathbf{H}(\mathbf{curl}, \Omega))$ *and* $\boldsymbol{\lambda} \in L^2(0, T; \mathbf{H}_{\|}^{-\frac{1}{2}}(\mathrm{div}_\Gamma 0, \Gamma))$ *which solve* (5.19).

Proof. The idea of the proof is similar to Cartensen & Stephan [16, Corollary 2] and Bachinger *et al.* [4, Theorem 1].

As $\mathbf{H}(\mathbf{curl}, \Omega)$ is separable and reflexive, the embedding $\mathbf{H}(\mathbf{curl}, \Omega) \subset \mathbf{L}^2(\Omega)$ is continuous and $\mathbf{H}(\mathbf{curl}, \Omega)$ is dense in $\mathbf{L}^2(\Omega)$. Hence,

$$\mathbf{H}(\mathbf{curl}, \Omega) \subset \mathbf{L}^2(\Omega) \subset \mathbf{H}(\mathbf{curl}, \Omega)' \ .$$

Moreover, the nonlinear reluctivity ν implies a nonlinear operator

$$A : \mathbf{H}(\mathbf{curl}, \Omega) \to \mathbf{H}(\mathbf{curl}, \Omega)'$$

which is defined as

$$(A(\boldsymbol{u}), \boldsymbol{v}) := \mathcal{A}_\nu(\boldsymbol{u}, \boldsymbol{v}) = (\nu\,(|\mathbf{curl}\,\boldsymbol{u}|)\,\mathbf{curl}\,\boldsymbol{u}, \mathbf{curl}\,\boldsymbol{v})_\Omega \ .$$

This nonlinear operator is monotone, due to the function $s \to \nu(s)\,s$ is monotone and strictly positive and there exists a positive constant α_0 such that

$$(A(\boldsymbol{u}) - A(\boldsymbol{v}), \boldsymbol{u} - \boldsymbol{v}) = (\nu\,(|\mathbf{curl}\,\boldsymbol{u}|)\,\mathbf{curl}\,\boldsymbol{u} - \nu\,(|\mathbf{curl}\,\boldsymbol{v}|)\,\mathbf{curl}\,\boldsymbol{v}, \mathbf{curl}\,(\boldsymbol{u} - \boldsymbol{v}))_\Omega$$
$$\geq \alpha_0 \|\,\mathbf{curl}(\boldsymbol{u} - \boldsymbol{v})\|^2_{\mathbf{L}^2(\Omega)} \geq 0\ .$$

Moreover, the bilinear form $\mathcal{A}(\boldsymbol{u}, \boldsymbol{\lambda}; \boldsymbol{v}, \boldsymbol{\zeta})$ from (5.18) is also monotone.

Using Lemma 1.3.3 we have that the operators $\mathcal{V}$ and $-\mathcal{W}$ are elliptic, and the operator $\mathcal{K}$ is adjoint to $\mathcal{K} - \mathcal{I}$. Therefore, we obtain

$$\mathcal{A}(\boldsymbol{u}, \boldsymbol{\lambda}; \boldsymbol{u}, \boldsymbol{\lambda}) = \tilde{\lambda}\,(\boldsymbol{u}, \boldsymbol{u})_\Omega - \langle \mathcal{W}\boldsymbol{u}_\Gamma, \boldsymbol{u}_\Gamma \rangle_\Gamma + \left\langle \widetilde{\mathcal{K}}\boldsymbol{\lambda}, \boldsymbol{u}_\Gamma \right\rangle_\Gamma + \langle (I - \mathcal{K})\boldsymbol{u}_\Gamma, \boldsymbol{\lambda} \rangle_\Gamma + \langle \mathcal{V}\boldsymbol{\lambda}, \boldsymbol{\lambda} \rangle_\Gamma$$
$$= \tilde{\lambda}\,(\boldsymbol{u}, \boldsymbol{u})_\Omega - \langle \mathcal{W}\boldsymbol{u}_\Gamma, \boldsymbol{u}_\Gamma \rangle_\Gamma + \langle \mathcal{V}\boldsymbol{\lambda}, \boldsymbol{\lambda} \rangle_\Gamma$$
$$\gtrsim (\boldsymbol{u}, \boldsymbol{u})_\Omega + \|\,\mathrm{curl}_\Gamma\,\boldsymbol{u}_\Gamma\|^2_{H^{-1/2}(\Gamma)} + \|\boldsymbol{\lambda}\|^2_{\mathbf{H}_\|^{-\frac{1}{2}}(\mathrm{div}_\Gamma, \Gamma)}$$
$$\gtrsim \|\boldsymbol{u}\|^2_{\mathbf{L}^2(\Omega)} + \|\boldsymbol{\lambda}\|^2_{\mathbf{H}_\|^{-\frac{1}{2}}(\mathrm{div}_\Gamma, \Gamma)} \geq 0.$$

Thus $\mathcal{C}_\nu(\boldsymbol{u}, \boldsymbol{\lambda}; \boldsymbol{v}, \boldsymbol{\zeta})$ satisfies

- **Monotonicity.**

$$\mathcal{C}_\nu(\boldsymbol{u}, \boldsymbol{\lambda}; \boldsymbol{u} - \boldsymbol{v}, \boldsymbol{\lambda} - \boldsymbol{\zeta}) - \mathcal{C}_\nu(\boldsymbol{v}, \boldsymbol{\zeta}; \boldsymbol{u} - \boldsymbol{v}, \boldsymbol{\lambda} - \boldsymbol{\zeta}) = (A(\boldsymbol{u}) - A(\boldsymbol{v}), \boldsymbol{u} - \boldsymbol{v})$$
$$+ \mathcal{A}(\boldsymbol{u} - \boldsymbol{v}, \boldsymbol{\lambda} - \boldsymbol{\zeta}; \boldsymbol{u} - \boldsymbol{v}, \boldsymbol{\lambda} - \boldsymbol{\zeta})$$
$$\geq 0.$$

- **Coercivity.**

$$\mathcal{C}_\nu(\boldsymbol{u}, \boldsymbol{\lambda}; \boldsymbol{u}, \boldsymbol{\lambda})) = (A(\boldsymbol{u}), \boldsymbol{u}) + \mathcal{A}(\boldsymbol{u}, \boldsymbol{\lambda}; \boldsymbol{u}, \boldsymbol{\lambda})$$
$$\gtrsim \|\,\mathbf{curl}\,\boldsymbol{u}\|^2_{\mathbf{L}^2(\Omega)} + \|\boldsymbol{u}\|^2_{\mathbf{L}^2(\Omega)} + \|\boldsymbol{\lambda}\|^2_{\mathbf{H}_\|^{-\frac{1}{2}}(\mathrm{div}_\Gamma, \Gamma)}$$
$$= \|(\boldsymbol{u}, \boldsymbol{\lambda})\|^2_{\mathbf{H}(\mathbf{curl}, \Omega) \times \mathbf{H}_\|^{-\frac{1}{2}}(\mathrm{div}_\Gamma, \Gamma)}.$$

- **Continuity.** It is an immediate consequence of the continuity of the boundary integral operators (see Lemma 1.3.2) and because the reluctivity ν is bounded from above. Hence there exist a positive constant α_1 such that

$$|\mathcal{C}_\nu(\boldsymbol{u}, \boldsymbol{\lambda}; \boldsymbol{v}, \boldsymbol{\zeta}))| \leq \alpha_1 \|(\boldsymbol{u}, \boldsymbol{\lambda})\|_{\mathbf{H}(\mathbf{curl}, \Omega) \times \mathbf{H}_\|^{-\frac{1}{2}}(\mathrm{div}_\Gamma, \Gamma)} \|(\boldsymbol{v}, \boldsymbol{\zeta})\|_{\mathbf{H}(\mathbf{curl}, \Omega) \times \mathbf{H}_\|^{-\frac{1}{2}}(\mathrm{div}_\Gamma, \Gamma)}\ .$$

In conclusion, due to the assumptions of the main theorem on existence and uniqueness of nonlinear parabolic problems are fulfilled (see Zeidler [79, Theorem 30.A]) there exist unique $\boldsymbol{u} \in W^1(0, T; \mathbf{H}(\mathbf{curl}, \Omega))$ and $\boldsymbol{\lambda} \in L^2(0, T; \mathbf{H}_\parallel^{-\frac{1}{2}}(\mathrm{div}_\Gamma 0, \Gamma))$ which solve (5.19) ∎

For the numerical solution of (5.19) we obtain a full-discrete system using a standard Galerkin method for the space discretization and for the discretization in time the discontinuous Galerkin method in time (see Section 3.2).

5.2 Solution procedure

Let $\mathcal{T}_h$ be a triangulation (with tetrahedral or hexahedral elements) of the domain Ω. We assume that $\mathcal{T}_h$ is quasi-uniform with mesh size $h > 0$ and shape-regular (cf. Section 3.1.2). This mesh induces a mesh $\mathcal{K}_h := \{\mathfrak{T} \cap \Gamma : \mathfrak{T} \in \mathcal{T}_h\}$ of triangles or quadrilaterals on the boundary.

In the interior domain we use Nédélec functions of first order $\mathcal{ND}_1(\mathcal{T}_h)$, a conforming finite element space of $\mathbf{H}(\mathbf{curl}, \Omega)$, for the discretization of the unknown $\boldsymbol{u} = \boldsymbol{u}(t, \boldsymbol{x})$ with $\boldsymbol{u} \in W^1(0, T; \mathbf{H}(\mathbf{curl}, \Omega))$, furthermore we use the divergence free Raviart-Thomas functions space $\mathcal{RT}_1^0(\mathcal{K}_h)$ a conforming finite element space of $\mathbf{H}_\parallel^{-\frac{1}{2}}(\mathrm{div}_\Gamma 0, \Gamma)$, for the discretization of the boundary unknown $\boldsymbol{\lambda} = \boldsymbol{\lambda}(t, \boldsymbol{x}) = \mathbf{curl}\, \boldsymbol{u} \times \boldsymbol{n}$, with $\boldsymbol{\lambda} \in L^2(0, T; \mathbf{H}_\parallel^{-\frac{1}{2}}(\mathrm{div}_\Gamma 0, \Gamma))$. Now, if $\{\Phi_k\}_{k=1,\dots,M}$ denotes a basis of $\mathcal{ND}_1(\mathcal{T}_h)$ and $\{\boldsymbol{\psi}_k\}_{k=1,\dots,m}$ denotes a basis of $\mathcal{RT}_1^0(\mathcal{K}_h)$, we can identify the vector $\boldsymbol{U}^h := (\boldsymbol{U}_i^h)_{i=1,\dots,M}$ with the discrete function $\boldsymbol{U}^h = \boldsymbol{U}^h(\boldsymbol{x}) := \sum_{i=1}^M \boldsymbol{U}_i^h \Phi_i(\boldsymbol{x}) \in \mathcal{ND}_1(\mathcal{T}_h)$ without loss of generality. Analogously we identify the function $\boldsymbol{\lambda}^h = \boldsymbol{\lambda}^h(\boldsymbol{x}) := \sum_{i=1}^M \boldsymbol{\lambda}_i^h \boldsymbol{\psi}_i(\boldsymbol{x}) \in \mathcal{RT}_1^0(\mathcal{K}_h)$ with the vector $\boldsymbol{\lambda}^h = (\boldsymbol{\lambda}_i^h)_{i=1,\dots,m}$.

Aditionally we consider a partition $0 = t_0 < t_1 < t_2 < \dots < t_N = T$ of the time interval $[0, T]$ into subintervals $I_n := (t_{n-1}, t_n]$ of length $k_n := t_n - t_{n-1}$ and associate with each such time interval a triangulation $\mathcal{T}_h^n := \mathcal{T}_{h_n}$ (of tetrahedral or hexahedral elements) of Ω and an induced mesh $\mathcal{K}_{h_n}$ of triangles or quadrilaterals on the boundary Γ.

The approximate solution of (5.19) is obtained by solving the following problem (cf. (3.20)):

For $n = 1, \dots, N$, find $\mathbf{U}_n^h \in \mathbf{V}_h^{n,l}$ and $\boldsymbol{\lambda}_n^h \in \widetilde{\mathbf{V}}_h^{n,l}$ such that

$$\int_{I_n} \left\{ (\sigma \dot{\mathbf{U}}^h{}_n, \boldsymbol{v}) + \mathcal{C}_\nu(\mathbf{U}_n^h, \boldsymbol{\lambda}_n^h; \boldsymbol{v}, \boldsymbol{\zeta}) \right\} dt + (\sigma [\mathbf{U}^h]_{n-1}, \boldsymbol{v}_{n-1}^+) = \int_{I_n} \mathcal{L}(\boldsymbol{v})\, dt, \qquad (5.20)$$

for all $\boldsymbol{v} \in \mathbf{V}_h^{n,l}$ and all $\boldsymbol{\zeta} \in \widetilde{\mathbf{V}}_h^{n,l}$.

Here we use the definitions

$$\boldsymbol{v}_n^+ := \lim_{t \to 0+} \boldsymbol{v}(t_n + t), \quad \boldsymbol{v}_n^- := \lim_{t \to 0-} \boldsymbol{v}(t_n + t) \quad \text{and} \quad [\boldsymbol{v}]_n := \boldsymbol{v}_n^+ - \boldsymbol{v}_n^-.$$

We solve this nonlinear problem by means of Newton's method. The widespread use of this technique is due to its fast convergence: Newton's method is locally superlinearly (or even quadratically) convergent.

Considering the bilinear form

$$\mathcal{Q}_{\boldsymbol{w}}(\boldsymbol{u},\boldsymbol{\lambda};\boldsymbol{v},\boldsymbol{\zeta}) := \int_{I_n} \left\{ (\sigma\dot{\boldsymbol{u}},\boldsymbol{v}) + (\tilde{\nu}(\operatorname{\mathbf{curl}}\boldsymbol{w})\operatorname{\mathbf{curl}}\boldsymbol{u},\operatorname{\mathbf{curl}}\boldsymbol{v})_{\Omega} + \mathcal{A}(\boldsymbol{u},\boldsymbol{\lambda};\boldsymbol{v},\boldsymbol{\zeta}) \right\} dt$$
$$+ (\sigma\left[\boldsymbol{u}\right]_{n-1},\boldsymbol{v}_{n-1}^{+})$$

where for $\boldsymbol{x} \in \mathbb{R}^3$, $\tilde{\nu}(\boldsymbol{x}) \in \mathbb{R}^{3\times3}$ denotes the Jacobian of $\boldsymbol{x} \mapsto \nu(|\boldsymbol{x}|)\boldsymbol{x}$, i.e.,

$$\tilde{\nu}(\boldsymbol{x}) = \nu(|\boldsymbol{x}|)\boldsymbol{I}_{3\times3} + \nu'(|\boldsymbol{x}|)\frac{\boldsymbol{x}\cdot\boldsymbol{x}^{\top}}{|\boldsymbol{x}|}.$$

Newton's scheme for the solution of the nonlinear system (5.20) is presented in Algorithm 4.

We seek to find solution for (5.24) by means of the discontinuous Galerkin method using piecewice linear functions in time, i.e., we choose $l = 1$.

Analogously to the Section 3.2.1, we define the trial functions as

$$\boldsymbol{D}_n(\boldsymbol{x},t) := \boldsymbol{D}_{n,1}(\boldsymbol{x}) + \frac{t-t_{n-1}}{k_n}\boldsymbol{D}_{n,2}(\boldsymbol{x}),$$

$$\boldsymbol{\delta}_n(\boldsymbol{x},t) := \boldsymbol{\delta}_{n,1}(x) + \frac{t-t_{n-1}}{k_n}\boldsymbol{\delta}_{n,2}(\boldsymbol{x})$$

for some $\boldsymbol{D}_{n,1}(\boldsymbol{x}),\boldsymbol{D}_{n,2}(\boldsymbol{x})$ in $\mathcal{N}\mathcal{D}_1(\mathcal{T}_{h_n})$ and $\boldsymbol{\delta}_{n,1}(x),\boldsymbol{\delta}_{n,2}(\boldsymbol{x})$ in $\mathcal{R}\mathcal{T}_1^0(\mathcal{K}_{h_n})$. Moreover, our test functions are defined by

$$\Phi_1(\boldsymbol{x},t) := \Phi(\boldsymbol{x}), \quad \Phi_2(\boldsymbol{x},t) := \frac{t_n-t}{k_n}\Phi(\boldsymbol{x}) \quad \text{and} \quad \Phi(\boldsymbol{x}) \in \mathcal{N}\mathcal{D}_1(\mathcal{T}_{h_n}) \ .$$

Similary we define the test functions for $\boldsymbol{\psi} \in \mathcal{R}\mathcal{T}_1^0(\mathcal{K}_{h_n})$.

Then, considering the bilinear operator

$$\mathcal{B}_{\boldsymbol{w}}(\boldsymbol{u},\boldsymbol{\lambda};\boldsymbol{v},\boldsymbol{\zeta}) := \int_{I_n} \left\{ (\tilde{\nu}(\operatorname{\mathbf{curl}}\boldsymbol{w})\operatorname{\mathbf{curl}}\boldsymbol{u},\operatorname{\mathbf{curl}}\boldsymbol{v})_{\Omega} + \mathcal{A}(\boldsymbol{u},\boldsymbol{\lambda};\boldsymbol{v},\boldsymbol{\zeta}) \right\} dt$$

the problem (5.24) is equivalent to:

For $n = 1,\ldots,N$, find $\boldsymbol{D}_{n,1},\boldsymbol{D}_{n,2} \in \mathcal{N}\mathcal{D}_1(\mathcal{T}_{h_n})$ and $\boldsymbol{\delta}_{n,1},\boldsymbol{\delta}_{n,2} \in \mathcal{R}\mathcal{T}_1^0(\mathcal{K}_{h_n})$, such that

$$\mathcal{B}_{\mathbf{U}_n^{(j)}}(\boldsymbol{D}_{n,1},\boldsymbol{\delta}_{n,1};\boldsymbol{v},\boldsymbol{\zeta}) + \frac{1}{k_n}(\sigma\boldsymbol{D}_{n,1},\boldsymbol{v}) + \frac{1}{2}\mathcal{B}_{\mathbf{U}_n^{(j)}}(\boldsymbol{D}_{n,2},\boldsymbol{\delta}_{n,2};\boldsymbol{v},\boldsymbol{\zeta}) + \frac{1}{k_n}(\sigma\boldsymbol{D}_{n,2},\boldsymbol{v}) =$$
$$= \frac{1}{k_n}(\sigma\boldsymbol{D}_{n-1}^{-},\boldsymbol{v}) - \frac{1}{k_n}\mathfrak{b}_n(\boldsymbol{U}_n^{(j)},\boldsymbol{\lambda}_n^{(j)};\boldsymbol{v},\boldsymbol{\zeta}) \qquad (5.21)$$

and

$$\frac{1}{2}\mathcal{B}_{\mathbf{U}_n^{(j)}}(\boldsymbol{D}_{n,1}, \boldsymbol{\delta}_{n,1}; \boldsymbol{v}, \boldsymbol{\zeta}) + \frac{1}{k_n}(\sigma \boldsymbol{D}_{n,1}, \boldsymbol{v}) + \frac{1}{6}\mathcal{B}_{\mathbf{U}_n^{(j)}}(\boldsymbol{D}_{n,2}, \boldsymbol{\delta}_{n,2}; \boldsymbol{v}, \boldsymbol{\zeta}) + \frac{1}{2k_n}(\sigma \boldsymbol{D}_{n,2}, \boldsymbol{v}) =$$

$$= \frac{1}{k_n}(\sigma \boldsymbol{D}_{n-1}^-, \boldsymbol{v}) - \frac{1}{2k_n}\mathfrak{b}_n(\boldsymbol{U}_n^{(j)}, \boldsymbol{\lambda}_n^{(j)}; \boldsymbol{v}, \boldsymbol{\zeta}) \qquad (5.22)$$

for all $\boldsymbol{v} \in \mathcal{ND}_1(\mathcal{T}_{h_n})$ and all $\boldsymbol{\zeta} \in \mathcal{RT}_1^0(\mathcal{K}_{h_n})$.

Notice that (5.21) and (5.22) are equivalent to the following linear system of equations:

$$\begin{pmatrix} \left(\tilde{\lambda}+\frac{\sigma}{k_n}\right)\mathcal{M}+\mathcal{R}^*-\mathcal{W} & \mathcal{C} & \left(\frac{\tilde{\lambda}}{2}+\frac{\sigma}{k_n}\right)\mathcal{M}+\frac{1}{2}\mathcal{R}^*-\frac{1}{2}\mathcal{W} & \frac{1}{2}\mathcal{C} \\ \mathcal{B} & \mathcal{V} & \frac{1}{2}\mathcal{B} & \frac{1}{2}\mathcal{V} \\ \hline \left(\frac{\tilde{\lambda}}{2}+\frac{\sigma}{k_n}\right)\mathcal{M}+\frac{1}{2}\mathcal{R}^*-\frac{1}{2}\mathcal{W} & \frac{1}{2}\mathcal{C} & \left(\frac{\tilde{\lambda}}{6}+\frac{\sigma}{2k_n}\right)\mathcal{M}+\frac{1}{6}\mathcal{R}^*-\frac{1}{6}\mathcal{W} & \frac{1}{6}\mathcal{C} \\ \frac{1}{2}\mathcal{B} & \frac{1}{2}\mathcal{V} & \frac{1}{6}\mathcal{B} & \frac{1}{6}\mathcal{V} \end{pmatrix} \begin{pmatrix} \boldsymbol{D}_{n,1} \\ \boldsymbol{\delta}_{n,1} \\ \boldsymbol{D}_{n,2} \\ \boldsymbol{\delta}_{n,2} \end{pmatrix} = \begin{pmatrix} \mathfrak{A}_1 \\ \mathfrak{G}_1 \\ \mathfrak{A}_2 \\ \mathfrak{G}_2 \end{pmatrix} \qquad (5.23)$$

where right hand side is abreviated by

$$\mathfrak{A}_1 := \frac{\sigma}{k_n}\mathcal{M}\left(\boldsymbol{D}_{n-1}^- + \mathbf{U}_{n-1}^-\right) + \frac{1}{k_n}\mathcal{F}_1 - \frac{\sigma}{k_n}\mathcal{M}(\mathbf{U}_{n,1}^{(j)} + \mathbf{U}_{n,2}^{(j)}) - \mathcal{R}^{NL} + \mathcal{W}\mathbf{U}_n^{(j)} - \mathcal{C}\boldsymbol{\lambda}_n^{(j)} ,$$

$$\mathfrak{A}_2 := \frac{\sigma}{k_n}\mathcal{M}\left(\boldsymbol{D}_{n-1}^- + \mathbf{U}_{n-1}^-\right) + \frac{1}{k_n^2}\mathcal{F}_2 - \frac{\sigma}{2k_n}\mathcal{M}(2\mathbf{U}_{n,1}^{(j)} + \mathbf{U}_{n,2}^{(j)}) - \frac{1}{2}\mathcal{R}^{NL} + \frac{1}{2}\mathcal{W}\mathbf{U}_n^{(j)} - \frac{1}{2}\mathcal{C}\boldsymbol{\lambda}_n^{(j)} ,$$

$$\mathfrak{G}_1 := -\mathcal{B}\mathbf{U}_n^{(j)} - \mathcal{V}\boldsymbol{\lambda}_n^{(j)} ,$$

$$\mathfrak{G}_2 := -\frac{1}{2}\mathcal{B}\mathbf{U}_n^{(j)} - \frac{1}{2}\mathcal{V}\boldsymbol{\lambda}_n^{(j)}$$

and

$$(\mathcal{F}_1)_i := \left(\int_{I_n} \boldsymbol{f} \, dt, \Phi_i\right), \qquad \left(\mathcal{R}^{NL}\right)_i := (\nu(|\mathbf{curl}\,\mathbf{U}_n^{(j)}|)\,\mathbf{curl}\,\mathbf{U}_n^{(j)}, \mathbf{curl}\,\Phi_i),$$

$$(\mathcal{F}_2)_i := \left(\int_{I_n} (t_n - t)\boldsymbol{f} \, dt, \Phi_i\right), \qquad \left(\mathcal{R}^*\right)_{ik} := (\tilde{\nu}(\mathbf{curl}\,\mathbf{U}_n^{(j)})\,\mathbf{curl}\,\Phi_i, \mathbf{curl}\,\Phi_k),$$

$$(\mathcal{M})_{ik} := (\Phi_i, \Phi_k), \qquad (\mathcal{W})_{ik} := \langle \mathcal{W}(\gamma_D \Phi_i), \gamma_D \Phi_k \rangle,$$

$$(\mathcal{B})_{ik} := \langle (I - \mathcal{K})\gamma_D \Phi_i, \psi_k \rangle, \qquad (\mathcal{C})_{ik} := \langle \widetilde{\mathcal{K}}(\gamma_N \psi_i), \gamma_D \Phi_k \rangle,$$

$$(\mathcal{V})_{ik} := \langle \mathcal{V}\psi_i, \psi_k \rangle,$$

where $\{\Phi_k\}_{k=1,\dots,M}$ is a basis of $\mathcal{ND}_1(\mathcal{T}_{h_n})$ and $\{\psi_k\}_{k=1,\dots,m}$ a basis of $\mathcal{RT}_1^0(\mathcal{K}_{h_n})$.

Algorithm 4   Newton's Algorithm for the solution of the nonlinear system

---

Require: • Set the partition $0 = t_0 < t_1 < \cdots < t_N = T$ of the time interval $[0, T]$ into subintervals $I_n := (t_{n-1}, t_n]$ of length $k_n := t_n - t_{n-1}$.

      • Set the initial condition

$$\mathbf{U}_0^- = \lim_{t \to 0^-} \mathbf{U}_1(0 + t) = 0 \ .$$

      • Set the tolerance $\epsilon > 0$.

      • Set initial solution $(\mathbf{U}_1^{(0)}, \boldsymbol{\lambda}_1^{(0)})$, which can be the solution of the linear problem, i.e., $\nu \equiv \text{const.}$, or choose $(\mathbf{U}_1^{(0)}, \boldsymbol{\lambda}_1^{(0)}) = (0, 0)$.

for $n = 1, 2, \cdots, N$ **do**

(a) **for** $j = 0, 1, 2, \cdots$ **do**

    (i) Compute the load vector

$$\mathfrak{b}_n(\boldsymbol{U}_n^{(j)}, \boldsymbol{\lambda}_n^{(j)}; \boldsymbol{v}, \boldsymbol{\zeta}) := \int_{I_n} \Big\{ (\boldsymbol{f}, \boldsymbol{v}) - (\sigma \dot{\boldsymbol{U}}_n^{(j)}, \boldsymbol{v}) - \mathcal{C}_\nu(\boldsymbol{U}_n^{(j)}, \boldsymbol{\lambda}_n^{(j)}; \boldsymbol{v}, \boldsymbol{\zeta}) \Big\} \, dt$$
$$- (\sigma \big[\boldsymbol{U}_n \big]_{n-1}, \boldsymbol{v}_{n-1}^+)$$

    (ii) If $\|\mathfrak{b}_n\|_{l_2} := \sqrt{\mathfrak{b}_n \cdot \mathfrak{b}_n} \leq \epsilon$, then goto (b)

    (iii) Find the increment $(\boldsymbol{D}_n^{(j+1)}, \boldsymbol{\delta}_n^{(j+1)}) \in \mathbf{V}_h^{n,l} \times \widetilde{\mathbf{V}}_h^{n,l}$ by solving the problem

$$\mathcal{Q}_{\mathbf{U}_n^{(j)}}(\boldsymbol{D}_n^{(j+1)}, \boldsymbol{\delta}_n^{(j+1)}; \boldsymbol{v}, \boldsymbol{\zeta}) = \mathfrak{b}_n(\boldsymbol{U}_n^{(j)}, \boldsymbol{\lambda}_n^{(j)}; \boldsymbol{v}, \boldsymbol{\zeta}) \qquad (5.24)$$

    for all $\boldsymbol{v} \in \mathbf{V}_h^{n,l}$ and all $\boldsymbol{\zeta} \in \widetilde{\mathbf{V}}_h^{n,l}$.

    (iv) Update the solution

$$(\mathbf{U}_n^{(j+1)}, \boldsymbol{\lambda}_n^{(j+1)}) = (\mathbf{U}_n^{(j)}, \boldsymbol{\lambda}_n^{(j)}) + (\boldsymbol{D}_n^{(j+1)}, \boldsymbol{\delta}_n^{(j+1)}) \in \mathbf{V}_h^{n,l} \times \widetilde{\mathbf{V}}_h^{n,l}.$$

    (v) Set $j = j + 1$ and goto (a)

(b) **Initialise the next time step:**

    • Set

$$\boldsymbol{U}_n^- = \lim_{t \to 0^-} \mathbf{U}_{n+1}(t_n + t) = \mathbf{U}_n^{(j)}(t_n).$$

    • Set initial solution $(\mathbf{U}_{n+1}^{(0)}, \boldsymbol{\lambda}_{n+1}^{(0)})$, which can be the solution of the linear problem, i.e., $\nu \equiv \text{const.}$, or $(\mathbf{U}_{n+1}^{(0)}, \boldsymbol{\lambda}_{n+1}^{(0)}) := (0, 0)$.

(c) If $n < N$, goto (a). Otherwise exit, if the final time T is achieved.

---

5 A nonlinear, time dependent eddy current problem

Example 5.2.1 *We define $\Omega := (-1, 1)^3$ and for $t \in [0, 1]$ we consider that the exact solution of (5.2) - (5.7) is given by*

$$\boldsymbol{u}(t, \boldsymbol{x}) = g(t)\boldsymbol{v}(\boldsymbol{x}) = te^{-\frac{1}{3}t}\,\mathbf{curl}\,\mathfrak{I}_\Omega(\boldsymbol{\rho}(\boldsymbol{y}))(\boldsymbol{x}), \quad \boldsymbol{x} \in \Omega,$$

where

$$\mathfrak{I}_\Omega(\boldsymbol{\rho}(\boldsymbol{y}))(\boldsymbol{x}) = \int_\Omega \frac{1}{\|\boldsymbol{x} - \boldsymbol{y}\|}\boldsymbol{\rho}(\boldsymbol{y})\,d\boldsymbol{y}$$

with

$$\boldsymbol{\rho}(\boldsymbol{x}) := ((1 - x_1^2)(1 - x_2^2)(1 - x_3^2))^2 x_1 x_2 x_3 (1, 1, 1)^\mathsf{T}, \quad \boldsymbol{x} \text{ in } \Omega,$$

(cf. Example 4.2.2).

We consider a linear and a nonlinear problem, i.e., we choose $\nu = \nu^{(1)}$ or $\nu = \nu^{(2)}$ in (5.19a) where

$$\nu^{(1)}(s) = 1.0, \tag{5.25}$$

$$\nu^{(2)}(s) = 0.001 + (1.0 - \alpha)\frac{s^8}{s^8 + \beta} \tag{5.26}$$

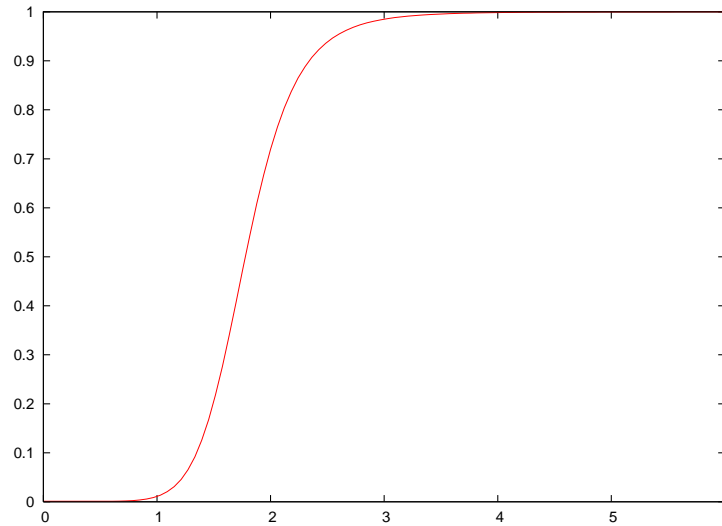*with $\alpha = 0.001$ and $\beta = 100$. The right hand side is chosen to yield the exact solution*

Figure 5.1: Graph of the function $\nu^{(2)}(s)$.

(see Page 79) in both cases.

*We obtain the solution of the scheme (5.20) by applying the Newton method presented in Algorithm 4, which stops if the Euclidean norm of $(\boldsymbol{D}, \boldsymbol{\delta})$ on each nodal point t_n is less than 10^{-6} The linear system (5.23) are solved using Inverse block preconditioners (see Section 4.2.1) and HMCR as fast solver.*

Figures 5.2 and 5.3 give the error $e_1 := \|\boldsymbol{u} - \boldsymbol{U}^h\|_{\mathbf{L}^2(\Omega)}$ and the error in energy norm e_2 and their respectives convergence rates with respect to the degree of freedom DOF. Column 6 on Figure 5.2 gives the Newton's steps needed for convergence.
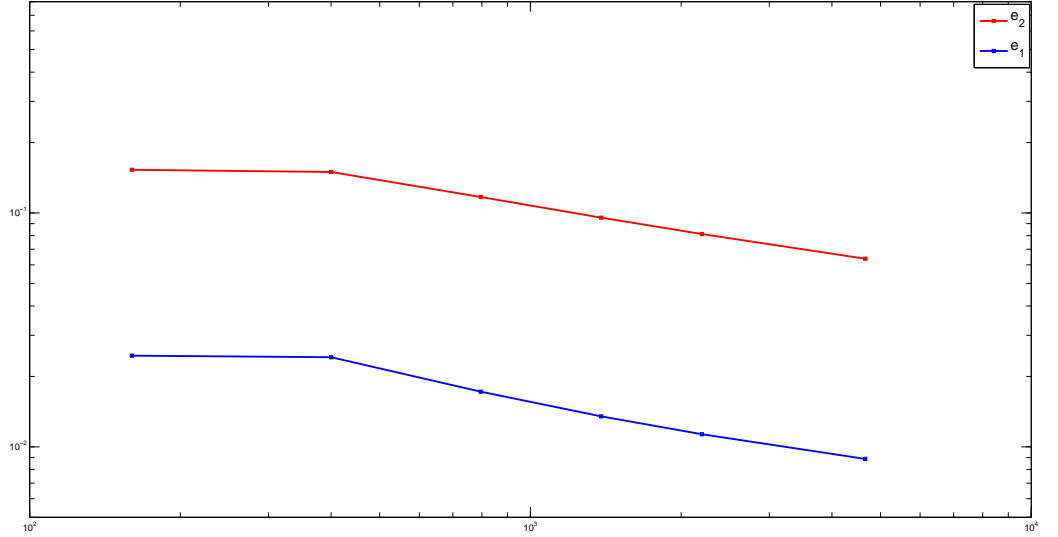
DOF	e_1	α_{nl1}	e_2	α_{nl2}	Iter
160	0.0245	-	0.1529	-	10
400	0.0242	-0.0163	0.1497	-0.0231	16
796	0.0172	-0.4934	0.1170	-0.3582	19
1384	0.0135	-0.4386	0.0955	-0.3678	23
2200	0.0113	-0.3805	0.0812	-0.3485	27
4660	0.0089	-0.3230	0.0637	-0.3228	36

Figure 5.2: $\mathbf{L}^2-$error $e_1 := \|\boldsymbol{u}-\boldsymbol{U}^h\|_{\mathbf{L}^2(\Omega)}$, error in energy norm e_2, convergence rates α_{nl1}, α_{nl2} and Newton's iterations in $t_n = 0.6$ for the non-linear case in Example 5.2.1.
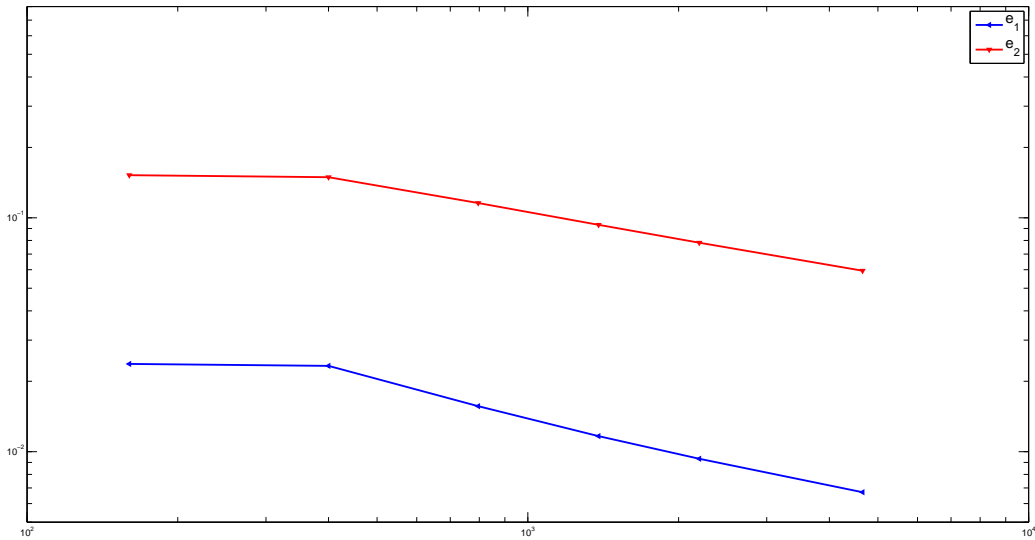
DOF	e_1	α_{li1}	e_2	α_{li2}
160	0.0237	-	0.1521	-
400	0.0233	-0.0208	0.1492	-0.0216
796	0.0157	-0.5756	0.1157	-0.3696
1384	0.011	-0.53347	0.0933	-0.3885
2200	0.009	-0.48133	0.0783	-0.3785
4660	0.006	-0.43827	0.0594	-0.3675

Figure 5.3: $\mathbf{L}^2-$error $e_1 := \|\boldsymbol{u} - \boldsymbol{U}^h\|_{\mathbf{L}^2(\Omega)}$, error in energy norm e_2 and convergence rates α_{li1}, α_{li2} for the linear case in Example 5.2.1.

Bibliography

[1] A. ALONSO AND A. VALLI, *Some remarks on the characterization of the space of tangential traces of $H(\mathrm{rot}; \Omega)$ and the construction of an extension operator*, Manuscripta Math., 89 (1996), pp. 159–178.

[2] C. AMROUCHE, C. BERNARDI, M. DAUGE, AND V. GIRAULT, *Vector potentials in three-dimensional non-smooth domains*, Math. Methods Appl. Sci., 21 (1998), pp. 823–864.

[3] F. ASSOUS, P. DEGOND, E. HEINTZE, P.-A. RAVIART, AND J. SEGRE, *On a finite-element method for solving the three-dimensional Maxwell equations*, J. Comput. Phys., 109 (1993), pp. 222–237.

[4] F. BACHINGER, U. LANGER, AND J. SCHÖBERL, *Numerical analysis of nonlinear multiharmonic eddy current problems*, Numer. Math., 100 (2005), pp. 593–616.

[5] N. BASTOS, JOÃO PEDRO A. ; SADOWSKI, *Electromagnetic modeling by finite element methods*, vol. 117 of Electrical engineering and electronics, Dekker, New York, 2003.

[6] R. BECK, R. HIPTMAIR, R. H. W. HOPPE, AND B. WOHLMUTH, *Residual based a posteriori error estimators for eddy current computation*, M2AN Math. Model. Numer. Anal., 34 (2000), pp. 159–182.

[7] A. BOSSAVIT, *The computation of eddy-currents, in dimension 3, by using mixed finite elements and boundary elements in association*, Math. Comput. Modelling, 15 (1991), pp. 33–42. Boundary integral equation methods (boundary element methods).

[8] F. BREZZI AND M. FORTIN, *Mixed and hybrid finite element methods*, vol. 15 of Springer Series in Computational Mathematics, Springer-Verlag, New York, 1991.

[9] A. BUFFA, *Hodge decompositions on the boundary of nonsmooth domains: the multi-connected case*, Math. Models Methods Appl. Sci., 11 (2001), pp. 1491–1503.

[10] A. BUFFA AND P. CIARLET, JR., *On traces for functional spaces related to Maxwell's equations. I. An integration by parts formula in Lipschitz polyhedra*, Math. Methods Appl. Sci., 24 (2001), pp. 9–30.

Bibliography

[11] ——, *On traces for functional spaces related to Maxwell's equations. II. Hodge decompositions on the boundary of Lipschitz polyhedra and applications*, Math. Methods Appl. Sci., 24 (2001), pp. 31–48.

[12] A. BUFFA, M. COSTABEL, AND C. SCHWAB, *Boundary element methods for Maxwell's equations on non-smooth domains*, Numer. Math., 92 (2002), pp. 679–710.

[13] A. BUFFA, M. COSTABEL, AND D. SHEEN, *On traces for* $\mathbf{H}(\mathbf{curl}, \Omega)$ *in Lipschitz domains*, J. Math. Anal. Appl., 276 (2002), pp. 845–867.

[14] A. BUFFA AND R. HIPTMAIR, *Galerkin boundary element methods for electromagnetic scattering*, in Topics in computational wave propagation, vol. 31 of Lect. Notes Comput. Sci. Eng., Springer, Berlin, 2003, pp. 83–124.

[15] A. BUFFA, R. HIPTMAIR, T. VON PETERSDORFF, AND C. SCHWAB, *Boundary element methods for Maxwell transmission problems in Lipschitz domains*, Numer. Math., 95 (2003), pp. 459–485.

[16] C. CARSTENSEN AND E. P. STEPHAN, *Adaptive coupling of boundary elements and finite elements*, RAIRO Modél. Math. Anal. Numér., 29 (1995), pp. 779–817.

[17] P. CIARLET, JR. AND J. ZOU, *Finite element convergence for the Darwin model to Maxwell's equations*, RAIRO Modél. Math. Anal. Numér., 31 (1997), pp. 213–249.

[18] ——, *Fully discrete finite element approaches for time-dependent Maxwell's equations*, Numer. Math., 82 (1999), pp. 193–219.

[19] P. G. CIARLET, *The finite element method for elliptic problems*, vol. 40 of Classics in Applied Mathematics, Society for Industrial and Applied Mathematics (SIAM), Philadelphia, PA, 2002. Reprint of the 1978 original [North-Holland, Amsterdam; MR0520174 (58 #25001)].

[20] D. COLTON AND R. KRESS, *Inverse acoustic and electromagnetic scattering theory*, vol. 93 of Applied Mathematical Sciences, Springer-Verlag, Berlin, second ed., 1998.

[21] M. COSTABEL, *Symmetric methods for the coupling of finite elements and boundary elements (invited contribution)*, in Boundary elements IX, Vol. 1 (Stuttgart, 1987), Comput. Mech., Southampton, 1987, pp. 411–420.

[22] M. COSTABEL, *Boundary integral operators on Lipschitz domains: elementary results*, SIAM J. Math. Anal., 19 (1988), pp. 613–626.

[23] M. COSTABEL, V. J. ERVIN, AND E. P. STEPHAN, *Symmetric coupling of finite elements and boundary elements for a parabolic-elliptic interface problem*, Quart. Appl. Math., 48 (1990), pp. 265–279.

[24] R. DAUTRAY AND J.-L. LIONS, *Mathematical analysis and numerical methods*

for science and technology. Vol. 3, Springer-Verlag, Berlin, 1990. Spectral theory and applications, With the collaboration of Michel Artola and Michel Cessenat, Translated from the French by John C. Amson.

[25] L. DEMKOWICZ, J. KURTZ, D. PARDO, M. PASZYŃSKI, W. RACHOWICZ, AND A. ZDUNEK, *Computing with hp-adaptive finite elements. Vol. 2*, Chapman & Hall/CRC Applied Mathematics and Nonlinear Science Series, Chapman & Hall/CRC, Boca Raton, FL, 2008. Frontiers: three dimensional elliptic and Maxwell problems with applications.

[26] J. W. DEMMEL, *Applied numerical linear algebra*, Society for Industrial and Applied Mathematics (SIAM), Philadelphia, PA, 1997.

[27] K. ERIKSSON AND C. JOHNSON, *Adaptive finite element methods for parabolic problems. I. A linear model problem*, SIAM J. Numer. Anal., 28 (1991), pp. 43–77.

[28] K. ERIKSSON, C. JOHNSON, AND V. THOMÉE, *Time discretization of parabolic problems by the discontinuous Galerkin method*, RAIRO Modél. Math. Anal. Numér., 19 (1985), pp. 611–643.

[29] V. GIRAULT AND P.-A. RAVIART, *Finite element methods for Navier-Stokes equations*, vol. 5 of Springer Series in Computational Mathematics, Springer-Verlag, Berlin, 1986. Theory and algorithms.

[30] P. GRISVARD, *Elliptic problems in nonsmooth domains*, vol. 24 of Monographs and Studies in Mathematics, Pitman (Advanced Publishing Program), Boston, MA, 1985.

[31] W. HACKBUSCH, *Multigrid methods and applications*, vol. 4 of Springer Series in Computational Mathematics, Springer-Verlag, Berlin, 1985.

[32] ——, *Theorie und Numerik elliptischer Differentialgleichungen*, Teubner Studienbücher Mathematik. [Teubner Mathematical Textbooks], B. G. Teubner, Stuttgart, second ed., 1996.

[33] R. HIPTMAIR, *Multilevel Preconditioning for Mixed Problems in Three Dimensions*, PhD thesis, Mathematisches Institut, Universität Augsburg, Augsburg, Germany, 1996.

[34] ——, *Canonical construction of finite elements*, Math. Comp., 68 (1999), pp. 1325–1346.

[35] ——, *Multigrid method for Maxwell's equations*, SIAM J. Numer. Anal., 36 (1999), pp. 204–225 (electronic).

[36] ——, *Finite elements in computational electromagnetism*, Acta Numer., 11 (2002), pp. 237–339.

[37] ——, *Symmetric coupling for eddy current problems*, SIAM J. Numer. Anal., 40 (2002), pp. 41–65.

[38] ——, *Coupling of finite elements and boundary elements in electromagnetic scattering*, SIAM J. Numer. Anal., 41 (2003), pp. 919–944.

[39] F. LEYDECKER, *hp-version of the boundary element method for electromagnetic problems - error analysis, adaptivity, preconditioners*, PhD thesis, Institute of Applied Mathematics, Universität Hannover, Germany, 2006.

[40] J.-L. LIONS AND E. MAGENES, *Non-homogeneous boundary value problems and applications. Vol. I*, Springer-Verlag, New York, 1972.

[41] G. LIPPOLD, *Error estimates and step-size control for the approximate solution of a first order evolution equation*, RAIRO Modél. Math. Anal. Numér., 25 (1991), pp. 111–128.

[42] M. LUSKIN AND R. RANNACHER, *On the smoothing property of the Galerkin method for parabolic equations*, SIAM J. Numer. Anal., 19 (1982), pp. 93–113.

[43] R. C. MACCAMY AND E. STEPHAN, *A simple layer potential method for three-dimensional eddy current problems*, in Ordinary and partial differential equations (Dundee, 1982), vol. 964 of Lecture Notes in Math., Springer, Berlin, 1982, pp. 477–484.

[44] ——, *A boundary element method for an exterior problem for three-dimensional Maxwell's equations*, Applicable Anal., 16 (1983), pp. 141–163.

[45] ——, *Solution procedures for three-dimensional eddy current problems*, J. Math. Anal. Appl., 101 (1984), pp. 348–379.

[46] R. C. MACCAMY AND E. STEPHAN, *A skin effect approximation for eddy current problems*, Arch. Rational Mech. Anal., 90 (1985), pp. 87–98.

[47] M. MAISCHAK, *The analytical computation of the Galerkin elements for the Laplace, Lamé and Helmholtz equation in 2d-bem*, preprint, Gottfried Wilhelm Leibniz Hanover University, Germany, 1995.

[48] ——, *The analytical computation of the Galerkin elements for the Laplace, Lamé and Helmholtz equation in 3d-bem*, preprint, Gottfried Wilhelm Leibniz Hanover University, Germany, 1995.

[49] ——, *Technical manual of the program system maiprogs*, tech. rep., Gottfried Wilhelm Leibniz Hanover University, Germany, 1996.

[50] ——, *Manual of the software package maiprogs.* Report #48 (2001) Institute of Applied Mathematics, Hannover University, Germany, 2003.

[51] ——, *Book of numerical experiments (b.o.n.e.)*, preprint, Gottfried Wilhelm Leibniz Hanover University, Germany, 2008.

[52] M. Maischak and T. Tran, *A block preconditioner for an electromagnetic fembem coupling problem in r^3*, Recent Progress in Scientific Computing, (2007), pp. 302–318.

[53] W. McLean, *Strongly elliptic systems and boundary integral equations*, Cambridge University Press, Cambridge, 2000.

[54] S. Meddahi and V. Selgas, *A mixed-FEM and BEM coupling for a three-dimensional eddy current problem*, M2AN Math. Model. Numer. Anal., 37 (2003), pp. 291–318.

[55] S. Meddahi and V. Selgas, *A FEM-BEM formulation for a time-dependent eddy current problem*, in Numerical mathematics and advanced applications, Springer, Berlin, 2006, pp. 1155–1163.

[56] S. Meddahi and V. Selgas, *An H-based FEM-BEM formulation for a time dependent eddy current problem*, Appl. Numer. Math., 58 (2008), pp. 1061–1083.

[57] D. Mitrea, M. Mitrea, and J. Pipher, *Vector potential theory on nonsmooth domains in $\mathbf{R}^3$ and applications to electromagnetic scattering*, J. Fourier Anal. Appl., 3 (1997), pp. 131–192.

[58] P. Monk, *Analysis of a finite element method for Maxwell's equations*, SIAM J. Numer. Anal., 29 (1992), pp. 714–729.

[59] ——, *Finite element methods for Maxwell's equations*, Numerical Mathematics and Scientific Computation, Oxford University Press, New York, 2003.

[60] P. Mund, *Adaptive kopplung von finiten elementen und randelementen fuer ein elliptisch-parabolisches uebergangsproblem*, Master's thesis, Universitaet Hannover, 1994.

[61] P. Mund and E. P. Stephan, *Adaptive coupling and fast solution of FEM-BEM equations for parabolic-elliptic interface problems*, Math. Methods Appl. Sci., 20 (1997), pp. 403–423.

[62] J.-C. Nédélec, *Computation of eddy currents on a surface in $\mathbf{R}^3$ by finite element methods*, SIAM J. Numer. Anal., 15 (1978), pp. 580–594.

[63] ——, *Mixed finite elements in $\mathbf{R}^3$*, Numer. Math., 35 (1980), pp. 315–341.

[64] ——, *Integral equations with nonintegrable kernels*, Integral Equations Operator Theory, 5 (1982), pp. 562–572.

[65] ——, *A new family of mixed finite elements in* $\mathbf{R}^3$, Numer. Math., 50 (1986), pp. 57–81.

[66] ——, *Acoustic and electromagnetic equations*, vol. 144 of Applied Mathematical Sciences, Springer-Verlag, New York, 2001. Integral representations for harmonic problems.

[67] S. Oestmann, *Fehlerkontrollierte adaptive FEM-BEM Kopplungsmethoden und Anwendungen*, PhD thesis, Institute of Applied Mathematics, Universität Hannover, Germany, 2005.

[68] L. Paquet, *Problèmes mixtes pour le système de Maxwell*, Ann. Fac. Sci. Toulouse Math. (5), 4 (1982), pp. 103–141.

[69] P.-A. Raviart and J. M. Thomas, *A mixed finite element method for 2nd order elliptic problems*, in Mathematical aspects of finite element methods (Proc. Conf., Consiglio Naz. delle Ricerche (C.N.R.), Rome, 1975), Springer, Berlin, 1977, pp. 292–315. Lecture Notes in Math., Vol. 606.

[70] Y. Saad and M. H. Schultz, *GMRES: a generalized minimal residual algorithm for solving nonsymmetric linear systems*, SIAM J. Sci. Statist. Comput., 7 (1986), pp. 856–869.

[71] E. Stephan and A. J. Wathen, *Convergence of preconditioned minimum residual iteration for coupled finite element/boundary element computations*, Mathematics Department Report AM-94-03, University of Bristo, (1994).

[72] J. Stratton and L. Chu, *Diffraction theory of electromagnetic waves.*, Phys. Rev., II. Ser., 56 (1939), pp. 99–107.

[73] M. Teltscher, *A posteriori Fehlerschätzer für elektromagnetische Kopplungsprobleme in drei Dimensionen*, PhD thesis, Institute of Applied Mathematics, Hannover University, Germany, 2002.

[74] V. Thomée, *Galerkin finite element methods for parabolic problems*, vol. 25 of Springer Series in Computational Mathematics, Springer-Verlag, Berlin, second ed., 2006.

[75] T. von Petersdorff and E. P. Stephan, *On the convergence of the multigrid method for a hypersingular integral equation of the first kind*, Numer. Math., 57 (1990), pp. 379–391.

[76] ——, *Multigrid solvers and preconditioners for first kind integral equations*, Numer. Methods Partial Differential Equations, 8 (1992), pp. 443–450.

[77] H. Whitney, *Geometric integration theory*, Princeton University Press, Princeton, N. J., 1957.

[78] E. Zeidler, *Nonlinear functional analysis and its applications. II/A*, Springer-Verlag, New York, 1990. Linear monotone operators, Translated from the German by the author and Leo F. Boron.

[79] ———, *Nonlinear functional analysis and its applications. II/B*, Springer-Verlag, New York, 1990. Nonlinear monotone operators, Translated from the German by the author and Leo F. Boron.

Bibliography

116

Curriculum vitae

12.01.1973	Born in Barranquilla, Colombia.
1989	Bachiller at Gimnasio Pablo VI de Soledad, Soledad, Colombia.
02/1990 – 08/1994	Studies of Mathematics and Physics at Universidad del Atlantico, Barranquilla, Colombia.
08/1994	Bachelor degree.
since 01/1995	Docent at the Universidad del Norte, Barranquilla, Colombia
02/2000 – 07/2003	Master studies in Mathematics at the Universidad Nacional de Colombia, Sede Medellin, Colombia.
07/2003	Master in Mathematics.
since 10/2005	Ph. D. student at the Institut of Applied Mathematics, Gottfried Wilhelm Leibniz Universität Hannover.